

**Characterisation and mechanisms of thiol-
induced protection against myocardial infarction**

A thesis submitted in accordance with the requirements for
the degree of PHILOSOPHIÆ DOCTOR at Cardiff University

by

Qutuba Ghanim Karwi



School of Pharmacy and Pharmaceutical Sciences

Cardiff University

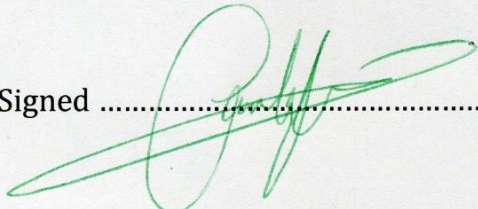
November 2016

Supervisor: Professor Gary F. Baxter

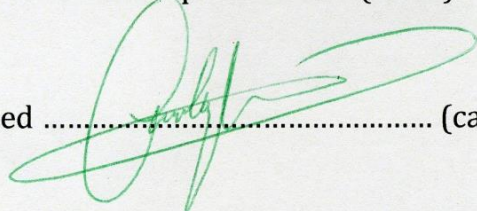


DECLARATION

This work has not been submitted in substance for any other degree or award at this or any other university or place of learning, nor is being submitted concurrently in candidature for any degree or other award.

Signed  (candidate) Date 06/04/17

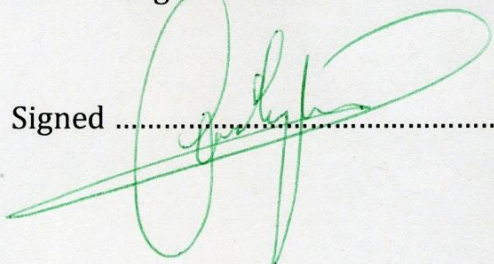
This thesis is being submitted in partial fulfillment of the requirements for the degree of Philosophiæ Doctor (Ph.D.).

Signed  (candidate) Date 06/04/17

This thesis is the result of my own independent work/investigation, except where otherwise stated. Other sources are acknowledged by explicit references. The views expressed are my own.

Signed  (candidate) Date 06/04/17

I hereby give consent for my thesis, if accepted, to be available for photocopying and for inter-library loan, and for the title and summary to be made available to outside organisations.

Signed  (candidate) Date 06/04/17

Summary

Hydrogen sulfide (H₂S) is the simplest endogenously produced thiol and has an indispensable role in cardiovascular homeostasis. It has been shown that exogenous H₂S supplementation protected the heart against myocardial ischaemia/reperfusion injury through a mechanism which is yet to be defined.

In this thesis, it was hypothesised that controlled application of thiol/H₂S donors at reperfusion would mitigate acute myocardial infarction. We sought to characterise the cardioprotection and molecular targets of three H₂S donors (mesna, GYY4137 (a slow-releasing, non-mitochondrial targeted H₂S donor) and AP39 (a mitochondria-targeting H₂S donor). This characterisation was conducted using a broad range of experimental models and techniques including anaesthetised rat model of ischaemia/reperfusion injury, Western blotting and mitochondrial studies using isolated cardiomyocyte mitochondria, namely subsarcolemmal and interfibrillar mitochondria.

Mesna did not limit infarct size when it was given pre-ischaemia or at reperfusion. GYY4137 and AP39 significantly limited infarct size when given specifically at the time of reperfusion through different mechanisms. Cardioprotection established by GYY4137 was mediated mainly by triggering of PI3K/Akt/GSK-3 β signalling at reperfusion with partial dependency on eNOS activity. Selective mitochondrial delivery of H₂S at reperfusion using AP39 had no effect on Akt, eNOS, GSK-3 β and ERK1/2. In isolated mitochondria, AP39 inhibited Ca²⁺-sensitive opening of PTP in subsarcolemmal and interfibrillar mitochondria through attenuation of mitochondrial reactive oxygen species generation.

The studies presented in this thesis provided novel mechanistic insights into cardioprotection by H₂S. These studies suggest that targeted delivery of H₂S represents a novel and effective adjunctive therapy to ameliorate the injurious effects of reperfusion which contribute to acute myocardial infarction.

Acknowledgements

This thesis signifies the completion of my doctoral studies and there are many people who have helped and supported me to make it such a wonderful journey and I would like to thank them. Firstly, I would like to thank my supervisor Professor Gary F. Baxter. Gary, thank you for giving me the opportunity to undertake my PhD study under your expert guidance. I thank you for sharing your wealth of knowledge with me and for all your support and advice. I was extremely privileged to have you with me in this fantastic journey as a mentor and friend. Thank you.

I am also very grateful to Professor Rainer Schulz and his team (Julia, Kerstin, Christine, Jacqueline, Elvira, Anna and Sabine) at Justus-Liebig University, Giessen, Germany. Rainer, thank you for the very special hospitality during the time which I spent in your lab. I highly appreciate sharing your extensive knowledge in mitochondrial physiology and your generous help in supporting the mitochondrial studies.

I would also thank Professor Matt Whiteman for sharing his critical thoughts on H₂S pharmacology with me and for the generous gifts of GYY4137 and AP39.

I must also thank my friends at the WSP for their help and support during my PhD. Special mention goes to Dr Justin Bice who has been a great friend and very supportive throughout my PhD.

I am very grateful to all my family for their support during my PhD especially my parents for their encouragement and love. Finally, special thanks to my wife and my daughter, my heart and soul. Laheeb, thank you for all your love, support and patience. This work would have been impossible without you.

Last but not least, I would like to thank the Iraqi Ministry of Higher Education and Scientific Research and University of Diyala for their unlimited support and for funding my PhD study, without which I wouldn't be able to conduct this project.

List of publications

Articles

- 1- **Karwi, Q. G.**, Bornbaum, J., Boengler, K., Torregrossa, R., Whiteman, M., Wood, M., Schulz, R., Baxter, G. F. 2017. AP39, a mitochondria-targeting hydrogen sulfide (H₂S) donor, protects against myocardial reperfusion injury independently of salvage kinase signalling. *British Journal of Pharmacology*, 174 (4), 287-301
- 2- **Karwi, Q. G.**, Whiteman, M., Wood, M. E., Torregrossa, R. & Baxter, G. F. 2016. Pharmacological postconditioning against myocardial infarction with a slow-releasing hydrogen sulfide donor, GYY4137. *Pharmacological Research*, 111, 442-451.

Abstracts

- 1- **Q. Karwi**, M. Whiteman, M. Wood, G. Baxter 2016. Postconditioning with H₂S: molecular pharmacology. *Journal of Molecular and Cellular Cardiology*, 97, S1-S18.
- 2- **Qutuba Karwi**, Matt Whiteman, Mark Wood, Gary Baxter 2016. Postconditioning with mitochondrial-targeting hydrogen sulfide donor (AP39). *Journal of Molecular and Cellular Cardiology*, 98, S1-S85.
- 3- **Karwi, Q. G.**; Whiteman, M.; Wood, M.; Ford, W.; Baxter, G. F. 2015. Infarct limitation by GYY4137 at reperfusion, a slow-releasing hydrogen sulfide donor, in the rat *in vivo*. *E-journal of British Pharmacological Society*. (<http://www.pa2online.org/abstract/abstract.jsp?abid=32759&author=karwi&cat=-1&period=61>).
- 4- **Karwi, Q. G.**; Whiteman, M.; Wood, M.; Ford, W.; Baxter, G. F. 2015. Infarct limitation by GYY4137 at reperfusion, a slow-releasing hydrogen sulfide donor, is PI3K/Akt-dependant with partial dependency on endothelial NO in the rat *in vivo*. *Journal of Molecular and Cellular Cardiology*, 86, S1-S78.

Manuscripts in preparation

- 1- **Karwi, Q. G.**, Bice, J, S., Baxter, G. F.. Conditioning the heart against ischaemia/reperfusion injury using hydrogen sulfide (H₂S): Systematic review and meta-analysis.
- 2- **Karwi, Q. G.**, Whiteman, M., & Baxter, G. F. The effect of different hydrogen sulfide donors on reperfusion-induced ventricular arrhythmias *in vivo*.

-
- 3- **Karwi, Q. G.**, Elsay, D.S., Whiteman, M., & Baxter, G. F. Divergent effects of MESNA (mercaptoethane sulfonate sodium) in myocardial ischaemia-reperfusion injury *ex vivo* and *in vivo*.
 - 4- **Karwi, Q. G.**; Baxter, G. F. Is it crosstalk or interaction between H₂S and NO in the cardiovascular system? *AJP-Heart and Circulatory Physiology* (manuscript in preparation).
 - 5- **Karwi, Q. G.**; Wang, R; Baxter, G. F. Biological implications of hydrogen sulfide-induced post-translational modifications.

Abbreviations

3-MST	3-mercaptopyruvate sulfurtransferase
AAR	area at risk
ADT-OH	anethole dithiolethione
ANT	adenine nucleotide translocase
ATP	adenosine triphosphate
ADP	adenosine diphosphate
Akt	protein kinase B
AMI	acute myocardial infarction
AP39	10-oxo-10-(4-(3-thioxo-3H-1, 2-dithiol-5-yl)phenoxy)decyl) triphenylphosphonium bromide
AP219	mitochondria-targeting moiety
BCA	bicinchoninic acid
BPM	beat per minute
cAMP	adenosine-3', 5'-cyclic monophosphate
CA/CPR	cardiac arrest and cardiopulmonary resuscitation
CAO	coronary artery occlusion
CAT	cysteine aminotransferase
CBS	cystathionine-beta-synthase
CSE	cystathionine-gamma-lyase
cGMP	guanosine-3', 5'-cyclic monophosphate, cyclic guanosine monophosphate
CHD	coronary heart disease
CsA	cyclosporine-A
CVD	cardiovascular disease
CypD	cyclophilin D
Cys	cysteine
DAO	D-aminoacid oxidase
DATS	diallyl trisulfide
DMSO	dimethyl sulfoxide
ECG	electrocardiogram
EDRF	endothelium derived relaxing factor
ERK1/2	extracellular signal-regulated kinase 1/2
FAD	flavin adenine dinucleotide
FAO	fatty acid oxidation
eNOS	endothelial nitric oxide synthase
GPx	glutathione peroxidase
GSH	glutathione
GSK-3 β	glycogen synthase kinase 3 beta
GSNO	s-nitrosoglutathione
GSSG	oxidised glutathione

GY4137	morpholin-4-ium 4-methoxyphenyl-morpholino-phosphinodithioate
H ₂ S	hydrogen sulfide
HIF-1 α	hypoxia induced factor-1 alpha
HNO	nitroxyl
HR	heart rate
HRP	horseradish peroxidase
HSP90	heat shock protein 90
HSNO	thionitrous acid
IFM	interfibrillar mitochondria
IPC	ischaemic preconditioning
IPost	ischaemic postconditioning
JAK	janus kinase
K _{ATP}	adenosine triphosphate-sensitive potassium channel
KLF5	kruppel like factor 5
LAD	left anterior descending
LDL	low density lipoprotein
L-NAME	n ^ω -nitro-l-arginine methyl ester
LV	left ventricle
MAP	mean arterial pressure
MAPK	mitogen activated protein kinase
Mesna	2-mercaptoethanesulfonate
Mito-ROS	mitochondrial reactive oxygen species
MVO	microvascular obstruction
PTP	permeability transition pore
Na ₂ S	sodium sulfide
NaHS	sodium hydrosulfide
NADPH	nicotinamide adenine dinucleotide phosphate
NF- κ B	nuclear factor-kappab
NO	nitric oxide
Nrf2	nuclear factor2
ODQ	1h-[1,2,4]oxadiazolo[4,3-a]quinoxalin-1-one
PDE	phosphodiesterase
PI3K	phosphoinositide 3-kinase
PiC	mitochondrial phosphate carrier
PIP2	phosphatidylinositol(4,5)bisphosphate
PKC	protein kinase C
PKG	protein kinase G
PLB	phospholamban
PostC-H ₂ S	postconditioning with H ₂ S
PPCI	primary percutaneous coronary intervention
PTM	post-translational modification
PVDF	polyvinylidene fluoride

RET	reverse electron transport
RISK	reperfusion injury salvage kinase
RNS	reactive nitrogen species
ROS	reactive oxygen species
RPP	rate pressure product
RV	right ventricle
RyR2	ryanodine receptor 2
SAFE	survivor activating factor enhancement
SDH	succinate dehydrogenase
SDO	sulfur dioxygenase
SDS-PAGE	sodium dodecyl sulfate polyacrylamide gel electrophoresis
sGC	soluble guanylyl cyclase
SHR	spontaneous hypertensive rat
SNAP	S-nitroso-N-acetylpenicillamine
SOD	superoxide dismutase
SO	sulfide oxidase
SO ₃ ²⁻	Sulfite
S ₂ O ₄ ²⁻	Sulfate
SP-1	specificity factor-1
SQR	sulfide quinone oxidase
SR	sarcoplasmic reticulum
SSM	subsarcolemmal mitochondria
SSO ₃ ²⁻	thiosulfate
STAT	signal transduction activator of transcription
STEMI	ST-elevation myocardial infarction
TR	thiosulfate reductase
Trx-1	thioredoxin-1
TST	thiosulfate sulfurtransferase
TPP ⁺	triphenylphosphonium
TTC	triphenyl tetrazolium chloride
VDAC	voltage-dependent anion channel
VEGF	vascular endothelial growth factor
VEGFR2	vascular endothelial growth factor receptor 2
VF	ventricular fibrillation
VPB	ventricular premature beat

Table of figures

Figure 1.1 Scheme of major cellular changes in the cardiomyocyte during ischaemia.	5
Figure 1.2 Scheme illustrating the major components the reperfusion injury. ..	7
Figure 1.3 Schematic represents the cardioprotective signal transduction of the Reperfusion Injury Salvage Kinase (RISK) and the Survival Activating Factor Enhancement (SAFE) pathways.	21
Figure 1.4 Schematic of enzymatic pathways of H ₂ S production.....	25
Figure 1.5 Schematic illustrates the catabolic fates of H ₂ S in the mitochondria.	28
Figure 2.1 Close-up image of the rat heart during the stabilisation period with a ligature around the left anterior descending coronary artery.	59
Figure 2.2 Close-up image showing the regional ischaemia in rat heart.	62
Figure 2.3 Infarct data for the preliminary study with different periods of regional myocardial ischaemia.	62
Figure 2.4 Diagram of the modified Langendorff constant pressure rig used to stain the non-ischaemic area of the heart with Evan's blue dye.	64
Figure 2.5 Perfusing the heart with Evan's blue dye through the aortic root to demarcate the non-ischaemic area after permanently occluding the left coronary artery.....	65
Figure 2.6 Scanned image for the heart slices after being stained with triphenyltetrazolium chloride (TTC) and fixed for 24 hours in formalin.....	67
Figure 2.7 Representative heart sections which have been excluded at the level of planimetry due to poor delineation between non-infarcted and infarcted areas within the AAR.	67

Figure 2.8 Representative dual staining technique with Evans' blue and TTC.	68
Figure 2.9 Schematic illustrating the heart sectioning for western blotting.....	70
Figure 3.1 Experimental protocol for the preliminary study.....	80
Figure 3.2 Experimental protocol for the model validation study with ischaemic preconditioning (IPC).....	81
Figure 3.3 Example of the cardiodynamics changes following the coronary artery occlusion (CAO).....	84
Figure 3.4 Examples of (A) the increase in R wave amplitude following coronary artery occlusion and (B) the ST-segment elevation.	85
Figure 3.5 Representative blood pressure (BP), heart rate (HR) and electrocardiography (ECG) traces during a single ventricular premature beat (VPB) that occurs during ischaemia/reperfusion protocol.	86
Figure 3.6 Representative blood pressure (BP), heart rate (HR) and electrocardiography (ECG) traces during ventricular tachycardia (VT) that occurs during ischaemia/reperfusion protocol.....	87
Figure 3.7 Representative blood pressure (BP), heart rate (HR) and electrocardiography (ECG) records during ventricular fibrillation (VF) that occurs during ischaemia/reperfusion protocol.....	88
Figure 3.8 Examples of cardiodynamics (blood pressure, heart rate and ECG) for (A) the control and (B) preconditioned hearts at early reperfusion.	91
Figure 3.9 Comparison of (A) rate pressure product (RPP) and (B) mean arterial pressure (MAP) among the control group.....	93
Figure 3.10 Comparison of (A) rate pressure product and (B) mean arterial pressure among ischaemic preconditioned rats.	94

Figure 3.11 Infarct size data for the model validation study with ischaemic preconditioning (IPC).....	95
Figure 4.1 Chemical structure of 2-mercaptoethanesulfonate sodium (Mesna).	101
Figure 4.2 Treatment protocol for Mesna study.	108
Figure 4.3 Summary of infarct size measurements for Mesna dose-response study.....	112
Figure 4.4 The oxidation of Mesna to dimesna in the circulation.	115
Figure 5.1 GYY4137 chemical structure (morpholin-4-ium 4-methoxyphenyl-morpholino-phosphinodithioate).	121
Figure 5.2 Treatment protocol for dose optimization study of GYY4137.	133
Figure 5.3 Treatment protocol for the mechanistic study of GYY4137.	135
Figure 5.4 Experimental protocol of tissue sampling following GYY4137 treatment in the presence and absence of LY294002 and L-NAME.	136
Figure 5.5 Infarct size data of GYY4137's dose-response study.	140
Figure 5.6 Infarct data of GYY4137 with pharmacological inhibitors.....	143
Figure 5.7 Representative blots and Western blot analysis of the phosphorylation of Akt in left ventricular myocardium, harvested from the area at risk 5 minutes after reperfusion, following GYY4137's postconditioning. .	145
Figure 5.8 Representative blots and Western blot analysis of the phosphorylation of eNOS in left ventricular myocardium, harvested from the area at risk 5 minutes after reperfusion, following GYY4137's postconditioning.	146
Figure 5.9 Representative blots and Western blot analysis of the phosphorylation of GSK-3 β in left ventricular myocardium, harvested from the	

area at risk 5 minutes after reperfusion, following GYY4137's postconditioning.	147
Figure 5.10 Representative blots and Western blot analysis of the phosphorylation of ERK1/2 in left ventricular myocardium, harvested from the area at risk 5 minutes after reperfusion, following GYY4137's postconditioning.	148
Figure 5.11 GYY4137, a donor of H ₂ S, induces marked limitation of myocardial infarct size when given shortly before reperfusion.	150
Figure 6.1 Chemical structures of (A) mitochondria-targeted H ₂ S donor AP39 with the two control compounds (B) AP219 and (C) ADT-OH.....	164
Figure 6.2 Experimental protocol of dose-response study of AP39.....	169
Figure 6.3 Experimental protocol of the mechanistic study of AP39.	171
Figure 6.4 Experimental protocol of myocardial biopsies sampling following postconditioning with AP39.	172
Figure 6.5 Scheme illustrating the protocol for isolation of rat-derived cardiomyocyte mitochondria using differential centrifugation.	175
Figure 6.6 Protocol for isolation of subsarcolemmal mitochondria (SSM) and stimulation with AP39 for GSH experiments.....	183
Figure 6.7 Protocol for isolation of SSM and IFM and stimulation with AP39 and SNAP for S-nitrosylation Assay.	186
Figure 6.8 Scheme illustrating the detection of mitochondrial S-nitrosylated protein post-translational modifications using Pierce S-Nitrosylation Western blot kit.....	189
Figure 6.9 Area at risk and infarct size data for dose-response study of AP39.	193

Figure 6.10 Area at risk and infarct size data for the mechanistic study of AP39 with the RISK pathway blockers.	197
Figure 6.11 Effect of postconditioning with AP39 on the phosphorylation of Akt and eNOS at early reperfusion.	199
Figure 6.12 Effect of postconditioning with AP39 on the phosphorylation of GSK-3B and ERK1/2 at early reperfusion.....	200
Figure 6.13 Toxicity study of AP39 on subsarcolemmal rat mitochondria in vitro.	202
Figure 6.14 Effect of AP39 on the opening of the mitochondria permeability transition pore (PTP).....	204
Figure 6.15 Effect of AP39 on mitochondrial-ROS generation.....	206
Figure 6.16 Effect of AP39 on mitochondrial oxygen consumption in subsarcolemmal (SSM) mitochondria.....	208
Figure 6.17 Effect of AP39 on mitochondrial oxygen consumption in interfibrillar (IFM) mitochondria.....	209
Figure 6.18 GSH and GSSG contents in the mitochondria following AP39 application.	210
Figure 6.19 Overall SSM proteins stained with Ponceau S following treatment with AP39.	212
Figure 6.20 Overall IFM proteins stained with Ponceau S following treatment with AP39.	213
Figure 6.21 Immunoidentification of the S-nitrosylated protein in subsarcolemmal mitochondria following AP39 application.	214
Figure 6.22 Immunoidentification of the mitochondrial S-nitrosylated protein in interfibrillar mitochondria following AP39 application.	215

List of tables

Table 3.1	Baselines and haemodynamic measurements throughout ischaemia/reperfusion protocol for the preliminary series of experiments	89
Table 3.2	Summary of baseline parameters and haemodynamics throughout ischaemia-reperfusion injury protocol for Ischaemic preconditioning study	92
Table 4.1	Summary of the baseline parameters and haemodynamics throughout ischaemia/reperfusion injury protocol for dose-response study of Mesna.....	111
Table 5.1	Summary of the experimental studies using the slow-releasing hydrogen sulfide donor, GYY4137, listed in chronological order	124
Table 5.2	Summary of Baselines and cardiodynamics for GYY4137 dose-effect study during ischaemia/reperfusion protocol.....	138
Table 5.3	Summary of baseline parameters and haemodynamics throughout acute myocardial infarction protocol for the mechanistic study of GYY4137 with the pharmacological inhibitors.....	142
Table 6.1	Summary of experimental studies utilising the mitochondria-targeted H ₂ S donor, AP39, listed in chronological order	163
Table 6.2	Summary of haemodynamic parameters for AP39 dose-response study during ischaemia/reperfusion protocol.....	192
Table 6.3	Summary of haemodynamic parameters throughout ischaemia/reperfusion protocol for mechanistic study of AP39 with the pharmacological inhibitors.....	195

Table of contents

Declaration	I
Summary	II
Acknowledgements	III
List of publications	IV
Abbreviations	VI
List of figures	IX
List of tables	XIV
Table of contents	XV
CHAPTER 1 GENERAL INTRODUCTION	1
1.1 Introduction.....	2
1.1.1 Coronary heart disease (CHD)	2
1.1.2 Acute myocardial infarction (AMI)	3
1.2 Pathogenesis of myocardial ischaemia	4
1.3 Reperfusion injury	6
1.3.1 Reperfusion-induced arrhythmia	6
1.3.2 Myocardial stunning	8
1.3.3 Microvascular obstruction (MVO)	8
1.3.4 Lethal myocardial reperfusion injury.....	8
1.3.5 Oxidative stress	9
1.3.6 Mitochondrial permeability transition pore (PTP)	11
1.4 Ischaemic conditioning	14
1.4.1 Ischaemic preconditioning (IPC)	14

1.4.2 Remote ischaemic preconditioning (RIPC)	17
1.4.3 Ischaemic postconditioning (IPost)	18
1.5 Hydrogen sulfide (H₂S)	22
1.5.1 The discovery of H ₂ S and origin of life	22
1.5.2 Production of H ₂ S	23
1.5.3 Metabolism of H ₂ S	26
1.5.4 Toxicity of H ₂ S	29
1.6 The effects of H₂S on the cardiovascular system.....	30
1.6.1 H ₂ S and vascular smooth muscle	30
1.6.2 H ₂ S and atherosclerosis	31
1.6.3 H ₂ S and angiogenesis	32
1.6.4 H ₂ S and hypertension	33
1.6.5 H ₂ S and myocardial ischaemia/reperfusion injury.....	35
1.7 Interaction between H₂S and NO	37
1.8 H₂S and mitochondria.....	38
1.9 H₂S and redox homeostasis	40
1.10 Rational and objectives of the studies presented in this thesis.....	43
1.11 Main points of interest	44
1.12 General thesis	44
1.13 Hypothesis and objectives.....	45
1.14 Synopsis of the thesis	45

CHAPTER 2 GENERAL METHODOLOGY	47
2.1 Materials and Methods	48
2.1.1 Chemicals	48
2.1.2 Buffers and solutions	51
2.1.3 Antibodies	54
2.1.4 Kits.....	55
2.2 Animals	56
2.3 General surgical procedures	57
2.3.1 Anaesthesia.....	57
2.3.2 Cannulation procedures	57
2.3.3 Coronary artery occlusion (CAO).....	58
2.3.4 Stabilization period	60
2.3.5 Induction of regional myocardial ischaemia.....	60
2.3.6 Reperfusion.....	63
2.4 Histology of myocardial infarction	63
2.4.1 Infarct size measurements	66
2.5 Inclusion/exclusion criteria	68
2.6 Protein level determination	69
2.6.1 Myocardial tissue sampling.....	69
2.6.2 Tissue homogenisation	71
2.6.3 Protein determination of myocardial samples	71
2.7 Western Blotting.....	72

2.7.1 Protein Separation	72
2.7.2 Proteins blotting.....	73
2.7.3 Immunodetection.....	73
2.8 Statistical analysis	76
CHAPTER 3 EXPERIMENTAL MODEL: DEVELOPMENT AND VALIDATION	77
3.1 Introduction.....	78
3.1.1 Aims.....	79
3.2 Materials and Methods	80
3.2.1 Model development: preliminary study.....	80
3.2.1.1 Experimental protocol	80
3.2.2 Model validation: using ischaemic preconditioning	80
3.2.2.1 Experimental protocol	81
3.3 Results.....	82
3.3.1 Preliminary study.....	82
3.3.1.1 Inclusion/exclusion criteria	82
3.3.1.2 The effect of coronary artery occlusion on cardiodynamics	82
3.3.1.3 Infarct data.....	90
3.3.2 Model validation study with IPC	90
3.3.2.1 Inclusion/exclusion criteria	90
3.3.2.2 The effect of IPC on cardiodynamics	90
3.3.2.3 Infarct size data	95
3.4 Discussion	96

3.5 Conclusion.....	99
----------------------------	-----------

CHAPTER 4 INVESTIGATING THE POTENTIAL INFARCT-LIMITING EFFECT OF 2-MERCAPTOETHANESULFONATE (MESNA) AGAINST MYOCARDIAL ISCHAEMIA/REPERFUSION INJURY <i>IN VIVO</i>	100
---	-----

4.1 Introduction.....	101
------------------------------	------------

4.1.1 Mesna: 2-mercaptoethanesulfonate sodium	101
---	-----

4.1.2 Aim.....	105
----------------	-----

4.1.3 Hypotheses	105
------------------------	-----

4.1.4 Objectives.....	105
-----------------------	-----

4.2 Materials and Methods	107
--	------------

4.2.1 Animals.....	107
--------------------	-----

4.2.2 The <i>in vivo</i> rat model of myocardial ischaemia/reperfusion injury	107
---	-----

4.2.3 Treatment protocols	107
---------------------------------	-----

4.2.3.1 Mesna dose-response study	107
---	-----

4.3 Results.....	109
-------------------------	------------

4.3.1 Inclusion/exclusion criteria	109
--	-----

4.3.2 Effect of Mesna on cardiodynamics	109
---	-----

4.3.3 Infarct size data	109
-------------------------------	-----

4.4 Discussion	113
-----------------------------	------------

4.5 Study limitations.....	117
-----------------------------------	------------

4.6 Conclusion.....	117
----------------------------	------------

CHAPTER 5 PHARMACOLOGICAL POSTCONDITIONING AGAINST MYOCARDIAL
INFARCTION WITH A SLOW-RELEASING HYDROGEN SULFIDE DONOR, GYY4137

.....	119
5.1 Introduction.....	120
5.1.1 GYY4137: a slow-releasing hydrogen sulfide (H ₂ S) donor.....	120
5.1.2 The biological activity of GYY4137	121
5.1.3 Aim.....	129
5.1.4 Hypotheses	129
5.1.5 Objectives.....	129
5.2 Materials and Methods	131
5.2.1 Animals.....	131
5.2.2 Acute myocardial infarction model	131
5.2.3 Treatment protocols	131
5.2.3.1 Dose-response study of GYY4137	131
5.2.3.2 Mechanistic study with the pharmacological inhibitors.....	133
5.2.3.3 Preparation of myocardial samples for protein analysis.....	135
5.2.3.4 Western blotting analysis	136
5.3 Results.....	137
5.3.1 Inclusion/exclusion criteria	137
5.3.2 Dose-response study of GYY4137	137
5.3.2.1 Hemodynamic parameters	137
5.3.2.2 Infarct size following GYY4137 postconditioning.....	139
5.3.3 Mechanistic study: involvement of PI3K/Akt and eNOS.....	141
5.3.3.1 Haemodynamic parameters	141

5.3.3.2 Infarct size data	141
5.3.4 Protein phosphorylation following postconditioning with GYY4137 ..	144
5.4 Discussion	149
5.4.1 Infarct limitation by GYY4137.....	150
5.4.2 GYY4137 postconditioning activates PI3K/Akt signalling	153
5.4.3 Dependency of GYY4137-postconditioning on NO.....	154
5.4.4 GYY4137 postconditioning attenuates GSK-3 β phosphorylation	156
5.5 Study limitations.....	157
5.6 Conclusion.....	157
CHAPTER 6 AP39, A MITOCHONDRIA-TARGETING HYDROGEN SULFIDE (H ₂ S) DONOR, PROTECTS AGAINST MYOCARDIAL REPERFUSION INJURY INDEPENDENTLY OF SALVAGE KINASE SIGNALLING	159
6.1 Introduction.....	160
6.1.1 AP39: mitochondria-targeting H ₂ S donor	161
6.1.2 Aims.....	165
6.1.3 Hypotheses	165
6.1.4 Objectives.....	166
6.2 Materials and Methods	167
6.2.1 Animals.....	167
6.2.2 Acute myocardial infarction model	167
6.2.3 Treatment protocols	167
6.2.3.1 Dose-response study of AP39	167
6.2.3.2 Mechanistic study of AP39 postconditioning	169

6.2.3.3 Myocardial tissue sampling for protein analysis.....	172
6.2.4 Isolation of cardiac mitochondria	173
6.2.4.1 Protein quantification of the mitochondrial samples	176
6.2.5 Mitochondrial functions	176
6.2.5.1 Mitochondrial membrane potential	176
6.2.5.2 Mitochondrial autofluorescence	177
6.2.5.3 Ca ²⁺ retention capacity (CRC).....	178
6.2.5.4 Mitochondrial ROS generation.....	179
6.2.5.5 Mitochondrial oxygen consumption.....	180
6.2.5.6 Effect of AP39 on mitochondrial GSH production	181
6.2.6 Effect of AP39 on S-nitrosylation of mitochondrial proteins	184
6.2.6.1 Mitochondrial preparations	184
6.2.6.2 Detecting AP39-induced S-nitrosylation using Ponceau dye	187
6.2.6.3 Detecting AP39-induced S-nitrosylation using Pierce S-nitrosylation Western blot kit	187
6.3 Results.....	190
6.3.1 Inclusion/exclusion criteria	190
6.3.2 Pharmacological postconditioning with AP39	190
6.3.2.1 Haemodynamic parameters	190
6.3.2.2 Infarct limitation with AP39 postconditioning.....	191
6.3.3 Mechanistic study of AP39: involvements of PI3K/Akt and NO	194
6.3.3.1 Haemodynamic parameters	194
6.3.3.2 Infarct size data	196
6.3.4 Protein phosphorylation following postconditioning with AP39	198

6.3.5 Direct mitochondrial effects of AP39.....	201
6.3.5.1 Toxicity study of AP39 on the mitochondria	201
6.3.5.2 AP39's impact on Ca ²⁺ overload-induced PTP opening.....	203
6.3.5.3 The effect of AP39 on mito-ROS generation	205
6.3.5.4 The effect of AP39 on mitochondrial oxygen consumption	207
6.3.5.5 Mitochondrial GSH and GSSG levels after AP39 application	210
6.3.5.6 The pattern of S-nitrosylation following AP39 application <i>in vitro</i>	211
6.4 Discussion	216
6.4.1 Postconditioning the heart with AP39	217
6.4.2 Cytosol independent cardioprotection by AP39	219
6.4.3 Inhibition of PTP opening by AP39.....	220
6.4.4 Limitation of mito-ROS generation by AP39.....	222
6.4.5 Selective delivery of H ₂ S into the mitochondria by AP39 does not affect respiratory complexes I and II	223
6.4.6 Mitochondrial GSH/GSSG ratio is not altered by AP39 application.....	225
6.4.7 The effect of AP39 on posttranslational modifications (PTMs)	226
6.5 Study limitations.....	228
6.6 Conclusion.....	229
CHAPTER 7 GENERAL DISCUSSION.....	231
7.1 General discussion	232
7.1.1 Principal findings	232
7.1.2 Context validation of the work.....	234
7.1.3 Limitations and future perspectives.....	237

7.1.4 Concluding remarks	241
REFERENCES	243
PUBLICATIONS	281

Chapter 1 General Introduction

1.1 Introduction

1.1.1 Coronary heart disease (CHD)

Cardiovascular disease (CVD) is the main cause of death and disability worldwide according to the World Health Organization (2014). Globally, it was responsible for 30% of deaths (more than 17 million) in 2008 (Mendis et al., 2011) and it is predicted to cause more than 23 million deaths by 2030 (World Health Organisation 2014). Approximately half of these deaths (8 millions) were caused by coronary heart disease (CHD) which is an umbrella term for an impairment in the coronary circulation. CHD is most commonly caused by accumulation of atherosclerotic plaques inside the coronary arteries. Plaques causes vascular stenosis impairing the blood flow to the cardiac tissue through the coronary artery. In the United Kingdom, CHD caused around 74,000 deaths among 127,000 acute myocardial infarctions (AMIs) that patients suffered in 2012 (Bhatnagar et al., 2015). The mortality rate for CHD has significantly decreased in recent years where 7 out of 10 people survive the heart attack by the virtue of risk factor reduction, new pharmacological protocols for primary prevention and earlier diagnosis (Bhatnagar et al., 2015). However, 1 in every 4 patients currently admitted for early reperfusion treatment will either die or develop heart failure within a year of the treatment (Cung et al., 2015). There are 1.5 million people in the UK living with either heart failure or other after effects of AMI (Bhatnagar et al., 2015). Therefore, there is still a great global demand for safe and effective therapies for CHD.

1.1.2 Acute myocardial infarction (AMI)

The rupture of an unstable atherosclerotic plaque in the coronary artery is the principal contributor to AMI. The exact mechanism by which atherosclerotic plaque develops in the coronary artery is not yet known. However, it is thought to involve an intricate interaction between the inflammatory/innate immune cells and the innermost layer of the coronary artery intima. High levels of low-density lipoprotein cholesterol (LDL) is proposed to cause damage to the intima and trigger a series of inflammatory responses which lead to further accumulation of blood-borne inflammatory and immune cells such as macrophage and T-lymphocyte, forming what is so-called “foam cells” (Stary et al., 1995). Foam cells comprise the core of the atheroma, along with dead cells, debris and connective tissue (Stary et al., 1995), while the outer fibrous cover of the plaque is composed of connective tissue and smooth muscle (Ross, 1993). Rupture of the fibrous cap usually occurs suddenly and triggers platelet aggregation and thrombus formation that can block the vessel lumen and cause myocardial ischaemia. If the thrombotic occlusion is sustained, it will cause irreversible myocardial damage that is termed as “infarction”. The clinical manifestation of infarction is dependent upon the degree and duration of thrombotic coronary artery occlusion. When the occlusion affects a major vessel, a myocardial ischaemic risk zone (area at risk, AAR) will rapidly develop with a high propensity of arrhythmia and decrease in contractility. In the United Kingdom, 190 out of the daily 515 patients presenting to the hospital with AMI will not survive the first few hours and the survivors will live with chronic irreversible myocardial damage in the AAR predisposing to development of chronic heart failure (Bhatnagar et al., 2014).

1.2 Pathogenesis of myocardial ischaemia

Ischaemia causes several biochemical alterations in the myocardium (Figure 1.1). The levels of adenosine tri- (ATP) and di-phosphates (ADP) rapidly fall after the onset of ischaemia as a result of cessation of oxidative phosphorylation, the main source of ATP. Glycogen swiftly becomes the main source of energy production by anaerobic metabolism (i.e. glycolysis) which leads to intracellular acidosis due to accumulation of hydrogen ion (H^+), lactate and inorganic phosphate. Acidosis itself can inhibit glycolysis and residual energy metabolism as well as disturbs ions transport across the sarcolemma. Na^+H^+ exchanger is activated in an attempt to extrude the excess H^+ ion in exchange for Na^+ which associated with more water and Cl^- entering the cell, leading to cell swelling (Reimer et al., 1981). The sarcoplasmic reticulum tries to extrude the accumulated Na^+ ions by activating the $2Na^+-Ca^{2+}$ exchanger and that results in intracellular Ca^{2+} overload (Pisarenko et al., 1988). The reduction in the energy yield of glycolysis impairs the activity of $3Na^+-K^+$ ATPase (sodium pump) which limits Na^+ extrusion and aggravates Na^+ overload in the sarcolemma. Energy shortage also limits the activity of sarcoplasmic/endoplasmic Ca^{2+} -ATPase reducing sequestration of cytoplasmic Ca^{2+} (Kaplan et al., 1992). Despite the high intracellular Ca^{2+} concentration, there is a decline in the contractility due to the desensitisation of the contractile proteins by acidosis, phosphate and Ca^{2+} overload (Fiolet and Baartscheer, 2000). Ischaemia-induced acidosis maintains mitochondrial permeability transition pore (PTP) closed during ischaemia. PTP is a nonselective protein pore generated in the inner membrane of the mitochondria during pathological conditions such as stress or ischaemia (Ong et al., 2015). The PTP opening could be triggered during the first few minutes of

reperfusion due to restoration of cytosolic pH and the overwhelming ROS generation as well as further Ca^{2+} overload.

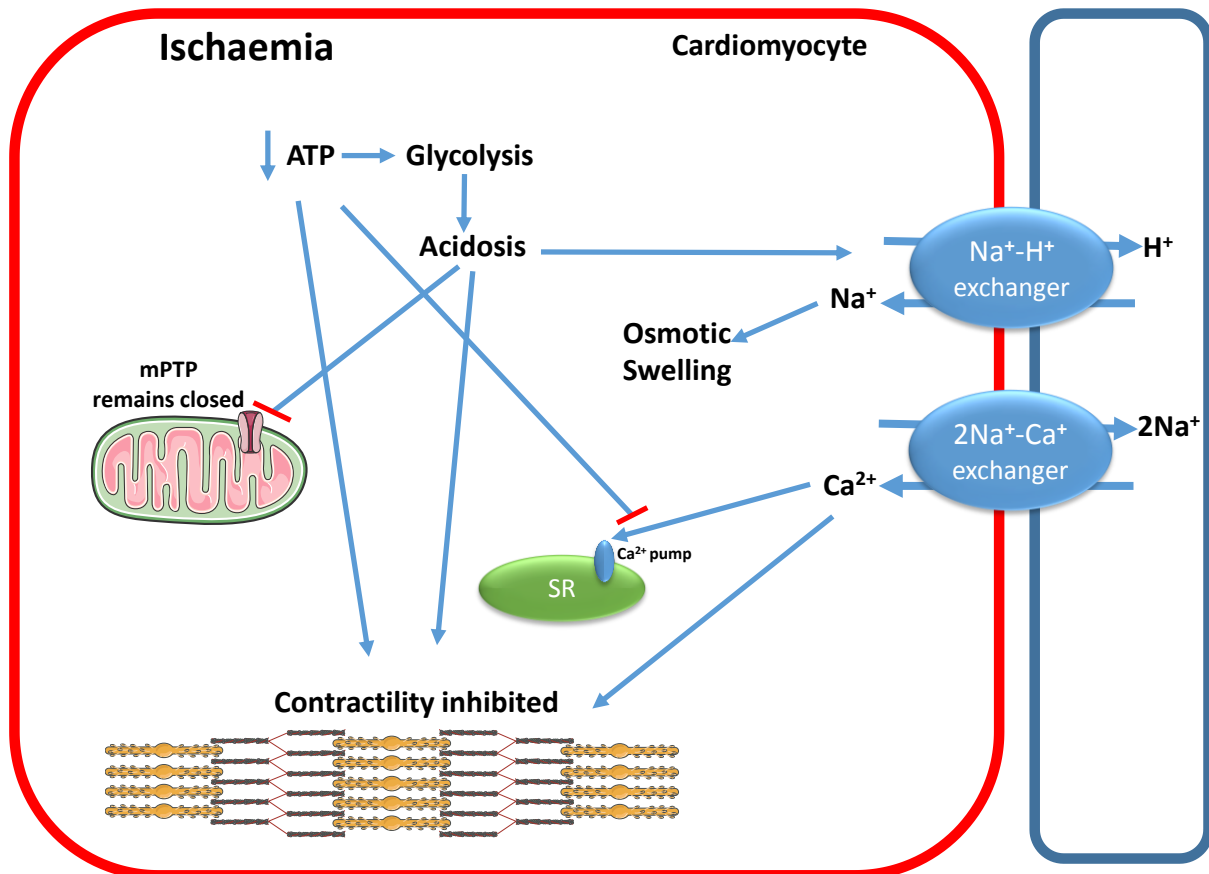


Figure 1.1 Scheme of major cellular changes in the cardiomyocyte during ischaemia. Ischaemia suppresses mitochondrial oxidative phosphorylation and glycolysis rapidly becomes the major source of energy. Anaerobic metabolism results in intracellular acidosis that activates $\text{Na}^+\text{-H}^+$ exchanger to extrude H^+ outside the cell and causing Na^+ overload. Activation of $2\text{Na}^+\text{-Ca}^{2+}$ exchanger reduces the Na^+ overload and results in Ca^{2+} overload instead that cannot be sequestered inside the sarcoplasmic reticulum by Ca^{2+} pump due to the ATP limitation. In acute myocardial ischaemia, acidosis prevents the opening of the mitochondrial permeability transition pore (PTP). ATP shortage and Ca^{2+} overload also inhibit the contractility of the cardiomyocyte.

1.3 Reperfusion injury

Reperfusion refers to re-introducing the blood through a previously occluded vessel. If applied in a timely fashion, reperfusion can ensure viability of the ischaemic tissue and limit the cellular damage. Paradoxically, reperfusion has been termed a "double-edged sword" because it has a pivotal role in maintaining viable myocardium and at the same time it is associated with deleterious effects collectively termed "reperfusion injury" (Braunwald and Kloner, 1985). It has long been understood that the main mediators of reperfusion injury are generation of reactive oxygen species (ROS), Ca^{2+} overload and pH restoration at early reperfusion (Figure 1.2). Rapid restoration of physiological pH in early reperfusion removes the inhibitory effect of acidosis on the PTP opening while ROS generation and Ca^{2+} overload are believed to trigger its opening (Hausenloy et al., 2003).

The mechanism of reperfusion injury is not yet fully understood but there are four recognized forms of myocardial reperfusion injury: two of them cause reversible damage and the others cause irreversible insult.

1.3.1 Reperfusion-induced arrhythmia

It was first reported by Hearse's group in the early 1980s that early reperfusion of an acutely ischaemic heart can induce arrhythmias in different experimental models and in the clinic. The type and severity of induced-arrhythmias can vary according to the severity and duration of the preceding ischaemia (Manning and Hearse, 1984). After brief ischaemia, there are severe reperfusion arrhythmias while prolonged ischaemia is associated with mild reperfusion arrhythmia due to the fact that dead tissue does not contract. The underlying

cause of these arrhythmias is suggested to be the oxidative stress during early reperfusion (Hearse and Tosaki, 1987). This type of arrhythmia can be self-terminating or can be easily controlled in a clinical environment.

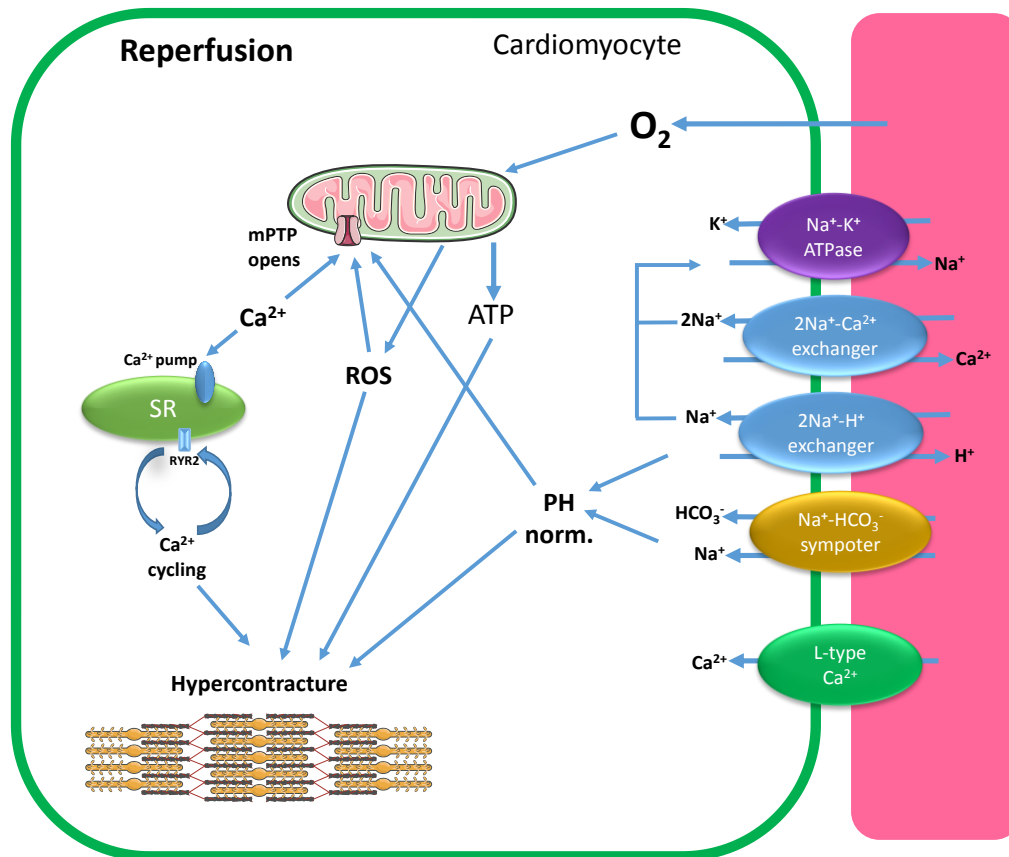


Figure 1.2 Scheme illustrating the major components the reperfusion injury. Re-oxygenation of the mitochondria restores the ATP level and reactivates the electron transport chain which is believed to be the main source of reactive oxygen species (ROS) generation. Reperfusion also activates the H^+ extruding mechanisms (Na^+-H^+ exchanger and $Na^+-HCO_3^-$ symporter), normalising the intracellular pH. The H^+ extrusion combines with Na^+ influx that can, unless sufficiently removed by Na^+ extrusion machinery, reverse the $2Na^+-Ca^{2+}$ exchanger mode of action again and exacerbate the existing Ca^{2+} overload. The overload of Ca^{2+} is initially sequestered by the sarcoplasmic reticulum by Ca^{2+} -ATPase that then releases via the ryanodine receptor 2 (RyR2) because overwhelms its capacity, creating cyclic Ca^{2+} oscillation. Rapid pH normalisation and Ca^{2+} oscillation cause hypercontracture and sarcoplasmic reticulum rupture. Collectively, these events mediate the opening of the mitochondrial permeability transition pore (PTP) which initiates cell apoptosis and necrosis.

1.3.2 Myocardial stunning

Stunning is a reversible dysfunction of the contractile apparatus after reperfusing acutely ischaemic myocardium and resolves within days or weeks. It has been suggested that impairment in myocardial contractility is caused by the overwhelming generation of ROS and Ca^{2+} overload at reperfusion, leading to temporary insensitivity of the myofilament to Ca^{2+} (Bolli and Marban, 1999).

1.3.3 Microvascular obstruction (MVO)

Krug et al. (1966) first documented microvascular obstruction in cat heart describing this phenomenon as “inability to reperfuse a previously ischaemic region” after temporary occlusion of the coronary artery. Microvessel abnormalities within the infarcted area have been reported in around 30-40% of patients after primary percutaneous coronary intervention (PPCI) with no effective therapy currently available (Bogaert et al., 2007, White et al., 2012). The main causes of MVO include: capillary collapse; impaired vasodilation; vessel plugging with neutrophil and debris from atherosclerotic plaque; platelet aggregation; external compression due to endothelial and cardiac cells swelling; release of inflammatory; vasoconstrictor and thrombogenic mediators (Ito, 2006, Heusch et al., 2009). MVO has a significant impact on clinical outcome by increasing the cell damage by continued ischaemia, reducing left ventricular ejection and promoting adverse remodelling (Hombach et al., 2005).

1.3.4 Lethal myocardial reperfusion injury

Lethal reperfusion injury refers to the cell death caused by reperfusion itself that is additive to the preceding irreversible tissue damage caused during ischaemia.

The existence of reperfusion injury and whether it compromises the salutary effects of reperfusion were topics of debate in the 1990s. There is no direct method to either quantify the cells which injured irreversibly during ischaemia or distinguish the cells which survived the ischaemic event. However, different mechanical and pharmacological interventions applied solely at the commencement of reperfusion have significantly limited the extent of cell death by 40-50% in different experimental models of myocardial ischaemia/reperfusion injury and in patients who underwent primary percutaneous coronary intervention (PPCI) (Hausenloy and Yellon, 2013). Moreover, those studies also helped in identifying possible mechanisms of reperfusion injury that can potentially be targeted to limit the lethal myocardial reperfusion injury and consequently, improve the clinical outcomes of PPCI. Unfortunately, there is no effective therapy currently used as adjunct to PPCI which could mitigate the reperfusion injury. Therefore, there is still a need to fulfil this gap.

1.3.5 Oxidative stress

ROS generation occurs normally during oxidative metabolism and is neutralised by the cellular antioxidant systems represented by endogenous reductants, such as glutathione (GSH) and thioredoxin-1 (Trx-1), and antioxidant enzymes, such as superoxide dismutase (SOD, EC 1.15.1.1) catalase (EC 1.11.1.6) and glutathione peroxidase (GPx, EC 1.11.1.9). However, endogenous antioxidant network could be overwhelmed during pathological conditions such as ischaemia or inflammation, leading to cellular stress. There is strong evidence that the first burst of superoxide (O_2^-) in the first few minutes of reperfusion is responsible for the detrimental changes at cellular and mitochondrial levels

which eventually leads to cell injury (Burwell et al., 2009). The mitochondrial respiratory chain in particular has long been recognised as the main source of ROS at early reperfusion (Chouchani et al., 2016). In addition, other cellular components have also been implicated in reperfusion-induced ROS such as xanthine oxidase (Xia and Zweier, 1995), NADPH oxidase (Braunersreuther et al., 2013) and catecholamines (Vishnevskii et al., 1995). Nevertheless, the contribution of these sources to the overall oxidative stress at reperfusion is suggested to be secondary and determined by the initial mitochondrial burst of ROS (Abramov et al., 2007). The general consensus over the last two decades has been that sudden entry of oxygen (O_2) into the electron transport complexes at the commencement of reperfusion charges these complexes leading to a considerable leak of electrons. With the availability of O_2 , electrons which escaped from the respiratory chain will create O_2^- that can, by itself or through generating of hydroxyl radical (OH^\cdot), cause irreversible cellular damage (Hausenloy and Yellon, 2013, Chouchani et al., 2016). Among the five respiratory complexes, complex I has attracted considerable attention since there is a compelling evidence that selective shut-down of its activity limited ROS production and protected the heart against ischaemia/reperfusion injury (Lesnefsky et al., 2004, Chen et al., 2006).

Seminal work by Murphy and colleagues (Chouchani et al., 2014) have recently revealed a more detailed and persuasive mechanism for ROS production through complex I at reperfusion. They showed that anaerobic metabolism during ischaemia could lead succinate dehydrogenase (SDH) to function in a reverse mode converting overproduced fumarate during ischaemia into succinate (Chouchani et al., 2014). In the first minutes of reperfusion, complexes

III and IV are at their full capability to maintain positive protonmotive force to derive ATP synthesis. Therefore, oxidation of accumulated succinate by SDH will cause backward flow of electrons from complex II to complex I in what is known as reverse electron transport (RET). RET into complex I leads to O_2^- generation possibly from its electron acceptor moiety, namely flavin mononucleotide moiety (Chouchani et al., 2014). Pharmacological blockade of ischaemia-induced succinate accumulation using dimethylmalonate, a SDH blocker, before ischaemia was demonstrated to limit mitochondrial ROS production and infarct size *in vivo* in a mouse ischaemia/reperfusion injury model (Chouchani et al., 2014). Garcia-Dorado's group (Valls-Lacalle et al., 2016) recently reported that perfusing malonate for the first 15 minutes of reperfusion limited infarct size and improved post-ischaemia contractility in Langendorff perfused mouse heart. This cardioprotection was associated with attenuation in mitochondrial ROS (mito-ROS) generation at reperfusion (Valls-Lacalle et al., 2016). Whether malonate at reperfusion could exert comparable cardioprotection *in vivo* is yet to be tested. In addition, whether succinate accumulation is of any clinical relevance is still to be determined. Furthermore, it is also yet to be investigated whether attenuation of succinate oxidation at reperfusion contributes to the cardioprotective mechanism of ischaemic conditioning, will be both discussed later in this Chapter.

1.3.6 Mitochondrial permeability transition pore (PTP)

The thorough characterisation studies undertaken by Haworth and Hunter in the late 1970s persuasively introduced the concept that Ca^{2+} overload induced loss of the inner mitochondrial membrane (IMM) which results in mitochondrial

permeability transition (Hunter and Haworth, 1979a, Haworth and Hunter, 1979, Hunter and Haworth, 1979b). In the late 1980s, these findings were confirmed using patch-clamp technique showing evidence of a megachannel in the IMM which is responsive to the cytosolic and mitochondrial Ca^{2+} contents, the basic features of what is recognised today as PTP (Kinnally et al., 1989, Petronilli et al., 1989). The seminal study by Al-Nasser and Crompton (1986) first showed the modulatory effect of cyclosporine A (CsA) on a mitochondrial Ca^{2+} -sensitive permeability channel. The transient opening of PTP, also known as flickering, regulates important cellular and mitochondrial physiological functions including Ca^{2+} homeostasis (Bernardi and von Stockum, 2012) and ROS signalling (Zorov et al., 2000). However, prolonged opening of PTP has been demonstrated to have detrimental effects on mitochondrial integrity in particular and cell viability in general. The crucial role of pathological PTP opening in irreversible myocardial injury has been characterised by Griffiths and Halestrap (1993) even before recognition of the role of mitochondria in apoptosis (Susin et al., 1996). Griffiths and Halestrap (1993) first reported that pre-ischaemic CsA treatment improved post-ischaemia cardiac contractility and preserved ATP/ADP ratio in Langendorff perfused rat heart subjected to acute myocardial infarction. It should be mentioned here that the time of PTP opening during ischaemia/reperfusion injury was not known at that time. The same group later found that ischaemia-induced acidosis maintains the PTP in close conformation during ischaemia despite existence of sufficient excitatory Ca^{2+} and oxidative stress in the matrix (Griffiths and Halestrap, 1995). However, rapid normalisation of cellular pH at early reperfusion removes this inhibition, permits the opening of PTP and initiates cell injury. Hausenloy et al. (2002) first reported that application of CsA specifically at reperfusion limited ischaemia/reperfusion-induced infarction in

isolated rat heart. This infarct limitation was absent when a PTP inhibitor, sanglifehrin-A, was applied 15 minutes post-reperfusion (Hausenloy et al., 2003), emphasising the need to target PTP at the immediate onset of reperfusion.

The composition of the PTP has been under debate since its discovery 30 years ago and is still unclear. However, a number of components have been suggested to either regulate its function or compose the pore itself. Early studies showed that the two mitochondrial membranes are connected with a number of protein-protein junctions which could comprise the PTP. These proteins included adenine nucleotide translocase (ANT) (Hunter and Haworth, 1979a, Haworth and Hunter, 1979, Hunter and Haworth, 1979b); voltage-dependent anion channel (VDAC) (Szabó et al., 1993); mitochondrial phosphate carrier (PiC) (Al-Nasser and Crompton, 1986); hexokinase (Kottke et al., 1988); Bcl-2 related proteins (Marzo et al., 1998). Nevertheless, selective genetic ablation of these targets have ruled out the necessity for any of these components for the PTP to be formed (Kokoszka et al., 2004, Krauskopf et al., 2006). Instead, experimental studies have suggested that these components could act as modulators to the PTP opening. Cyclophilin D (CypD) has also been implicated with the PTP formation since it was first shown by Crompton's group (Al-Nasser and Crompton, 1986) that the sensitivity of PTP to Ca^{2+} was attenuated by inhibiting the activity of CypD. In 2005, three independent laboratories came to the same conclusion regarding the critical role of CypD in the formation of PTP and cell death induced by its opening (Basso et al., 2005, Baines et al., 2005, Nakagawa et al., 2005). CypD^{-/-} mitochondria were more tolerant to Ca^{2+} -induced PTP opening and eventually cell death which was comparable to the effect of CsA.

However, PTP opening was still observed with higher concentrations of Ca^{2+} suggesting the formation of the pore in CypD-deficient mitochondria and that CypD could act as a facilitator for PTP opening. This hypothesis was then supported by the work of Giorgio et al. (2009) who proposed that mitochondrial F_0F_1 ATP synthase, which is the fifth mitochondrial respiratory complex (complex V), could play a major role in PTP formation. They suggested that, in response to Ca^{2+} overload or oxidative stress, CypD can bind to ATP synthase at its lateral stalk and decrease complex activity. This binding was enhanced by inorganic phosphate and abrogated by CsA, principle features of PTP. A subsequent study by Bonora et al. (2013) showed that ablation of the c-subunit of F_0 ATP synthase rendered the mitochondria more resistant to Ca^{2+} overload and oxidative stress. Alavian et al. (2014) further demonstrated that purified reconstructed c-subunit ring of F_0 ATP synthase was enlarged in response to high concentrations of Ca^{2+} , forming a voltage sensitive channel similar to PTP. More interestingly, deletion of the c-subunit enhanced mitochondrial tolerance against Ca^{2+} overload and oxidative stress while, conversely, c-subunit overexpression or long exposure to Ca^{2+} promoted cell death.

1.4 Ischaemic conditioning

1.4.1 Ischaemic preconditioning (IPC)

A major focus of research for the past 30 years has been to identify potential mechanism(s) or cellular target(s) that can be manipulated to mitigate ischaemia/reperfusion injury. Different approaches have been adopted to clearly understand the molecular pathology which underlies ischaemia/reperfusion

injury aiming to target its causes. The first milestone came from Reimer and Jennings's laboratory, in a series of experiments carried out by Charles Murry. Murry et al. (1986) demonstrated that subjecting dog heart to four episodes of 5 minutes ischaemia and 5 minutes reperfusion before sustained ischaemia (40 minutes) and 3 hours reperfusion dramatically reduced the infarct size by 75%. In his seminal paper, Murry termed this manoeuvre as "preconditioning with ischaemia" (Murry et al., 1986) which was then termed as ischaemic preconditioning (IPC). IPC is demonstrated to have two discrete windows of protection. The first window affords cardioprotection immediately after the application of IPC and lasts for 2-3 hours and it is called classical IPC or acute IPC. The second window of protection (SWOP or delayed IPC) was simultaneously reported by Marber et al. (1993) and Kuzuya et al. (1993) and it becomes functional 12-24 hours after the IPC manoeuvre has been applied. Although it is less protective than the classic IPC, SWOP can last up to 72 hours (Baxter et al., 1997) which might have significant clinical implications. The cardioprotection of IPC has not been limited to infarct size reduction, but it can also protect against life-threatening ischaemia- and reperfusion-induced arrhythmia and myocardial stunning. These effects are reproducible in all animal models studied hitherto and even in man (Murry et al., 1986, Schott et al., 1990, Liu et al., 1991, Yellon et al., 1993, Sumeray and Yellon, 1998). Moreover, IPC protocols are shown to function in isolated tissue and organs, suggesting a neural-independent mechanism (Bulluck and Hausenloy, 2015).

The mechanism of action of IPC is not yet fully understood. It was initially thought that the main salvage mechanism of IPC is mediated by slowing energy utilisation during ischaemia (Murry et al., 1990). Intriguingly, it has recently been

suggested that IPC could limit ATP depletion through its inhibitory effect on ATP synthase (complex V) (Murphy and Steenbergen, 2013). However, accumulated body of evidence suggests that the key endogenous survival mechanism activated by IPC act during reperfusion. Griffiths and Halestrap (1995) first documented that the PTP remains close during ischaemia and opens in the early reperfusion. Experimental studies showed that IPC could inhibit the opening of PTP through attenuating rapid intracellular pH restoration at reperfusion potentially through two different mechanisms. First, limitation in anaerobic metabolism mediated by IPC could result in less level of ischaemia-induced acidosis and eventually minimises the pH change at reperfusion (Asimakis et al., 1992, Wolfe et al., 1993). Second, Xiao and Allen (1999) found that IPC inhibits the activity of Na⁺-H⁺ exchanger at reperfusion allowing a slow normalisation of intracellular pH. Several studies have also demonstrated that IPC could influence the activity of the PTP at reperfusion through attenuation of the oxidative stress at reperfusion, another major trigger of PTP opening (Crestanello et al., 1996, Hoek et al., 2000, Clarke et al., 2008). However, the exact antioxidant mechanism by which IPC inhibits oxidative stress awaits clarification.

Yellon's laboratory (Hausenloy et al., 2005) first showed that the cardioprotection of IPC could mainly be mediated by activation of pro-survival anti-apoptotic kinase signalling pathway at reperfusion. This pathway consisted of PI3K/Akt and Erk1/2 signalling cascades which were collectively called the Reperfusion Injury Salvage Kinase (RISK) pathway (Hausenloy and Yellon, 2004). These data proposed an irrefutable role of the RISK pathway in IPC's cardioprotection. However, the exact mechanism by which this signalling

pathway actually inhibits the opening of PTP to confer its cardioprotection remains to be directly tested. It seems more convincing that the activation of the RISK pathway components could inhibit the opening of PTP indirectly via modulating Ca^{2+} overload, oxidative stress and pH restoration at reperfusion. Furthermore, emerging evidence showed direct “mitochondrial preconditioning” by IPC through enhancing the activity of Connexin 43 (Cx43), a hemi-channel in the IMM, in a cytosol-independent fashion (Ruiz-Meana et al., 2014).

1.4.2 Remote ischaemic preconditioning (RIPC)

This intriguing phenomena was first described by Przyklenk et al. (1993) in dogs where application of transient ischaemia in one region of the heart paradoxically preconditioned a remote region of the myocardium (virgin myocardium). This intriguing phenomenon was later extended to remotely precondition other organs (Hausenloy et al., 2016). The exact mechanism of this cardioprotective manoeuvre remains unresolved but there is compelling evidence that it involves a complex neuro-humoral pathway. Pharmacological (Gho et al., 1996), surgical (Lim et al., 2010) or genetic (Mastitskaya et al., 2012) dissipation of the neuronal pathway in the preconditioned tissue has been demonstrated to abolish infarct limitation of RIPC. This emphasises the crucial role of neural transmission in exerting the cardioprotection of RIPC. Similarly, it has been shown experimentally that RIPC stimuli generate humoral factors which are proposed to be 3.0-8.5 kDa in size, heat-labile and lipophilic (Lang et al., 2006, Breivik et al., 2011). Several blood-borne molecules have been implicated in RIPC including nitrite (Rassaf et al., 2014), miRNA-144 (Li et al., 2014), leukotrienes (Singh et al., 2016). Interestingly, Redington and colleagues (2009) found that

humoral factors which are generated in preconditioned rabbit are transferable and can protect a Langendorff perfused naïve rabbit heart against myocardial infarction.

1.4.3 Ischaemic postconditioning (IPost)

Okamoto et al. (1986) first described that “gradual” or “staged” reperfusion can be cardioprotective against ischaemia/reperfusion injury in dog heart. Later work Zhao et al. (2003) demonstrated that early interruption of reperfusion with three cycles of a brief ischaemia/reperfusion (30 seconds) protected the heart against ischaemia/reperfusion injury in a canine model. The salvage effect (44%) was comparable to IPC protection (40%) in that study and accordingly, they called it “ischaemic postconditioning (IPost)” in their seminal paper referring to the similarity to IPC (Zhao et al., 2003). It has been proposed that maintaining acidic intracellular pH in the first minutes of reperfusion by interrupting reflow allows a gradual restoration of cellular osmosis and a slow reactivation of the respiratory machinery which, collectively, protected against myocardial infarction. Similar to IPC, Vinten-Johansen’s group (Zhao et al., 2003, Sun et al., 2005) also reported that hypoxic postconditioning exerted its salvage effects by mitigating oxidative stress via a mechanism which is yet to be determined. Moreover, IPost could also exert cardioprotection by attenuating Ca^{2+} overload at reperfusion (Sun et al., 2005). Nevertheless, the contribution of Ca^{2+} overload, compared to oxidative stress and pH, in PTP opening-induced injury at reperfusion has recently been questioned. Mitochondrial calcium uniporter (MCU) knockout mice had a similar infarct size to their wild-type littermates following acute myocardial infarction (Pan et al., 2013).

Unlike IPC, IPost-evoked cardioprotection has more potential for clinical application as it is applied after the ischaemic event, onset of which is unpredictable by nature. Interestingly, late application of IPost by 60 seconds results in complete loss of the cardioprotection (Kin et al., 2004). This further emphasises the importance of early events at the commencement of reperfusion in determination of the final infarct size. Furthermore, IPost-induced cardioprotection also provided persuasive evidence for the existence of reperfusion-induced cell death. Several studies have unravelled a number of cellular signalling circuits which could possibly be triggered at reperfusion by IPost to elicit its cardioprotection. Yellon's laboratory (Tsang et al., 2004) was the first to provide evidence suggesting that IPost triggers the RISK pathway at early reperfusion to mediate protection similar to IPC. Inhibition of PI3K/Akt in isolated rat heart (Tsang et al., 2004) or Erk1/2 in isolated rabbit heart (Darling et al., 2005) abolished IPost-induced cardioprotection. Another signalling cascade has been associated with IPost cardioprotection which is called the Survival Activating Factor Enhancement (SAFE) pathway. The SAFE pathway is activated when proteins of the interleukin-6 family bind to cell surface receptors and trigger JAK/STAT phosphorylation. The level of phosphorylated STAT3 has been reported to directly relate to infarct-sparing effect of IPost as well as IPC (Lecour et al., 2005, Boengler et al., 2008b). Inhibition of the JAK/STAT3 cascade using AG490 abrogated the salvage effects of IPC (Negoro et al., 2001) as well as IPost (Lecour, 2009). Studies with STAT3 knockout mice reported that both IPC and IPost failed to show any infarct-sparing effect in these mice (Smith et al., 2004, Boengler et al., 2008a).

The relationship between the SAFE and the RISK pathways is not fully understood and requires further delineation. However, it can be postulated that there is a cross-talk between them under certain circumstances. STAT3 phosphorylation was abolished by the PI3K/Akt inhibitor wortmannin (Suleman et al., 2008). In addition, IPC did not show a significant increase in Akt phosphorylation in STAT3 knockout mice (Suleman et al., 2008). Interestingly, work by Lecour and colleagues (Lecour et al., 2005) showed that the cardioprotection of IPC, which is mediated by activating the SAFE and the RISK pathways, was abolished by inhibition of either of these pathways. In addition, exogenous TNF- α has been shown to mimic the salvage effect of IPC in isolated rat heart (Deuchar et al., 2007) and IPost in isolated mouse heart (Lacerda et al., 2009). Whether targeting the downstream effectors of these pathways individually or simultaneously can potentiate the cardioprotection also remains to be investigated.

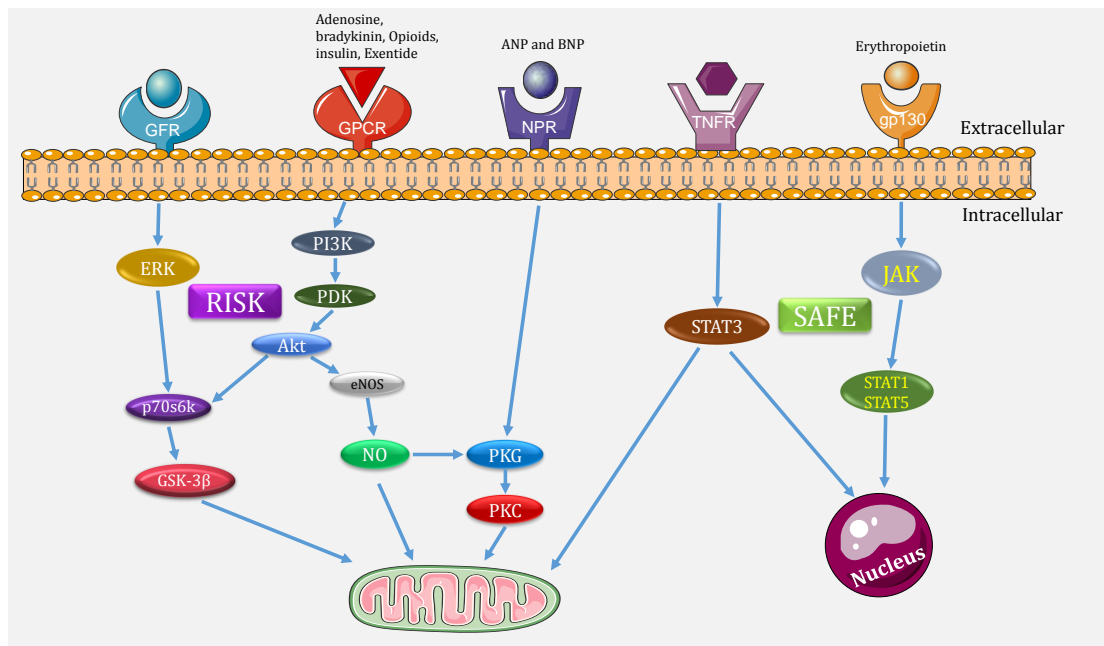


Figure 1.3 Schematic represents the cardioprotective signal transduction of the Reperfusion Injury Salvage Kinase (RISK) and the Survival Activating Factor Enhancement (SAFE) pathways modified from that presented in (Bulluck et al., 2016). PI3K: phosphatidylinositol 3-kinase; PDK: phosphoinositol-dependent kinase; Akt: protein kinase B; ERK: extracellular signal-regulated kinase; GSK-3 β : glycogen synthase kinase-3 beta; GPCR: G-protein coupled receptor; TNFR: tumor necrosis factor receptor; gp130: glycoprotein 130; JAK: janus kinase; STAT: signal transducer and activator of transcription; eNOS: endothelial nitric oxide synthase; NO: nitric oxide; ANP: atrial natriuretic peptide; BNP: brain natriuretic peptide; NPR: natriuretic peptide receptor; PKG: protein kinase G; PKC: protein kinase C; GFR: growth factor receptor.

1.5 Hydrogen sulfide (H₂S)

1.5.1 The discovery of H₂S and origin of life

Hydrogen sulfide (H₂S) is the simplest thiol-containing compound. It is thought to have served as the primordial energy source to support the earliest eukaryotes on earth in euxinic oceans (anoxic and sulfidic) more than 250 million years ago (Wille et al., 2008). With the gradual increase in O₂ production by cyanobacteria and plants, eukaryotic mitochondria then started to energise the electron transport chains using O₂ instead of oxidation of H₂S (Olson and Straub, 2016). However, an enzymatic sulfide oxidation system, represented by sulfide quinone reductase (SQR, EC 1.8.5.4), is still present in mammalian mitochondrion, supporting the long phylogenetic relationship with their ancestors. Despite being long recognised as the unpleasant odour of rotten egg, the first investigation into the occupational hazard of H₂S was carried out by Bernardino Ramazzini in early 18th century in cesspit workers presenting with irritated eyes and secondary blindness (Lambert et al., 2006). The discovery of endogenous H₂S in rat (Warencya et al., 1989), bovine (Savage and Gould, 1990) and human (Goodwin et al., 1989) brain in the early 1990s attracted great attention toward potential physiological actions of H₂S. Since then, H₂S has joined the family of gasotransmitters along with nitric oxide (NO) and carbon monoxide (CO) as a freely permeable gaseous signal transmitter exerting multiple versatile biological activities in the cell.

1.5.2 Production of H₂S

The level of endogenous H₂S under normal physiological conditions is constantly maintained by enzymatic and non-enzymatic pathways. H₂S can also be directly released from its intracellular sulfur stores, which is in the form of sulfane sulfur pools, under certain conditions (Ishigami et al., 2009). The non-enzymatic generation of H₂S occurs by reducing endogenous and exogenous thiol-containing molecules. There are four enzymes known so far which catalyse endogenous H₂S production and maintain a stable H₂S level in the cell. These enzymes have different localisation within the cell as well as diverse distribution in the body. Cystathionine-β-synthase (CBS, EC 4.2.1.22) and cystathionine-γ-lyase (CSE, EC 4.4.1.1) are pyridoxal-5'-phosphate-dependent cytosolic enzymes and they are thought to be the primary contributors to the global H₂S level. Although equally expressed in the liver and kidney, CBS is the dominant H₂S synthase in the central nervous system while CSE is the main H₂S synthase in the peripheral tissue including the cardiovascular system. Both CBS and CSE can separately condense L-homocysteine and L-cysteine molecules to produce L-cystathionine and H₂S (Figure 1.4). Also, CBS alternatively catalyses the reaction between two L-homocysteine or two L-cysteine to generate H₂S with either lanthionine or homolanthionine depending on the starting substrate conformation (Singh et al., 2009).

The process of H₂S production in the mitochondria is collaboratively governed by two enzymes, namely cysteine aminotransferase (CAT, EC 2.6.1.3) and 3-mercaptopyruvate sulfurtransferase (3-MST, EC 2.8.1.2). The transamination from mitochondrial L-cysteine to α-ketoglutarate is mediated by CAT to produce 3-mercaptopyruvate and L-glutamate. 3-MST then converts 3-mercaptopyruvate

into pyruvate and H₂S in the presence of mitochondrial reductants such as dihydrolipoic acid or thioredoxin. In the absence of mitochondria reductants, 3-MST could transfer 3-mercaptopyruvate into sulfane sulfur and pyruvate (Mikami et al., 2011). A similar mechanism has recently been unveiled which mediates the H₂S production in the mitochondria specifically in the brain and kidney. This pathway involves oxidation of dietary D-cysteine by D-aminoacid oxidase (DAO, EC 1.4.3.3) to produce 3-mercaptopyruvate which is then converted to H₂S and pyruvate by 3-MST (Shibuya et al., 2013). It has also been shown that cytosolic CBS and CSE can be translocated to the mitochondria as an adaptation mechanism to maintain physiological level of H₂S when the mitochondrial H₂S-producing system is dramatically compromised during oxidative stress (Fu et al., 2012, Modis et al., 2013a, Szabo et al., 2013).

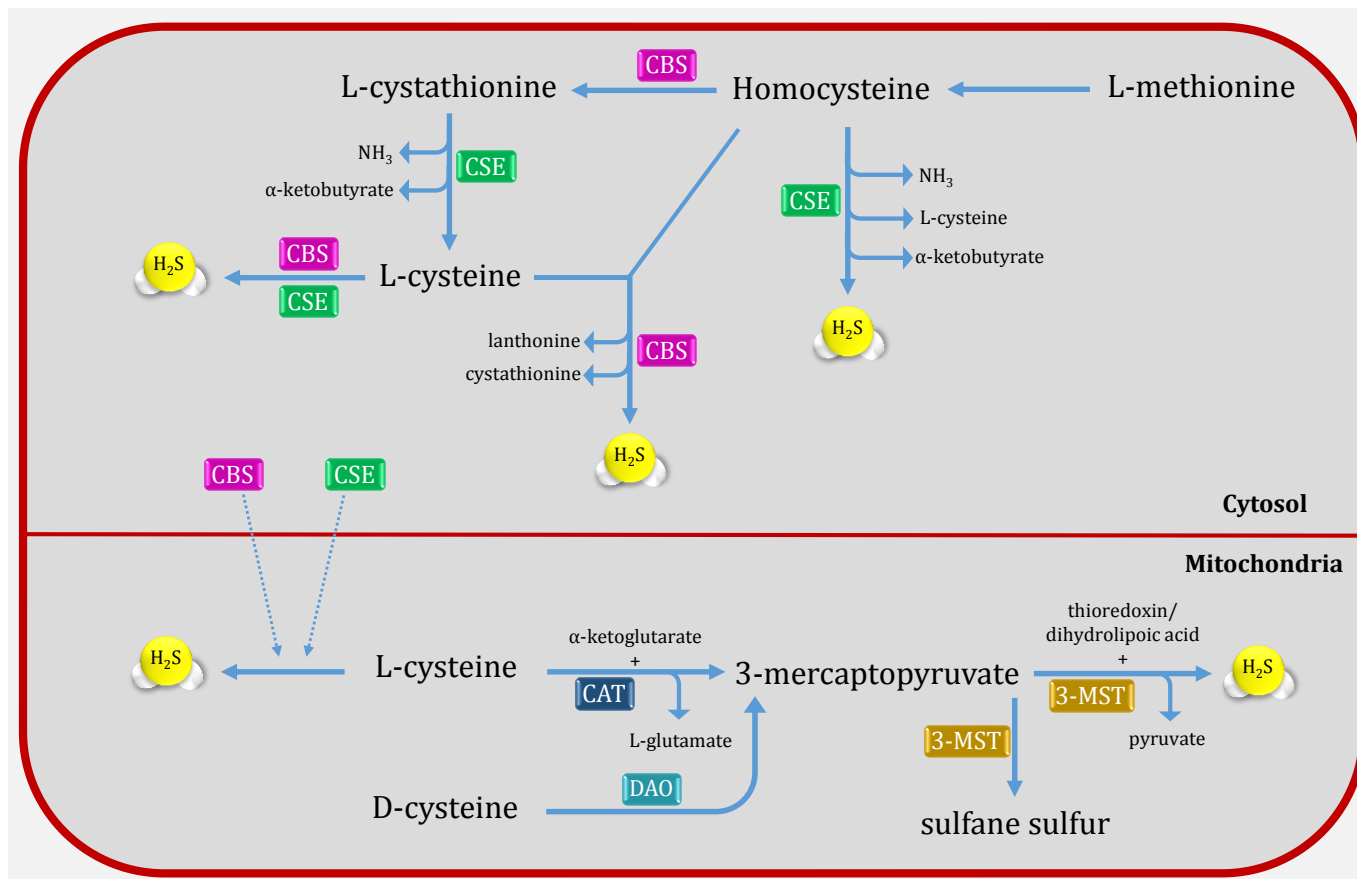


Figure 1.4 Schematic of enzymatic pathways of H₂S production. Cystathionine-β-synthase (CBS) and cystathionine-γ-lyase (CSE) utilise L-cysteine and homocysteine to generate H₂S in the cytosol. In the mitochondria, cysteine aminotransferase (CAT) and 3-mercaptopyruvate sulfurtransferase (3-MST) are working in a concert to convert L-cysteine into H₂S and pyruvate. D-aminoacid oxidase (DAO) could also participate to maintain mitochondrial H₂S production in kidney and brain.

1.5.3 Metabolism of H₂S

H₂S can be metabolised by a number of enzymatic pathways in the mitochondria, the major source of H₂S production. There are different catabolic fates of H₂S in the cell. In eukaryotes, H₂S can easily diffuse in and out of the cell. However, there is a general consensus that the first step in H₂S metabolism begins with oxidation of H₂S by sulfide quinone reductase (SQR, Figure 1.5). This step generates two electrons which could be transferred to the ubiquinone pool by flavin adenine dinucleotide (FAD) and then passed forward to complex III and complex IV (Olson, 2012). Therefore, SQR is arguably the third source of electrons, in addition to NADH dehydrogenase and succinate dehydrogenase, to the mitochondrial respiratory chain which feeds the electrons directly to complex III.

Oxidation of H₂S by SQR also generates sulfane sulfur of SQR (SQR-sulfane sulfur) which could interact with mitochondrial GSH to produce glutathione persulfide. In the presence of O₂, persulfide can be oxidised to sulfite (SO₃²⁻) by sulfur dioxygenase (SDO, EC 1.13.11.18). Alternatively, persulfide could be converted to SO₃²⁻ by thiosulfate sulfurtransferase (TST, EC 2.8.1.1). Further oxidation of sulfite by sulfite oxidase (SO, EC 1.8.3.1) could generate two electrons which add to the total electrons gain of H₂S oxidation. This step also produces two protons (H⁺) which could be pumped into the intermembrane space to maintain positive protonmotive force that drives ATP synthesis. Sulfite might also interact with SQR to produce thiosulfate (S₂O₃²⁻) in the presence of H₂S (Helmy et al., 2014). S₂O₃²⁻ is considered as a reliable marker of H₂S metabolism; it can also be reduced to pyruvate by thiosulfate-thiol

sulfurtransferase (TTST, EC 2.8.1.3) and releases H₂S. An alternative catabolic pathway of S₂O₃²⁻ is by 3-MST in the presence of endogenous reductants, such as thioredoxin or dihydrolipoic acid, that also generates H₂S and pyruvate.

Although it is classified as an “emergency fuel” for electron transport chain, the process of H₂S oxidation consumes more oxygen compared to other organic substrates as the oxidation of each molecule of sulfide utilises three moles of O₂. In addition, oxidation of sulfide generates a lower yield of electrons (two sulfide molecules produce two electrons) in comparison with organic substrates. Thus, H₂S oxidation arguably is an inefficient approach to energise the mitochondrial respiratory chain under normal physiological conditions. However, it can play a crucial in the cell survival during hypoxia.

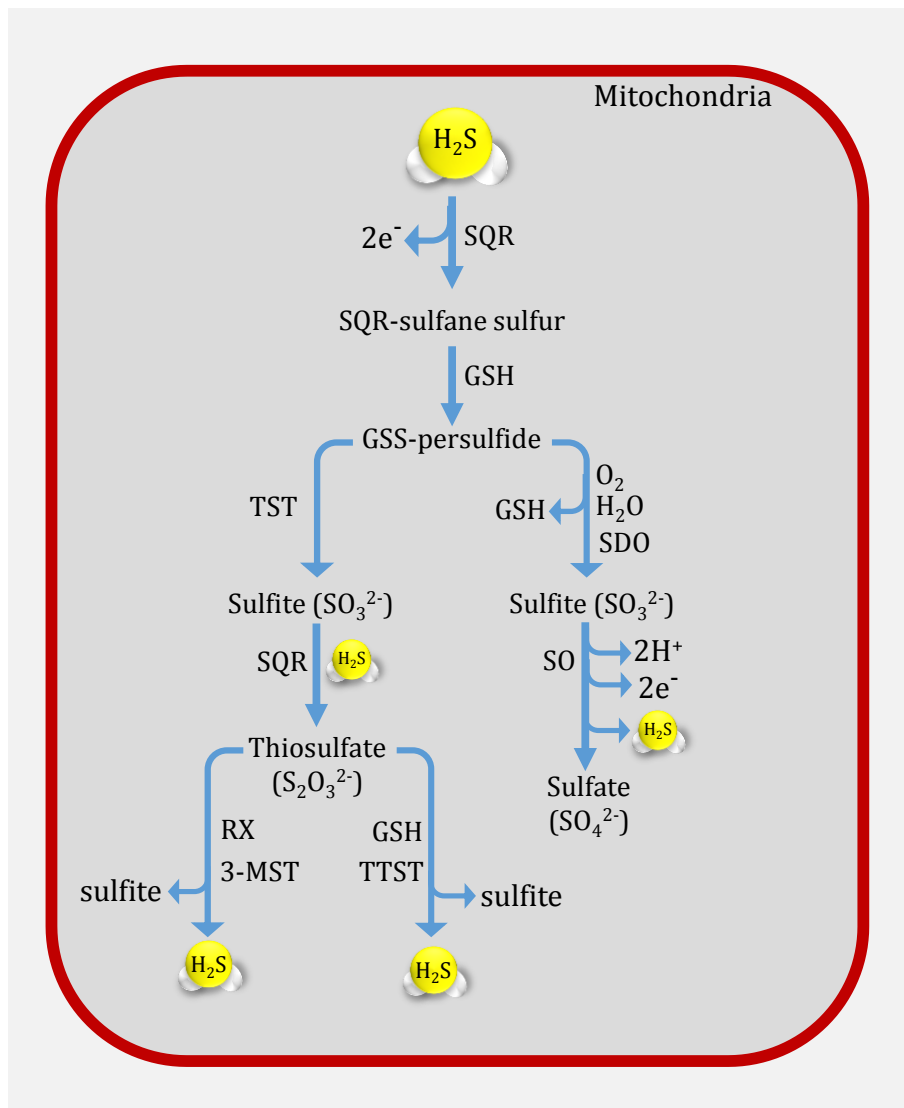


Figure 1.5 Schematic illustrates the catabolic fates of H₂S in the mitochondria. H₂S binds to Sulfide Quinone Oxidoreductase (SQR) forming SQR-sulfane sulfur and generating two electrons which feed into the respiratory chain at the level of CoenzymeQ to complex III. Sulfane sulfur is then transferred to sulfite by either thiosulfate sulfurtransferase (TST) or sulfur dioxygenase (SDO). H₂S can be generated through sulfite oxidation by sulfite oxidase (SO) which also generates two electrons that add up to the total electronic gain. Interestingly, sulfite might consume H₂S to convert to thiosulfate which could be metabolised by either thiosulfate-thiol sulfurtransferase (TTST) or 3-mercaptopyruvate sulfurtransferase (3-MST) to recover H₂S. RX, endogenous reductant.

1.5.4 Toxicity of H₂S

In humans, acute exposure to H₂S gas (>10000 ppm) can be fatal as it causes severe respiratory depression (Costigan, 2003). Low concentrations of H₂S (lower than 10 μM) can stimulate mitochondrial oxygen consumption and ATP synthesis by entering the mitochondrial oxidative phosphorylation. However, high concentrations (10 μM-100 μM) inhibit the activity of mitochondrial cytochrome c oxidase (complex IV) by reversibly binding to its active heme-side and competitively prevents the binding O₂ to this site. On a mole to mole basis, H₂S is even more toxic than cyanide (Haouzi, 2016). The inhibition of complex IV leads to accumulation of electrons in the respiratory chain, disruption in the inner membrane potential and cessation of aerobic ATP synthesis (Szabo et al., 2014). The activity of complex IV was demonstrated to be restored within 10-30 minutes after acute H₂S exposure in tissue homogenates (Di Meo et al., 2011). However, it has been reported that the complex IV inhibition might last longer *in vivo* (Khan et al., 1990). It seems conceivable that this prolonged inhibition of complex IV *in vivo* could be mediated by H₂S release from the mitochondrial sulfane sulfur pool which forms following H₂S administration, although this needs further investigation. H₂S could also inhibit the activity of carbonic anhydrase with no specific consequences of this inhibition, although it could arguably contribute to the inhibition of mitochondrial respiratory chain and bioenergetics (Nicholson et al., 1998). Interestingly, the toxic dose of H₂S (~100 μM) is almost twice the normal physiological concentration of H₂S (45.2 μM) in the brain (Warenycia et al., 1989). This suggests a steep dose-response curve for H₂S. In addition, it is also likely that there is tight control on constitutive H₂S production. However, I still think that the reported level of H₂S in the brain is actually

relatively high and this could be due to the limited accuracy of the method which has been used.

1.6 The effects of H₂S on the cardiovascular system

1.6.1 H₂S and vascular smooth muscle

The crucial regulatory role of H₂S on vascular bed homeostasis has been extensively studied. The expression of CSE as a H₂S-producing enzyme in vascular smooth muscle was first demonstrated by Hosoki et al. (1997) in rat thoracic artery and portal vein. CSE was found to be localised in the endothelium and to mediate 70-80% of the cholinergic relaxation of the vasculature (Yang et al., 2008). Moreover, dose-dependent relaxation by H₂S was present following vascular denervation but absent when the endothelium was removed (Zhao and Wang, 2002). Taken together, these results suggested that H₂S could be another endothelium derived relaxing factor (EDRF) in addition to NO. There is an accumulating body of evidence suggests a complex interaction between H₂S and NO in the vasculature. Low concentration of sodium hydrosulfide (NaHS) has been shown to synergise NO-induced relaxation of the thoracic aorta compared to high concentration of NaHS (Hosoki et al., 1997). Similar to eNOS knockout mice, CSE^{-/-} mice showed an age-dependent increase in blood pressure (up to 20 mmHg) which emphasises the importance of a constitutive H₂S-relaxing effect.

The relaxing effect of H₂S has been demonstrated to be related to the O₂ partial pressure and to the vasculature under investigation as well as H₂S tissue concentration (Koenitzer et al., 2007). Zhao et al. (2001) demonstrated that the

relaxing effect of NaHS on rat aortic tissue was via increased K_{ATP} channel permeability causing hyperpolarization of the tissue. This conclusion was derived from the observation that H_2S -induced relaxation was mimicked by pinacidil, a K_{ATP} channel activator, and abolished by glibenclamide, a K_{ATP} channel blocker. Further work by the same group showed that the H_2S -induced vasorelaxation was not attenuated by blocking soluble guanylyl cyclase (sGC) activity using ODQ or NS-2028 but in fact enhanced its effect (Zhao and Wang, 2002). These results suggested a molecular mechanism which is, at least in vasculature, independent of cyclic guanosine monophosphate (cGMP). The conductance of K_{ATP} channel is physiologically regulated by phosphatidylinositol(4,5)bisphosphate (PIP₂) which binds to the cysteine-43 (Cys⁴³) residue to open the channel. It has been shown that CSE-derived H_2S is necessary for PIP₂'s binding to K_{ATP} channel as it S-sulfhydrates Cys⁴³ and facilitates its binding to PIP₂ (Mustafa et al., 2011).

1.6.2 H_2S and atherosclerosis

There is a convincing body of evidence suggesting that the reduction in H_2S bioavailability has a major role in developing atherosclerotic plaque. Wang's laboratory (Mani et al., 2013) demonstrated that CSE $-/-$ mice had an elevation in blood levels of total cholesterol, low density lipoprotein (LDL) and homocysteine. H_2S supplement with NaHS effectively corrected these levels (Mani et al., 2013, Mani et al., 2015). H_2S also has anti-inflammatory properties and can attenuate the development of the atherosclerotic lesion. Macrophages have the capacity to release CSE-derived H_2S when stimulated by inflammatory mediators, such as lipopolysaccharide, and inhibits the inflammation process

(Zhu et al., 2010). Moreover, it has been demonstrated that exogenous H₂S limited leukocyte adhesion to the endothelium by inhibiting the expression of intracellular and extracellular adhesion molecules, such as ICAM-1 and P-selectin (Wang et al., 2009), as well as chemokine receptors, such as CX3CL1 and CX3CR1 (Zhang et al., 2012). The anti-atherogenic effects of H₂S might also be attributable to its antioxidant activity. It has been reported that oxidative stress-induced endothelial damage was exacerbated in CSE^{-/-} mice (Mani et al., 2013). This endothelial damage was mitigated by GYY4137, a slow-releasing H₂S donor (Liu et al., 2013b).

1.6.3 H₂S and angiogenesis

Angiogenesis is mainly induced by hypoxia which provides a preferential environment for the activity of proangiogenic signalling kinases such as hypoxia inducible factor-1 α (HIF-1 α) and vascular endothelium growth factor (VEGF) (Rey and Semenza, 2010). The concept that tissue concentration of H₂S is inversely proportion to the level of O₂ has now become more acceptable whereby H₂S can act as an inorganic fuel to energise oxidative phosphorylation during hypoxia (Olson et al., 2006). In addition, ischaemia-induced acidosis due to anaerobic metabolism could also facilitate the release of H₂S from a cellular acid labile pool (Yuan and Kevil, 2016). It has been reported that H₂S plays a crucial role in the signalling cascade of angiogenesis and can affect the stability of pro-angiogenic signalling kinases during ischaemia. Bir et al. (2012) reported that HIF-1 expression was upregulated in ischaemic skeletal muscle compared to normal tissue in a mouse model of hind-limb ischaemia. They also demonstrated that H₂S treatment ameliorated the expression of HIF-1 α and

VEGF expressions in the ischaemic tissue. Recent work by Flannigan and colleagues showed that decreased expression of CSE significantly compromised the stability of HIF-1 α and exacerbated the severity of colitis in a mouse model of dinitrobenzene sulfonic acid-induced colitis (Flannigan et al., 2015). The severity of colitis was reduced by H₂S treatment which substantiated the stability of HIF-1 α and upregulated the hypoxia-responsive genes. Interestingly, stabilisation of HIF-1 α resulted in a reduction in the endogenous production of H₂S suggesting a negative feedback mechanism and emphasised the role of H₂S/HIF-1 α signalling in angiogenesis (Flannigan et al., 2015). Posttranslational modification (PTM) by H₂S is also proposed to influence the signalling response to other proangiogenic factors. It has been suggested that constitutive H₂S regulates the transcription of VEGF receptor (VEGFR2) and neuropilin-1 (NRP-1) through its influence on their transcription factor, namely specificity factor (SP-1) (Saha et al., 2016). S-sulfhydration of SP-1 at the Cys⁶⁸ and Cys⁷⁵⁵ residues enhanced its stability and upregulated VEGFR1 and NRP-1. These effects were absent in CBS^{-/-} endothelial cells and restored by NaHS application (Saha et al., 2016). These data further emphasise the critical role of H₂S in the mediation of angiogenesis.

1.6.4 H₂S and hypertension

The contribution of H₂S in regulating the basal blood pressure was first characterised in spontaneously hypertensive rat (SHR) which was reported to have attenuated H₂S level and suppressed CSE activity compared to normotensive rat (Yan et al., 2004). Further inhibition of constitutive H₂S synthesis by CSE using propargylglycine (PAG) as an enzyme inhibitor caused

an additional elevation in the blood pressure and exacerbated vascular remodelling (Yan et al., 2004). This crucial role of H₂S in the pathogenesis and development of hypertension is of a clinical relevance. Hypertensive patients of grades 2 and 3 (Whiteman et al., 2010a) and diabetic patient with hypertension (Sun et al., 2007) have been shown to have a low plasma level of H₂S. Shi et al. (2007) reported that the protective effect of H₂S against hypertension-induced vascular hypertrophy and tissue fibrosis in SHR was abolished by glibenclamide, suggesting a K_{ATP} channel-dependent mechanism. Recent work by (Sun et al., 2015) demonstrated that NaHS upregulates the expression of K_{ATP} subunits in the vascular smooth muscle in the same animal model (i.e. SHR). The crosstalk between H₂S and NO has also been studied in the context of hypertension. Zhong et al. (2003) found that hypertension induced by inhibiting NO synthase using L-NAME in rat downregulated CSE expression and limited H₂S bioavailability which was reversed by H₂S therapy. These results are consistent with a recent study by Al-Magableh et al. (2015) which showed that NaHS treatment corrected low NO level and reduced systolic blood pressure in an angiotensin II-induced hypertensive rat model. It has also been shown that in dexamethasone-induced hypertension, impaired arterial relaxation was associated with downregulation of constitutive H₂S synthases (CSE and CBS) expression and low plasma H₂S level. Subsequent work by the same group demonstrated that a sulfhydrated form of zofenoprilat (S-zofenoprilat) reduced blood pressure and restored the relaxation capacity of aorta and carotid artery in SHR through its H₂S-releasing mechanism (Bucci et al., 2014).

1.6.5 H₂S and myocardial ischaemia/reperfusion injury

The contribution of impaired constitutive H₂S levels to myocardial pathologies has been investigated in various ways. Geng and colleagues (2004) were the first to provide evidence that CSE-derived H₂S could contribute in the pathology of isoproterenol-evoked cardiac injury. They also demonstrated that NaHS treatment mitigated the cardiac toxicity, as evidenced by an improved cardiac contractility and a decrease in the mortality rate. This observation is of clinical importance since patients with heart disease show low levels of H₂S (Jiang et al., 2005). In line, Zhu et al. (2007) reported a 30% decrease in mortality rate and infarct size in NaHS-treated rats compared to PPG-treated ones following ischaemia/reperfusion injury. Work by Johansen et al. (2006) was the first to test the potential cardioprotection of exogenous H₂S against ischaemia/reperfusion injury in isolated rat heart. As proof of concept, constant perfusion of NaHS pre-ischaemia and up to 10 minutes of reperfusion showed a concentration-dependent limitation in the infarct size. This infarct limitation was abolished in hearts which were pre-treated with either glibenclamide or 5-hydroxydecanoate, suggesting the involvement of K_{ATP} channel in the observed cardioprotection. Later studies from Lefer's laboratory sought to validate this observation *in vivo* and to elucidate the underlying mechanism(s). They first showed that overexpression of CSE synthase could be as protective as Na₂S therapy, given at reperfusion, against myocardial ischaemia/reperfusion injury in mice (Elrod et al., 2007). Cardioprotection established by either approach was shown to preserve mitochondrial integrity and mitigate mitochondrial dysfunction following ischaemia/reperfusion injury. They then demonstrated that H₂S could attenuate oxidative stress-induced mitochondrial

dysfunction when administered as a preconditioning mimetic before ischaemia via enhanced endogenous antioxidant expression (Calvert et al., 2009). Similarly, the same group later reported that overexpression of CSE or pharmacological H₂S therapy, (Na₂S 100 µg kg⁻¹) started after the ischaemia episode, mitigated left ventricle hypertrophy and cardiac dysfunction in ischaemia-induced heart failure in mice (Calvert et al., 2010). This protection was associated with increased Akt phosphorylation, enhanced Nrf2 expression and promoted mitochondrial biogenesis.

The involvement of NO in the cardioprotection mediated by H₂S has been studied in different species. In mice, Minamishima et al. (2009) found that improved survival rate and cardiac function following cardiac arrest and cardiopulmonary resuscitation mediated by H₂S treatment was absent in endothelial nitric oxide synthase (eNOS)-deficient mice. Consistently, enhanced NO bioavailability, as evidence by increased eNOS activation and plasma NO metabolites, was correlated with the infarct-limiting effect of garlic-derived diallyl trisulfide (DATS) as H₂S donor (Predmore et al., 2012). Moreover, the injury-limiting effect of H₂S was also abrogated by abolishing NOS phosphorylation in isoproterenol-induced cardiac injury (Sojitra et al., 2012). Interestingly, impaired NO bioavailability and eNOS activity were associated with exacerbated myocardial infarction in CSE^{-/-} mice which were restored with H₂S therapy (King et al., 2014). In a head-to head comparison across species, Papapetropoulos's group (Bibli et al., 2015) demonstrated that infarct limitation by H₂S was present when concomitantly administered with L-NAME in a rabbit model of acute myocardial infarction while it was absent in phospholamban (PLN) knockout mice.

It has been demonstrated that H₂S could mediate its infarct limitation by triggering prosurvival signalling pathways at reperfusion. Several *in vitro* and *in vivo* studies have demonstrated that exogenous H₂S mediated its cardioprotection via activation of the RISK signalling pathway at reperfusion (Yong et al., 2008, Osipov et al., 2009, Calvert et al., 2010, Yao et al., 2010, Hu et al., 2011, Predmore et al., 2011). This protective mechanism appears to function despite the existence of comorbidities such as diabetes (Peake et al., 2013, Lambert et al., 2014) and in aged cardiomyocytes (Li et al., 2015b, Li et al., 2015a). Alternatively, the SAFE pathway is also implicated in H₂S-induced cardioprotection (Luan et al., 2012, Li et al., 2016). Modulation of Ca²⁺ homeostasis is another proposed mechanism by which H₂S can reduce cardiac contractility and inhibit ischaemia-induced Ca²⁺ overload to protect cardiomyocyte against simulated ischaemia/reperfusion *in vitro* (Sun et al., 2008, Hu et al., 2011).

1.7 Interaction between H₂S and NO

There is an increasing body of evidence supporting the possibility of chemical interaction between H₂S and NO in the cellular milieu, although this remains to be detected *in vivo*. It has been proposed that the direct interaction between H₂S with available NO under aerobic conditions could generate S-nitrosothiols which potentially limit NO-induced vasorelaxation. NO could also interact with the protein cysteine residue to produce S-nitrosothiols with the possibility of NO release from these complexes (King et al., 2013). Under aerobic conditions, the simplest S-nitrosothiol is thionitrous acid (HSNO) which has been proposed to restrict the availability of NO in the presence of low H₂S concentration (Filipovic

et al., 2012, King, 2013). Under anaerobic conditions, HSNO itself could also interact with endogenous H₂S to produce hydrogen disulfide (H₂S₂) and nitroxyl (HNO), the reduced form of NO (Cortese-Krott et al., 2015). Like NO, HNO could act as an activator of sGC and stimulates vasorelaxation. Nevertheless, it has superior activity over NO as it resists ROS-induced degradation and less tolerance develops following long exposure (Beltowski, 2015). It has also been reported that HNO increases myocardial contractility via increasing the availability of Ca²⁺ in the cytosol and increasing the sensitivity of myofibrils to Ca²⁺ (Gao et al., 2012). Moreover, Sivakumaran et al. (2013) found that HNO has not only a positive inotropic effect on the heart but also a lusitropic effect by allowing muscle relaxation following contraction by activating Ca²⁺-ATPase. These beneficial effects make HNO a potential therapy to treat heart failure.

1.8 H₂S and mitochondria

H₂S exerts two different effects on the mitochondrial respiratory chain depending on its local concentration. At low concentration, H₂S can enter the oxidation process and feeds electrons into the electron transport chain at complex III. H₂S-derived electrons flow forward to bind to oxygen and aid in ATP production. Conversely, high concentration of H₂S can inhibit the activity of complex IV and consequently hinder the flow of electrons through the mitochondrial respiratory chain. This toxic effect of H₂S is seen as inhibition of ATP production and the accumulated pool of electrons in the respiratory chain which could be a potential source for ROS generation. Despite its narrow therapeutic window, it has been demonstrated that the basal level of H₂S, maintained by the constitutive H₂S production machinery, is essential for cell survival. Kondo et al. (2013) reported

that isolated mitochondria derived from CSE^{-/-} mice exhibited severe malfunction which was improved with SG-1002 as H₂S donor. Moreover, the cardiac dysfunction and mortality rate, following an acute myocardial infarction protocol, were markedly higher in CSE^{-/-} mice compared to wild type (Miao et al., 2016).

Alternative mechanisms by which endogenous H₂S could stimulate the electron transport chain have been proposed which involves stimulation of mitochondrial cAMP/PKC signalling cascade. Apart from its cytosolic functions, mitochondrial cyclic AMP is shown to interact with different constituents in the mitochondria (Acin-Perez et al., 2009). Mitochondrial cAMP concentration is controlled by mitochondrial phosphodiesterases (PDEs) and can stimulate the electron transport chain by phosphorylation of respiratory complexes (Acin-Perez et al., 2011). Szabo's laboratory has recently reported that H₂S abolished the inhibitory effect of mitochondrial PDE2A on cAMP in rat-derived liver mitochondria (Modis et al., 2013c). The resulting enhanced level of cAMP stimulated the mitochondrial respiratory chain through a PKC-dependent mechanism.

Another modulatory role of H₂S on mitochondrial bioenergetics in M2-polarized macrophage has recently been proposed by Miao et al. (2016). NaHS induced polarisation of M2-macrophage with significant enhancement of fatty acid oxidation (FAO) and lipolysis, the two main energy sources for these cells. This conclusion was drawn based on the observation that NaHS-treated M2-macrophages showed an increase in oxygen consumption rate, spare respiratory capacity and ratio of oxidative phosphorylation to aerobic glycolysis. These data unveiled a novel pathway through which H₂S could energise the mitochondria by stimulating lipolysis and FAO.

1.9 H₂S and redox homeostasis

It has been suggested that H₂S is a potent reducing agent and mediates its cytoprotective effects, at least in part, through its direct quenching of ROS. Dissolved H₂S under normal physiological conditions (37 °C, pH 7.4) is in fact present mainly as HS⁻ which is known to be a strong reductant of ROS (Al-Magableh et al., 2014) and reactive nitrogen species (RNS) (Whiteman et al., 2006). However, a compelling body of evidence suggests that these effects could be artificial due to the supraphysiological concentration of H₂S employed in these studies compared to the actual physiological level of H₂S (Furne et al., 2008). Rapid catabolism of sulfide maintains the tissue level in the low micromolar range which is far less than the high micromolar or even low millimolar range applied to explore the quenching effect of H₂S on ROS and RNS. Moreover, tissue level of H₂S in the various organs (brain, heart, and kidney) is suggested to be maintained within the low micromolar range *in vivo* (Haouzi et al., 2016). Accordingly, it seems more convincing that H₂S could have a modulatory/regulatory effect on the endogenous defence machinery against oxidative damage.

Previous work by Kimura's laboratory (Kimura and Kimura, 2004) showed that H₂S protected primary cortical neurons against oxidative glutamate toxicity (oxygenotoxicity) by enhancing the production of GSH, a powerful endogenous reductant. Further work by the same group revealed that H₂S promotes cysteine transport into the cell for GSH production, reduces cystine to cysteine in the extracellular space and enhances the redistribution and localisation of GSH to the mitochondria (Kimura et al., 2010). Furthermore, recent work by Jain et al. (2014) demonstrated that H₂S enhanced GSH production by upregulating the

cellular glutamate/cysteine exchange mechanism, represented by glutamate/cysteine ligase catalytic subunit and glutamate/cysteine ligase modifier subunit. Trx-1 is another powerful endogenous reductant, along with GSH, which can modulate ROS signal transduction as well as directly scavenge ROS to protect the cell against oxidative stress (Nordberg and Arnér, 2001). Using a murine model of hepatic ischaemia/reperfusion injury, Lefer's group (Jha et al., 2008) reported that the H₂S donor, IK1001 at reperfusion protected the liver, as evaluated by reduction in liver injury biomarkers namely alanine aminotransferase and aspartate aminotransferase. The hepatoprotective mechanism was suggested to be through improving GSH/GSSG ratio and upregulated expression of Trx-1. These data were later confirmed by the same group in a murine model of myocardial ischaemia/reperfusion injury (Calvert et al., 2009) where Na₂S treatment (100 µg kg⁻¹) was given 24 hours before the onset of ischaemia. Preconditioning the heart with H₂S resulted in infarct limitation, attenuation of oxidative stress and reduction in circulating troponin I via upregulated Trx-1 expression. Similarly, Bian and colleagues have demonstrated that H₂S treatment before subjecting to oxidative stress could render the SH-SY5Y neuronal cells and MC3T3-E1 osteoblastic cells more tolerant against oxidative stress via stimulation of endogenous reductants including GSH and Trx-1 (Xu et al., 2011, Liu et al., 2013a). Trx-1 expression is of clinical relevance as its plasma level is elevated in patients with heart failure (Kishimoto et al., 2001). Calvert and colleagues (Nicholson et al., 2013) explored the potential salvage effect of H₂S in a murine model of ischaemia-induced heart failure. In wild type mice, seven days Na₂S treatment (100 µg kg⁻¹ day⁻¹) started at the onset of reperfusion improved cardiac contractility and limited cardiac remodelling by abolishing HF-activated apoptosis signalling kinase-1 and

histone deacetylase-4 expression. The same treatment failed to show any protection in dominant negative mutant Trx-1 mice which emphasises the crucial role of Trx-1 in H₂S-induced cardioprotection.

It has been shown that H₂S could also mitigate oxidative stress by directly influencing endogenous enzymatic antioxidants. Early reports showed that direct interaction between H₂S and SOD dramatically increased ROS quenching activity of this enzyme (Searcy et al., 1995). In different experimental models, enhanced level of H₂S was shown to protect against oxidative stress-induced cell death via preserving the levels of SOD, catalase and GPx *in vitro* (Sun et al., 2012, Wen et al., 2013) and *in vivo* (Su et al., 2009, Zhu et al., 2013, Huang et al., 2013). However, it is still not fully understood how H₂S actually upregulates these enzymes. One possibility could be through triggering specific transcription factors for endogenous antioxidant enzymes such as nuclear factor- κ B (NF- κ B). It has been reported that NF- κ B regulates the activity of SOD (Kim et al., 1994) and modulate the transcription of catalase and GPx (Zhou et al., 2001). Interestingly, application of H₂S was shown to suppress inflammatory mediators and oxidative stress through upregulation of NF- κ B in an array of pathologies such as ischaemia/reperfusion injury (Guo et al., 2014), cardiac arrest (Wei et al., 2015) and sepsis (Chen et al., 2014). Attenuation of oxidative stress by H₂S is also thought to signal through nuclear factor-2 (Nrf2) (Calvert et al., 2009). Wang's laboratory provided a mechanistic insight into how H₂S could promote Nrf2 signalling (Yang et al., 2013). They demonstrated that H₂S S-sulphydrated Klech-like ECH-associated protein1 (Keap1), an inhibitory modulator of Nrf2, at Cys¹⁵¹ allowing unrestricted expression of Nrf2 which attenuated aging-induced oxidative stress. Very recently, this signalling pathway has also been implicated

in GYY4137-induced suppression of accelerated atherosclerosis in diabetic mice (Xie et al., 2016). In the same study, dissipation of this signalling pathway by Nrf2 knockout or mutating the Cys¹⁵¹ residue of Keap1 *in vitro* was showed to suppress the salvage effect of GYY4137.

S-sulfhydration (also called persulfidation) by H₂S has also been proposed to specifically limit mito-ROS generation by modulating the activity of p66Shc, a Src homologous-collagen homologue (Shc) adaptor protein. It has been shown that cytosolic p66Shc is translocated into the mitochondria in response to cell stress after being phosphorylated at serine-36 (Ser³⁶) by protein kinase C-βII (PKC- βII). Phosphorylated p66Shc disturbs the electron transfer in the mitochondrial respiratory chain, by cytochrome c (complex III) in particular, causing electron leakage from the respiratory complexes that leads to ROS generation (Giorgio et al., 2005). In SH-SY5Y neuroblastoma cells, enhanced level of H₂S, either by NaHS or by overexpression of CBS, limited H₂O₂-induced mito-ROS generation by S-sulfhydration of p66Shc at Cys⁵⁹ (Xie et al., 2014). S-sulfhydration of this residue, which is in close proximity to Ser³⁶, dissipates the association between p66Shc and PKC- βII and limits its translocation into the mitochondria.

1.10 Rational and objectives of the studies presented in this thesis

Ischaemic heart disease is still the main cause of death and disability in the world, projected to remain in the lead for the next 20 years according to the WHO. A major focus over the last two decades has been on developing therapeutic approaches which could be employed at the reperfusion phase, as a clinically relevant point of intervention, to protect against reperfusion injury and

improve the clinical outcome of thrombotic coronary artery occlusion. Compelling experimental evidence has identified endogenous salvage signalling cascades which could mitigate the cell injury when they are targeted at reperfusion including the RISK and SAFE pathways. Despite the tremendous efforts and the very promising preclinical data, the cardioprotection field has, hitherto, failed to introduce any drug which can be used clinically to reduce myocardial infarction. H₂S is one of the endogenously produced gaseous mediators which plays key roles in cardiovascular homeostasis in health and disease. The growing interest in the biology of H₂S over the last three decades has unveiled potential cardioprotective mechanisms which could have significant clinical applications. However, a general consensus has not been reached yet regarding the cardioprotective mechanism(s) of this gas. Moreover, the clinical translation of these beneficial effects has been hindered by the lack of potential H₂S-releasing drug prototypes.

1.11 Main points of interest

The main objective of this work is to characterise the potential cardioprotective effect of thiol-containing compounds as potential H₂S donors *in vivo* and to decipher the underlying mechanisms of cardioprotection.

1.12 General thesis

Elevation of H₂S at reperfusion, through the use of thiol-containing compounds, limits myocardial infarct size.

1.13 Hypothesis and objectives

The specific questions to be address in this work:

1. Does Mesna at reperfusion protect the heart from ischaemia/reperfusion injury *in vivo*?
2. Does Mesna trigger the RISK pathways at reperfusion to protect the heart against myocardial infarction *in vivo*?
3. Does administration of GYY4137 at reperfusion limit acute myocardial infarction *in vivo*?
4. Does GYY4137 activate the RISK pathway components to mediate its infarct limitation?
5. Does GYY4137 reply on NO signalling to mediate its cardioprotection?
6. Does mitochondrial delivery of H₂S by AP39 protect against myocardial ischaemia/reperfusion *in vivo*?
7. Does AP39 trigger any of the RISK pathway components to exert its protection against reperfusion injury?
8. What effects does AP39 have on cardiomyocyte mitochondria?

1.14 Synopsis of the thesis

This work was dedicated to characterisation of the potential injury-limiting effect of three thiol-containing molecules, namely Mesna, GYY4137 and AP39, with different H₂S-releasing profiles using an *in vivo* rat model of acute myocardial infarction. The onset of reperfusion was chosen as the time to apply these

compounds because it represents the most clinically relevant time point of intervention. The model of ischaemia/reperfusion injury in rat was developed in the early phase of this work and validated using IPC as a positive control (Chapter 3). Evaluation of infarct-limiting effect of Mesna was carried out using the well-known dual staining technique with Evans' blue and tetrazolium chloride (Chapter 4). Likewise, the cardioprotection of GYY4137 (Chapter 5) and AP39 (Chapter 6) was also characterised using the same approach. The influence of H₂S donors, namely GYY4137 and AP39, on the phosphorylation of the RISK kinases in the left ventricle at early reperfusion was determined using Western blotting (Chapter 5 and 6). The direct effect of selective delivery of H₂S into the mitochondria by AP39 was assessed using isolated cardiomyocyte mitochondria, namely subsarcolemmal and interfibrillar mitochondria (Chapter 6). These mitochondrial studies included measuring mitochondrial oxygen consumption by complexes I and II using Clark oxygen electrode. It also incorporated assessing the direct effect of AP39 on the mito-ROS generation using Amplex UltraRed fluorescence dye. The effect of mitochondrially delivered H₂S on the PTP opening was also evaluated as a function of mitochondrial Ca²⁺ retention capacity.

Chapter 2 General Methodology

2.1 Materials and Methods

2.1.1 Chemicals

Chemical	Source
2,3,5-triphenyltetrazolium chloride (TTC)	Sigma-Aldrich, UK
3-(N-morpholino)propanesulfonic acid (MOPS)	Sigma-Aldrich, Germany
Acrylamide	BioRad, UK
ADT-OH (anethole dithiolethione, H ₂ S-releasing moiety of AP39, MW = 226.3 g mol ⁻¹)	A generous gift from Prof Matt Whiteman/Exeter University
Ammonium persulfate (APS)	BioRad, UK
Amplex UltraRed reagent	Thermo Fisher Scientific Inc., Germany
AP219 (triphenylphosphonium, mitochondrial-targeting scaffold of AP39, MW = 433.5 g mol ⁻¹)	A generous gift from Prof Matt Whiteman/Exeter University
AP39 (10-oxo-10-(4-(3-thioxo-3H-1, 2-dithiol-5-yl)phenoxy)decyl) triphenylphosphonium bromide, MW = 722.2 g mol ⁻¹), mitochondria-targeted H ₂ S donor	A generous gift from Prof Matt Whiteman/Exeter University
Bovine serum albumin	Sigma-Aldrich, Germany

Calcium green 5N	Invitorgen, Canada
Chemiluminescent substrate	Thermo Scientific, UK
Complete™ tablets (protease inhibitor cocktail tablets)	Sigma-Aldrich, Germany
Dimethylsulfoxide (DMSO)	Sigma-Aldrich, UK
Evans' blue dye	Sigma-Aldrich, UK
Ethylene diamine tetraacetic acid (EDTA)	Sigma-Aldrich, UK
Ethylene glycol-bis(β-aminoethyl ether)-N,N,N',N'-tetraacetic acid	Sigma-Aldrich, UK
Formalin	Fisher Scientific, UK
Heparin	AAH hospital service, UK
HEPES	Roth, Germany
Horseradish peroxidase (HRP)	Roche Diagnostics, Germany
S-nitrosoglutathione (GSNO)	Sigma-Aldrich, Germany
GY4137 (morpholin-4-ium 4-methoxyphenyl-morpholino-phosphinodithioate, MW = 376.7 g mol ⁻¹)	A generous gift from Prof Matt Whiteman/Exeter University
Isoflurane Forane®	Abott GmbH, Germany
Magnesium chloride (MgCl ₂)	Fisher Scientific, UK

Magnesium sulfate (MgSO ₄)	Roth, Germany
Mesna (2-mercaptoethanesulfonate sodium)	Sigma-Aldrich, UK
Methanol	Fisher Scientific, UK
Nargase protease	Sigma-Aldrich, Germany
Neocuproine	Sigma-Aldrich, Germany
L-NAME, MW = 269.7 g mol ⁻¹	Sigma-Aldrich, UK
LY294002, 343.8 g mol ⁻¹	Sigma-Aldrich, UK
ODQ, 187.2 g mol ⁻¹	Sigma-Aldrich, UK
Percoll	GE Healthcare, Germany
Phosphate buffered saline tablets	Fisher Scientific, UK
Phosphatase inhibitor cocktail 1	Sigma-Aldrich, UK
PhosSTOP™ tablets (phosphatase inhibitor tablets)	Sigma-Aldrich, Germany
Ponceau S solution	Serva, Germany
Potassium chloride (KCl)	Fisher Scientific, UK
Potassium dihydrogen phosphate (KH ₂ PO ₄)	Merck, Germany
Protease inhibitor cocktail	Sigma-Aldrich, UK
Protein marker Precision Plus Protein™	BioRad, Germany
Rotenone 123	Sigma-Aldrich, Germany
S-nitrosoglutathione (GSNO)	Santa Cruz, Germany

S-nitroso-N-acetyl-DL-penicillamine (SNAP)	Life Technologies, Germany
Sodium dodecyl sulfate (SDS)	BioRad, UK
Sodium chloride (NaCl)	Fisher Scientific, UK
Super Signal West Dura Extended Duration Substrate	Thermo Scientific, UK
Succinate	Sigma-Aldrich, Germany
Tetramethylethylenediamine (TEMED)	Sigma-Aldrich, UK
Thiobutabarbital sodium salt hydrate (Inactin [®] hydrate)	Sigma-Aldrich, UK
Tris-Base	Fisher Scientific, UK
Triton X-100	Sigma-Aldrich, UK
Tween 20	Sigma-Aldrich, UK
XT Sample buffer (4x)	Bio-Rad, Germany

2.1.2 Buffers and solutions

30% Percoll solution	30% Percol (sterile filtered) in isolation buffer 1
Incubation buffer	125 mM KCl, 10 mM MOPS, 1.2 mM KH ₂ PO ₄ , 1.2 mM MgCl ₂ , 20 μM EGTA,

	pH 7.4
Blocking solution	5% w/v blotting grade blocker non-fat dry milk in TBST
Buffer A	0.0551 g ATP in 100 mL incubation buffer
Buffer B	80 mg bovine serum albumin (BSA) in 20 mL incubation buffer
Glutamate/Malate buffer	5 mM glutamate, 2.5 mM malate in incubation buffer
HENS buffer	100 mM HEPES (pH 7.8), 1 mM EDTA, 0.1 mM Neocuproine, and 1% SDS
Isolation buffer 1	0.146 g EDTA, 1.19 g HEPES and 42.79 g sucrose (for 500 mL), pH 7.4 adjusted with Tris-base
Isolation buffer 2	Isolation buffer 1 with Complete® tablet
Isolation buffer 3	25 µL of 200 mM Neocuproine, 3 tablets of Complete® and 3 tablets of PhosSTOP® (for 50 mL)
2-(N-morpholino)ethanesulfonic acid (MES) buffer	0.1 M 2-(N-morpholino)ethanesulphonic acid, 0.05 M phosphate, and 1 mM EDTA, pH 6.0
Physiological saline (NaCl 0.9% w/v)	Fisher Scientific, UK

Lysis buffer	1.46 g NaCl, 0.91 g KCl, 0.15 g MgCl and 0.93 g EDTA were first dissolved in 230 mL distilled water, then 20 mL Tris-buffer (pH 7.6) and 0.3% (v/v) of Triton X-100 were added with stirring
Running (Tank) buffer	30.28 g Tris-base, 142.5 g Glycine and 5 g SDS in 1 L distilled water (pH 8.3)
Sample buffer (Laemmli) 2X-concentrate	4% SDS w/v, 20% v/v glycerol, 10% v/v 2-mercaptoethanol, 0.004% v/v bromophenol blue and 0.125 M Tris HCl (pH approx. 6.8), Sigma-Aldrich, UK
Separating gel	5.27 mL distilled water, 3.33 mL Acrylamide, 1.25 mL Tris-HCl, 100 μ L of 10% w/v SDS, 50 μ L APS and 5 μ L TEMED
Stacking gel	5.77 mL distilled water, 1.67 mL acrylamide, Tris-HCL/SDS 2.5 mL, APS 50 μ L and 8 μ L TEMED
Succinate buffer	5 mM succinate, 2 μ M rotenone 123 in incubation buffer
Tris-buffered saline (TBS)	2.42 g Tris-Base and 8.8 g NaCl dissolved in 1 L distilled water (pH 7.5)

1% Tris-buffered saline with 1 mL Tween 20 in 1 L TBS
 tween 20 (1% TBST)

Transfer buffer 3.03 g Tris-buffer, 14.4 g Glycine and 200 mL Methanol in 1 L distilled water (pH 8.3)

Tris-HCl/SDS 0.4 g SDS and 6.056 g Tris-base dissolved in 100 mL distilled water and the pH was adjusted with concentrated HCl

2.1.3 Antibodies

Antibody	Company	Dilution
Rabbit polyclonal anti-human Akt	(#9272), Cell signalling, UK	1:1000
Rabbit polyclonal anti-human phosphor-Akt (Ser473)	(#9271), Cell signalling, UK	1:1000
Rabbit polyclonal anti-human eNOS	(9572), Cell signalling, UK	1:500
Rabbit polyclonal anti-human phospho-eNOS (Ser1177)	(9571), Cell signalling, UK	1:500
Rabbit polyclonal anti-human GSK-3 β	(#9315), Cell signalling, UK	1:1000
Rabbit polyclonal anti-human phospho-GSK-3 β (Ser9)	(#9336), Cell signalling, UK	1:1000
Rabbit polyclonal anti-human ERK1/2	(#9102), Cell signalling, UK	1:1000
Rabbit polyclonal anti-human phosphor-ERK1/2 (Thr202/Tyr204)	(#9101), Cell signalling, UK	1:1000
Rabbit polyclonal anti-human translocase of the outer membrane 20 (Tom20)	(sc-11415), Santa Cruz, USA	1:2000

Rabbit polyclonal anti-human GAPDH	(#2118), Cell signalling, UK	1:50000
Anti-rabbit IgG, HRP-linked	(#7074) , Cell signalling, UK	1:15000
Anti-mouse IgG-HRP	(#7076), Cell Signalling, Germany	1:10000

2.1.4 Kits

DC protein assay kit II (for Lowry assay)	5000112, BioRad, Germany
Glutathione assay kit	703002, Cayman chemical, USA
Pierce™ BCA Protein Assay Kit	ThermoFisher Scientific, UK
Pierce™ S-nitrosylation Western blot kit	90105, Thermo Scientific, USA

2.2 Animals

Male Sprague Dawley (SD) rats, 300-350 g (9-11 weeks), were obtained from Harlan, UK and used for infarct size and myocardial tissue sampling studies. For mitochondrial bioenergetics studies undertaken in Justus-Liebig University/Giessen/Germany, male Wistar rats, 300-350 g (9-11 weeks), were purchased from Harlan, France. Rats were housed in the animal facility for at least 1 week after delivery before any procedure. All animals were housed in polyethylene cages in groups of 2-4 rats on wood shaving litter with free access for normal small animal food (Teklad global 14% protein rodent maintenance diet) and fresh tap water *ad libitum*. The temperature was maintained between 18-22 °C with relative humidity around 50% and 12 hours light/dark cycle was applied. Animals were housed in a small cardboard box on the day of experiment for a minimal time before being anaesthetised. All handling and procedures for *in vivo* experiments were carried out in accordance with UK Home Office Guidelines on the Animals (Scientific Procedures) Act 1986, (published by the Stationery Office, London, UK) and was approved by the Animal Welfare Ethical Review Board, Cardiff University. Studies involving mitochondria isolation were approved by the Animal Welfare Office of the Justus-Liebig University, Giessen, Germany. Animals studies were reported in accordance with ARRIVE guidelines (Kilkenny et al., 2010, McGrath et al., 2010).

2.3 General surgical procedures

2.3.1 Anaesthesia

Sodium thiobutobarbital (Inactin[®], Sigma-Aldrich, UK) was chosen as the anaesthetic agent because it can provide a stable plane of anaesthesia for up to 6 hours with minimal interference with cardiovascular function and renal output (Buelke-Sam et al., 1978). Anaesthesia was induced by intraperitoneal injection of Inactin[®] (200 mg kg⁻¹) and maintained by bolus doses of Inactin[®] (20 mg kg⁻¹) given intravenously as required to abolish reflexes. Depth of anaesthesia was monitored throughout the experiments to avoid insufficient anaesthesia or excessive cardiac or respiratory depression. The surgical plane of anaesthesia is characterized by muscle relaxation, lack of response to stimulation such as surgical stimulation or toe pinch (pedal reflex), slow depth and rate of spontaneous respiration. The body temperature was maintained at 37 ± 1 °C using a thermo-regulated blanket unit (Harvard Apparatus Ltd, Kent, UK) and monitored by a rectal thermometer.

2.3.2 Cannulation procedures

Once the surgical plane of anaesthesia was achieved, the left jugular vein was carefully located and cannulated for intravenous administration of the anaesthetic agent and experimental treatments. The jugular vein was chosen as it allows drug administration directly into the heart first before it systematically circulated in around the body. The right common carotid artery was then cannulated and connected to fluid-filled pressure transducer, previously calibrated, to measure arterial blood pressure and heart rate using the Powerlab

data acquisition system (AD instruments, Abington, UK). Cannulations of arterial and venous vessels were performed using polyethylene tube 50 (PE 50) of 0.5 mm internal diameter, 0.9 mm outer diameter (AD Instruments Ltd, Oxford, UK), connected to a 23G (0.6 x 25 mm) syringe needle and attached to three way taps. Cannulae were filled with heparinized saline solution (0.9% w/v NaCl and 10 IU ml⁻¹ heparin) to maintain patency and for flushing the cannula as required. The trachea was separated from the surrounding tissue, a tracheotomy was performed and the trachea intubated with a Y-shaped polyethylene tube. The lungs were inflated with room air using a small rodent volume controlled ventilator (Hugo Sachs Elektronik, March, Germany) at a rate of 75 strokes min⁻¹ and with tidal volume of 1.0 to 1.25 mL 100 g⁻¹.

Heart rhythm was monitored and recorded during each experiment using standard lead II electrodes inserted subcutaneously into the rat's limbs and connected to the Powerlab data acquisition system (AD instruments, Abington, UK). Electrocardiogram (ECG) was used to identify any arrhythmia during stabilisation period and to confirm induction of myocardial ischaemia and reperfusion.

2.3.3 Coronary artery occlusion (CAO)

After cannulating the arterial and venous lines and commencing artificial respiration, a longitudinal incision was made along the midline of the chest to separate the muscle layers over the sternum using a scalpel. A midline sternotomy was then performed with Mayo scissors from xiphoid process up to the manubrium and the two side of the chest were separated using a metal retractor in order to visualize the heart. The pericardium was then carefully

dissected from the heart. A 4/0 braided thread, attached to a 17 mm 3/8 circle taper point needle (Mersilk W581, Ethicon Ltd, Edinburgh, UK), was placed around the left anterior descending (LAD) coronary artery close to its origin and below the pulmonary conus with 2-3 mm margins around the LAD (Figure 2.1).

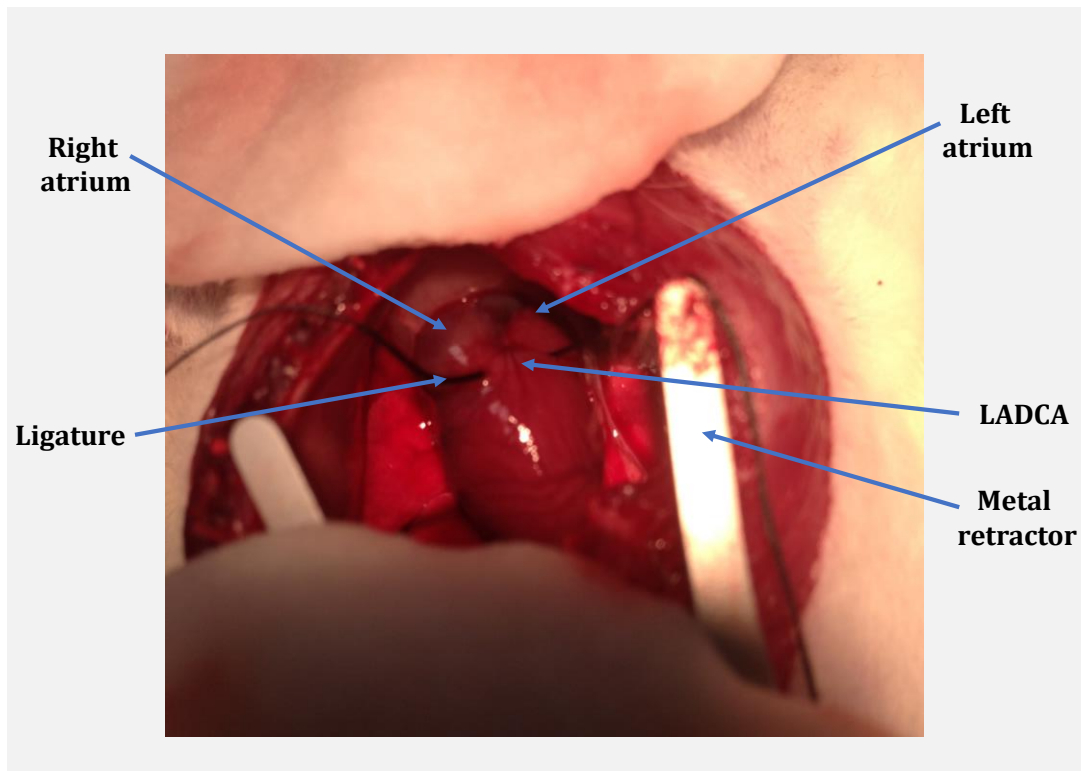


Figure 2.1 Close-up image of the rat heart during the stabilisation period with a ligature around the left anterior descending coronary artery. At this period, the ligature was loose without any interference and inclusion/exclusion criteria were applied. LADCA, left anterior descending coronary artery.

2.3.4 Stabilization period

After successfully placing the ligature around the left coronary artery, the animal was left to stabilise for 20 minutes during which the two ends of the ligature remained loose with no further interference (Figure 2.1). This period allowed adjustment of ventilation, normal sinus rhythm to be re-established, and evaluation of baseline haemodynamics. At the end of this period it was determined if animal had met the inclusion criteria for the study which were the following:

Heart rate greater than 250 beat per minutes (BPM), diastolic blood pressure greater than 50 mmHg, steady sinus rhythm, no visual signs of ischaemia, no arrhythmia during the stabilisation period.

These criteria were chosen based on previous conventions and to ensure that the rat has reasonable haemodynamics be subjected to ischaemia/reperfusion protocol. They also aimed to minimise intra- and inter-assay variation between the series of experiments and compare the data with others.

2.3.5 Induction of regional myocardial ischaemia

Two shortened pipette tips were used to form a snare around the left coronary artery to induce regional myocardial ischaemia. After 20 minutes of stabilisation, both ends of the ligature were passed through one of the shortened pipette tips and regional ischaemia was induced by pulling the two ends of the snare taut against the epicardium. The snare was then secured by placing the second pipette tip inside the first one (Figure 2.2). Ischaemia was induced for 30 minutes and confirmed by a drop in the mean arterial pressure (MAP), a colour change

of the left ventricle (from red to pale purple), and ECG changes (ST-segment elevation). The duration of myocardial ischaemia was chosen based on a preliminary series of experiments (Figure 2.3) used different ischaemia periods (20, 25 and 30 minutes) aimed to produce a reproducible area at risk (about 50-60% of the total ventricular area) and a survivable infarct size (about 50% of the ischaemic zone). Infarct size produced by 20, 25 and 30 minutes of ischaemia was 12.7 ± 4.0 , 36.2 ± 3.6 and 52.4 ± 3.1 , respectively. Therefore, 30 minutes period of ischaemia was chosen and used for the subsequent series of experiments.

Haemodynamic and ischaemia-induced arrhythmias were monitored and recorded during the 30 minutes of regional ischaemia. During this time the core temperature was maintained at 37 ± 1 °C and the chest opening was covered with a layer of cotton gauze to maintain cardiac temperature.

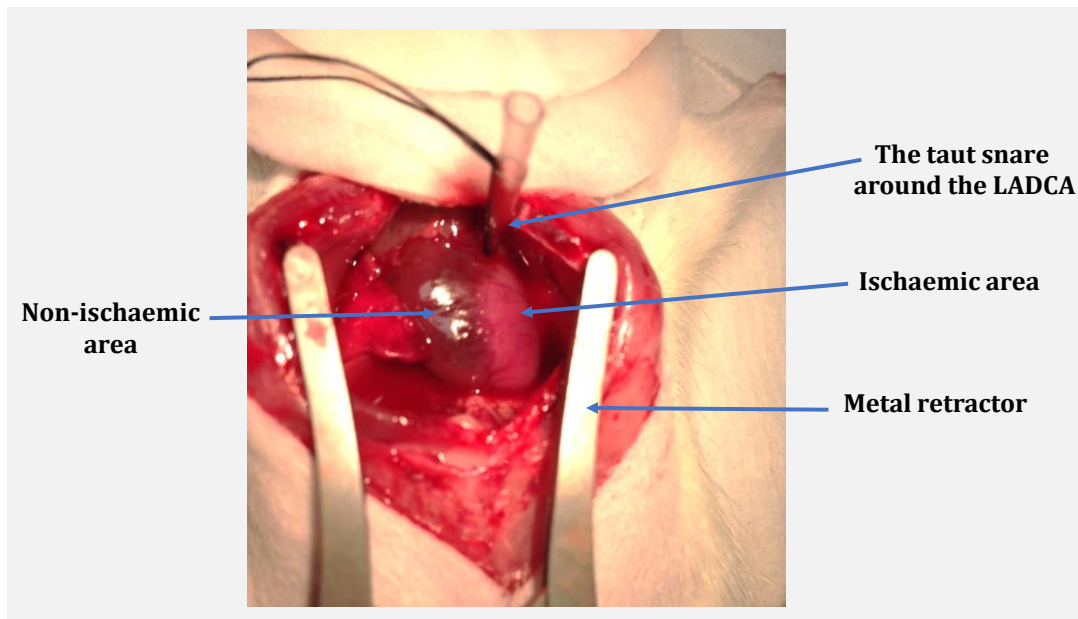


Figure 2.2 Close-up image showing the regional ischaemia in rat heart. The ischaemic bed appears as a pale purple area while the normally perfused tissue appears in red colour. The coronary artery was occluded by pulling the snare against the epicardium and securing it with another shortened pipette tip. The artery was occluded for 30 minutes, then the snare was released to reperfuse the ischaemic area for 120 minutes. LADCA, left anterior descending coronary artery.

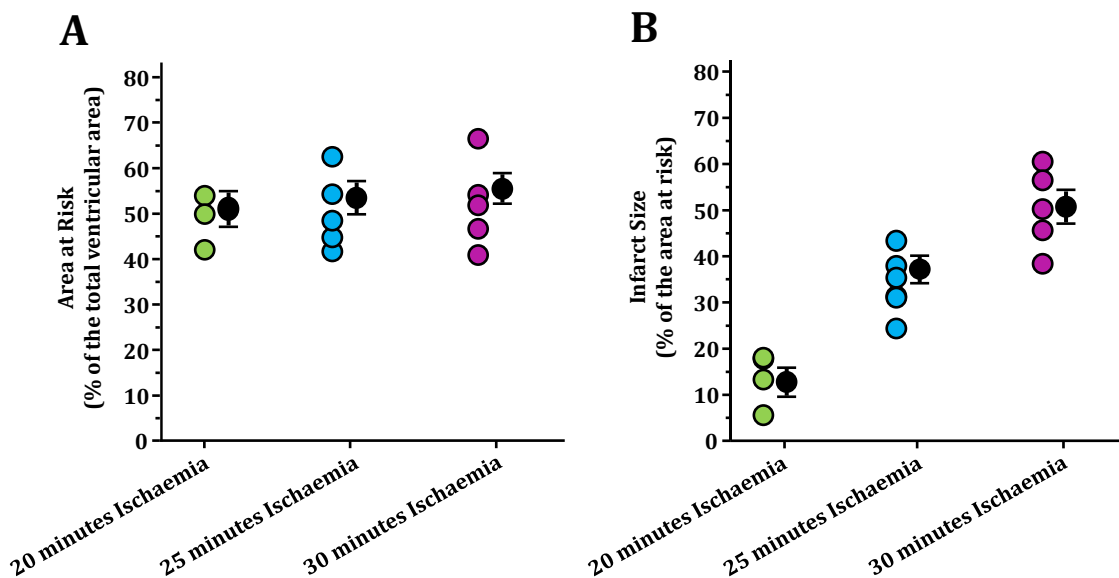


Figure 2.3 Infarct data for the preliminary study with different periods of regional myocardial ischaemia. Ischaemia was established by occluding the left descending coronary artery for 20 minutes (n=3), 25 minutes (n=5) and 30 minutes (n=5). Infarction was delineated using TTC staining and the infarct size was expressed as a percentage of the area at risk. Data are presented as mean \pm SEM.

2.3.6 Reperfusion

If the animal survived the 30 minutes of regional ischaemia, the snare was released to allow the blood to reflow through the left coronary artery again, initiating the reperfusion phase for 120 minutes. Successful reperfusion was confirmed by colour change of the ischaemic bed (from pale purple to bright red), occurrence of reperfusion-induced arrhythmia in the first minutes of reperfusion, and increase in the mean arterial pressure (MAP). Two hours of reperfusion was sufficient for the reperfusion injury to be developed. It also allows the co-factors and reducing enzymes to be cleared from the ischaemic bed which could interfere with the tertazolium staining procedure and to have a good red/white contrast within the risk zone. Cardiodynamics were recorded and respiratory adjustments was made, as required, throughout the reperfusion period. Any animal that failed to survive 120 minutes reperfusion was excluded.

2.4 Histology of myocardial infarction

Infarct size measurements were obtained using dual staining technique with Evans' blue and triphenyltetrazolium chloride (TTC). This is a gold-standard technique employed to determine infarct size in the setting of myocardial ischaemia reperfusion injury *ex vivo* and *in vivo* (Csonka et al., 2010, Bell et al., 2011). When the animal successfully survived the reperfusion period, the heart was excised with sufficient length of ascending aorta. The beating heart was washed with cold phosphate buffered saline (PBS) then transfer to a petri dish to remove any extra-cardiac tissue. The heart was then picked up by the aortic root using fine forceps and cannulated with a metal cannula to a modified Langendorff apparatus (Figure 2.4). The heart was perfused with PBS at

hydrostatic pressure of 74 mmHg (100 cm H₂O) at room temperature to remove the blood/heme residues trapped in the heart chambers. Removal of heme-containing proteins at this stage is important as any heme-residue might appear as a brownish colour and affect the red/white contrast with TTC staining later on (Pitts et al., 2007). The ligature around the LAD coronary artery was re-occluded with a surgeon's knot using fine forceps and 0.5-1.0 mL of 2% Evans blue dye slowly perfused through the aortic root to stain the non-ischaemic tissue (Figure 2.5). The stained heart was then detached from the cannula, suspended in a small plastic pot to maintain its shape and frozen at -20 °C for 3-72 hours. It is worth mentioning that this could be considered as a relatively slow freezing process for a very sensitive PTMs but this needs to be direct tested, however.

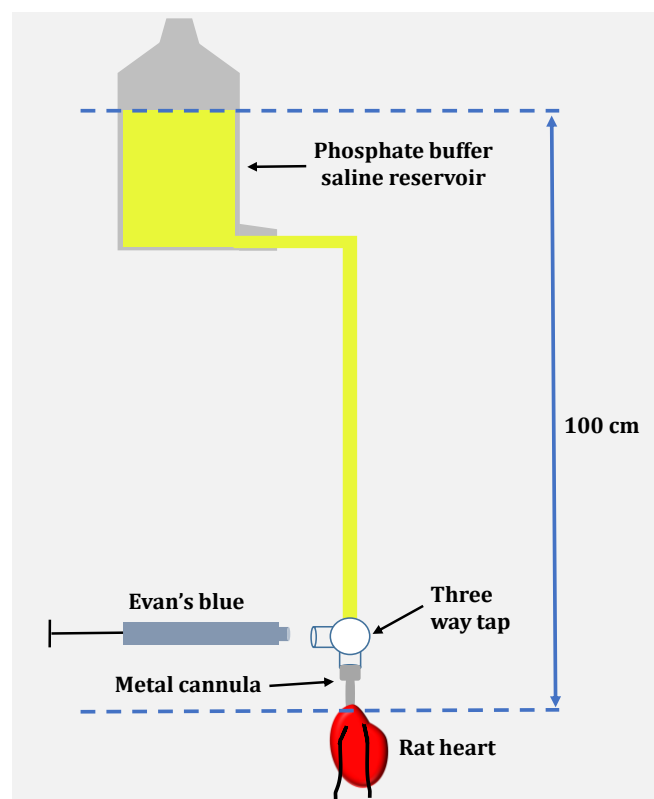


Figure 2.4 Diagram of the modified Langendorff constant pressure rig used to stain the non-ischaemic area of the heart with Evan's blue dye. At the end of ischaemia and reperfusion protocol, the heart was excised and perfused with phosphate buffer saline at 74 mmHg constant pressure *ex vivo*. The ligature was permanently tied off using a surgeon's knot before perfusing the non-ischaemic area with 2% Evan's blue dye. The heart was then frozen at -20 °C for 3-72 hours.

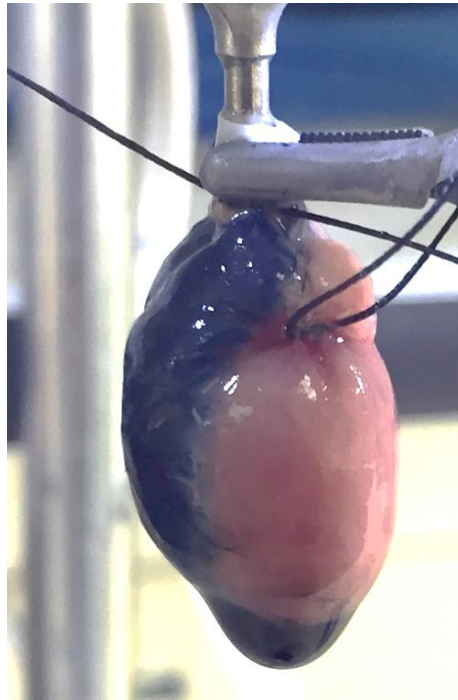


Figure 2.5 Perfusing the heart with Evan's blue dye through the aortic root to demarcate the non-ischaemic area after permanently occluding the left coronary artery. At this stage, the ischaemic area is delineated and highlighted in red colour.

The frozen heart was placed on a glass surface and left for 2-3 minutes to thaw slightly before being transversely sliced at 2 mm thickness into 5-6 sections from apex to base using metal scalpel. Sections were blotted on absorbent surface and left to fully thaw at room temperature before incubating them with the TTC solution. This step is important for two reasons: (1) to avoid any “smearing/leaching” from Evans’ blue dye from its territories which might affect the delineation of the non-ischaemic area (2) incubating the sections in 1% TTC solution at 37 °C whilst they are cool will lead to tissue contraction which affects the geometry of the sections.

TTC is used in biochemical analysis as a redox indicator to differentiate between metabolically active and inactive cells. TTC is a colourless dye but is

enzymatically reduced to brick-red 1,3,5, triphenylformazan in viable tissue by dehydrogenases (such as NADH), while necrotic tissue does not retain these enzymes and remains unstained (Birnbaum et al., 1997, Schwarz et al., 2000). Therefore, it is crucial that the reperfusion phase is of adequate duration to wash-out the dehydrogenases from the infarcted area to have proper delineation of the infarcted territories. Sections were then incubated with 1% solution of TTC in PBS (pH=7.4) in a small conical flask at 37 °C for 15 minutes in a water bath. It is important to agitate the sections every minute as the side of the section which faces the flask wall would not be stained. Sections were then fixed in 4% formalin in PBS for 24 hours to improve red/white contrast between the viable tissue and the infarcted area within the risk zone. This step also removes the fatty surface gloss of the section which might affect the contrast when the section is scanned (Bohl et al., 2009).

2.4.1 Infarct size measurements

Fixed sections were placed in order from the apex to the base over the glass of the digital scanner (HP Scanjet 4370, USA) with another piece of glass over them to keep them flat (Figure 2.6). A ruler was scanned with the sections to allow calibration of the image analysis program and transfer the area from pixel scale to metric scale (cm). Sections were then imaged from both sides and the images were coded using random number generator (<https://www.random.org>). Planimetry was conducted on coded sections (so that I was blind to the treatments to avoid any bias to any of the experimental groups) using the image analysis program Image J (version 1.48, National institute of Health, USA). Infarct size quantification included measuring the total ventricular area of the

heart (TVA, Evans' blue and TTC stained areas), area at risk (AAR, Evans' blue-negative area), and the infarcted area (I, TTC-negative stained area) (Figure 2.8). Infarct size was reported as a percentage of the area at risk (I/AAR %).

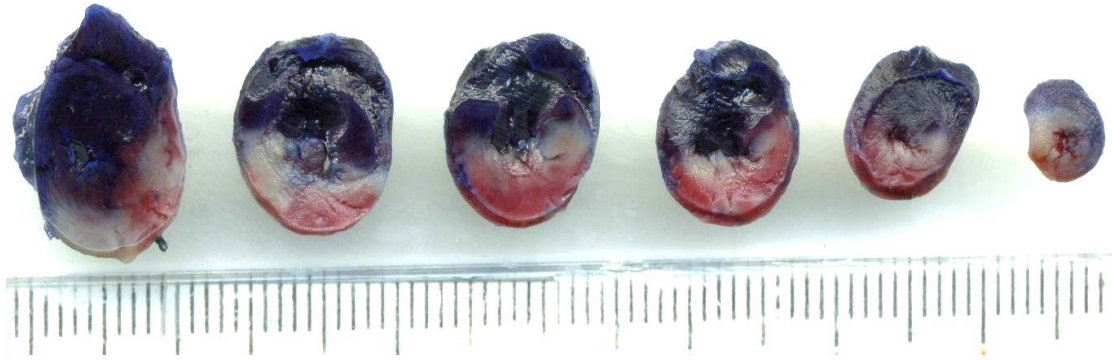


Figure 2.6 Scanned image for the heart slices after being stained with triphenyltetrazolium chloride (TTC) and fixed for 24 hours in formalin. Non ischaemic tissue appears as blue area while the ischaemic bed is delineated by the brick-red colour. Infarcted tissue is indicated by the white colour. Area at risk (risk zone) includes the red and white areas. Sections were traced using an image analysis program (Image J) to calculate the total ventricular volume (i.e. left and right ventricles area), area at risk, and the infarcted area. These values were then converted into volumes by multiplying the total of each area by 0.2. Infarct size was reported as a percentage of the area at risk.



Figure 2.7 Representative heart sections which have been excluded at the level of planimetry due to poor delineation between non-infarcted and infarcted areas within the AAR.

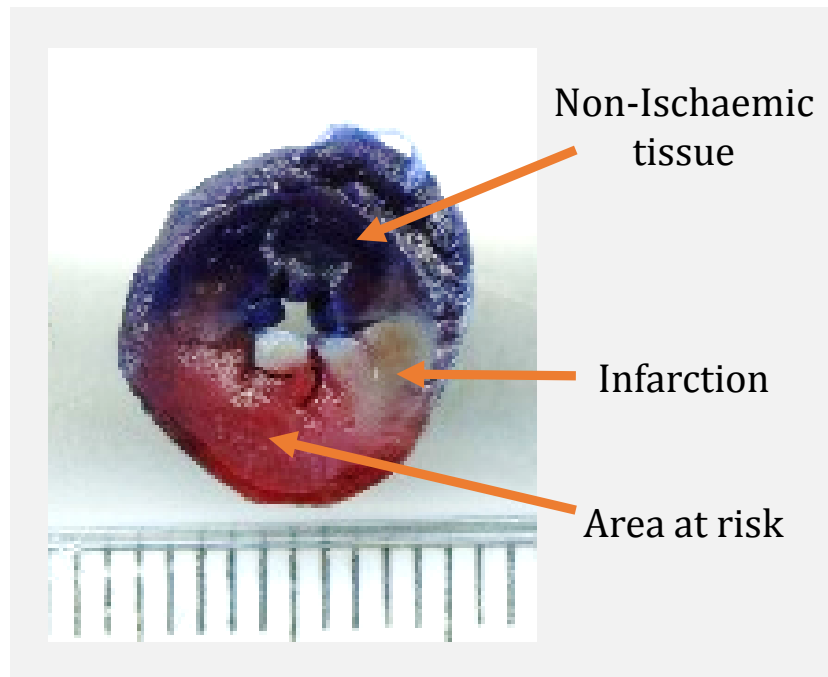


Figure 2.8 Representative dual staining technique with Evans' blue and TTC. Both sides of each heart section were scanned using digital scanner then the planimetry was performed using ImageJ software. Total ventricular area (ischaemic and non-ischaemic area), area at risk (Evans' blue negative area) and the infarction (TTC negative area) were quantified in cm after calibrating the software with the known scale roller scanned with each image. Area at risk was reported as a percentage of the total ventricular volume and the infarct size was expressed as a percentage of the area at risk.

2.5 Inclusion/exclusion criteria

In order to ensure that data were reproducible and to avoid any kind of bias between the experimental groups, strict criteria of inclusion/exclusion were followed. For each animal to be included and employed to the ischaemia/reperfusion protocol it had to achieve the haemodynamic parameters which were mentioned in section (2.3.4) during the stabilisation period.

During ischaemia, the animal was excluded if there was no evidence of developed ischaemia after tightening the ligature, such as ST-segment elevation, change in the colour of the left ventricle. This could be either because the snare was not tight enough to restrict the blood supply through the left

coronary artery or the ligature was not placed around the coronary artery. Moreover, the animal was excluded if ventricular fibrillation persisted for more than 2 minutes during ischaemia despite attempts to defibrillate it by gentle flicking of the heart. Exclusions also occurred where there was no evidence of reperfusion, such as reperfusion arrhythmia after releasing the snare, no change in the colour of the left ventricle. The animal was excluded if it died any time before the end of 120 minutes reperfusion.

The heart was also excluded during analysis when either the area at risk was < 30% of total ventricular area (AAR/TVA %); or when there was failure of staining due to either leaching of Evan's blue dye to the area at risk or poor red/white contrast between the viable and infarcted tissues within the area at risk (Figure 2.7).

2.6 Protein level determination

2.6.1 Myocardial tissue sampling

The effects of different hydrogen sulfide (H₂S) donors and a number of other pharmacological interventions on the phosphorylation of the RISK pathway kinases in the ischaemic tissue was evaluated as will be discussed in more detail in Chapters 5 and 6. Generally, all the treatments were given either during ischaemia or before reperfusion and the heart was reperfused for 5 minutes. The heart was quickly excised, washed with saline to remove blood residues and placed on glass surface where the base, including both atria, was removed (Figure 2.9). The right ventricle was isolated then the left ventricle was cut into two halves and each half was cut further divided in two as it is explained in Figure

2.7. Sections 1 and 3 were then collected together in 2 mL Eppendorf tube in order to reduce the possible variability in the infarcted area between the sections. Sections 2 and 4 were treated similarly. It is worth mentioning that these extra cuts, to some extent, could probably subject the tissue to some extra stress, however, it was almost equal across all experimental groups. Biopsies were then snap frozen in liquid nitrogen then stored at -80°C until required for Western blotting. The time of tissue preparation was 40-60 seconds.

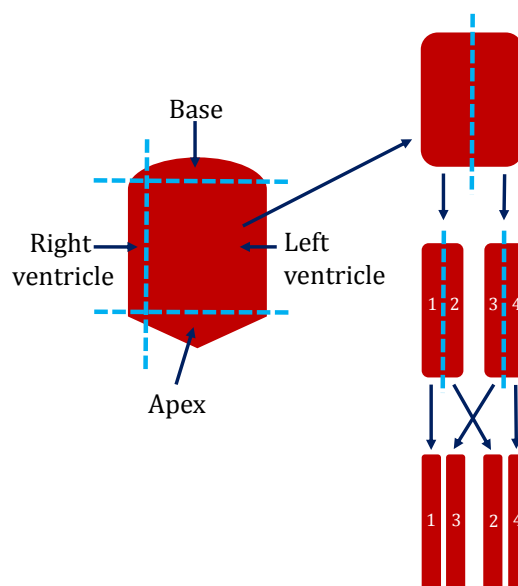


Figure 2.9 Schematic illustrating the heart sectioning for western blotting. The heart was excised after 5 minutes of reperfusion and washed with phosphate buffer saline to remove any remaining blood in the heart chambers. The base was separated and discarded, while the apex and the right ventricle were isolated and each of them was cut into 3-4 pieces and snap frozen. The left ventricle was cut in half and each half was cut in half again. The produced sections 1 and 3 were collected together, cut into 3-4 pieces and snap frozen until required for analysis. Sections 2 and 4 were treated similarly to 1 and 3.

2.6.2 Tissue homogenisation

Tissue homogenisation was carried out at ice-cold temperature to maintain the integrity and stability of the kinases. Frozen myocardial biopsies (40-60 mg) were placed in 2 mL Precellys tube (Bertin, UK) with 200 μ L lysis buffer, 20 μ L phosphate inhibitor cocktail and 10 μ L protease inhibitor cocktail. Samples were homogenised with 3 cycles of 20 seconds homogenisation period at (5500 rpm) using a Precellys 24 (Bertin, UK). Homogenate was recovered and centrifuged at 14000 rpm for 15 minutes at 4 $^{\circ}$ C. The supernatant was then collected in 2 mL Eppendorf tube and kept on ice. To prepare samples for Western blotting, the tissue homogenate (supernatant) was mixed with Laemmli buffer (2X-concentrated) in 1:1 ratio and heated in a dry bath at 90 $^{\circ}$ C for 10 minutes then stored at -20 $^{\circ}$ C until required.

2.6.3 Protein determination of myocardial samples

Bicinchoninic acid (BCA) assay was used to determine the total concentration of proteins in the myocardial samples. This assay is based on the interaction between the peptide bonds with the alkaline copper media (Cu^{2+}) medium. The product of this interaction is Cu^+ ion which is chelated by two molecules of bicinchoninic acid, forming a purple complex (Smith et al., 1985). The amount of this complex is directly proportional to the protein concentration in the sample and can be measured using colorimetric techniques at 560 nm. Serial dilutions of bovine serum albumin were prepared (0, 0.125, 0.25, 0.5, 1, 2, 4, 8 mg mL^{-1}) in lysis buffer and used to construct the standard curve. Standards and samples (10 μ L) were loaded in duplicate onto a 96-well plate. Reagents A and B of PierceTM BCA protein assay kit were mixed in 50:1 ratio, according to

manufacturer's instructions, and (200 μ L) of the mixture was added to each well. The plate was incubated for 30 minutes at 37 °C then the absorbance was measured at 560 nm using an ELISA reader (LT-5000MS, LabTech, UK).

2.7 Western Blotting

2.7.1 Protein Separation

Protein samples were routinely separated using 10% w/v sodium dodecyl sulfate-polyacrylamide gel (SDS-PAGE) using Mini-PROTEAN® Tetra Handcast system (Bio-Rad, UK). Handcasting was carried out by pouring the separating gel between two glass plates, which are fixed in a cassettes stand. A thin layer methanol was overlaid on the top of the gel to ensure that the top of the separating layer is flat and left to set for 20-30 minutes. Methanol was then decanted once the gel set and washed with distilled water. The stacking gel was then freshly prepared and added on the top of the separating gel before a well comb quickly inserted into it to create the protein loading lanes. The stacking gel was left to set for 15-20 minutes then the comb was gently removed. The created loading lanes were washed with tank buffer then the cassettes were placed in the electrode assembly which was then placed in the buffer tank. Protein samples were heated at 70 °C for 5 minutes before equal amounts (30 μ g) from each sample were loaded in each well. A protein ladder (Precision Plus Protein™ All Blue Standards, Bio-Rad, UK) was added to each gel to enable protein bands sizing. Electrophoresis of protein samples was carried out at 50 mV for 15 minutes then at 120 mV for 2.5 hours in an ice bath.

2.7.2 Proteins blotting

Once the proteins were separated, the cassettes were opened and the gels were removed and placed in transfer buffer. Nitrocellulose membrane (Amersham, Germany), two precut thick blot filter papers (Bio-Rad, UK) and two cotton pads were used to build each transfer sandwich. They were immersed in transfer buffer for 10 minutes before building the transfer sandwich to transfer the separated proteins. The separated proteins were transfer onto nitrocellulose membrane using a wet electrophoresis system (Mini Trans-Blot® Cell, Bio-Rad, UK). The transfer sandwich was built by placing a cotton pad on the cathode side of the gel holder cassette (Bio-Rad, UK) then a wet filter paper upon it. The nitrocellulose membrane was then place on the top followed the gel. Another filter paper was added upon the gel and any trapped air between the layers was removed by gently rolling a plastic rod on the top of the filter paper. Finally, the other cotton pad was placed on the top and the cassette was place the transferring Assembly. The assembly was placed in the transfer tank and the tank was filled with the transfer buffer. Proteins were transferred at 400 mA for 90 minutes in an ice bath.

2.7.3 Immunodetection

The membrane was incubated with 5% skimmed milk on a gyratory rocker (Stuart Scientific, UK) for 2 hours. The rationale of this step is to block any nonspecific binding of the antibodies to the membrane surface. This will subsequently reduce the background signal that might appear when the protein bands are visualised on an X-ray film. In some cases, the membrane was cut horizontally with 20 kDa margin based on the molecular weight for the protein of

interest. This approach was used to allow the detection of different proteins with different molecular weights at the same. Nevertheless, the main disadvantage of cutting the immunoblot is that it prevents the detection of any other protein modifications which could be detectable by the primary antibody but appear outside the limited range of screened molecular weight. The transferred proteins were probed with a specific primary antibody, which is diluted with 1% TBST and 1 % skimmed milk to a final volume of 1 mL, against each protein of interest overnight at 4 °C on a roller mixer (Stuart Scientific, UK). The probed membrane was then washed 3 X 15 minutes with 1% TBST on a gyratory rocker to remove the unbound residues of primary antibody. Probed proteins were detected indirectly by probing the primary antibody with an enzyme-labelled secondary antibody. To do so, the immunoblot was transferred to a 50 mL Falcon tube and incubated with the secondary antibody. Secondary antibody was diluted with 1% TBST and 1% skimmed milk to a final volume of 15 mL. The probed membrane was incubated with the secondary antibody on a roller mixer for 1 hour at room temperature. The immunoblot was then washed three times with 1% TBST for 15 minutes on a gyratory rocker to remove the excess and unbound secondary antibody.

Protein bands were visualised using Enhanced Chemiluminescence (ECL) detection technique. The probed membrane was placed on a polyethylene film in the developing cassette with the probed side of the membrane up. Solutions A and B of the chemiluminescent substrate kit (Super Signal West Dura Extended Duration Substrate, Pierce Biotechnology, UK) were mixed in 1:1 ratio, added to the probed side of the immunoblot and incubated for 5 minutes at room temperature. Chemiluminescent substrate produces photons as a by-product

when it is oxidised by the peroxidase. Protein bands were visualised on ECL Hyperfilm (GE Healthcare, Buckinghamshire, UK) placed against the immunoblot in a dark room for different exposure time to optimise the clarity of the developed film. The film was then developed using X-ray developer and fixer (Photo Imaging Systems, UK). The intensity of each band is directly correlated to the abundance of the protein on the immunoblot and ultimately, to its level in the harvested tissue.

The developed film was scanned using a digital scanner (HP scanjet 4370, USA) and the images were coded using random number generator (<https://www.random.org>). Densitometry was conducted in a blinded fashion using Image J software. Phosphorylated and total protein bands were normalised to corresponding GAPDH bands as an internal control to minimise the intra-assay variability which might occur due to the protein loading variation in the same immunoblot. Nevertheless, it needs to be acknowledge that there might be some inevitable changes in GAPDH level as a metabolic enzyme due to ischaemia/reperfusion injury and that requires further investigation. Protein bands were then normalised to a “baseline sample”, which was a myocardial sample harvested from the left ventricle after 20 minutes of stabilisation and before the regional myocardial ischaemia, loaded at either side of each gel. The rational of normalising the protein bands to the baseline sample was to minimise the possible inter-assay variations which could occur due to difference in the exposure time for each developed x-ray film.

2.8 Statistical analysis

Sample size for infarct size and mitochondrial studies was determined using R package for statistical analysis (R 3.3.3 version, www.stats.bris.ac.uk). Data were analysed using GraphPad software (Prism® 2007, Version 5.01). All numerical data were reported as arithmetic mean values \pm standard error of the mean (SEM) and passed the Kolmogorov-Smirnov normality test of distribution except when the sample size was small ($n=4$). For small sample size ($n=4$), non-parametric test (Kruskal-Wallis) was used as these data were not normally distributed. Unless otherwise indicated, two-tailed student's t-test was used to statistically compare between two experimental groups while one-way ANOVA followed by Newman Keuls *post hoc* test was employed for multiple comparison. Cardiodynamics, including mean arterial pressure (MAP) and rate pressure product (RPP), and mitochondrial data were analysed using repeated measures ANOVA followed by Bonferroni *post hoc* test. Differences between groups were considered significant if the p-value was <0.05 . Post hoc tests were only carried out if p value <0.05 was achieved in the ANOVA.

Chapter 3 Experimental Model: Development and Validation

3.1 Introduction

The *in vivo* model of myocardial ischaemia and reperfusion in the anaesthetized rat has been employed in this work. The rat has been used as a model of choice for cardiac ischaemia and reperfusion studies for more than four decades due to its relatively low cost compared to other species such as rabbits and dogs. Rat heart also has a negligible collateral circulation, which are minor blood vessels that can bypass the coronary vessel occlusion and provide adequate blood supply to the ischaemic area (Ytrehus, 2000, Ytrehus, 2006). In addition, it affords a high degree of standardization and repeated validation of the model in multiple laboratories confirms the homogeneity of response (Ytrehus, 2000, Ytrehus, 2006). Furthermore, it offers the possibility of measuring the cardiodynamics (for example: blood pressure, heart rate), cardiac electrophysiology and arrhythmias and assessment of therapeutic interventions (Hearse and Sutherland, 2000). The rat heart, however, has a major limitation which is its exceptionally short action potential duration that may influence electrophysiological assessments (Hearse and Sutherland, 2000).

Myocardial ischaemia could be simulated in this model by occlusion of the LAD coronary artery to establish regional ischaemia in the left ventricle. Regional ischaemia is associated with ventricular tachycardia and ventricular fibrillation. The severity of ischaemia-induced arrhythmias varies depending on the position of the ligature and the duration of ischaemia (Clark et al., 1980, Curtis et al., 1987). This model also offers the possibility to simulate early reperfusion treatment as restoration of the blood supply to the ischaemic myocardium can be achieved by releasing the ligature around the coronary artery. Reperfusion is also associated with ventricular arrhythmias which can vary depending on the duration of preceding ischaemia and how successfully reperfusion was achieved.

The early phase of this work aimed to develop the model of myocardial ischaemia/reperfusion injury in anaesthetised rat for the first time in the Cardiff laboratory. Initially, preliminary studies were carried out to validate my surgical skills and to build confidence in having consistent area at risk and infarct size. Different periods of regional ischaemia were employed (20-40 minutes) aiming to induce reproducible area at risk (~ 50% of the total ventricular volume) and survivable infarct size (~ 50% of the area at risk).

3.1.1 Aims

The main aims of this study were to:

- 1- Develop a model of ischaemia/reperfusion injury in anaesthetised rat with stable haemodynamics and reproducible myocardial infarction.
- 2- Investigate the feasibility to produce and detect potential infarct limitation using ischaemic preconditioning as a positive infarct-limiting approach, to validate the model.

3.2 Materials and Methods

3.2.1 Model development: preliminary study

The preliminary study aimed to develop the *in vivo* model of myocardial ischaemia/reperfusion injury in anaesthetised rat for the first time in Cardiff University. This series of experiments was used to validate the skills of the experimentalist in executing the surgical procedures and to ensure the reproducibility of data due to the complexity of this model.

3.2.1.1 Experimental protocol

In the preliminary series, rats underwent 30 minutes regional ischaemia and 120 minutes of reperfusion after stabilisation period for 20 minutes (Figure 3.1).

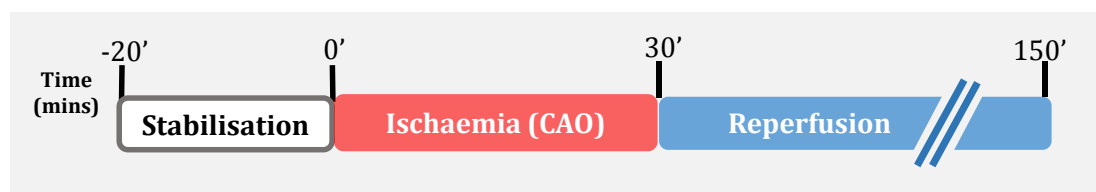


Figure 3.1 Experimental protocol for the preliminary study. After the surgical procedure, animals were stabilised for 20 minutes then subjected to 30 minutes coronary artery occlusion followed by 2 hours of reperfusion.

3.2.2 Model validation: using ischaemic preconditioning

An ischaemic preconditioning (IPC) manoeuvre was used, as a positive control, to validate the model of myocardial ischaemia/reperfusion injury in anaesthetized rat. IPC refers to brief episodes of ischaemia and reperfusion which render the myocardium more tolerant to acute myocardial infarction (see Chapter 1, section 1.4.1). This

manoeuvre is considered a gold standard cardioprotective intervention in the field of cardioprotection and has reproducibly protected the myocardium against ischaemia/reperfusion injury in all animal models and human studied hitherto (Murry et al., 1986, Schott et al., 1990, Liu et al., 1991, Yellon et al., 1993, Sumeraay and Yellon, 1998).

3.2.2.1 Experimental protocol

During the stabilisation period and after meeting the inclusion criteria, animals were randomly assigned to one of the following groups (Figure 3.2):

Group 1: Control (n=15). Animals received no intervention and were subjected to 30 minutes of regional myocardial ischaemia followed by 120 minutes reperfusion.

Group 2: IPC (n=10). Animals underwent 2 cycles of 3 minutes regional myocardial ischaemia/ 3 minutes reperfusion before the index regional myocardial ischaemia.

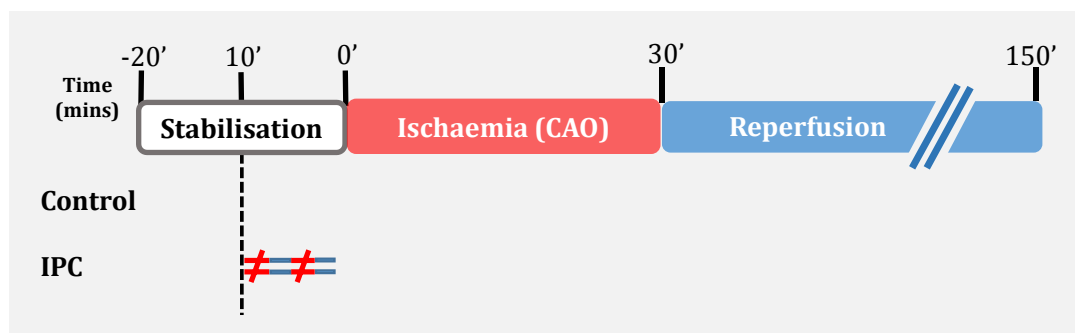


Figure 3.2 Experimental protocol for the model validation study with ischaemic preconditioning (IPC). During stabilisation period, animals were received either no further intervention or 2 episodes of 3 minutes regional myocardial ischaemia followed by 3 minutes reperfusion. Animals in both groups were underwent 30 minutes regional myocardial ischaemia and 120 minutes reperfusion.

3.3 Results

3.3.1 Preliminary study

3.3.1.1 Inclusion/exclusion criteria

In the preliminary experiments, a total of 44 rats underwent the ischaemia/reperfusion protocol. Twenty animals were excluded; 11 rats died before completion of the ischaemia/reperfusion protocol (8 animals due to VF during ischaemia and 3 animals because of ventilation failure); 2 animals due to problems with the ligature that led either to unsuccessful occlusion of the coronary artery or unsuccessful reperfusion; 7 experiments were excluded during analysis due to poor delineation between the area at risk and the infarcted tissue. Therefore, data for 24 successfully completed experiments are reported in this study.

3.3.1.2 The effect of coronary artery occlusion on cardiodynamics

Baseline parameters and haemodynamics throughout the ischaemia and reperfusion protocol are presented in Table 3.1. RPP and MAP were reported at the baseline before occluding the coronary artery, at 20 minutes of ischaemia as it is the time of intervention and at the end of the reperfusion. Successful occlusion of the left coronary artery caused a gradual decrease in the mean arterial pressure (MAP) and rate pressure product (RPP) which continued until the end of ischaemia (Figure 3.3). The induced ischaemia caused an increase in the R wave amplitude (Figure 3.4A) and ST segment elevation (Figure 3.4B) with a particular pattern of arrhythmias. The onset of arrhythmias typically occurred 4 minutes after coronary occlusion and lasted until around 15 minutes of ischaemia. The types of arrhythmias were: ventricular premature

beats (VPBs, discrete premature, in relation to P-wave, QRS complexes, Figure 3.5), ventricular tachycardia (VT, run of four or more consecutive VPBs, Figure 3.6), and ventricular fibrillation (VF, signal from which individual QRS deflections cannot longer be distinguished, Figure 3.7). Mean arterial pressure [MAP, diastolic blood pressure + $\frac{1}{3}$ (systolic blood pressure/diastolic blood pressure)] and rate pressure product [RPP, heart rate X systolic blood pressure] initially recovered gradually during the early phase of reperfusion before declining toward the end of reperfusion.

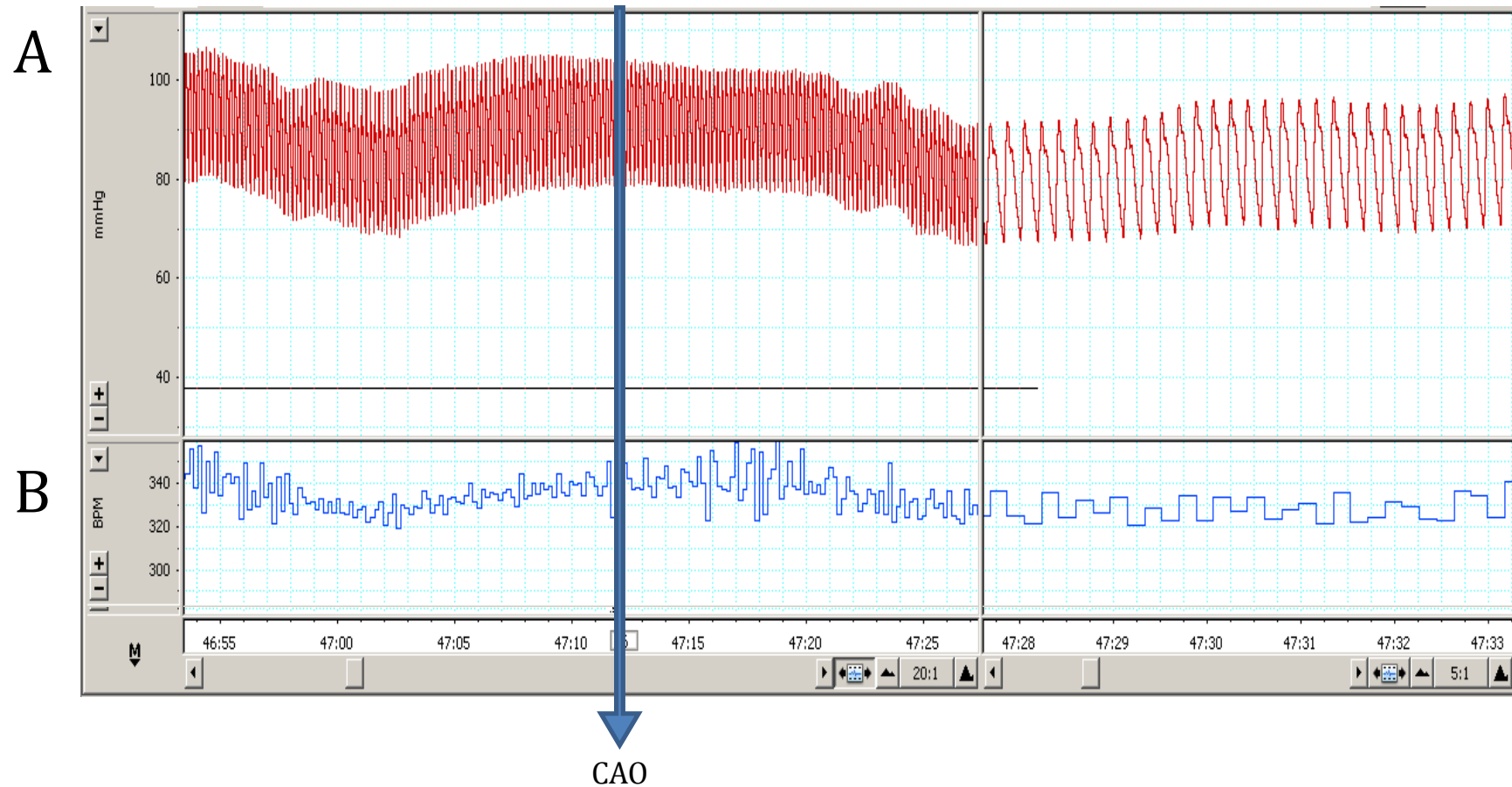


Figure 3.3 Example of the cardiodynamics changes following the coronary artery occlusion (CAO). The x-axis represent the time (second).

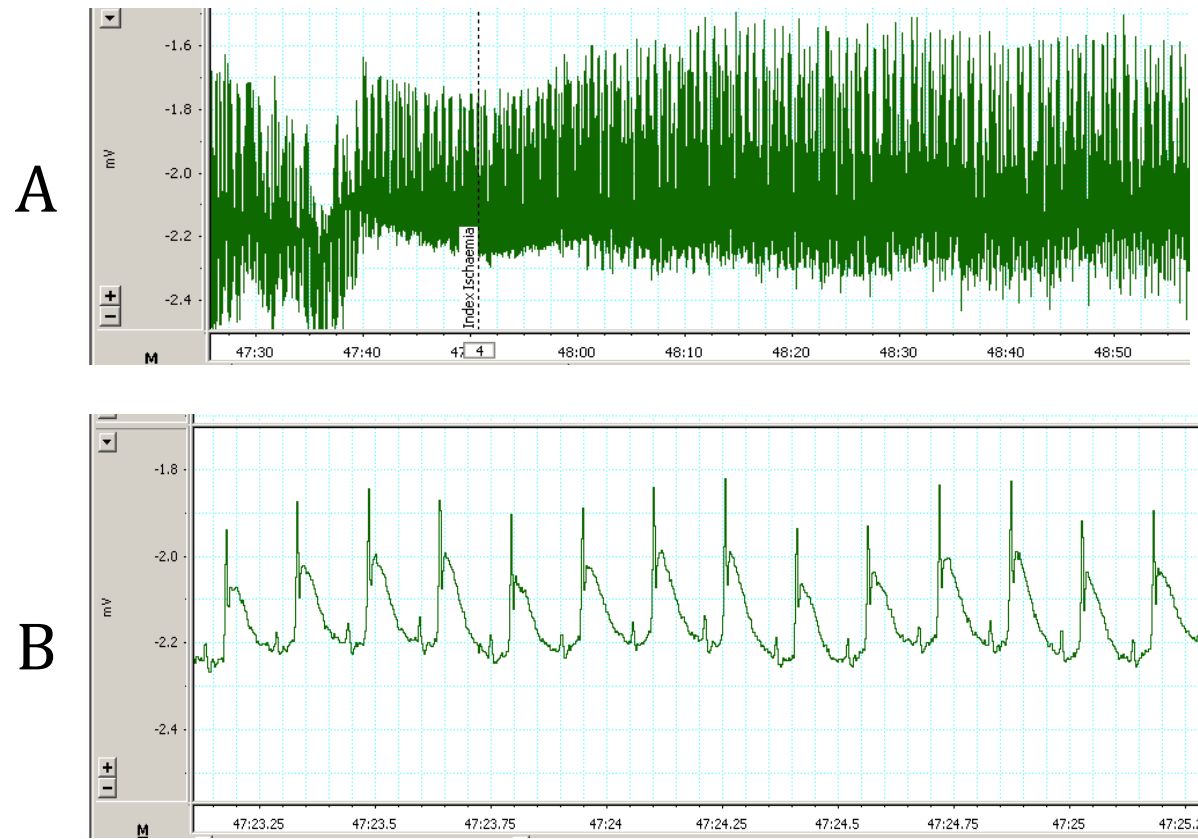


Figure 3.4 Examples of (A) the increase in R wave amplitude following coronary artery occlusion and (B) the ST-segment elevation.

Ventricular Premature Beat (VPB)

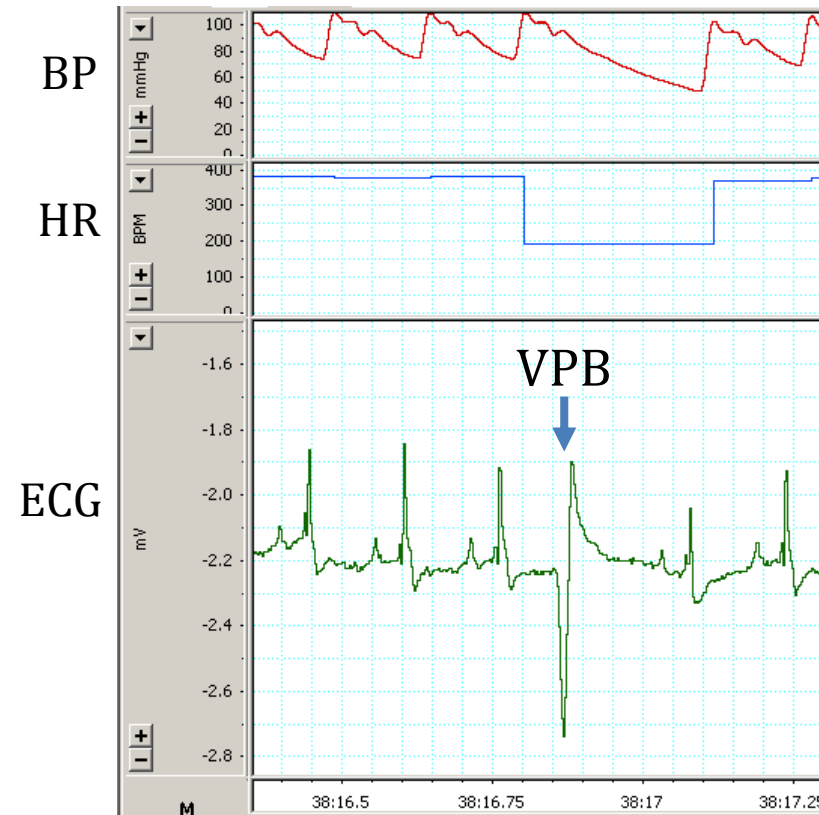


Figure 3.5 Representative blood pressure (BP), heart rate (HR) and electrocardiography (ECG) traces during a single ventricular premature beat (VPB) that occurs during ischaemia/reperfusion protocol. The arrow indicates the time of the single VPB and the x-axis represent the time (0.5 second).

Ventricular Tachycardia (VT)

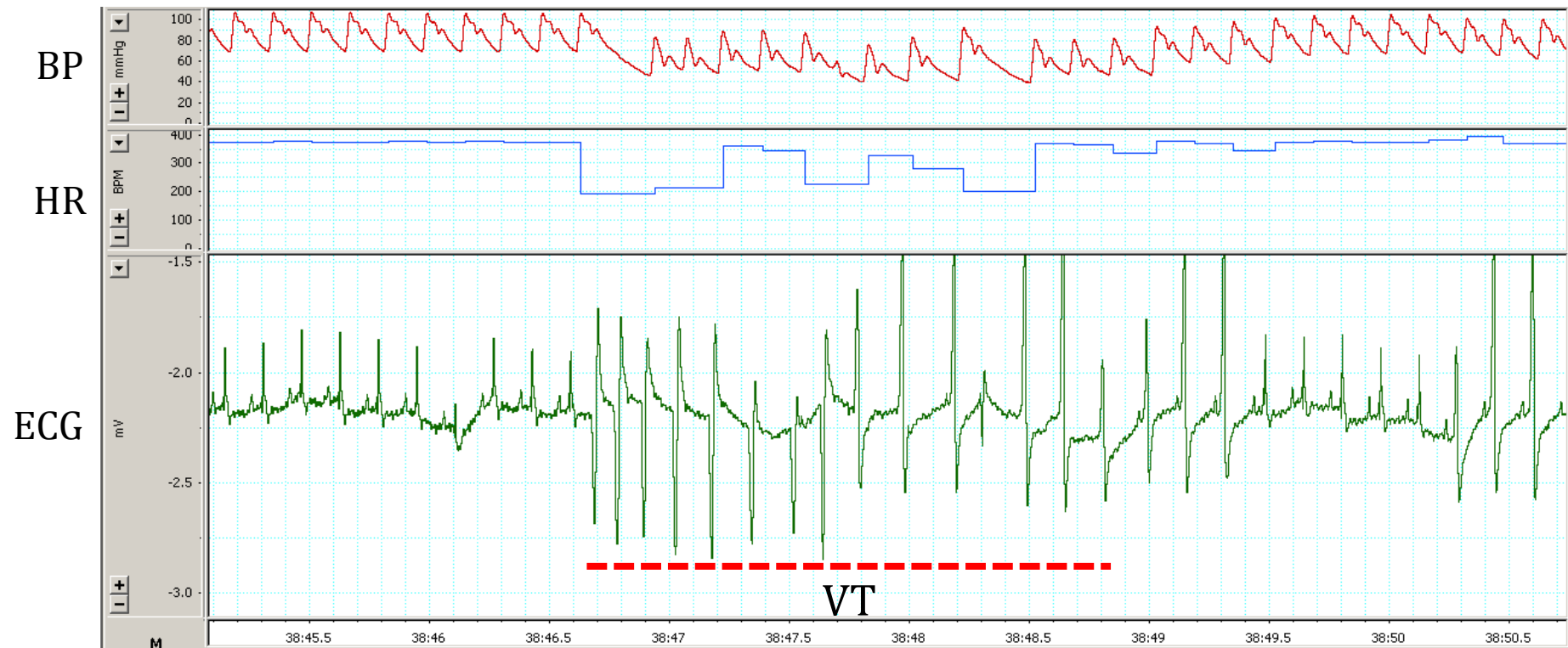


Figure 3.6 Representative blood pressure (BP), heart rate (HR) and electrocardiography (ECG) traces during ventricular tachycardia (VT) that occurs during ischaemia/reperfusion protocol. The episode of VT is underlined by the dotted red line. The decrease in the heart rate during the episode of VT is an artefact as a result of measuring the heart rate based on the ECG trace by Labchart® software and it does not mean that there was a real drop in the heart rate during this period. The x-axis represent the time (0.5 second).

Ventricular Fibrillation (VF)

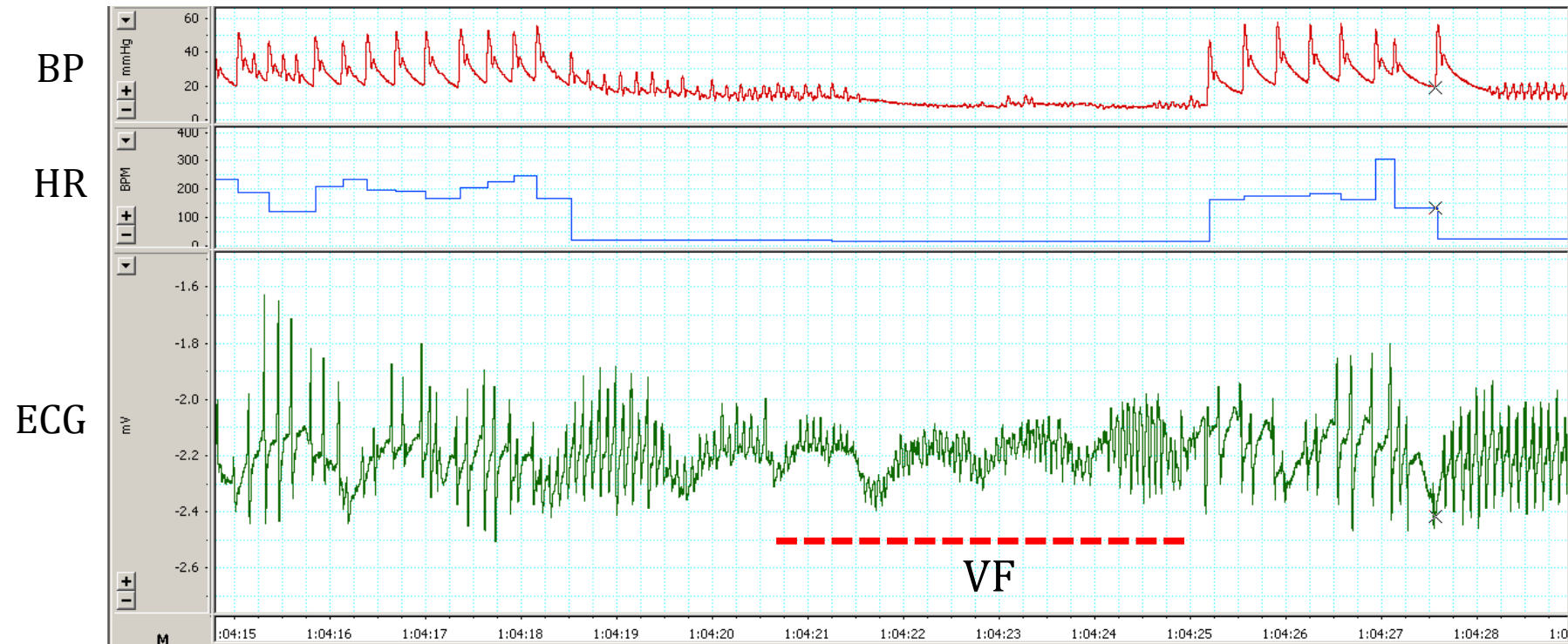


Figure 3.7 Representative blood pressure (BP), heart rate (HR) and electrocardiography (ECG) records during ventricular fibrillation (VF) that occurs during ischaemia/reperfusion protocol. The episode of VF is underlined by the dotted red line. This record also shows how VF can spontaneously reverses to normal rhythm which is a common feature of this model in rat. The drop in the heart rate during ventricular fibrillation is an artefact as the Labchart® software was measuring the heart rate based on the ECG trace and it does not mean that the heart rate was almost zero during this period. The x-axis represent the time (second).

Table 3.1 Baselines and haemodynamic measurements throughout ischaemia/reperfusion protocol for the preliminary series of experiments

Experimental Protocol	n	BW (g)	Baseline		20 min Ischaemia		120 min Reperfusion	
			RPP (mmHg min ⁻¹)*10 ³	MAP (mmHg)	RPP (mmHg min ⁻¹)*10 ³	MAP (mmHg)	RPP (mmHg min ⁻¹)*10 ³	MAP (mmHg)
Control	24	339 ± 11	42.3 ± 1.8	97 ± 4	28.9 ± 1.2	66 ± 3	18.0 ± 1.5	61 ± 5

n number of animals per group; *BW* body weight; *RPP* rate pressure product; *MAP* mean arterial pressure. Data are reported as mean ± SEM.

3.3.1.3 Infarct data

In the preliminary study, the area at risk (AAR/T %) for the 24 reported experiments was 60.6 ± 2.8 % of the total ventricular volume. Infarct size (I/AAR %) was 50.7 ± 2.6 %, expressed as a percentage of area at risk.

3.3.2 Model validation study with IPC

3.3.2.1 Inclusion/exclusion criteria

In IPC experiments, a total of 40 animals were used. Fifteen rats were excluded; 5 died before the completion of ischaemia/reperfusion protocol (4 animals due to ischaemia-induced VF and one animal due to respiratory failure); 5 were excluded due to problems with the ligature that caused either unsuccessful occlusion of the left coronary artery or unsuccessful reperfusion; 5 were excluded during analysis due to poor staining. Therefore, data from 25 successful experiments are reported.

3.3.2.2 The effect of IPC on cardiodynamics

The baselines and changes in haemodynamic parameters of the model validation study with IPC are presented in Table 3.2. Statistical analysis showed no significant difference between groups for any of the baseline parameters. The two cycles of short ischaemia/reperfusion significantly caused a reduction in the pre-ischaemic MAP (67 ± 4 versus 93 ± 5 , $p < 0.05$) and RPP (32.1 ± 1.0 versus 40.1 ± 1.0 , $p < 0.01$). There was no significant difference in either MAP or RPP during ischaemia and at the end of the reperfusion phase between the experimental groups. The variation in RPP and MAP among the rats in each experimental group is shown in Figures 3.9 and 3.10.

Moreover, IPC manoeuvre limited ischaemia- and reperfusion-induced arrhythmia compared to the control (Figure 3.8).

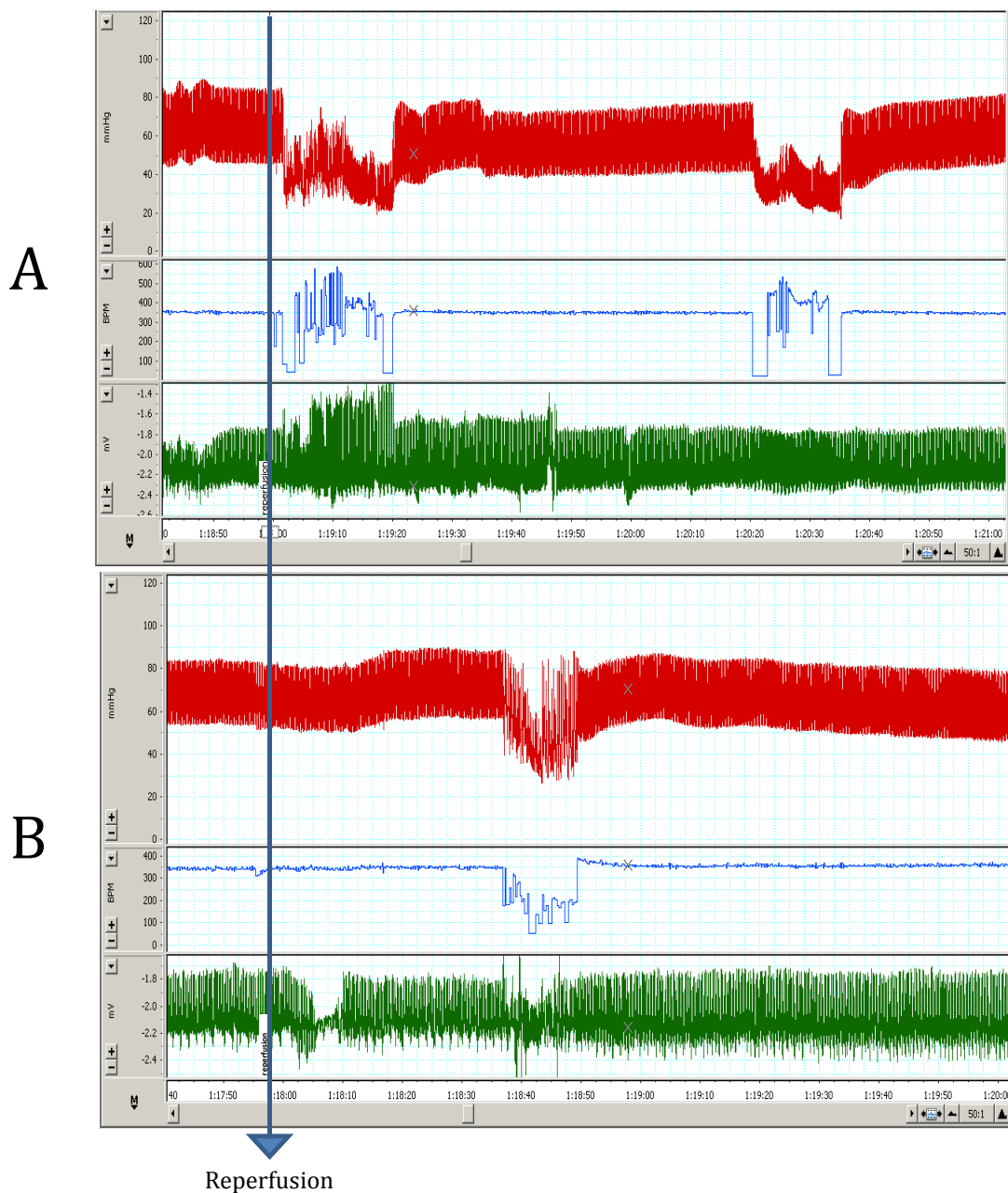


Figure 3.8 Examples of cardiodynamics (blood pressure, heart rate and ECG) for (A) the control and (B) preconditioned hearts at early reperfusion. There is a significant limitation in reperfusion induced arrhythmia in the early phase of reperfusion by IPC. The arrow indicates the time at which the ligature was released to commence the reperfusion phase for two hours. The x-axis represents the time (second).

Table 3.2 Summary of baseline parameters and haemodynamics throughout ischaemia-reperfusion injury protocol for Ischaemic preconditioning study

Experimental Protocol	n	BW (g)	Baseline				20 min Ischaemia		120 min Reperfusion	
			SBP mmHg	HR BPM	RPP (mmHg min ⁻¹)*10 ³	MAP (mmHg)	RPP (mmHg min ⁻¹)*10 ³	MAP (mmHg)	RPP (mmHg min ⁻¹)*10 ³	MAP (mmHg)
Control	15	403 ± 18	126 ± 13	318 ± 17	40.1 ± 1.0	93 ± 5	27.6 ± 1.3	63 ± 6	24.0 ± 0.9	48 ± 5
IPC	10	453 ± 31	100 ± 15	321 ± 14	32.1 ± 1.0 *	67 ± 4**	25.3 ± 1.4	53 ± 7	25.5 ± 1.0	45 ± 4

n number of animals per group; *BW* body weight; *RPP* rate pressure product; *MAP* mean arterial pressure; *IPC* ischaemic preconditioning.

Data are reported as mean ± SEM. (Two way ANOVA with Bonferroni *post hoc* test), **p* < 0.05, ***p* < 0.01 vs the control group.

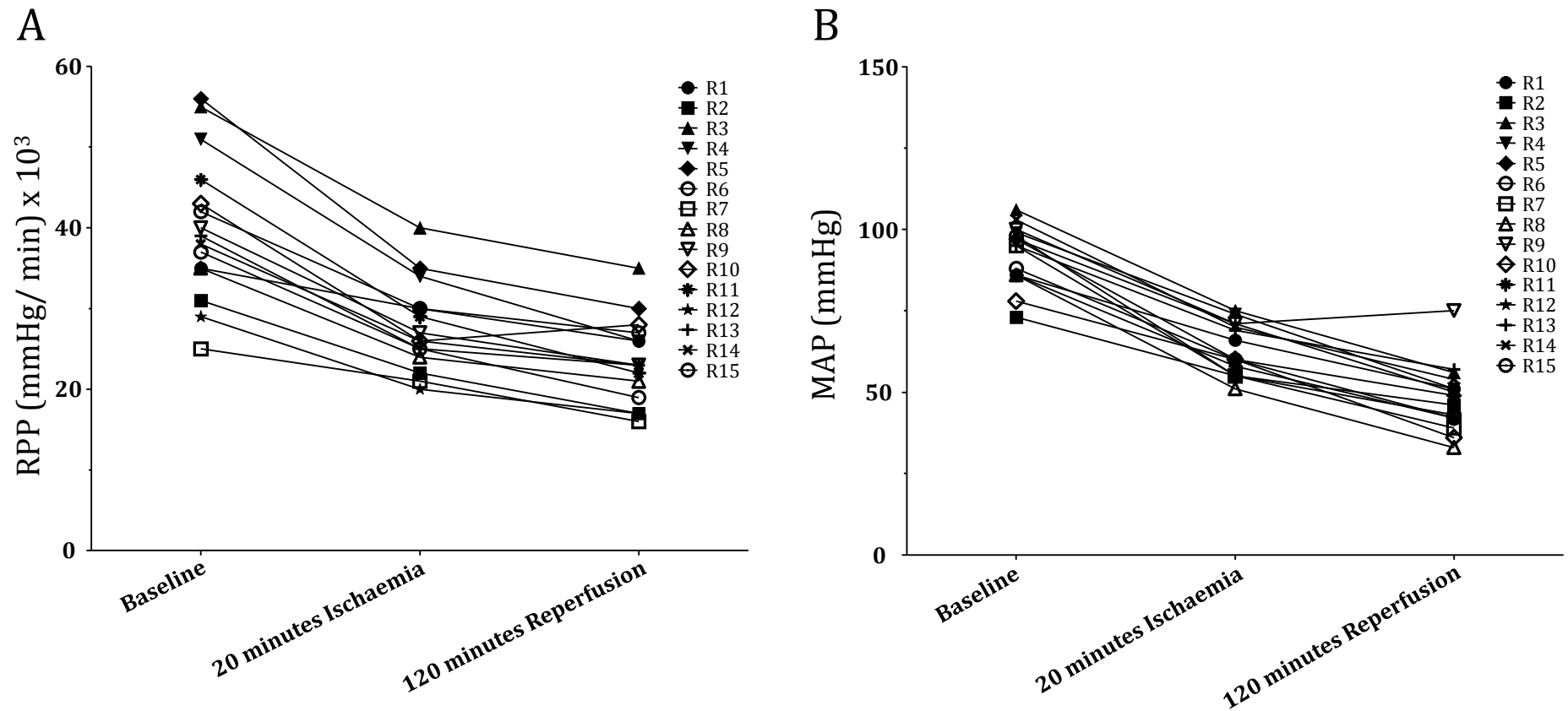


Figure 3.9 Comparison of (A) rate pressure product (RPP) and (B) mean arterial pressure (MAP) among the control group. The figure shows the possible variability in haemodynamics in the same experimental group when longitudinally paired. RPP and MAP were reported at the baseline, 20 minutes of ischaemia and at the end of reperfusion.

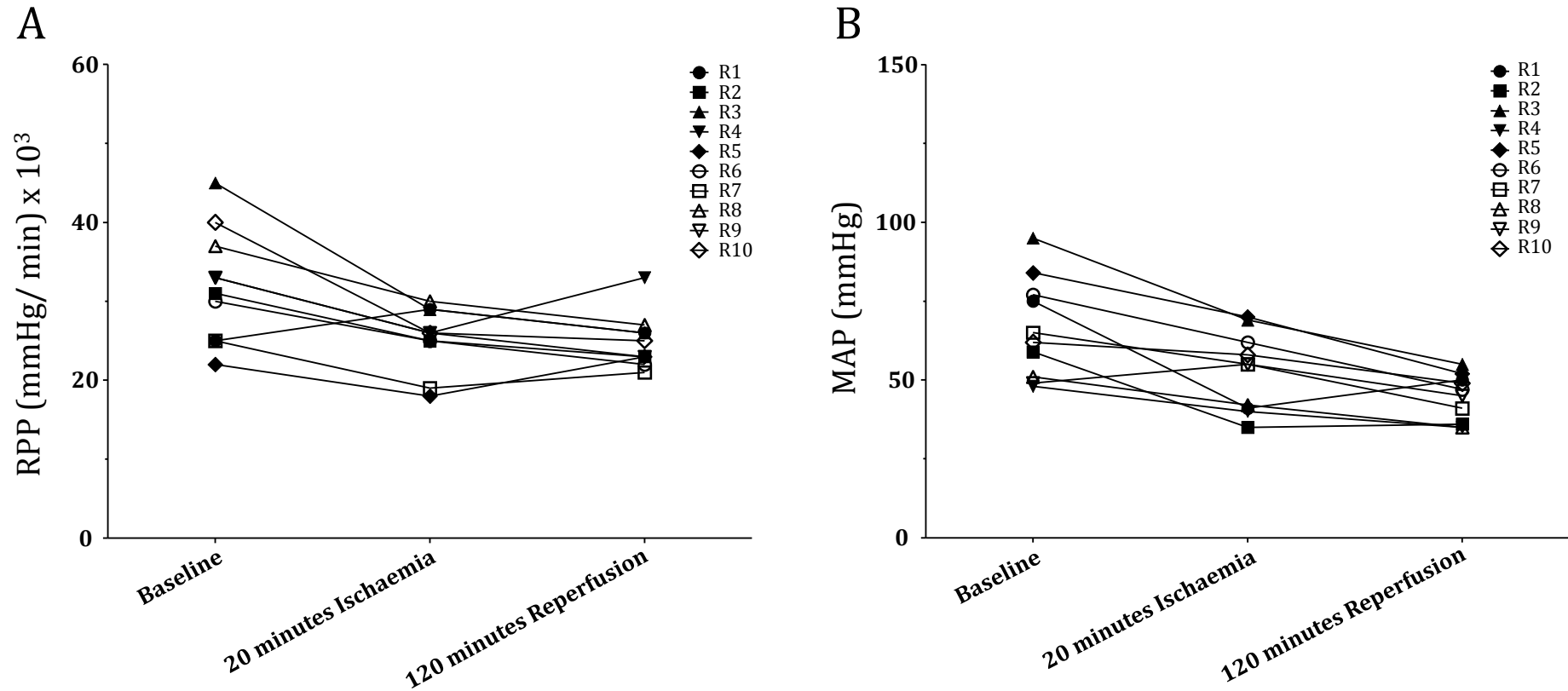


Figure 3.10 Comparison of (A) rate pressure product and (B) mean arterial pressure among ischaemic preconditioned rats. The figure illustrates the possible variability in cardiodynamics among the rats in the same experimental group when they longitudinally paired. RPP and MAP were reported at the baseline, 20 minutes of ischaemia and at the end of reperfusion.

3.3.2.3 Infarct size data

IPC was used to validate the model's potential for infarct size limitation in response to a gold standard cardioprotective manoeuvre. There was no significant difference in the area at risk between the experimental groups (Figure 3.11C). Two cycles of 3 minutes ischaemia/3 minutes reperfusion applied before the index regional ischaemia (30 minutes) significantly limited the infarct size from $51.4 \pm 6.5\%$ to $16.8 \pm 3.7\%$ of the area at risk ($p < 0.001$, Figure 3.11D). This represents 67% limitation in infarct size.

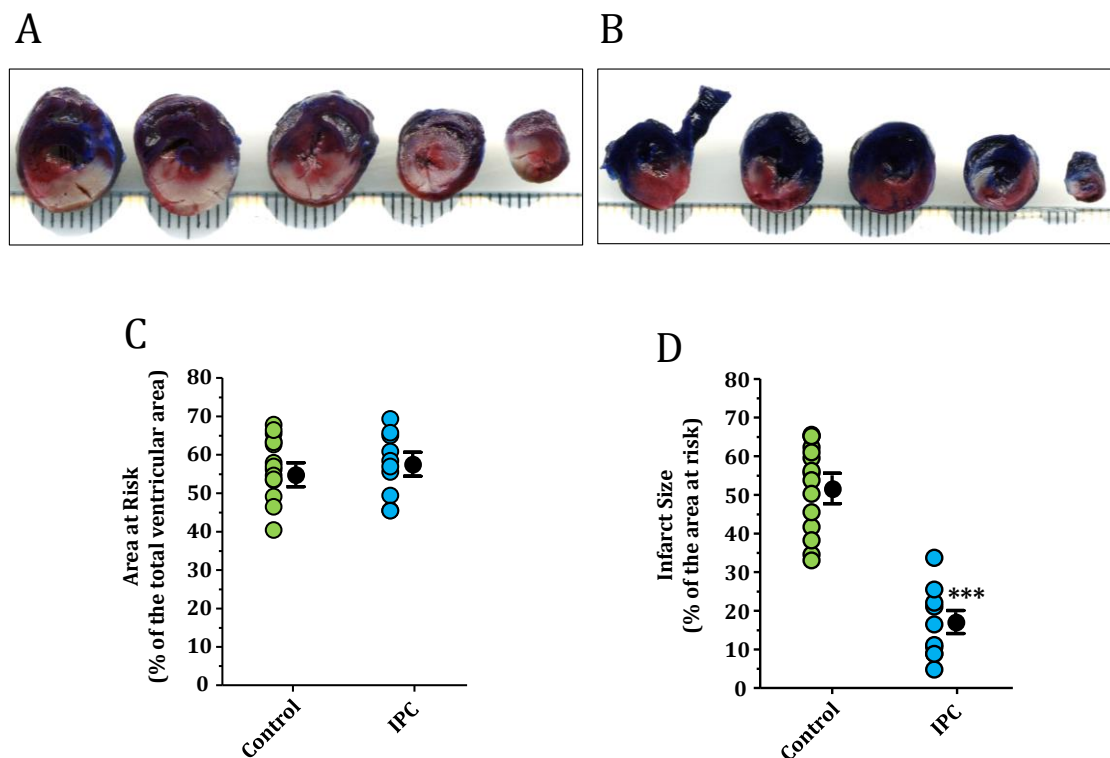


Figure 3.11 Infarct size data for the model validation study with ischaemic preconditioning (IPC). Representative heart sections for (A) Control (n=15) and (B) IPC group (n=10). Ischaemic preconditioning significantly limited the infarct size in the *in vivo* model of ischaemia-reperfusion injury. Heart was stained using Evans' blue/TTC staining. (C) Area at risk is expressed as a percentage of the total myocardium and (D) the infarction is reported as a percentage of the area at risk. Data were analysed using unpaired student *t*-test and expressed as mean \pm SEM, *** $p < 0.001$ vs control. The mean of infarct size for each group is represented by a filled circle (with error bar) next to the individual values (open circles).

3.4 Discussion

Rat has been employed extensively to characterise the pathophysiology of ischaemic heart disease. The rat model of myocardial ischaemia/reperfusion injury was first characterised by Johns and Olson in (1954). It has then become the model of choice (Curtis et al., 1987) to study myocardial infarction and associated arrhythmia during ischaemia and reperfusion. This model has several advantages over other animal models including simple instrumentation required compared to the larger animals (Ytrehus, 2000). In addition, cannulation of the arterial and venous lines enables monitoring of arterial-venous differences throughout the ischaemia/reperfusion experiments, drug delivery and blood sampling compared to mouse model (Ytrehus, 2000). Rat model also affords the possibility to expose the heart either by left or mid-line thoracotomy to occlude the left coronary artery with minimum interventions compared to large animals (Hearse and Sutherland, 2000). Permanent occlusion of the rat left coronary artery has also been used to develop heart failure and study post-infarction modelling and inflammation (Qvigstad et al., 2005). Furthermore, rat heart also has a sparse collateral circulation (Maxwell et al., 1987) which is important for reproducible ischaemic area (risk zone) that determines the severity of arrhythmia and infarct size (Curtis et al., 1987). Therefore, a reperfusion phase is essential to study the infarct development and limitation (Ytrehus, 2006). Nevertheless, there are some limitations to the rat model which have to be acknowledge when compared to human. The rat considerably has a high heart rate compared to human. In addition, rat's heart has a short action potential which means that there is a long inter-AP duration (i.e. prolonged phase 0). Taken together, these elements have a considerable impact on the incidence of

ventricular arrhythmias and the reversibility of ischaemia- and reperfusion-induced VF. Furthermore, the heart size/body size is higher in rat compared to this ratio in human. Transient ligation of the proximal left coronary artery for 30 minutes followed by reperfusion leads to an infarct which is reported to be 40-60% of the ischaemic area (are at risk) (Dillmann, 2008), which is in line with our results.

Another characteristic feature of the *in vivo* rat model is the pattern of ischaemia- and reperfusion-induced arrhythmias which is similar to that seen in large animals (dog and pig) compared to other small animal models (mouse and rabbit) in terms of vulnerability and reversibility. Regional ischaemia induces a first phase of arrhythmias after 4-5 minutes which lasts up to 15 minutes of ischaemia; a second phase of arrhythmia after 1.5-2.5 hours of occlusion; and a third phase occurs after 24 hours (Clark et al., 1980, Curtis et al., 1987). In our study, the first phase of ischaemia-induced arrhythmias was experienced only. Reperfusion also induces even more severe arrhythmias in comparison with ischaemia-induced arrhythmias but over a short period (first 1-5 minutes of reperfusion). However, variability in the incidence of ventricular tachycardia (VT), ventricular fibrillation (VF) and mortality emphasises that researchers need to randomise control experiments parallel to the treated group aiming to minimise that variation and to avoid any possible bias (Hearse and Sutherland, 2000).

The preliminary series of experiments were used to optimise the *in vivo* model of myocardial ischaemia/reperfusion injury in terms of haemodynamic parameters, successful induction of ischaemia and reperfusion, achieving a survivable infarct size, and having sufficient delineation for infarct size

determination. Regional myocardial ischaemia was induced in 60.6 ± 2.8 % of the total ventricular volume of the heart. Ischaemia was established by a transient occlusion of the left coronary artery for 30 minutes and followed by 2 hours of reperfusion. It should be acknowledged here that the AAR is relatively large which might have its implications on the resulted infarction. The incidence and pattern of VT and VF during ischaemia did not significantly vary with an onset 4-5 minutes that is consistent with others (Clark et al., 1980). Irreversible VF during ischaemia and shortly after 30 seconds of reperfusion was the main cause of death during ischaemia/reperfusion protocol. Myocardial infarction resulting from this protocol represented 50.7 ± 2.6 % of the area at risk which is consistent with other investigators using the same protocol (Wajima et al., 2006, Baker et al., 2007, De Paulis et al., 2013). Infarct size quantification was performed using a dual staining technique with Evans' blue and triphenyltetrazolium chloride. This technique has been used routinely in myocardial infarction studies where regional myocardial ischaemia was induced. Indirect delineation of the ischaemic myocardium is performed by staining the non-ischaemic area with Evans' blue to ascertain that the area at risk was similar between experimental groups (Black and Rodger, 1996). Infarcted tissue was then demarcated using TTC which precipitates as white particles in the dead (infarcted) tissue within the territories of the area at risk.

Ischaemic preconditioning (IPC) is the first cardioprotective mechanical manoeuvre introduced by Murry et al (1986). In the canine model, Murry et al. (1986) reported that applying a series of ischaemic episodes before the onset of long ischaemia can render the heart more resistant to ischaemia/reperfusion injury. The cardioprotective effects of IPC were then demonstrated in different

animal models including rabbit (Liu et al., 1991), rat (Li and Kloner, 1993), mouse (Suveren et al., 2012), swine (Schott et al., 1990) and in human (Kloner and Yellon, 1994). Therefore, we utilised IPC in the second phase of this study as a positive control to validate the model and ascertain that the cardioprotection of IPC can be detected. Two cycles of 3 minutes ischaemia/3 minutes reperfusion before the index ischaemia caused a significant limitation in the infarct size by 67%. It also showed a powerful antiarrhythmic effect on both ischaemia- and reperfusion-induced VT and VF. None of the preconditioned hearts suffered from VF during ischaemia in comparison to the control group. It is worth noting that this IPC protocol (2x3 min IPC cycles) is non-standard protocol and it is first time to report cardioprotection with this protocol in an *in vivo* rat model of myocardial ischaemia/reperfusion injury. Accordingly, it needs to be acknowledged that whether other IPC protocols could show similar cardioprotection is yet to be characterised. These results confirm that the established model can be used as a preclinical model and it is valid for screening potential cardioprotective agents.

3.5 Conclusion

These data show that the experimentalist had acquired the necessary skills to perform the surgical procedures required to establish the model of acute myocardial infarction in rat. The effects of IPC on haemodynamic parameters and infarct size were both detectable in our rat model. This demonstrates the validity of this model as a preclinical model to test the cardioprotection of any other potential targets or molecules.

Chapter 4 Investigating the potential infarct-limiting effect of 2-mercaptoethanesulfonate (Mesna) against myocardial ischaemia/reperfusion injury *in vivo*

4.1 Introduction

4.1.1 Mesna: 2-mercaptoethanesulfonate sodium

The first clinical trial of Mesna was conducted in the early 1970s by UBC Pharmaceuticals to test its mucolytic efficacy for bronchial diseases (Figure 4.1). After successful results, it was launched as an inhaled dosage form (Mistabron®) in France for treatment of respiratory disorders such as cough and chronic bronchitis, especially for children. The free thiol group of Mesna is suggested to disrupt the disulfide bonds between the mucus glycoproteins, rendering the secretion less viscous and more readily able to be eliminated from the respiratory airways (Shaw and Graham, 1987). This suggested that the sulfhydryl group of Mesna is prerequisite for its activity. Intriguingly, it has also been shown that Mesna is a co-enzyme in bacterial methanogenesis and is responsible for methyl transfer (Taylor and Wolfe, 1974).

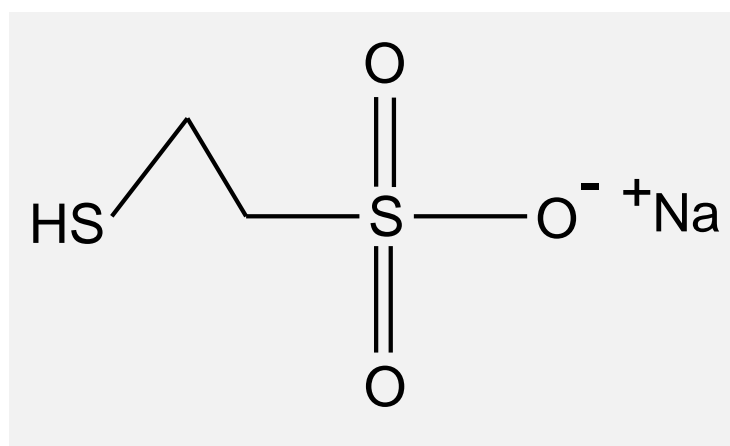


Figure 4.1 Chemical structure of 2-mercaptoethanesulfonate sodium (Mesna).

In the early 1980s, Brock and colleagues carried out a comprehensive study to identify the causative agent of haemorrhagic cystitis during oxazophosphorine cancer therapy, notably with cyclophosphamide and ifosfamide. They later reported in their seminal paper that the main causative factor was the renal excretion of the two urotoxic metabolites of oxazophosphorine, namely 4-hydroxy-oxazaphosphorines and acrolein (Brock et al., 1981a). The level of GSH in urine is very low which makes the bladder and the efferent urinary ducts vulnerable for these reactive chemicals that are renally excreted. Brock et al. (1981b) then conducted a comparative study using different thiol-containing compounds as potential adjunct therapies to oxazophosphorines without interfering with the anticancer activity. This screening study was the first to report uroprotection by Mesna and showed that Mesna can interact with the urotoxic chemicals, by virtue of the free sulfhydryl group, forming a nontoxic compound. The anticancer activity of oxazophosphorines was not affected by co-administration of Mesna as the latter does not enter most of the body tissues and has a small volume of distribution (Brock et al., 1982). This unique pharmacokinetic profile endorsed the addition of Mesna to the standard regimen of oxazophosphorine therapy which was confirmed by later clinical trials (Brock and Pohl, 1983). Since then, Mesna has revolutionized the use of high doses of oxazophosphorines in cancer therapy by abolishing the main adverse effect (i.e. haemolytic cystitis). Moreover, it has been demonstrated that Mesna can also prevent the chronic nephrotoxicity as well as the acute urotoxicity (Kempf and Ivankovic, 1987). Although it has small volume of distribution, Mesna has also shown potential to mitigate the systemic adverse effects of doxorubicin *in vitro* (Aluise et al., 2011).

Another form of Mesna-induced uroprotection was first demonstrated by Mashiach et al. (2001) where they reported that Mesna can protect against acute renal failure in

rat through its antioxidant activity. They showed that a bolus dose of Mesna (180 mg kg⁻¹, i.v.) 5 minutes before reperfusing ischaemic renal tissue restored 90-100% of glomerular filtration rate (GFR) with 75% improvement in the fractional sodium excretion (FE_{Na}). Later work by Kabasakal et al. (2004) demonstrated that Mesna protected the kidney against renal ischaemia/reperfusion injury via enhancing endogenous antioxidant capacity to attenuate the oxidative stress. Similarly, Sener et al. (2004) found that Mesna restored the GSH level and reduce the oxidative stress-induced damage in a rat model of burn-induced renal injury. The antioxidant effect of Mesna has also been tested against other types of ischaemia/reperfusion injury. Ypsilantis et al. (2006) reported that pre-ischaemia Mesna therapy protected the intestinal mucosa against intestinal ischaemia/reperfusion injury in a time-dependant manner. In addition to being directly antioxidant, later work by Ypsilantis's group (Ypsilantis et al., 2008) showed that Mesna could indirectly inhibit oxidative stress by targeting NF- κ B, which is involved in the inflammatory and immune responses, and inhibiting its activity following intestinal ischaemia/reperfusion. They also reported that a bolus dose of Mesna (400 mg kg⁻¹, i.p.) ameliorated the peritoneal puncture-induced oxidative stress in other splanchnic organs (stomach, liver, and kidney) in a rat model (Ypsilantis et al., 2009b). The protective effect of Mesna was also investigated against hepatic ischaemia/reperfusion injury. Sener and colleagues (Sener et al., 2005b) showed that administration of two bolus doses of Mesna (150 mg kg⁻¹, i.p.), one before ischaemia and the other at reperfusion, can improve hepatic function and structure by reducing the tissue damage in a rat model of hepatic ischaemia/reperfusion mediated via its antioxidant action. Later work by Ypsilantis's group (2009a) reported that Mesna also protected the liver against the anti-mitotic effect of Pringle-manoeuvre, inducing hepatic ischaemia by interrupting the blood flow through the hepatic artery

and the portal vein, by suppressing the activity of NF- κ B and scavenging of generated ROS. Interestingly, the protective effects of Mesna have also been shown in other pathologies. For instant, Shusterman et al. (2003) demonstrated that intrarectal administration of Mesna was protective against trinitrobenzene sulfonic acid-induced colitis in rat.

To our best knowledge, the first work investigating the potential cardioprotective action of Mesna against myocardial ischaemia/reperfusion injury was carried out in our laboratory in 2009, by David Elsey (Elsey, 2009). Elsey was exploring the cardioprotective properties of hydrogen sulfide (H₂S). As a part of his PhD work, Mesna was selected for comparison as an alternative sulfhydryl-containing compound and potentially a donor of H₂S. He reported a significant reduction in infarct size when Mesna (50 μ M) was perfused through the heart either pre-ischaemically or at reperfusion in an isolated buffer-perfused rat heart preparation. Further mechanistic study revealed that the cardioprotection established by Mesna was abrogated in the presence of the PI3K inhibitor, LY294002, suggesting that Mesna's cardioprotection might be mediated by triggering the RISK pathway.

In view of the significant contribution of oxidant stress to the development of lethal reperfusion injury and the preceding evidence suggesting that Mesna ameliorates oxidant stress, we sought to characterise the potential protective effect of Mesna as an adjunct to reperfusion against myocardial ischaemia/reperfusion injury *in vivo*. These studies are important because Mesna represents a drug with potential to be repurposed for clinical use as an adjunct to PPCI.

4.1.2 Aim

The aims of this study were to:

1. Test for the first time the cardioprotection of Mesna at early reperfusion *when given specifically as an adjunct to reperfusion* in an *in vivo* rat model of acute myocardial infarction.
2. Elucidate the mechanism of Mesna's cardioprotection in the early phase of reperfusion.

4.1.3 Hypotheses

We hypothesised the following:

- 1- Mesna will limit ischaemia/reperfusion injury when given just prior to reperfusion, thereby limiting ultimate infarct size.
- 2- The cardioprotective effect of Mesna is dependent on triggering the RISK pathway, namely PI3K/Akt and eNOS, at the commencement of reperfusion.

4.1.4 Objectives

The aforementioned hypotheses were tested with the following specific experimental objectives:

- 1- Establish a dose-response study to determine the optimum cardioprotective dose of Mesna using an *in vivo* rat model of acute myocardial infarction.

- 2- Assess the phosphorylation of the key kinases and effector proteins of the RISK pathway, namely Akt, eNOS, GSK-3 β and ERK1/2, at the first minutes of reperfusion using Western blot analysis.

4.2 Materials and Methods

4.2.1 Animals

Male Sprague Dawley rats, 300-350 g (9-11 weeks old), were sourced from Harlan, UK and used for Mesna study. Animals handling, housing and reporting are all explained in Chapter 2, section 2.2.

4.2.2 The *in vivo* rat model of myocardial ischaemia/reperfusion injury

Rats underwent 30 minutes of myocardial ischaemia and 2 hours reperfusion to induce survivable infarct size as described in Chapter 2, section 2.3. Infarct size determination was performed using dual staining with Evans' blue/TTC staining technique as described in Chapter 2, section 2.4.

4.2.3 Treatment protocols

4.2.3.1 Mesna dose-response study

This series of experiments was carried out to investigate the potential infarct-sparing effect of Mesna. A dose-response study was undertaken using different dosing regimens at different time points throughout the ischaemia/reperfusion protocol (Figure 4.1). Animals were subjected to 30 minutes regional myocardial ischaemia and 120 minutes reperfusion. Rats were randomised to receive one of the following treatments:

Group 1: Control (n=10). Animals received saline as a bolus dose 5 minutes before reperfusion.

Group 2: Mesna pre-ischaemia infusion (800 mg kg^{-1}) ($n=8$). After 10 minutes stabilisation, animals received Mesna (200 mg kg^{-1}) as a bolus loading dose followed by intravenous infusion of Mesna ($20 \text{ mg kg}^{-1}\text{min}^{-1}$, i.v.) until the first 20 minutes of ischaemia (total dose = 800 mg kg^{-1}).

Group 3-5: Mesna pre-reperfusion bolus (1, 10, 100 mg kg^{-1} , i.v.) (Each group $n=8$) received a bolus dose of Mesna (1, 10, 100 mg kg^{-1}) 5 minute before reperfusion.

Group 6: Mesna post-ischaemia infusion (1100 mg kg^{-1}) ($n=8$). Rats received a bolus loading dose of Mesna (200 mg kg^{-1}) at 15 minutes of ischaemia followed by intravenous infusion ($20 \text{ mg kg}^{-1}\text{min}^{-1}$, i.v.) until 30' minute of reperfusion (total dose = 1100 mg kg^{-1}).

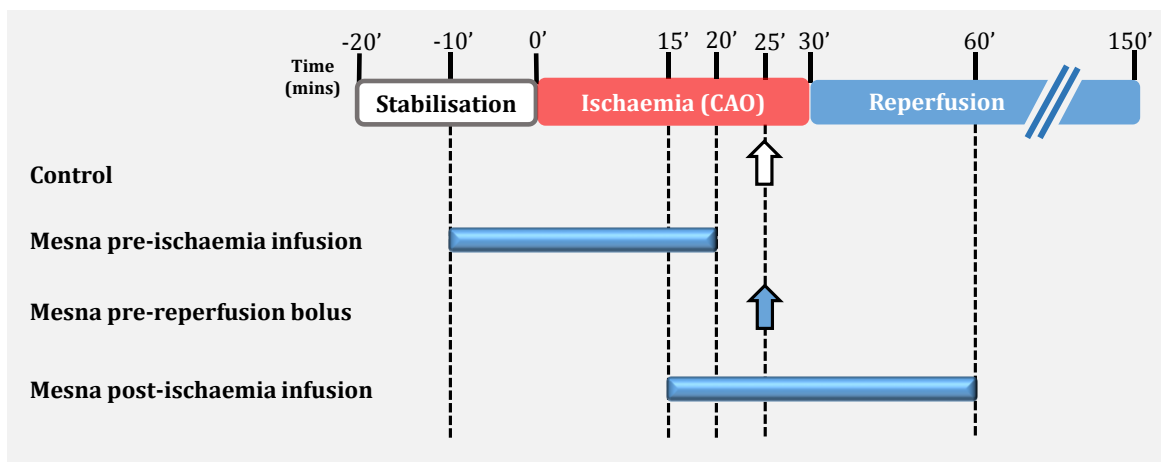


Figure 4.2 Treatment protocol for Mesna study. All hearts were subjected to regional ischaemia by tightening the snare around the left coronary artery. By releasing the snare, reperfusion was induced for 90-120 minutes following 30 minutes of ischaemia. Arrows and lines indicate the time of pharmacological interventions. $n=8-10$.

4.3 Results

4.3.1 Inclusion/exclusion criteria

In the dose-response study, 58 rats were employed, of which six did not successfully complete the ischaemia/reperfusion protocol and two were excluded due to failure in staining. Therefore, results of 50 successfully completed experiments were reported.

4.3.2 Effect of Mesna on cardiodynamics

There were no significant differences between the baseline parameters between experimental groups as can be seen in Table 4.1. Administration of Mesna in different doses of Mesna (1, 10, 100 mg kg⁻¹) as a bolus at 25 minutes of ischaemia showed no significant change in any of the haemodynamic parameters. However, Mesna (10 mg kg⁻¹) improved both RPP and MAP at the end of reperfusion but did not reach a statistical significance. The pre-ischaemia dosing regimen with Mesna caused a significant drop in both MAP and RPP by 30% compared to the control group. RPP transiently improved toward the end of ischaemia while the MAP was significantly lower by 26% at 20 minutes of ischaemia compare to the control. Similarly, postischaemia dosing of Mesna resulted in a decrease in both MAP and RPP that continued till the end of reperfusion.

4.3.3 Infarct size data

There was no significant difference in the area at risk (AAR) between the experimental groups where AAR of the control group represented (53.9 ± 2.7%) of the total ventricular volume of the heart (Figure 4.3A). Application of Mesna 5 minutes before

reperfusion did not have a significant effect on infarct size (Figure 4.3B). Moreover, neither pre-ischaemic nor post-ischaemic infusion of Mesna exerted a detectable effect on the myocardial infarction compare to the control group.

In the view of the failure to identify any cardioprotective dose of Mesna, no further mechanistic studies (Objective 2) were undertaken.

Table 4.1 Summary of the baseline parameters and haemodynamics throughout ischaemia/reperfusion injury protocol for dose-response study of Mesna

Experimental Protocol	n	BW (g)	Baseline		20 min Ischaemia		120 min Reperfusion	
			RPP (mmHg min ⁻¹)*10 ³	MAP (mmHg)	RPP (mmHg min ⁻¹)*10 ³	MAP (mmHg)	RPP (mmHg min ⁻¹)*10 ³	MAP (mmHg)
Control	10	363 ± 10	45.9 ± 1.4	100 ± 4	28.5 ± 1.7	64 ± 4	25.6 ± 1.8	56 ± 4
Mesna pre-ischaemia infusion (800 mg kg ⁻¹)	8	359 ± 6	32.1 ± 2.6 ***	71 ± 5 ***	21.4 ± 1.6	47 ± 3 *	19.0 ± 2.0 *	42 ± 4 *
Mesna pre-reperfusion bolus (1 mg kg ⁻¹)	8	378 ± 12	43.1 ± 0.8	99 ± 4	28.0 ± 1.5	63 ± 8	22.1 ± 1.4	48 ± 6
Mesna pre-reperfusion bolus (10 mg kg ⁻¹)	8	346 ± 6	46.4 ± 0.3	102 ± 1	31.5 ± 1.1	75 ± 5	27.9 ± 0.7	63 ± 3
Mesna pre-reperfusion bolus (100 mg kg ⁻¹)	8	345 ± 7	41.7 ± 1.2	93 ± 7	26.9 ± 1.3	61 ± 6	23.4 ± 0.8	47 ± 3
Mesna post-ischaemia infusion(1100 mg kg ⁻¹)	8	377 ± 9	47.2 ± 2.2	105 ± 5	28.9 ± 3.0	65 ± 5	18.2 ± 4.2 *	40 ± 7 *

n number of animals per group; BW body weight; RPP rate pressure product; MAP mean arterial pressure. Data are presented as mean ± SEM and analysed using Two way ANOVA test with Bonferroni *post hoc* test, *p < 0.05, ***p<0.001 vs control.

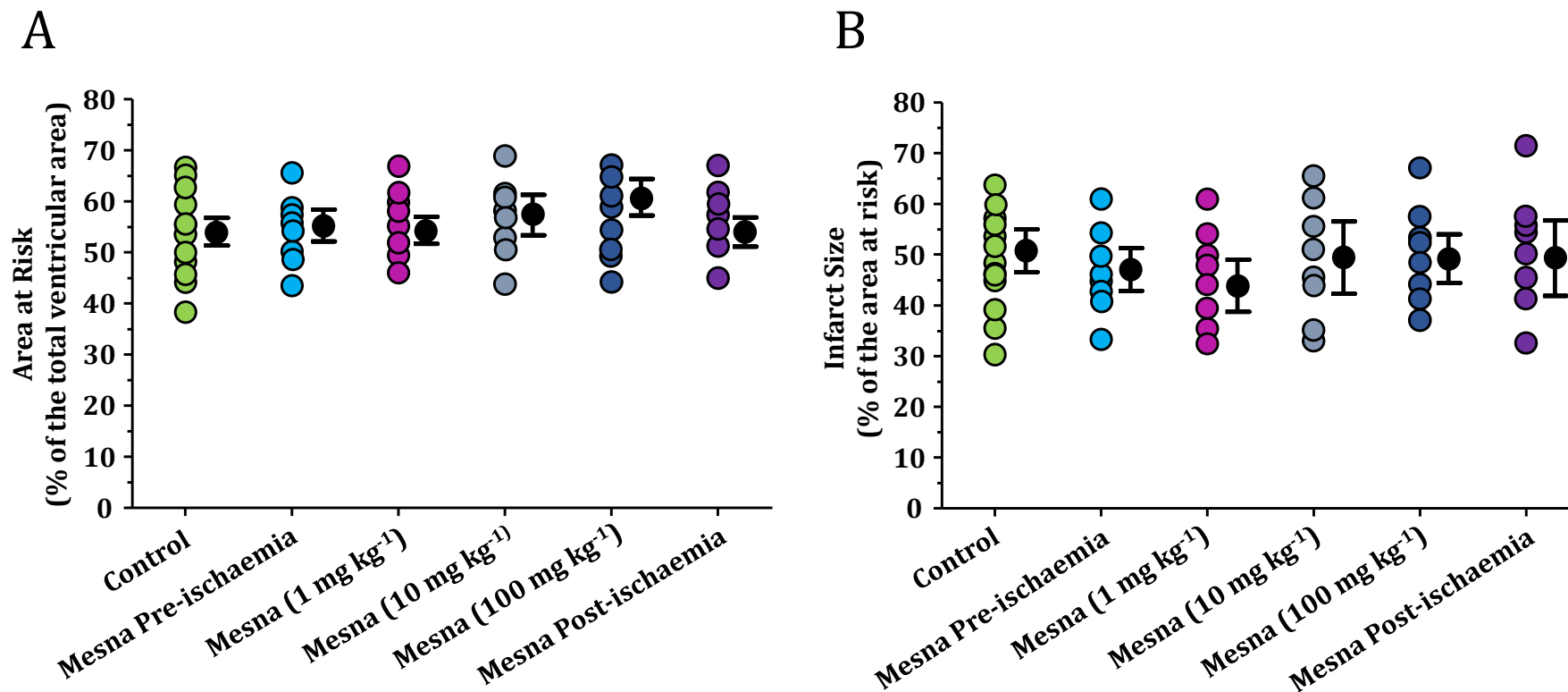


Figure 4.3 Summary of infarct size measurements for Mesna dose-response study. (A) Area at risk was expressed as a percentage of the total ventricular area and (B) infarct size was reported as a percentage of the area at risk. There was no significant difference between groups (p value > 0.05). Data were presented as a mean \pm SEM and analysed using one-way ANOVA. The mean of infarction for each group is represented a filled circle (with error bars) next to the individual values (open circles).

4.4 Discussion

Mesna has been used for almost four decades as an adjunct antioxidant therapy to prevent haemolytic cystitis induced by particular chemotherapy agents such as the oxazaphosphorines, cyclophosphamide and ifosfomide. It also elicits protection against different types of ischaemia/reperfusion injury in kidney, liver and intestine. Eelsey was the first to show cardioprotection by Mesna against myocardial ischaemia/reperfusion injury in Langendorff perfused rat heart. In that work, Mesna showed infarct limitation when perfused before the onset of ischaemia or at reperfusion. Interestingly, the latter effect was abrogated by PI3K inhibitor, suggesting that Mesna mediates its protection by activating the RISK pathway. The next step was naturally to test Mesna cardioprotection in an *in vivo* model of myocardial ischaemia/reperfusion injury as a necessary step for further development. A series of dose-response experiments were conducted to determine the optimum dose with infarct size measurement as an end-point of interest. The dose range was estimated according to Eelsey's work and the pharmacokinetic profile of Mesna (Verschraagen et al., 2004). Mesna was administered across a wide dose range: (1) 10 minutes before ischaemia (200 mg kg⁻¹ as a bolus) followed by IV infusion (20 mg kg⁻¹ min⁻¹) till 20 minutes of ischaemia, (2) as a bolus of 1, 10, 100 mg kg⁻¹ at 25 minutes of ischaemia, (3) at 15 minutes of ischaemia as a bolus (200 mg kg⁻¹) followed by IV infusion (20 mg kg⁻¹ min⁻¹) till 30 minutes of reperfusion. Mesna showed no infarct-limiting effect with any of the dosing schedules (p-value > 0.05).

The first reason for the absence of any cardioprotective effect by Mesna *in vivo* might be the short plasma half-life of Mesna (~17 minutes) (Shaw and Graham,

1987). It has been reported that Mesna is almost immediately oxidised into its disulfide form (dimesna, Figure 4.4) once it enters the circulation by a metal-dependent reaction (Shaw and Graham, 1987, Yilmaz et al., 2013). Alternatively, Mesna could also interact with endogenous thiol-containing compounds such as cysteine (a precursor for GSH) forming cysteine-Mesna complex, enhancing the excretion of cysteine in the urine. This has been detected in animals (Wright et al., 1985) and human (Duran et al., 1981, Sidau and Shaw, 1984, Jones et al., 1985), causing GSH depletion (Smith et al., 2003a). The two sulfonate groups and large size of dimesna make it difficult to enter most cells, with a small volume of distribution estimated to be 0.3 L kg^{-1} (Shaw and Graham, 1987). Collectively, these inactivation reactions are beneficial for the use of Mesna as an adjunct to neoplastic therapies because it limits its potential interference with their anticancer activities as they both travel through the blood to reach their targets. However, this could limit the antioxidant activity of Mesna in other tissues which lack the ability to retrieve Mesna from dimesna *in vivo*. The cell permeability of Mesna has also been questioned due to its high hydrophilicity which possibility hinders passive crossing through the hydrophobic cellular membranes. It is also emphasises that its absorption into the cell might need a carrier system similar to what is happening in the kidney (Shaw and Graham, 1987).

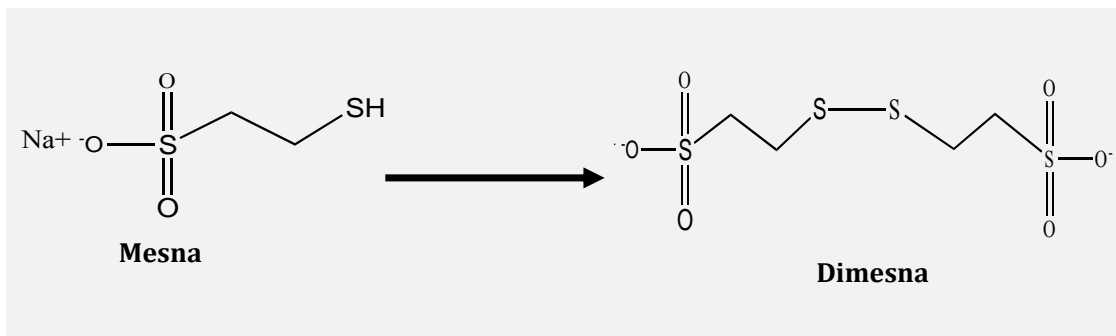


Figure 4.4 The oxidation of Mesna to dimesna in the circulation.

Taken together, these findings lead us to propose that the auto-oxidation of Mesna into disulfide forms *in vivo* limits antioxidant activity of Mesna only to the tissues which are able to retrieve Mesna from its inactive forms. This proposed model in fact can explain the majority of protective effect which have been associated with Mesna therapy. For example, it has been proposed that hepatocytes are not able to reuptake dimesna or reduce it to Mesna (Ormstad et al., 1983). However, later work by Goren et al. (1998) demonstrated that isolated liver has a glutathione-dependent capability of reducing perfused dimesna to Mesna. This evidence suggests that hepatoprotection established by Mesna treatment against ischaemia/reperfusion injury reported by a number of investigators (Sener et al., 2005a, Sener et al., 2005b, Ypsilantis et al., 2009a) could have been mediated by the retrieved Mesna in the liver. Similarly, a compelling body of evidence suggests that renal tubular epithelium can efficiently reuptake dimesna from the circulation and reduce it back to Mesna via cytosolic thiol transferase and GSH reductase to be finally excreted in the urine (Ormstad et al., 1983, Shaw et al., 1986). The capacity could arguably elucidate the urothelial protection elicited by Mesna against renal ischaemia/reperfusion

injury (Mashiach et al., 2001, Sener et al., 2004, Kabasakal et al., 2004). Oral dose of either Mesna or dimesna can be absorbed by the intestine epithelium where dimesna can be reduced and enter the blood as Mesna in similar manner to the renal reuptake. Accordingly, the availability of free sulfhydryl form of Mesna in the intestine could possibly be responsible for the observed antioxidant activity of Mesna therapy in different forms of intestinal ischaemia/reperfusion injury (Ypsilantis et al., 2006, Ypsilantis et al., 2008, Ypsilantis et al., 2009b). It should also be mentioned here that this capacity of intestinal endothelium to retrieve Mesna from dimesna can explain the reduction in intestinal inflammation with intrarectal injections of Mesna in the study of (Shusterman et al., 2003). Conceivably, this could also be the case with Elsey's work in Langendorff perfused heart model of myocardial infarction. In that model, the heart was perfused with Krebs-Henseleit buffer containing Mesna (50 μ M). Therefore, it seems very plausible that cardioprotection established by Mesna *ex vivo* was elicited by the active form of Mesna as it is stable in diluted solutions and only oxidises to dimesna in negligible quantity over a long period of time (Goren et al., 1991). Arguably, this could explain the reason why Mesna did not show a comparable cardioprotection in the *in vivo* model as it might be oxidised to its inactive dimesna and lost its efficacy when injected directly into the circulation. In line with these results, it is plausible to suggest that the observed anti-inflammatory effect of locally applied Mesna solution against experimental colitis reported by Shusterman et al. (2003) is also conferred by the active form of Mesna. Intriguingly, Yilmaz et al. (2013) reported that Mensa treatment given intraperitoneally at the time of traumatic brain injury did not effectively either mitigate oxidative stress or attenuate cell injury. Whether this failure was due to

the inactivation of Mesna in the blood which limited its antioxidant activity needs further investigation.

4.5 Study limitations

The main focus of this study was to characterise the potential cardioprotection of Mesna using an *in vivo* rat model of ischaemia/reperfusion injury. Since there was no significant effect of Mesna on myocardial infarction, a number of aspects have not been addressed here and need further investigation in future studies. The concentrations of Mesna and its disulfide form have not been measured in this study. The lack of sensitive probes or assay to selectively detect and differentiate between exogenous and endogenous thiol-containing compounds still represents a major challenge in measuring the plasma concentration of Mesna following administration and to estimate the rate of its conversion to Dimesna. Therefore, the pharmacokinetic profile of Mesna is yet to be fully elucidated.

4.6 Conclusion

In summary, Mesna represented a potential drug to be re-purposed clinically as adjunct to PPCI because it is a licenced, effective, well-tolerated and inexpensive drug. Previous studies by our group showed an infarct-limiting effect of Mesna in isolated rat heart that was, at least in part, related to triggering the RISK pathway at early reperfusion. We could not show cardioprotection with Mesna *in vivo* in term of infarct size reduction. We speculate that this could be due to its pharmacokinetic profile and its rapid auto-conversion to an inactive

disulfide form (i.e. dimesna) which limited its ability to enter most cells and enhance its clearance from body.

**Chapter 5 Pharmacological postconditioning
 against myocardial infarction with a slow-releasing
 hydrogen sulfide donor, GYY4137**

5.1 Introduction

Hydrogen sulfide (H_2S) has attracted considerable interest as a cardiovascular autacoid (see Chapter 1, section 1.6). Although produced endogenously within the myocardium and coronary vasculature (Liu et al., 2012, Hackfort and Mishra, 2016), in coronary artery disease, there may be reduced H_2S production (Yong et al., 2008, Han et al., 2015, Islam et al., 2015). The administration of exogenous H_2S donor compounds or increasing endogenous production of H_2S has been well documented to reduce ischaemia/reperfusion injury in experimental models (Elrod et al., 2007, Calvert et al., 2009, King et al., 2014). There is also evidence that H_2S is a mediator of IPost (Bian et al., 2006, Yong et al., 2008, Huang et al., 2012, Das et al., 2015). However, potential therapeutic extrapolation of this knowledge has been hindered by the limitations of H_2S donor compounds. Much of the experimental literature has reported studies with inorganic sulfide salts (Na_2S and NaHS) which are impure in commercial form and unstable. Despite them being water soluble and inexpensive, a particular issue is that the H_2S release is largely uncontrollable as the salts dissociate in aqueous medium instantly to generate H_2S at high concentration in a short-lasting burst (Papapetropoulos et al., 2015). However, these salts have helped in exploring the biological activities of H_2S .

5.1.1 GYY4137: a slow-releasing hydrogen sulfide (H_2S) donor

There have been a number of attempts to develop new thiol-containing compounds capable of acting as H_2S donors, to overcome the drawbacks of sulfide salts, aiming to deliver a stable and controllable level of H_2S to the cellular targets. GYY4137 (morpholin-4-ium 4-methoxyphenyl-morpholino-phosphinodithioate, Figure 5.1) was

the first water soluble H₂S donor reported to release H₂S at a slow steady rate at physiological pH and temperature that was characterised *in vitro* and *in vivo* (Li et al., 2008). Before that, GYY4137 was initially developed as an accelerator in the vulcanisation of natural rubber late in the 1950s (Rose et al., 2015). The H₂S release profile of GYY4137 has been characterised using different methods including fluorescence HPLC (Shen et al., 2012), H₂S selective polarographic electrode (Kolluru et al., 2013) and using fluorescence probe 2,6-dansyl azide and 5,5'-dithiobis(2-nitrobenzoic acid) (Qabazard et al., 2014).

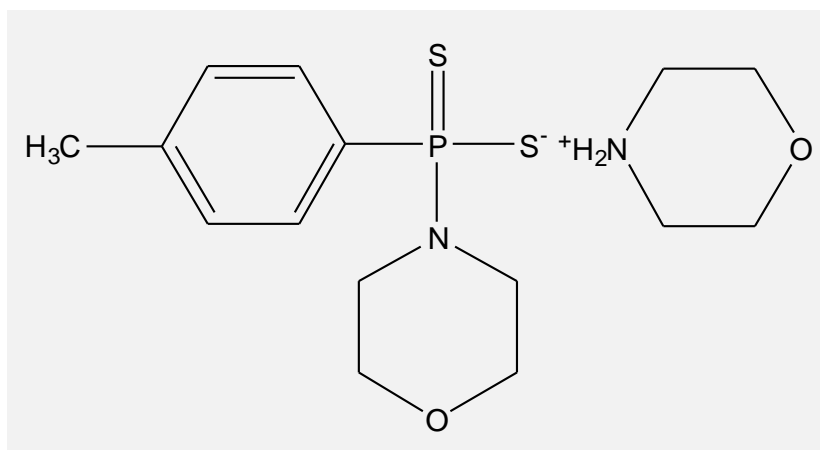


Figure 5.1 GYY4137 chemical structure (morpholin-4-ium 4-methoxyphenyl-morpholinophosphinodithioate).

5.1.2 The biological activity of GYY4137

Among the number of newly introduced and developed donors of H₂S, GYY4137 is the best characterised and studied compound hitherto in term of the mode of H₂S generation and biological activity (summarised in Table 5.1). The release of H₂S from GYY4137 occurs through a hydrolysis pathway of two-steps; first with a direct sulfur-oxygen exchange to produce a molecule of H₂S and arylphosphonamidothioate. The second step, which is relatively slower, involves another exchange to produce H₂S and arylphosphonate (Alexander et al., 2015). Li et al. (2008) first investigated the

vasodilatory effect of GYY4137 in rat aortic ring. They demonstrated a long-lasting vasodilatory response to GYY4137 which was mediated through opening of K_{ATP} channels. Using the same model, subsequent work by Bucci et al. (2012) showed that GYY4137-induced vasodilatation of aortic ring in a PKG-independent manner. Similarly, Chitnis et al. (2013) found that relaxant effect of GYY4137 mediated independently on eNOS signalling in bovine posterior ciliary artery. However, it has been suggested that GYY4137-released H_2S possibly interacts with NO to generate thiol-sensitive compound which exerts positive inotropic effect in rat cardiomyocytes (Yong et al., 2011). Interestingly, chronic treatment with GYY4137 reduced the blood pressure in normotensive rats and to a greater extent in SHR (Li et al., 2008). A part from its actions on vascular smooth muscle, it has also been shown that GYY4137 mediates muscle relaxation on other nonvascular smooth muscles including human myometrium (Robinson and Wray, 2012) and primary human airway (Fitzgerald et al., 2014) through the opening of ATP-sensitive K^+ channels. Other beneficial effects of GYY4137 on the cardiovascular system have been demonstrated including antithrombotic activity by inhibiting platelet activation in mouse (Grambow et al., 2014); anti-atherosclerotic action in apolipoprotein knockout mice fed with high fat diet (Li et al., 2013); and mitigated fibrosis progression in myocardial pathologies (Meng et al., 2015b, Lin et al., 2016).

The activity of GYY4137 therapy in cardiac pathologies has also been tested. It has recently been reported that GYY4137 therapy for 7 days following permanent ligation of the left descending coronary artery preserved cardiac contractility and attenuated remodelling via increased natriuretic peptide (ANP and BNP) release in rat myocardium (Lilyanna et al., 2015). Moreover, pre-ischaemia GYY4137 treatment for seven days elicited infarct limitation against myocardial ischaemia/reperfusion *in vivo*

by enhancing the expression of Bcl-2 and inhibiting the activity of MAPK, caspase-3 and Bax (Meng et al., 2015a). However, the therapeutically relevant time window for acute myocardial infarction implies administration as a postconditioning mimetic *i.e.* immediately prior to reperfusion since this is the time at which clinical therapeutic intervention can feasibly be made.

Table 5.1 Summary of the experimental studies using the slow-releasing hydrogen sulfide donor, GYY4137, listed in chronological order

Reference	Experimental model(s)	Main observed effect(s)	Mechanism(s)
Li et al. (2008)	Rat aortic ring, perfused rat kidney and anaesthetised rat	- Vasodilator and antihypertensive	- Opened the vascular smooth muscle K _{ATP} channels
Li et al. (2009)	Lipopolysaccharide (LPS)-induced endotoxic shock in rat	- Anti-inflammatory	- Inhibited LPS-induced TNF- α production and increased IL-10 in rat blood - Decreased the LPS-evoked rise in lung myeloperoxidase activity and upregulation liver transcription factors (NF- κ B and STAT-3)
Lee et al. (2011)	Human cancer cell lines and Xenograft study in mouse	- Pro-apoptotic and cell cycle arrest	- Enhanced the generation of cleaved PARP and cleaved caspase 9. - Partial G2/M arrest
Yong et al. (2011)	Rat cardiomyocytes	- Positive inotropic effect	- Interaction with nitric oxide to generate thiol-sensitive compound
Bucci et al. (2012)	Phenylephrine-contracted mouse aortic ring	- Vascular smooth muscle relaxation	- PKG-independent mechanism
Robinson and Wray (2012)	Human and rat myometrium	- Smooth muscle relaxation	- opening of K _{ATP} -channels
Fox et al. (2012)	Primary human articular chondrocyte and mesenchymal progenitor cells	- Cytoprotection	- Unknown
Chitnis et al. (2013)	Phenylephrine-contracted bovine posterior ciliary artery	- Vascular smooth muscle relaxation	- The activity was dependent on endogenous production of both prostanoids and H ₂ S and mediated by K _{ATP} channels with no role of either CBS or eNOS.

Li et al. (2013)	Human synoviocytes and articular chondrocytes and Complete Freund's adjuvant (CFA) model of acute joint inflammation in mouse	<ul style="list-style-type: none"> - Pro-inflammatory when given before CFA - Anti-inflammatory when administrated after CFA 	<ul style="list-style-type: none"> - Inhibited TNF-α, IL-1β, IL-6 and IL-8.
Lencesova et al. (2013)	HeLa cell	<ul style="list-style-type: none"> - Pro-apoptotic 	<ul style="list-style-type: none"> - Upregulated the expression of IP3R1 and IP3R2 on both mRNA and protein levels - Increased cytosolic Ca²⁺ and depleted reticular Ca²⁺ in concentration dependent manner - Increased endoplasmic reticulum stress markers, such as X-box, CHOP and ATF4
Liu et al. (2013b)	High fat fed apolipoprotein (ApoE ^{-/-}) mice	<ul style="list-style-type: none"> - Anti-atherosclerotic 	<ul style="list-style-type: none"> - Abrogated TNF-α, ICAM-1 and IL-6 expression and activated aortic Akt and eNOS
Grambow et al. (2014)	Platelets activation and venular thrombus formation	<ul style="list-style-type: none"> - Anti-thrombotic 	<ul style="list-style-type: none"> - Increased S-sulfhydration of platelet proteins - Reduced TRAP-induced adhesion molecule expression
Fitzgerald et al. (2014)	Primary human airway smooth muscle	<ul style="list-style-type: none"> - Smooth muscle relaxant 	<ul style="list-style-type: none"> - Opened sarcolemmal K_{ATP} channels
Wei et al. (2014)	Diabetic cardiomyopathy in H9c2 cells	<ul style="list-style-type: none"> - Cytoprotection 	<ul style="list-style-type: none"> - Activated AMPK/mTOR signalling pathway
Burguera et al. (2014)	Human chondrocytes	<ul style="list-style-type: none"> - Anti-inflammatory and anti-catabolic 	<ul style="list-style-type: none"> - Reduced the activation of NF-κB by inhibiting IL-1β signal

Lu et al. (2014)	Human hepatocellular carcinoma cell line and subcutaneous HepG2 xenograft model	- Anti-cancer	- Inhibited STAT3 phosphorylation and altered its downstream proteins including Bcl-2, Mcl-2, VEGF, surviving, HIF1- α and cyclin D1
Lee et al. (2014)	Human cancer cell and normal cell	- Selective anti-cancer	- Increased lactate accumulation and impair cellular pH regulation mechanisms, leading to metabolic acidosis
Wang et al. (2015)	Neck model of itch in mice	- No scratching behaviour induced compare to NaHS	- Unknown
Meng et al. (2015b)	Spontaneous hypertensive rat	- Anti-fibrotic	- Inhibited oxidative stress, TGF- β 1/Smad2 pathway and α -SMA expression
Lilyanna et al. (2015)	Acute myocardial infarction model in rat	- Cardioprotection when GYY4137 was given pre-ischaemia	- Activated endogenous natriuretic peptide (ANP and BNP) at early post-ischaemic phase
Meng et al. (2015a)	Acute myocardial infarction model in rat	- antioxidant and anti-apoptosis when GYY4137 was given pre-ischaemia	- Suppressed MAPK phosphorylation, activity of caspase-3 and expression of Bax, while increased the expression of Bcl-2 in the myocardium
Wu et al. (2015)	Coxsackie virus B3-induced myocarditis in rat-derived cardiomyocytes	- Anti-inflammatory	- Suppressed NF- κ B and MAPK signalling pathway
Kubickova et al. (2016)	Cholinergic neuronal cell line	- Differentiating factor	- Unknown
Lin et al. (2016)	Unilateral ureteral obstruction model in rat	- Anti-fibrotic	- Attenuated TGF- β 1 and ANGII mediated mechanism of fibrosis

Chen et al. (2016b)	Patients with spinal cord ischaemia/reperfusion injury and TNF- α -stimulated neural human cell lines (AGE1.HN and SY-SH5Y)	- Anti-apoptotic	- Reduced serum TNF- α and, consequently, suppressed the activity of miR-485-5p/TRADD axis
Chen et al. (2016a)	Mouse model of endotoxemia	- Cytoprotective	- Inhibited the elevated levels of TNF- α /IFN- γ in the plasma
Salvi et al. (2016)	Isolated superfused bovine iris-ciliary bodies	- Inhibited sympathetic neurotransmission	- Opening of K _{ATP} channels
Ivanciuc et al. (2016)	Respiratory syncytial virus-induced lung disease in wild and CSE knockout mice	- Antiviral and anti-inflammatory effects	- Attenuated inflammatory mediators and cells infiltration
Meng et al. (2016)	SHR, human hypertrophic myocardium and neonatal rat cardiomyocytes	- Mitigated cardiac hypertrophy	- Abrogated KLF5-induced cardiac hypertrophy by S-sulphydrating its transcriptional factor SP1 at Cys ⁶⁶⁴
Xie et al. (2016)	STD-induced LDLr ^{-/-} mice, LDLr ^{-/-} Nrf2 ^{-/-} mice and HG/ox-LDL-treated endothelial cells	- Attenuated diabetes-accelerated atherosclerosis	- Enhanced Nrf2 activity via S-sulphydration of Keap1 at Cys ¹⁵¹ and attenuated oxidative stress
van den Born et al. (2016)	HCA plaque and HMEC-1 CSE ^{-/-} cell	- Destabilised atherosclerotic plaque	- Stimulated micro-angiogenesis to create intraplaque microvessels
Coavoy-Sanchez et al. (2016)	Murine model of pruritus	- Alleviated itching	- NO/cGMP-independent inhibition of PAR-2 through opening K _{ATP} channel
Grambow et al. (2016)	Human whole blood	- Antithrombotic	- Enhanced endogenous thrombolysis by disturbing platelet-leukocyte aggregation
Rodrigues et al. (2016)	Dorsal skin pruritus and inflammation in BALB/c mice	- No effect on either inflammation or pruritus	- No effect on histamine release from rat peritoneal mast cell

Lobb et al. (2016)	Renal I/R injury in mice and NRK-52E	- Anti-apoptotic	- Decreased mito-ROS generation and improved mitochondrial membrane potential
-----------------------	--------------------------------------	------------------	---

VEGF vascular endothelial growth factor; *HIF1- α* hypoxia-inducible factor-1 α , *MAPK* mitogen activated protein kinases; *TNF- α* tumor necrosis factor-alpha; *SHR* spontaneous hypertensive rat; *KLF5* Krüppel-Like Factor 5; *SP1* specificity factor 1; *STD* Streptozotocin; *LDLr* low-density lipoprotein receptor; *Nrf2* nuclear factor erythroid 2-related factor; *HG* high glucose; *ox-LDL* oxidised LDL; *Keap1* Kelch-like ECH-associated protein 1; *HCA* Human carotid atherosclerotic; *HMEC-1* human dermal microvascular endothelial cell, *NO* nitric oxide; *cGMP* cyclic guanosine monophosphate; *PAR-2* proteinase-activated receptor-2.

5.1.3 Aim

The aims of this study were to:

- 1- Investigate for the first time the injury-limiting effects of GYY4137 at early reperfusion *when given specifically as an adjunct to reperfusion* in a rat model of acute myocardial infarction.
- 2- Characterise whether GYY4137 triggers the RISK pathway at early reperfusion to limit infarct size.

5.1.4 Hypotheses

We hypothesised the following:

- 1- GYY4137 will limit reperfusion injury when given just prior to reperfusion, thereby limiting ultimate infarct size.
- 2- The protective action of GYY4137 is due to H₂S-releasing capacity.
- 3- GYY4137 relies on activation of key components of the RISK signalling cascade, namely PI3K/Akt and eNOS, at the first minutes of reperfusion to elicit its postconditioning effect.

5.1.5 Objectives

The aforementioned hypotheses were tested through the following specific experimental objectives:

- 1- Perform a dose-response study to determine the optimum cardioprotective dose of GYY4137 using an *in vivo* rat model of myocardial regional ischaemia/reperfusion injury.
- 2- Apply depleted (D-GYY4137), as a negative control, at reperfusion to investigate whether the parent structure of GYY4137 retains any cardioprotection.
- 3- Investigate the activity of the key kinases and effector proteins of the RISK pathway at the first minutes of reperfusion using Western blot analysis.

5.2 Materials and Methods

5.2.1 Animals

Male Sprague Dawley rats, 300-350 g (9-11 weeks old), were purchased from Harlan, UK and used to characterise the cardioprotection of GYY4137. Rats handling, housing and reporting are all explained in Chapter 2, section 2.2.

5.2.2 Acute myocardial infarction model

The potential infarct-limiting effect of GYY4137 was characterised using an *in vivo* rat model of myocardial ischaemia/reperfusion injury as was described in Chapter 2, section 2.3. Infarct quantification was carried out using TTC staining technique as described in Chapter 2, section 2.4.

5.2.3 Treatment protocols

5.2.3.1 Dose-response study of GYY4137

The first series of experiments examined the dose-dependent effects of GYY4137 on infarct size and the involvement of H₂S in mediating any responses. GYY4137 (morpholino salt) is a water-soluble compound (up to 100 mM) and was the gift of Professor Matt Whiteman from University of Exeter/Medical School. It was synthesised as reported previously (Li et al., 2008) and the purity of GYY4137 was determined by NMR spectroscopy (1H, 31P and 13C). It was identical to a commercial sample from SigmaAldrich, UK. The dose range employed in this study was derived from previous studies in the rat heart *ex vivo* by our group (Suveren et al., 2012) and

in vivo studies conducted by others (Li et al., 2008, Meng et al., 2015a). Based on its H₂S-releasing profile, GYY4137 was given 10 minutes before reperfusion to allow enough time for GYY4137 to significantly increase H₂S level in the blood at the time of reperfusion. Animals underwent 30 minutes myocardial ischaemia and 2 hours of reperfusion and randomly assigned to one of five groups (Figure 5.2):

- Group 1: Control (n=9). Animals were subjected to 30 minutes coronary artery occlusion and 120 minutes reperfusion with saline given as a slow i.v. bolus (500 $\mu\text{L min}^{-1}$) 10 minutes before reperfusion.
- Group 2-4: Each group (n=8) received GYY4137 at 26.6, 133 or 266 $\mu\text{mol kg}^{-1}$, respectively) as a slow i.v. bolus (500 $\mu\text{L min}^{-1}$) 10 minutes before reperfusion.
- Group 5: Depleted GYY4137 (n=6). GYY4137 solution (100 mg mL⁻¹) was prepared in saline and left uncovered for 72 hours at room temperature to dissipate all H₂S as described in (Alexander et al., 2015), then administered at a dose of 266 $\mu\text{mol kg}^{-1}$ as a slow i.v. bolus (500 $\mu\text{L min}^{-1}$) 10 minutes before reperfusion.

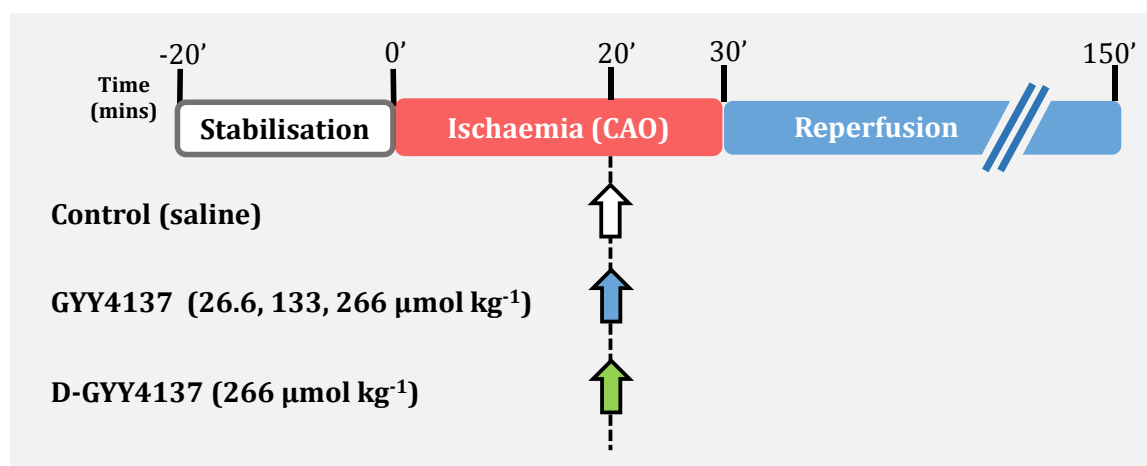


Figure 5.2 Treatment protocol for dose optimization study of GYY4137. After surgical preparation, rats were stabilised for 20 minutes then subjected to 30 minutes of left coronary artery occlusion (CAO) followed by 120 minutes of reperfusion. Control rats received saline, while treatment groups received one of three GYY4137 doses or depleted GYY4137 (D-GYY4137) 10 minutes before reperfusion. Hearts were excised at the end of reperfusion for infarct size determination, $n = 6-10$. Arrows indicate the time of pharmacological interventions.

5.2.3.2 Mechanistic study with the pharmacological inhibitors

The second series of experiments explored the involvement of the key elements of the RISK pathway in the cardioprotective effect of GYY4137. The optimum dose, within the applied dosing range, of GYY4137 (266 $\mu\text{mol kg}^{-1}$) was selected from the first series and animals were randomised into six treatment groups (Figure 5.3).

- Group 1: Control ($n=7$). Animals were subjected to coronary occlusion and reperfusion with saline or DMSO 5% (v/v) given as a slow i.v. bolus (500 $\mu\text{L min}^{-1}$) 15 minutes before reperfusion. DMSO was used as vehicle for LY294002. Since DMSO exerted no effect on either cardiodynamics or infarct size, saline- and DMSO-treated animals are reported collectively.

- Group 2: GYY4137 (n=7). A slow bolus dose of GYY4137 ($266 \mu\text{mol kg}^{-1}$, $500 \mu\text{L min}^{-1}$) was administered at 10 minutes before reperfusion.
- Group 3: GYY4137 + L-NAME (n=7). An intravenous bolus dose of L-NAME (20 mg kg^{-1}) was administered 15 minutes before reperfusion followed by GYY4137 ($266 \mu\text{mol kg}^{-1}$, $500 \mu\text{L min}^{-1}$) 10 minutes before reperfusion.
- Group 4: L-NAME (n=6). An intravenous bolus dose of L-NAME (20 mg kg^{-1}) was administered 15 minutes before reperfusion.
- Group 5: GYY4137 + LY294002 (n=6). An intravenous bolus dose of LY294002 (0.1 mg kg^{-1} in 5% DMSO) was given 15 minutes before reperfusion followed by GYY4137 ($266 \mu\text{mol kg}^{-1}$, $500 \mu\text{L min}^{-1}$) 10 minutes before reperfusion.
- Group 6: LY294002 (n=6). A bolus dose of LY294002 (0.1 mg kg^{-1} in 5% (v/v) DMSO) was administered intravenously 15 minutes before reperfusion.

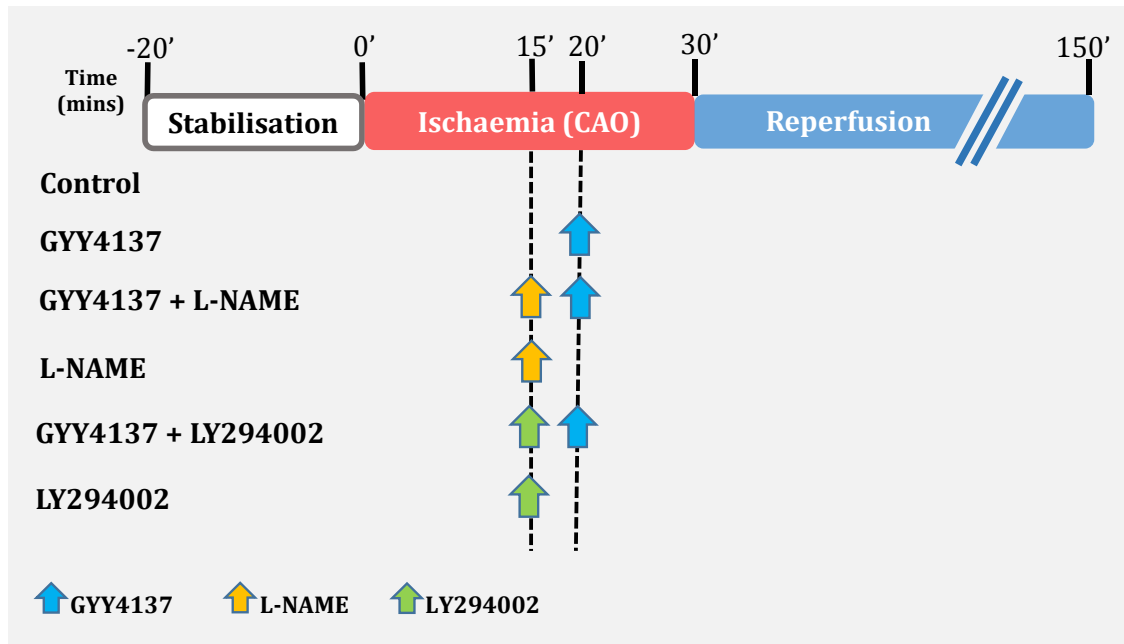


Figure 5.3 Treatment protocol for the mechanistic study of GYY4137. Following stabilisation, rats were subjected to 30 minutes of left coronary artery occlusion and 120 minutes of reperfusion. Animals were randomised into six groups. GYY4137 was administered 10 minutes before reperfusion. LY294002 and L-NAME were administered 15 minutes before reperfusion. Hearts were excised at the end of reperfusion for infarct size determination, $n = 6-7$. Arrows indicate the time of pharmacological interventions.

5.2.3.3 Preparation of myocardial samples for protein analysis

In a parallel series of experiments, rats were subjected to the same interventions as illustrated in section 5.2.3.2, to prepare myocardium samples for biochemical analysis. After 5 minutes of reperfusion, the experiment was terminated and myocardial biopsies were harvested from the left ventricle, rapidly frozen in liquid nitrogen then kept at $-80\text{ }^{\circ}\text{C}$ for Western blotting of Akt, eNOS, GSK-3 β and ERK1/2 (Figure 5.4).

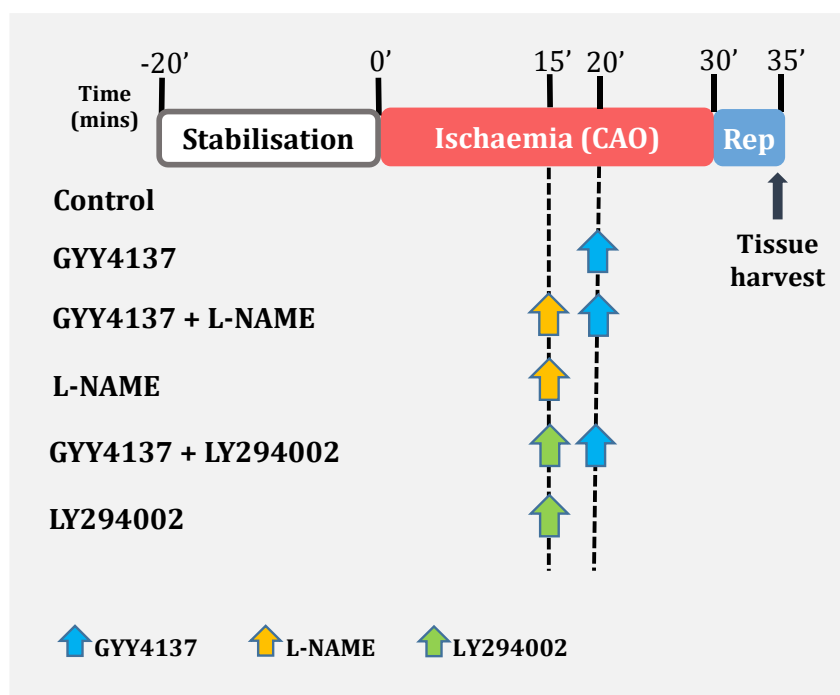


Figure 5.4 Experimental protocol of tissue sampling following GYY4137 treatment in the presence and absence of LY294002 and L-NAME. Animals were stabilised for 20 minutes and randomised into six groups. LY294002 and L-NAME were given at 15 minutes of ischaemia either alone or concomitantly with GYY4137. All rats underwent 30 minutes myocardial ischaemia and 5 minutes reperfusion followed by harvesting myocardial samples from the left ventricle. The tissue samples were snap frozen and kept under -80°C for analysis by immunoblotting. Arrows indicate the time of pharmacological interventions. $n=4$.

5.2.3.4 Western blotting analysis

Protein immunoblotting was carried out to analyse protein phosphorylation of the RISK pathway kinases, namely Akt, eNOS, GSK-3 β and ERK1/2, following GYY4137 treatment in the presence and absence of LY294002 and L-NAME. Myocardial samples were harvested from the left ventricle at 5 minutes of reperfusion as described in Chapter 2, section 2.6.1. Protein extraction was carried out as described in Chapter 2, section 2.6.2, and the protein level for the left ventricle biopsies was determined using bicinchoninic acid (BCA) assay as described in Chapter 2, section 2.6.3. Immunoblotting of the proteins of interest was performed as reported in Chapter 2, section 2.6.4.

5.3 Results

5.3.1 Inclusion/exclusion criteria

In dose-response study, 42 rats were used, of which two were excluded from final analysis, one due to failure of TTC staining and one rat which did not survive the ischaemia-reperfusion protocol. Thus data for 40 successfully completed experiments are reported. In the mechanistic study, 66 rats were employed, of which three did not complete the ischaemia-reperfusion protocol. Thus, data from a total of 63 completed experiments are reported in series 2: these comprised 39 completed infarct size experiments and 24 preparations for Western blot analysis (no exclusion). It is worth mentioning here that the number animals excluded is fewer than the previous series of experiments as the operator became more competent in conducting the surgery and developed the skills to carry out the intubation and cannulation.

5.3.2 Dose-response study of GYY4137

5.3.2.1 Hemodynamic parameters

Baseline hemodynamics for dose-response study are summarised in Table 5.2. There was no significant difference in any of the baseline parameters among the experimental groups. Cardiodynamics (MAP and RPP) measurements before ischaemia, during ischaemia and at the end of reperfusion are also presented in Table 5.2. GYY4137 had no detectable effect on cardiodynamics during the ischaemia/reperfusion protocol.

Table 5.2 Summary of Baselines and cardiodynamics for GYY4137 dose-effect study during ischaemia/reperfusion protocol.

Experimental Protocol	<i>n</i>	BW (g)	Baseline		20 min Ischaemia		120 min Reperfusion	
			RPP (mmHg min ⁻¹)*10 ³	MAP (mmHg)	RPP (mmHg min ⁻¹)*10 ³	MAP (mmHg)	RPP (mmHg min ⁻¹)*10 ³	MAP (mmHg)
Control	10	355 ± 6	37.5 ± 2.0	88 ± 4	27.9 ± 1.8	68 ± 4	24.0 ± 1.4	53 ± 3
GYY4137 26.6 μmol kg ⁻¹	8	360 ± 9	40.3 ± 3.0	90 ± 6	29.1 ± 2.1	71 ± 5	26.3 ± 2.0	59 ± 4
GYY4137 133 μmol kg ⁻¹	8	346 ± 7	41.4 ± 1.8	94 ± 6	29.5 ± 2.2	70 ± 6	24.3 ± 1.5	53 ± 4
GYY4137 266 μmol kg ⁻¹	8	368 ± 6	39.1 ± 1.7	83 ± 4	28.6 ± 2.0	65 ± 5	20.9 ± 1.6	45 ± 3
D-GYY4137	6	368 ± 6	38.4 ± 2.3	85 ± 5	26.3 ± 2.1	69 ± 4	22.7 ± 1.3	48 ± 4

n number of animals per group; *BW* body weight; *RPP* rate pressure product; *MAP* mean arterial pressure. Data are reported as mean ± SEM. There was no significant difference in any of the baselines between the experimental groups (repeated measures ANOVA followed by Bonferroni *post hoc* test).

5.3.2.2 Infarct size following GYY4137 postconditioning

Series 1 examined the response to three doses of GYY4137 on infarct size (Figure 5.5). AAR constituted approximately 40-60% of the total ventricular volume with no significant differences among the treatment groups (Figure 5.5A). Control infarct size (I/AAR%) was $52.5 \pm 4.7\%$ (Figure 5.5B). GYY4137 ($266 \mu\text{mol kg}^{-1}$) produced significant infarct limitation when given 10 minutes before reperfusion compared to control hearts ($27.9 \pm 3.8\%$ vs $52.5 \pm 4.7\%$, $p < 0.01$). This represents a 47% relative reduction in infarct size. In contrast, depleted-GYY4137, produced as described in section 5.2.3.1, which lacked H₂S donating potential but was otherwise structurally identical had no effect on infarct size at the same dose ($51.9 \pm 3.1\%$). These results confirm the dependency of GYY4137's infarct-limiting action on H₂S-releasing capacity.

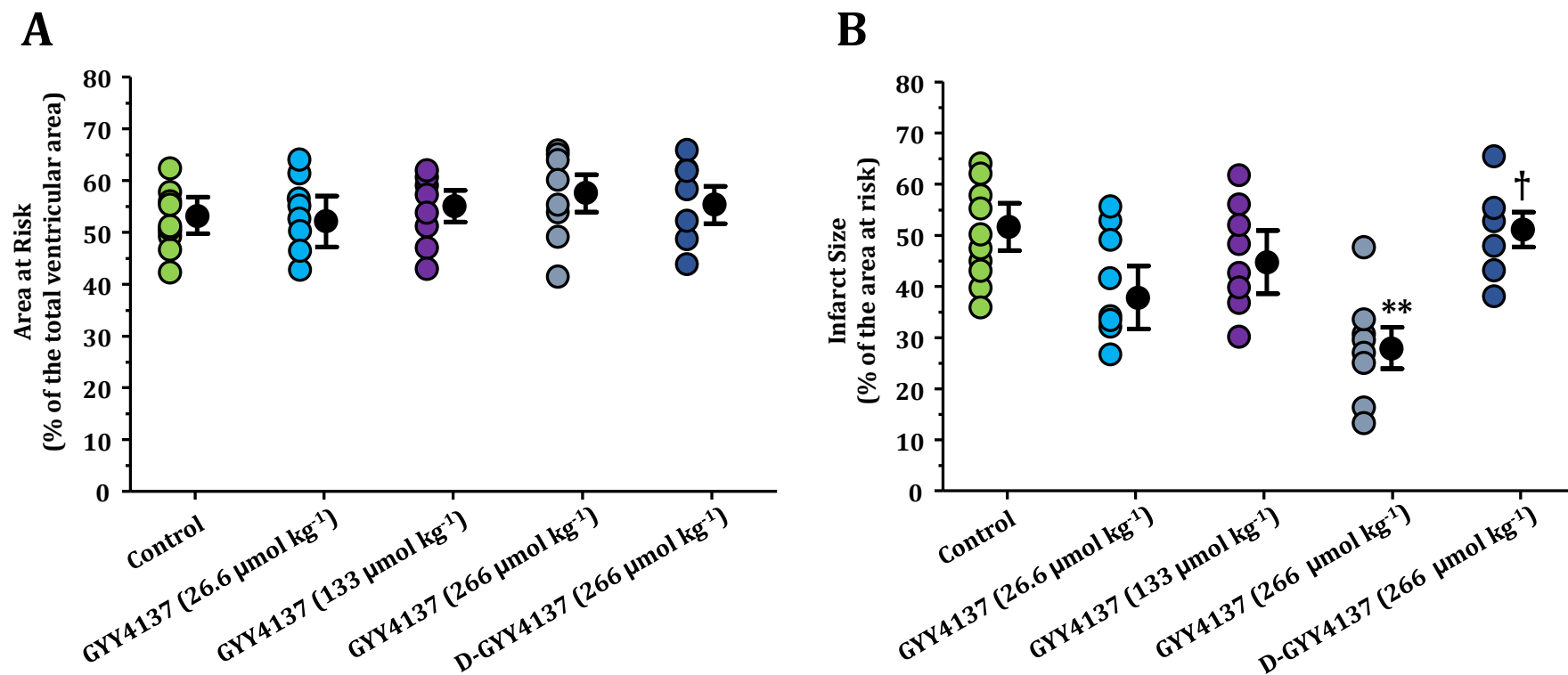


Figure 5.5 Infarct size data of GYY4137's dose-response study. Area at risk was determined Evans' blue exclusion and infarction was assessed by TTC staining. GYY4137 was administered at 26.6, 133, or 266 $\mu\text{mol kg}^{-1}$ 10 minutes before reperfusion. **A.** area at risk as a percentage of the total ventricular volume. **B.** myocardial infarction expressed as a percentage of the area at risk. The mean of infarct size is reported by a filled circle (with error bars) along with the individual values. ** $p < 0.01$ versus Control; † $p < 0.05$ versus GYY4137 266 $\mu\text{mol kg}^{-1}$ (one way ANOVA with Newman Keuls post hoc test).

5.3.3 Mechanistic study: involvement of PI3K/Akt and eNOS

5.3.3.1 Haemodynamic parameters

Baselines and cardiodynamics measurements throughout ischaemia/reperfusion protocol are presented in Table 5.3. There was no significant difference in the baseline parameters among the experimental groups. Similar to the first series, GYY4137 did not have any effect on either RPP or MAP. Blocking either PI3K with LY294002 or endogenous nitric oxide synthesis with L-NAME resulted in no change in either RPP or MAP in the presence or absence of GYY4137.

5.3.3.2 Infarct size data

The second series of experiments was undertaken to examine the role of components of the RISK signalling pathway in the protective effect of GYY4137 (Figure 5.6). There was no significant difference in the area at risk among the experimental groups (Figure 5.6A). GYY4137 ($266 \mu\text{mol kg}^{-1}$) elicited a significant reduction in %I/AAR compared to control ($27.6 \pm 2.0\%$ vs $56.8 \pm 3.5\%$, respectively, $p < 0.001$, Figure 5.6B). Pharmacological inhibition of eNOS with L-NAME prior to GYY4137 almost halved the cardioprotective effect of GYY4137 ($41.1 \pm 6.3\%$ vs $27.6 \pm 2.0\%$, respectively, $p < 0.05$), but did not abolish it ($41.1 \pm 6.3\%$ vs $56.8 \pm 3.5\%$, respectively, $p < 0.01$, Figure 5.6B). Concomitant administration of LY294002 to inhibit PI3K activity completely abrogated the cardioprotective effect of GYY4137 ($49.8 \pm 4.2\%$ vs $56.8 \pm 3.5\%$, respectively, $p > 0.05$). Neither L-NAME nor LY294002 had any effect on infarct size when given alone ($55.7 \pm 3.3\%$ and $51.2 \pm 2.7\%$ respectively, both $p > 0.05$ vs control).

Table 5.3 Summary of baseline parameters and haemodynamics throughout acute myocardial infarction protocol for the mechanistic study of GYY4137 with the pharmacological inhibitors

Experimental Protocol	n	BW (g)	Baseline	20 min Ischaemia	120 min Reperfusion			
			RPP (mmHg min ⁻¹)*10 ³	MAP (mmHg)	RPP (mmHg min ⁻¹)*10 ³	MAP (mmHg)	RPP (mmHg min ⁻¹)*10 ³	MAP (mmHg)
Control	7	384 ± 7	36.3 ± 2.2	85 ± 5	24.8 ± 2.2	61 ± 6	21.2 ± 2.0	48 ± 4
GYY4137	7	379 ± 8	41.3 ± 3.0	96 ± 6	26.8 ± 1.6	66 ± 6	21.6 ± 1.1	47 ± 2
GYY4137 + L-NAME	7	387 ± 7	39.3 ± 2.5	88 ± 5	29.5 ± 2.4	69 ± 5	19.4 ± 2.4	50 ± 6
L-NAME	6	381 ± 9	39.3 ± 1.6	97 ± 3	30.4 ± 2.1	76 ± 7	22.4 ± 5.1	57 ± 9
GYY4137 + LY294002	6	362 ± 8	39.3 ± 1.8	88 ± 4	30.2 ± 1.8	71 ± 5	24.2 ± 0.6	53 ± 1
LY294002	6	367 ± 11	44.5 ± 2.8	98 ± 4	29.6 ± 1.2	72 ± 4	25.0 ± 0.7	54 ± 2

n number of animals per group; BW body weight; RPP rate pressure product; MAP mean arterial pressure. Data are expressed as mean ± SEM. There was no significant difference in any of the baselines between the experimental groups (repeated measures ANOVA with Bonferroni *post hoc* test).

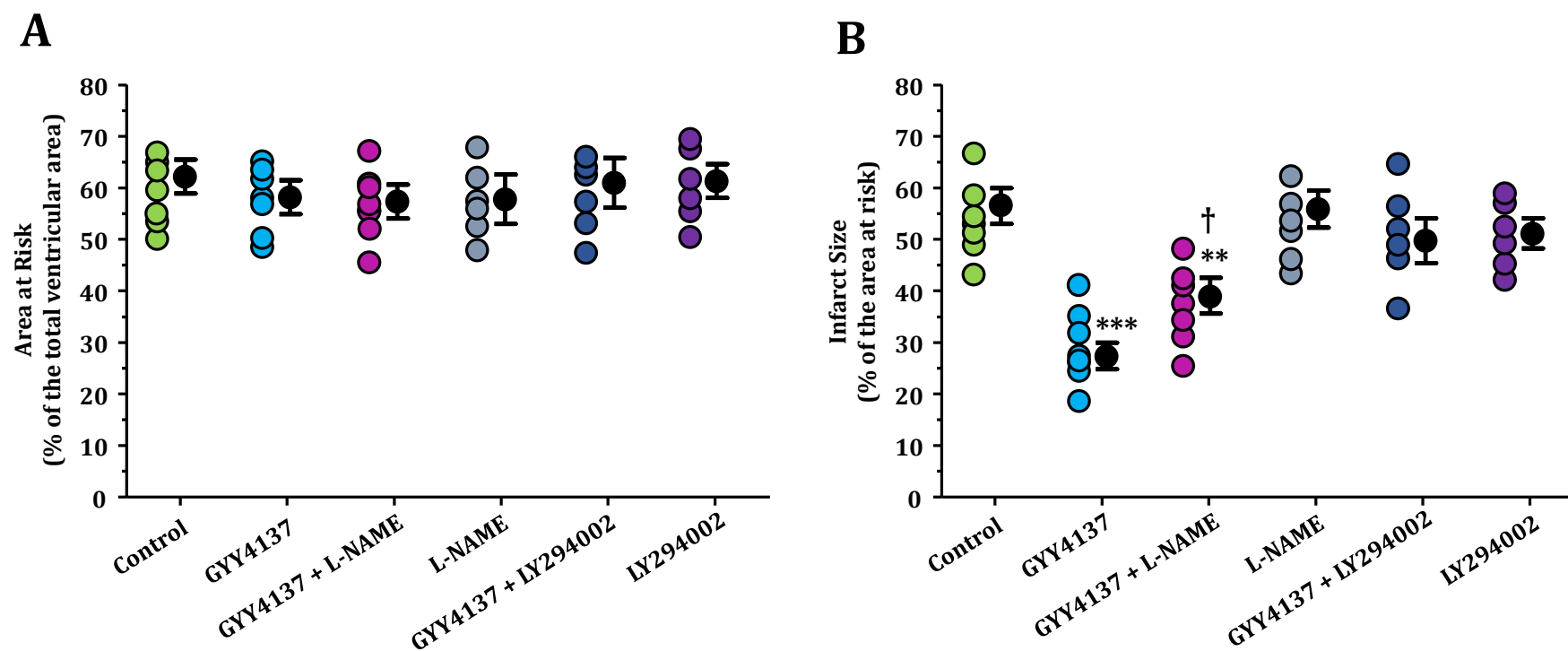


Figure 5.6 Infarct data of GYY4137 with pharmacological inhibitors. Infarct size quantification was carried out using dual staining with Evans' blue and TTC. GYY4137 was administered at $266 \mu\text{mol kg}^{-1}$ 10 minutes before reperfusion. LY294002 or L-NAME were given 15 minutes before reperfusion. **A.** area at risk expressed as a percentage of the total ventricular volume. **B.** infarct size expressed as a percentage of the area at risk. The mean of infarction presented by a filled circle (with error bars) next to the individual value of each group (open circles). ** $p < 0.01$ versus Control; *** $p < 0.001$ versus control; † $p < 0.01$ versus GYY4137 (one way ANOVA with Newman Keuls post hoc test).

5.3.4 Protein phosphorylation following postconditioning with GYY4137

The extent of phosphorylation of Akt, eNOS, GSK-3 β and ERK1/2 in early reperfusion was investigated with phospho-specific antibodies to determine the possible roles in cardioprotection by GYY4137. Hearts were postconditioned with GYY4137 at 10 minutes before reperfusion in the presence and absence of PI3K inhibitor (LY294402) or constitutive nitric oxide synthase inhibitor (L-NAME). Immunoreactivity measurements of the RISK pathway components, namely Akt, eNOS, GSK-3 β and ERK1/2, were performed using myocardial tissue sampled from the left ventricle 5 minutes after reperfusion. There was no significant difference in protein expression to GAPDH of Akt, eNOS, GSK-3 β or ERK1/2 among any of the experimental groups. There was a significant 2.8-fold increase ($p < 0.05$ vs. control) in phospho-ser⁴⁷³Akt at reperfusion following GYY4137 treatment (Figure 5.7A). Prior administration of L-NAME did not limit this increase in Akt phosphorylation. Both GYY4137 and L-NAME did not have an effect in the total Akt expression in the myocardium (Figure 5.7B). However, administration of LY294002 prior to GYY4137 abolished Akt phosphorylation (Figure 5.7A) with no effect on total Akt (Figure 5.7B). Postconditioning with GYY4137 also increased eNOS phosphorylation at the activating ser¹¹⁷⁷ site by 2.2-fold in early reperfusion ($p < 0.05$ vs. control; Figure 5.8A). This activation was abrogated by concomitant administration of L-NAME which interestingly showed a trend of increase in the total eNOS expression in the tissue in the presence and absence of GYY4137 (Figure 5.8B). However, this trend did not reach the significance threshold. Activation of eNOS with GYY4137 was also abolished by co-administration of LY294002 with no significant effect on the total eNOS expression in the myocardium (Figure 5.8B). Ser⁹ phosphorylation of GSK-3 β

was also increased 2.2-fold by GYY4137 (Figure 5.9A). This phosphorylation, leading to inactivation of GSK-3 β , was not affected L-NAME. However, pre-treatment with LY294002 prior to GYY4137 abrogated GSK-3 β phosphorylation. GYY4137 had no significant effect on the phosphorylation of ERK1/2 at early reperfusion (Figure 5.10A).

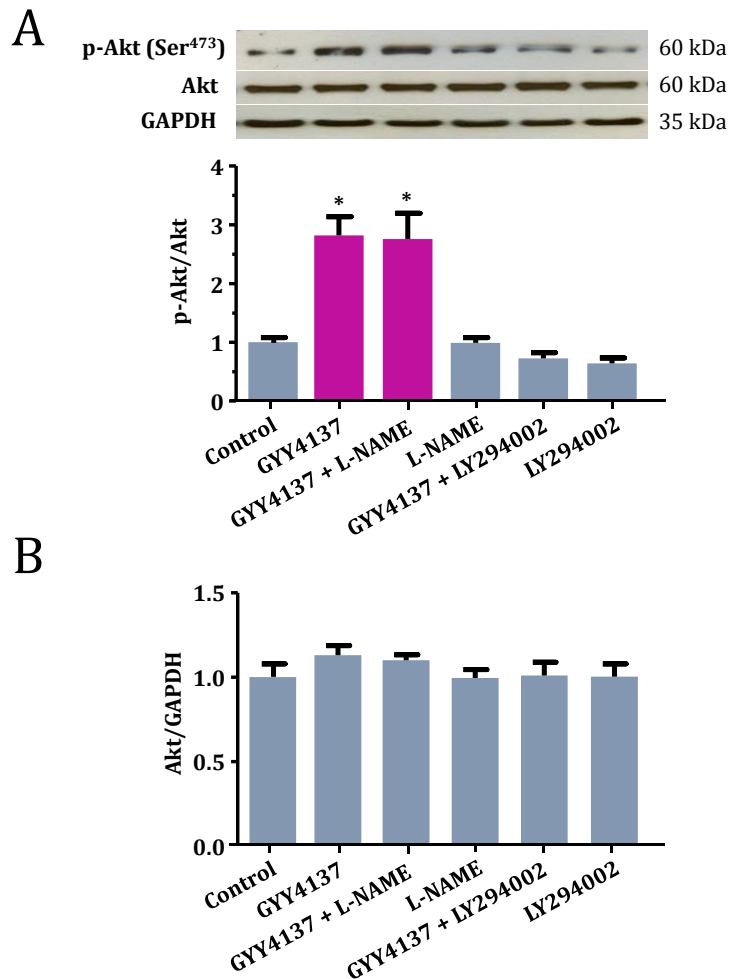


Figure 5.7 Representative blots and Western blot analysis of the phosphorylation of Akt in left ventricular myocardium, harvested from the area at risk 5 minutes after reperfusion, following GYY4137's postconditioning. Histograms show densitometric ratios of (A) phosphorylated Akt to total Akt (B) total Akt to GAPDH. GAPDH was used as loading control for all determinations. Data were analysed using Kruskal-Wallis followed by Dunn's post hoc test and reported as mean \pm SEM. * $p < 0.05$ versus control. In all groups, $n = 4$ hearts from 4 independent experiments.

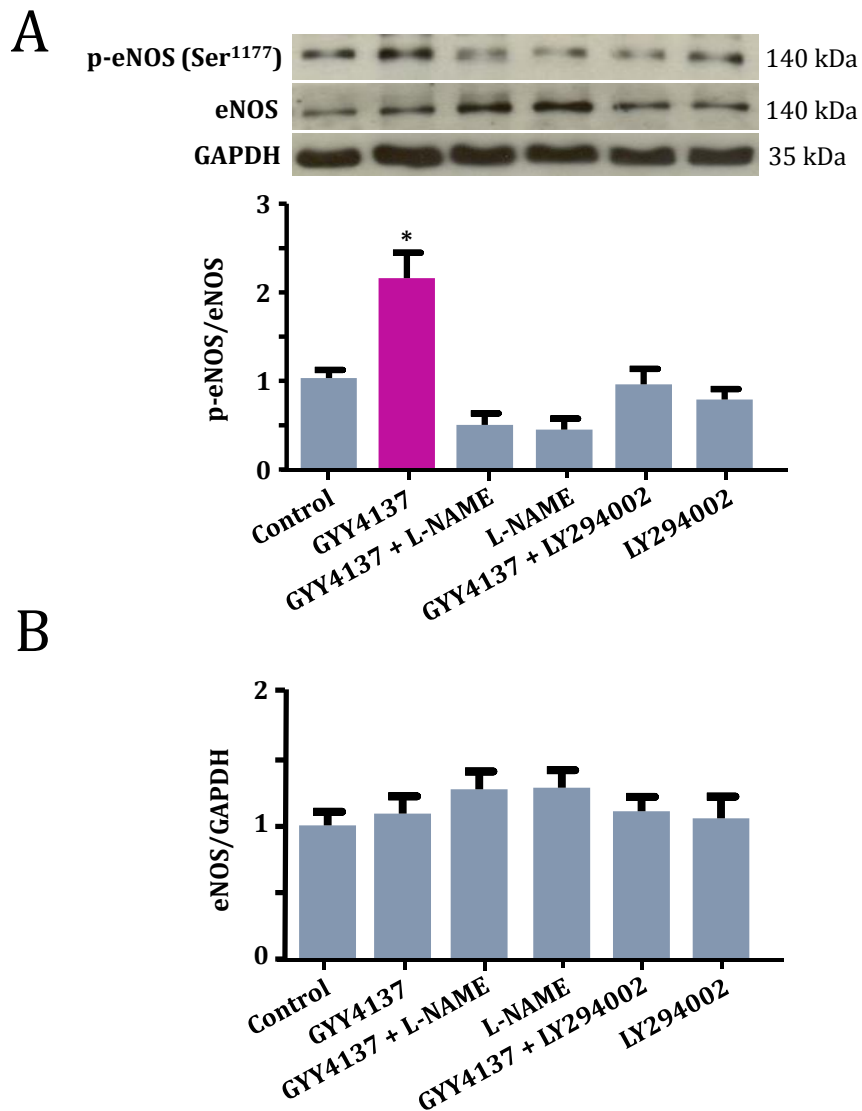


Figure 5.8 Representative blots and Western blot analysis of the phosphorylation of eNOS in left ventricular myocardium, harvested from the area at risk 5 minutes after reperfusion, following GYY4137's postconditioning. Histograms show densitometric ratios of (A) phosphorylated eNOS to total eNOS (B) total eNOS to GAPDH. GAPDH was used as loading control for all determinations. Data were analysed using Kruskal-Wallis followed by Dunn's post hoc test and reported as mean \pm SEM. * $p < 0.05$ versus control. In all groups, $n = 4$ hearts from 4 independent experiments.

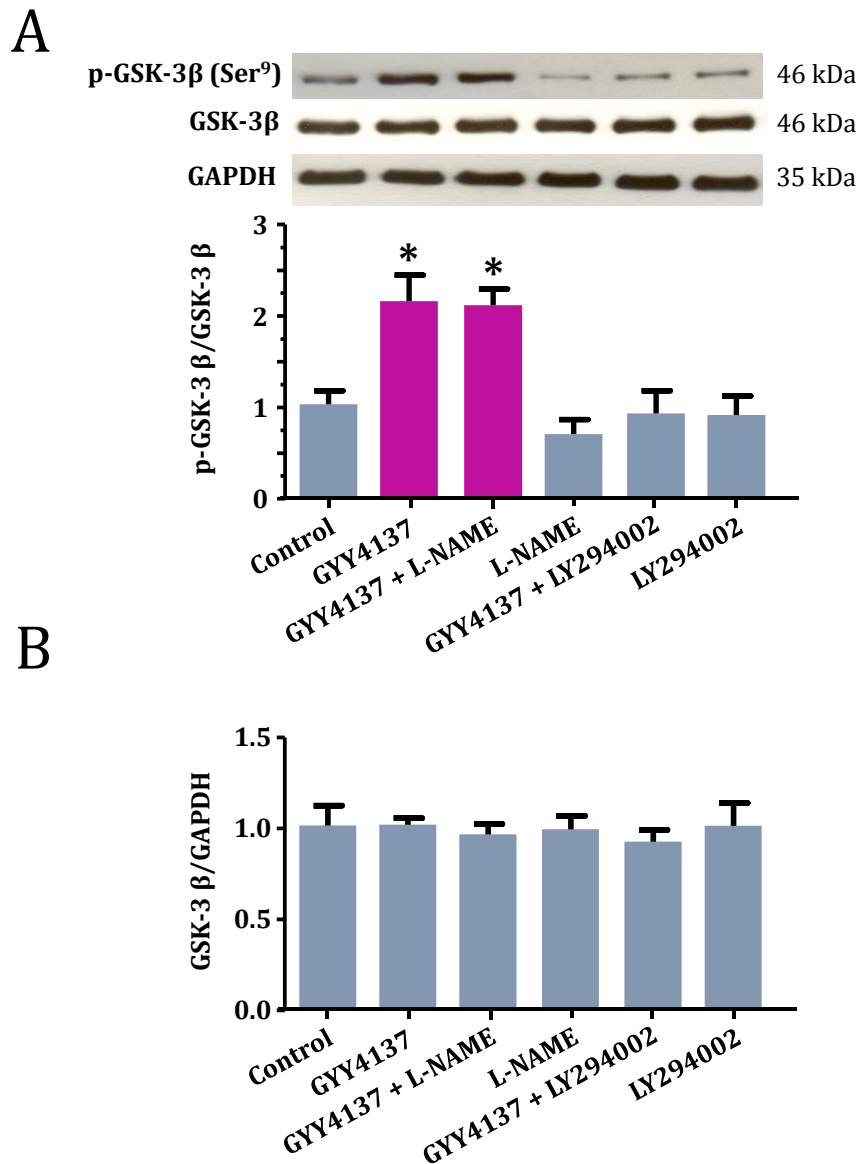


Figure 5.9 Representative blots and Western blot analysis of the phosphorylation of GSK-3 β in left ventricular myocardium, harvested from the area at risk 5 minutes after reperfusion, following GYY4137's postconditioning. Histograms show densitometric ratios of (A) phosphorylated GSK-3 β to total GSK-3 β (B) total GSK-3 β to GAPDH. GAPDH was used as loading control for all determinations. Data were analysed using Kruskal-Wallis followed by Dunn's post hoc test and reported as mean \pm SEM. * $p < 0.05$ versus control. In all groups, $n=4$ hearts from 4 independent experiments.

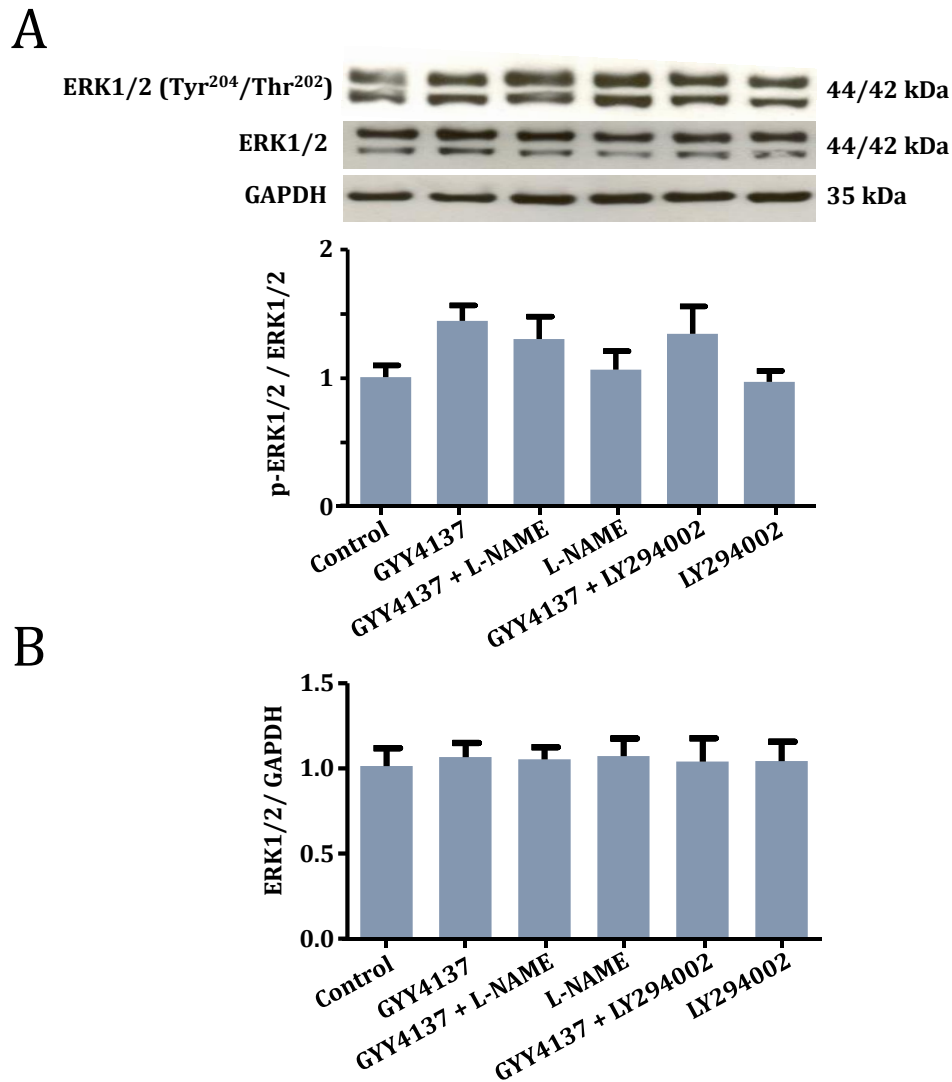


Figure 5.10 Representative blots and Western blot analysis of the phosphorylation of ERK1/2 in left ventricular myocardium, harvested from the area at risk 5 minutes after reperfusion, following GYY4137's postconditioning. Histograms show densitometric ratios of (A) phosphorylated ERK1/2 to total ERK1/2 (B) total ERK1/2 to GAPDH. GAPDH was used as loading control for all determinations. Data were analysed using Kruskal-Wallis and reported as mean \pm SEM. For all groups, $n = 4$ hearts from 4 independent experiments.

5.4 Discussion

The principal observations of this study can be summarised as follows:

- 1- GYY4137 limited myocardial infarction *in vivo* when given specifically prior to reperfusion indicating potent attenuation of lethal reperfusion injury in a postconditioning-like manner.
- 2- GYY4137 relied on its H₂S-generating capacity to elicit its cardioprotection against acute myocardial infarction.
- 3- The infarct-limiting effect of GYY4137 at early reperfusion was mediated through activation of the PI3K/Akt survival cascade.
- 4- There was a partial dependency of GYY4137's protective effect on increased eNOS phosphorylation.
- 5- GYY4137 inhibited GSK-3 β activity at early reperfusion by increasing the phosphorylation of its ser⁹ site downstream of PI3K/Akt signalling.

These findings support the hypothesis that administration of GYY4137 at reperfusion can protect the heart against reperfusion injury by activating the key components of the RISK cascade (PI3K/Akt/NO) and inhibition of GSK-3 β activity (Figure 5.11).

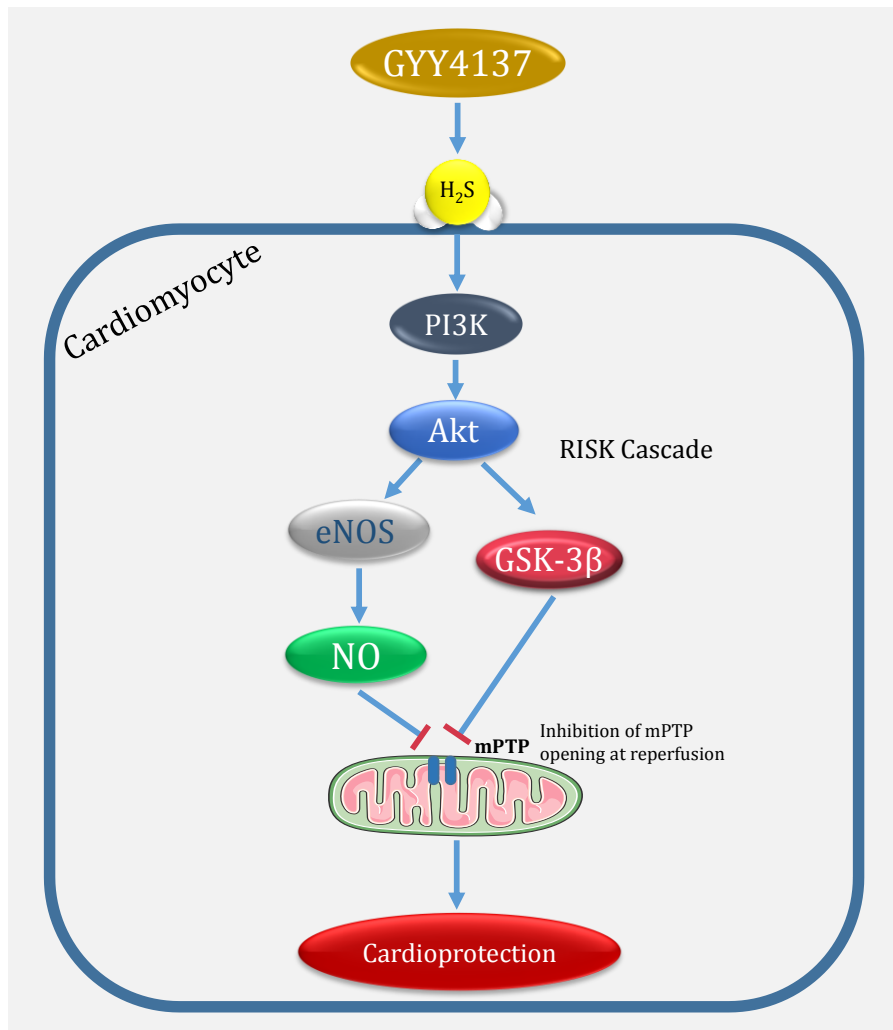


Figure 5.11 GYY4137, a donor of H₂S, induces marked limitation of myocardial infarct size when given shortly before reperfusion. Based on the present experimental data, we present a mechanistic scheme by which GYY4137 mediates its cardioprotection against reperfusion injury. GYY4137 releases H₂S which triggers a key component of the reperfusion injury salvage kinase cascade, namely PI3K/Akt activation at reperfusion. Downstream of activated Akt, phosphorylation of eNOS and GSK-3β are induced by GYY4137 treatment. Although not yet determined, it seems plausible that GYY4137 eventually inhibits the opening of PTP at early reperfusion as a result of the increase in NO level and inhibition GSK-3β activity, resulting in reduced cardiomyocyte susceptibility to lethal reperfusion injury.

5.4.1 Infarct limitation by GYY4137

The results show for the first time the effect of GYY4137, as a slow-releasing H₂S donor, on myocardial infarction in an *in vivo* model. Intracellular levels of

H₂S are reported to be decreased during ischaemia-reperfusion as a result of overwhelming ROS generation which limits H₂S synthesis and increases its degradation (Vandiver and Snyder, 2012). GYY4137 elicited significant infarct limitation when administered prior to reperfusion. Depleted GYY4137 (Alexander et al., 2015) was employed as a control to ensure that any detectable effect was due to H₂S released and not by the parent molecule or by-products formed from GYY4137 decomposition. Depleted GYY4137 had no effect on infarct size and this is consistent with previous studies where loss of H₂S from GYY4137 was shown to be associated with loss of biological activity (Li et al., 2009, Whiteman et al., 2010b, Fox et al., 2012, Jamroz-Wisniewska et al., 2014, Alexander et al., 2015).

This is the first study of pharmacological postconditioning against reperfusion injury *in vivo* using GYY4137 as a stable H₂S donor. Although inorganic H₂S generators (NaHS and Na₂S) have been used in different experimental species, the specific targeting of reperfusion injury by GYY4137 in this study is novel. Several studies have investigated the effect of H₂S against myocardial ischaemia/reperfusion when commercially available sulfide salts were perfused or given pre-ischaemia. For example, Johansen et al. (2006) were the first to show that NaHS limited infarct size in a rat isolated heart preparation, while Pan et al. (2009), Sivarajah et al. (2009), Zhuo et al. (2009) and Yao et al. (2012) all showed that NaHS limited infarct size in an *in vivo* rat model through diverse mechanisms. Part of this variation is arguably due to the unstable nature of these H₂S sources, in addition to the different experimental conditions and end-points of interest. Using garlic derivatives as organic sources of H₂S, Zhang et al. (2001) and Chuah et al (2007) reported that allitridum and S-allylcysteine

respectively also elicited cardioprotection against myocardial infarction when given before ischaemia. Preconditioning the heart with the thiol derivative S-diclofenac was also protective partially through the opening of mitochondrial K_{ATP} channels (Rossoni et al., 2008). Investigators have also examined the possibility of postconditioning the myocardium using NaHS and Na_2S . For example, Elrod et al. (2007), Sodha et al. (2009) and Lambert et al. (2014) all reported that Na_2S protected mouse heart against myocardial infarction *in vivo* when given at reperfusion. Bibli et al. (2015) showed that a bolus dose of NaHS 10 minutes before reperfusion then continuous infusion of NaHS till the end of reperfusion was required to significantly exert cardioprotection in rabbit. In comparison with these results, in this study we showed that a single bolus dose of GYY4137 at reperfusion had a significant cardioprotective effect against myocardial infarction in the rat. To our knowledge, the only other long-lasting H_2S donors that have been reported are the polysulfide diallyl trisulfide (DATS) and SG-1002, a thiol-activated H_2S donor. Despite generating 10 times less H_2S than Na_2S , DATS was shown to improve mitochondrial respiration and stimulate eNOS at reperfusion in an *in vivo* mouse model of ischaemia/reperfusion injury. However, DATS is a polysulfide compound, and thus cannot be considered a pure H_2S donor with the possibility of off-target effects. Moreover, H_2S release from GYY4137 is reported to last longer compare to DATS (Li et al., 2008, Predmore et al., 2012). In the setting of pressure-overload-induced heart failure, SG-1002-treated hearts were protected during transverse aortic constriction via triggering VEGF/Akt/eNOS/NO/cGMP pathway. Recently, SG-1002 has successfully passed Phase I clinical study in patient with heart failure (ClinicalTrials.gov #NCT01989208 and #NCT02278276), by increasing blood H_2S level and circulating NO bioavailability (Polhemus et al., 2015). However,

none of these studies have shown that the observed effects are due to H₂S release due to the lack of negative control (like depleted GYY4137, for example). Therefore, there is persuasive experimental evidence that a stable level of H₂S release confers effective cardioprotection against ischaemia/reperfusion injury. The present study confirms for the first time that administration of GYY4137 prior to reperfusion (postconditioning), rather than prior to coronary artery occlusion (preconditioning), exerts a marked cardioprotective effect due to H₂S-releasing capacity. This cardioprotection by GYY4137 did not have an effect on cardiodynamics which, to some extent, shows a potential cardiac safety that needs further investigation.

5.4.2 GYY4137 postconditioning activates PI3K/Akt signalling

The second series of experiments aimed to explore the signalling mechanisms underpinning the protective effect of GYY4137. The involvement during early reperfusion of specific kinase mechanisms, notably activation of PI3K/Akt and/or ERK1/2, activation of eNOS and inhibition of GSK-3 β , has attracted considerable attention in relation to cardiac conditioning phenomena, especially postconditioning. Elucidation of the RISK pathway has confirmed that it is a key modulator of protection against reperfusion injury in many species, although not all. Here, we explored the effects of pharmacological inhibition of two key components, PI3K/Akt and eNOS, confirmed by assessment of the phosphorylation status of these proteins. We found that the PI3K inhibitor LY294002 abrogated the infarct-limiting effect of GYY4137 which indicated the involvement of PI3K/Akt survival pathway in cardioprotection established by GYY4137. This was supported by the observation that GYY4137 increased Akt

phosphorylation in left ventricular myocardium during early reperfusion, an effect abolished by LY294002. Li et al. (2015a) showed that NaHS at reperfusion limited cell death by activating PI3K/Akt pathway in aging rat heart and cardiomyocytes. However, Lambert et al. (2014) demonstrated that in diabetic rats NaHS-induced postconditioning might signal through the other arm of the RISK pathway, namely ERK1/2. LY294002 alone had no significant effect on either the infarct size or Akt phosphorylation compared to control which is consistent with the findings of other investigators (Wang et al., 2013, Barsukevich et al., 2015). This suggests that the PI3K/Akt pathway is almost inactive at basal physiological levels of H₂S.

We also investigated the involvement of ERK1/2 in cardioprotection established by GYY4137. In contrast to Akt phosphorylation, we observed no significant increase in ERK1/2 phosphorylation at early reperfusion following postconditioning with GYY4137. It has been reported by others that a bolus dose of Na₂S at reperfusion could activate ERK1/2 and also inhibit GSK-3 β (Lambert et al., 2014, Li et al., 2015b, Bibli et al., 2015). However, since in our hands GSK-3 β phosphorylation (leading to enzyme inhibition) by GYY4137 was abrogated by LY294002, this suggests it is downstream of PI3K/Akt, rather than ERK1/2. It again emphasises the physiological differences between bolus sulfide (with NaHS or Na₂S) and H₂S generated in a more physiological manner (with GYY4137).

5.4.3 Dependency of GYY4137-postconditioning on NO

Inhibition of NO synthesis using L-NAME had no effect on the infarct size *per se* which is consistent with other investigators (Fradorf et al., 2010, Imani et al.,

2011). This observation implies that NO does not afford any cardioprotection against myocardial infarction at basal physiological levels. GYY4137 treatment induced an increase in the phosphorylation of eNOS at its activating site, ser¹¹⁷⁷ suggesting that NO bioavailability is increased following GYY4137 treatment. L-NAME prior to GYY4137 administration limited the phosphorylation of eNOS and partially attenuated infarct limitation but did not completely abolish the protective effect. These data suggest that enhancing NO bioavailability synergises the cardioprotection of GYY4137 against reperfusion injury but blocking eNOS phosphorylation only partially limits the cardioprotection of GYY4137, suggesting the involvement of parallel NO-independent pathway(s). There has been considerable interest in cross-regulation of NO and H₂S but the nature of their interactions is uncertain, at least in part because of the large variation in experimental conditions.

SG-1002, H₂S donor, was protective and increased NO bioavailability in an *in vivo* model of heart failure (Kondo et al., 2013). An increase in NO metabolites following DATS treatment was also observed by Lefer and co-workers (Predmore et al., 2012) in mouse heart. King et al. (2014) found that H₂S did not limit infarction in eNOS phospho-mutant (ser^{1179A}) or eNOS knockout mice. Considered together, these studies suggest that an increase in one of the gaseous mediators can eventually lead to an increase in the other but the picture is obscured by variations across species, pathological models and tissue types. The NO-dependency of H₂S has recently been studied by Bibli et al. (2015) in an *in vivo* model of myocardial infarction using two species, rabbit and mouse. Pharmacologically limiting NO availability with L-NAME did not limit the protection of NaHS in rabbits, while genetic mutation or pharmacological

blockade of eNOS totally abolished H₂S-induced protection in mice. Dependency of NaHS-induced cardioprotection on NO in mice was previously reported by Sojitra *et al.* (2012). Together and in line with our data, it seems plausible that NO involvement in the infarct-limiting effect of H₂S could be tissue and/or species-dependent. Further detailed work needs to be carried out for better understanding of the molecular pharmacology of these molecules and to enhance the clinical implementation of H₂S-delivering systems.

5.4.4 GYY4137 postconditioning attenuates GSK-3 β phosphorylation

GSK-3 β has been proposed as one of the key end effectors of some cardioprotective manoeuvres, particularly ischemic conditioning phenomena. It has been demonstrated that GSK-3 β promotes the opening of mitochondrial permeability transition pore (PTP) during reperfusion, an event thought to be a major determinant of cell death (Cabrera-Fuentes *et al.*, 2016). In isolated cardiomyocytes, Yao *et al.* (2010) and Li *et al.* (2015b) found that NaHS protected against hypoxia/reoxygenation induced cell death by inhibiting GSK-3 β -dependent opening of PTP. In line with these results, the present study demonstrated that GYY4137 increased the phosphorylation of GSK-3 β at Ser⁹ site at reperfusion. This was abolished by LY294002, but not by L-NAME, suggesting that GYY4137 induced inhibition of GSK-3 β is downstream of PI3K/Akt. There is evidence that the increase in Akt phosphorylation (Hausenloy *et al.*, 2009) and NO bioavailability (Burley *et al.*, 2007) at early reperfusion may also inhibit the opening of PTP. Considering these data together, it seems plausible that postconditioning with GYY4137 is associated with a reduced

susceptibility of PTP opening, although this remains to be determined by specific measurements of PTP opening.

5.5 Study limitations

There are still questions which this study did not address and they could be interesting topics for further investigations. This study found that GYY4137 activates the RISK pathway at early minutes of reperfusion to limit the infarct size where infarction was quantified after 2 hours of reperfusion. Nevertheless, whether GYY4137 could exert a comparable cardioprotection via similar or different mechanism(s) with longer reperfusion protocol, where there could be no-flow phenomena or late apoptosis, needs to be investigated. Although spent-GYY4137 did not exert any cardioprotection, the direct effect of GYY4137 administration on the level of H₂S in the heart and circulation needs to be measured. Similarly, measuring the proposed elevation in NO bioavailability as a result of activating eNOS at reperfusion by GYY4137 administration could also underpin the conclusion.

5.6 Conclusion

In summary, we have demonstrated that the slow-releasing H₂S donor GYY4137, but not its H₂S-depleted control, protected the heart against lethal reperfusion injury when administered as an adjunct treatment prior to reperfusion. This cardioprotective action is dependent on activation of PI3K/Akt signalling pathway at early reperfusion, which in turn, increases NO bioavailability by increasing eNOS phosphorylation, and increases the phosphorylation of GSK-3 β . Thus, stable slow-releasing H₂S donor compounds

may be promising candidates for the development of adjunct therapies to reperfusion for the treatment of acute myocardial infarction.

Chapter 6 AP39, a mitochondria-targeting hydrogen sulfide (H₂S) donor, protects against myocardial reperfusion injury independently of salvage kinase signalling

6.1 Introduction

As described in Chapter 1 (section 1.3.6), mitochondria play a pivotal role in cell survival, metabolism and proliferation (Murphy et al., 2016). In myocardial ischaemia/reperfusion injury, rapid pH normalisation, Ca²⁺ overload and overwhelming ROS and RNS generation disturb mitochondrial function and result in the opening of the PTP (Hausenloy and Yellon, 2007). PTP opening leads to collapse of mitochondrial membrane potential and swelling of the mitochondria, leading to loss of ATP-generating capacity and causing the release of cytochrome c into the cytoplasm which initiates apoptosis (Pell et al., 2016, Murphy et al., 2016). PTP opening at reperfusion is believed to be the no-return point of reperfusion injury (Hausenloy et al., 2009). Therapeutic targeting of these processes during the first minutes of reperfusion has been investigated intensively in experimental settings as early reperfusion appears to afford a window of opportunity to prevent PTP opening and ultimately reduce lethal cell injury during reperfusion following acute myocardial ischaemic episodes such as occur in acute myocardial infarction (Ferdinandy et al., 2014).

Hydrogen sulfide (H₂S) is the simplest bioactive thiol (Abe and Kimura, 1996). The long-recognised toxic effects of environmental or exogenous H₂S occur as a result of inhibition of cytochrome c oxidase, an essential enzyme for mitochondrial complex IV respiration, with perturbation of ATP production (Nicholls et al., 2013). However, the roles of endogenous H₂S, in a wide range of physiological systems, have been extensively explored following the discovery that it is produced by several regulated biochemical pathways in mammalian species and can act as a freely diffusible and degradable signalling mediator (Kimura et al., 2011). In myocardium, enhanced levels of H₂S, whether by H₂S supplement or increased endogenous production, has been

shown to protect the heart against ischaemia/reperfusion injury (Elrod et al., 2007, Karwi et al., 2016). However, whether H₂S directly interacts with mitochondria or triggers cytosolic salvage kinases arguably depends on the intracellular level of H₂S, although the majority of these kinases have downstream end effectors at the mitochondrial level that converge on the mitochondria. Therefore, targeting the mitochondria with selective H₂S donors is a plausible therapeutic approach to limit ischaemia/reperfusion injury.

6.1.1 AP39: mitochondria-targeting H₂S donor

The lipophilic triphenylphosphonium (TPP⁺) scaffold is highly positively charged and has been shown to accumulate selectively (100-500 fold compared to the cytosol) in the mitochondrial matrix (Smith et al., 2003b, James et al., 2007). Therefore, the TPP⁺ scaffold has become an attractive moiety for investigation of mitochondrial function by specific delivery of bioactive molecules and probes (Murphy and Smith, 2007, Smith et al., 2011). In previous work, Prime et al. (2009) demonstrated infarct limitation using a mitochondria-targeted NO donor (MitoSNO), where an NO-releasing moiety linked to TPP⁺ was shown to be rapidly and exclusively taken up by mitochondria and increased the mitochondrial NO level. Krieg's group (Methner et al., 2013) showed that MitoSNO works independently of cytosolic PKG, the mechanism which mediates the cardioprotective effect of non-mitochondrial-targeted NO donors. AP39 (10-oxo-10-(4-(3-thioxo-3H-1, 2-dithiol-5-yl)phenoxy)decyl) triphenylphosphonium bromide) represented the first successful prototype to deliver H₂S selectively and at a low concentration to the mitochondria (Figure 6.1A). By virtue of its highly cationic TPP⁺ moiety, AP39 accumulates in the mitochondria due to the mitochondrial membrane potential. It was first characterised by Le Trionnaire et al. (2014) and since then,

several studies have followed-up showing that AP39 could potentially have many therapeutic applications in various pathologies and in different tissues and organs (Table 6.1). Interestingly, this increase in mitochondrial H₂S level following AP39 application did not seem to upregulate or suppress any known endogenous H₂S synthetic pathway, namely CSE, CBS and 3-MST (Ikeda et al., 2015). The rationale for targeted delivery of H₂S to the mitochondria is based on the evidence that H₂S could work as an inorganic fuel for ATP production (Fu et al., 2012), attenuate mitochondrial ROS (mito-ROS) generation (Jha et al., 2008) and preserves mitochondrial integrity (Elrod et al., 2007). There are recent observations that AP39 can successfully deliver H₂S into the mitochondria when given at reperfusion and that the agent reproducibly protects the mitochondria in particular and the cell in general against ischaemia/reperfusion injury in the brain and kidney (Ikeda et al., 2015, Ahmad et al., 2016). We sought to investigate the potential cardioprotection by AP39 against myocardial ischaemia/reperfusion injury when given at reperfusion *in vivo* using the rat model and to elucidate the underlying mechanisms. Moreover, we also employed the mitochondrial targeting scaffold of AP39 (AP219, Figure 6.1B) and H₂S-generating moiety (ADT-OH, Figure 6.1C) individually as controls to characterise whether any of them possess any, cardioprotective effects. These controls are shown to lack any biological activity when used up to micromolar concentration range *in vitro* and *in vivo* (Le Trionnaire et al., 2014, Szczesny et al., 2014, Tomasova et al., 2015). Therefore, they offer the possibility to confirm whether the approach of selective delivery of H₂S into the mitochondria could successfully protect the heart independently of triggering any cytosolic salvage pathway.

Table 6.1 Summary of experimental studies utilising the mitochondria-targeted H₂S donor, AP39, listed in chronological order

Reference	Experimental model(s)	Main observed effect(s)	Mechanism(s)
Le Trionnaire et al. (2014)	HCMVEC/D3 and bEnd.3 MMVEC	- Antioxidant	- Enhanced the expression of Trx-1
Szczesny et al. (2014)	Glucose oxidase-induced oxidative stress in bEnd.3 MMVEC	- Antioxidant and cytoprotective	- Improved cellular bioenergetics and limited mitochondrial DNA damage
Tomasova et al. (2015)	Anaesthetised Wistar rat, HEK293 cell and rat-derived SR	- NO-independent Hypotensive effect	- Reduced heart rate, blood pressure and pulse wave velocity by attenuating Ca ²⁺ current, inhibited RyR2 channel activity and enhanced the conductance of Cl ⁻ channel
(Ikeda et al. (2015)	murine model of CA/CPR	- Improved survival rate and neurological functions	- Attenuated oxidative stress, preserve mitochondrial integrity by inhibiting PTP opening
Ahmad et al. (2016)	NRK-49F and rat model of renal I/RI	- Antioxidant and anti-inflammatory	- Inhibition of neutrophil infiltration and TUNEL staining
Gero et al. (2016)	HG-induced oxidative stress in bEnd.3 MMVEC	- Antioxidant and cytoprotective	- Mitigated mitochondrial oxidants generation and promoted cellular metabolism
Ahmad and Szabo (2016)	Rat model of burn injury	- Anti-inflammatory	- Decreased circulatory IL-6 and IL-10
Lobb et al. (2016)	Renal I/R injury in mice and NRK-52E	- Anti-apoptotic	- Decreased mito-ROS generation and improved mitochondrial membrane potential

HCMVEC human cerebral microvascular endothelial cell; *MMVEC* mouse microvascular endothelial cell; *SR* sarcoplasmic reticulum; *CA/CPR* cardiac arrest and cardiopulmonary resuscitation; *PTP* permeability transition pore; *I/RI* ischaemia/reperfusion injury; *HG* high glucose; *Trx-1* thioredoxin-1; *NRK-52E* rat kidney epithelial cells.

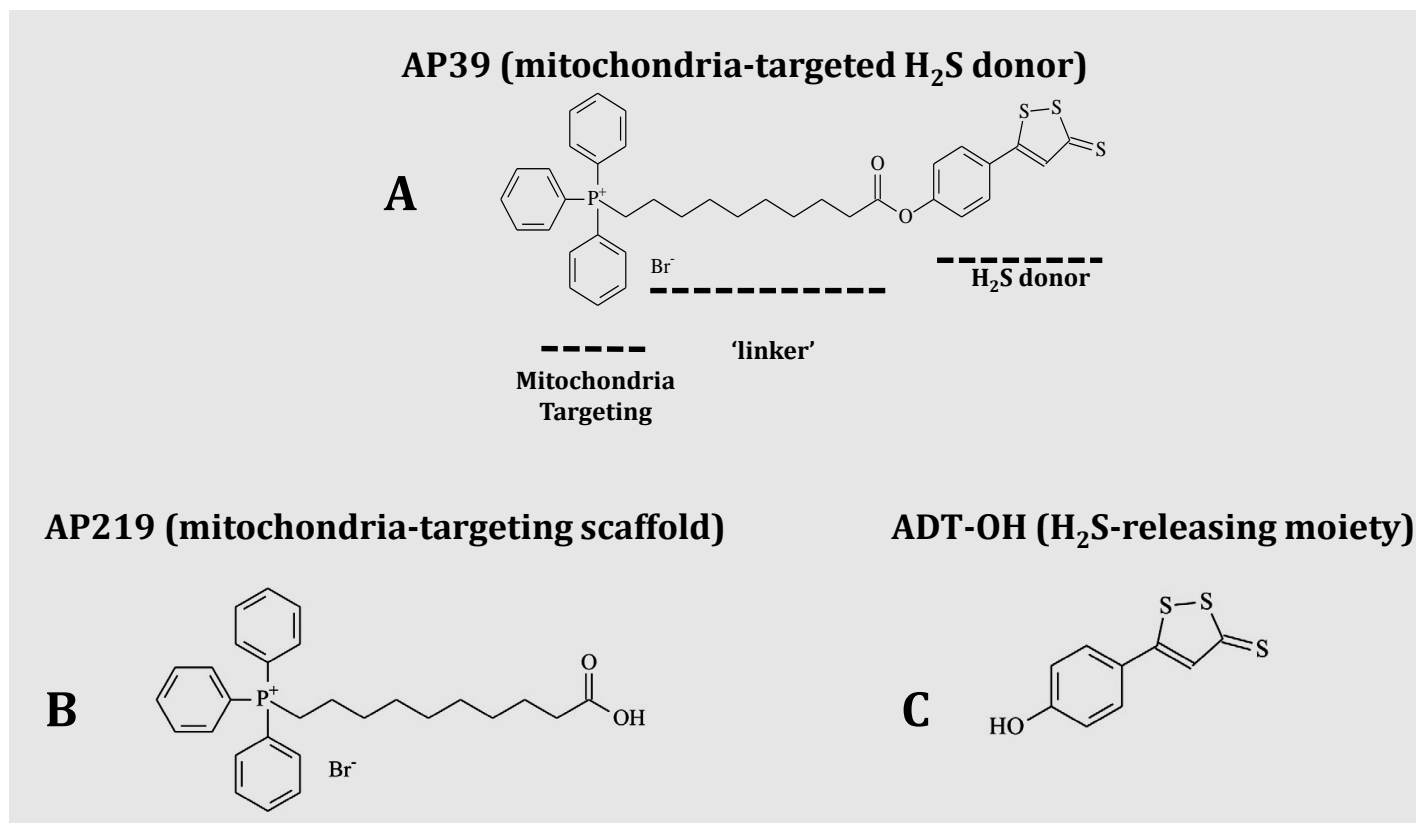


Figure 6.1 Chemical structures of (A) mitochondria-targeted H₂S donor AP39 with the two control compounds (B) AP219 and (C) ADT-OH. AP39 consists of a mitochondria-targeting moiety (triphenylphosphonium; TPP⁺) and a H₂S donor (anethole dithiolethione) attached via an ester to an aliphatic linker.

6.1.2 Aims

The aims of this study were to

1. Examine the potential cardioprotective effects of a novel mitochondria-targeting H₂S donor (AP39) when administrated as adjunct to reperfusion in an *in vivo* rat model of myocardial ischaemia/reperfusion injury.
2. Investigate whether the mitochondria-targeting scaffold (AP219, TPP⁺ moiety) or the H₂S donor (ADT-OH, anethole dithiolethione moiety) exerts any cardioprotection against ischaemia/reperfusion injury.
3. Identify the molecular pharmacology of AP39 and whether it acts directly on the mitochondria or within the cellular compartments to exert its cardioprotective effect.
4. Investigate the direct effects of AP39 on the cardiomyocyte mitochondria, namely subsarcolemmal (SSM) and interfibrillar (IFM) mitochondria, dynamics.

6.1.3 Hypotheses

- 1- Postconditioning with AP39 can protect the ischaemic myocardium against reperfusion injury when applied at reperfusion.
- 2- AP39's postconditioning effect is mediated independently of cardioprotective cytosolic signalling pathway at early reperfusion.
- 3- AP39 can inhibit the opening of the mitochondrial permeability transition pore (PTP).

- 4- Selectively delivered H₂S into the mitochondria via AP39 can improve mitochondrial respiration.
- 5- Targeted delivery of H₂S by AP39 can limit mito-ROS generation.

6.1.4 Objectives

The following experimental approaches have been used to test these hypotheses:

- 1- Perform a dose-response study to identify the optimum cardioprotective dose of AP39 when given at reperfusion using an *in vivo* rat model of myocardial ischaemia/reperfusion injury in comparison with AP219 and ADT-OH.
- 2- Investigate if AP39 limits infarct size through activating the RISK pathway, namely PI3K/Akt, eNOS and sGC, at reperfusion by concomitant administration of specific pharmacological inhibitors of these enzymes.
- 3- Characterise whether AP39 alters the activity of constituents of the RISK pathway, namely Akt, eNOS, GSK-3 β and ERK1/2, in the left ventricle at the first minutes of reperfusion using Western blotting.
- 4- Determine whether AP39 inhibits Ca²⁺-sensitive PTP opening using isolated cardiomyocyte mitochondria, namely, subsarcolemmal (SSM) and interfibrillar (IFM) mitochondria, *in vitro*.
- 5- Examine the effect of AP39 application on the mito-ROS generation *in vitro* using isolated SSM and IFM.
- 6- Characterise the effect of AP39 on the mitochondrial respiration using isolated SSM and IFM *in vitro*.

6.2 Materials and Methods

6.2.1 Animals

Male Sprague Dawley rats, 300-350 g (9-11 weeks), were obtained from Harlan, UK and used for infarct size and Western blotting studies. For mitochondrial functions and biochemistry undertaken in Giessen, Germany, male Wistar rats, 300-350 g (9-11 weeks), were purchased from Harlan, France. Animals handling and reporting are described in more details in Chapter 2, section 2.2.

6.2.2 Acute myocardial infarction model

Rat model of myocardial ischaemia and reperfusion injury was employed to model the acute myocardial infarction as described in Chapter 2, section 2.3. Briefly, the rat was anaesthetised and underwent 30 minutes regional myocardial ischaemia, obtained by left coronary artery occlusion, and 120 minutes reperfusion following 20 minutes stabilisation period when inclusion/exclusion criteria were applied. Myocardial infarct size was quantified using Evans' blue/TTC staining technique as described in Chapter 2, section 2.4.

6.2.3 Treatment protocols

6.2.3.1 Dose-response study of AP39

A series of infarct size experiments were carried out to characterise the dose-dependent infarct-limiting effect of AP39. Along with these doses, AP219

(mitochondria-targeting moiety) and ADT-OH (H₂S-releasing moiety) were also used individually to confirm the selective effect of H₂S delivery into the mitochondria. AP39 (MW = 722.2 g mol⁻¹), AP219 (MW = 433.5 g mol⁻¹) and ADT-OH (MW = 226.3 g mol⁻¹) were synthesised as previously reported (Tomasova et al., 2015, Szczesny et al., 2014, Le Trionnaire et al., 2014). The purity of the compound was determined by NMR spectroscopy (¹H, ³¹P and ¹³C). Doses of AP39, AP219 and ADT-OH used in these experiments derived from *in vitro* and *in vivo* studies undertaken by others (Szczesny et al., 2014, Ikeda et al., 2015, Ahmad et al., 2016). AP39 was given 10 minutes before reperfusion to allow enough time for AP39 to be accumulated in the mitochondria before reperfusion.

Animals were randomised to receive one of six interventions (Figure 6.2):

- Group 1: Control (n=10). Animals received a bolus dose of 0.05% DMSO (v/v), i.v. 10 min before reperfusion. DMSO was used as a vehicle for AP39, AP219 and ADT-OH.
- Group 2-4: Each group (n=8) received AP39 at 0.01, 0.1 or 1 µmol kg⁻¹, respectively as an i.v. bolus contains 0.05% DMSO (v/v) 10 min before reperfusion.
- Group 5: AP219 (n=8). Animals received AP219 (1 µmol kg⁻¹) as an i.v. bolus contains 0.05% DMSO (v/v) 10 min before reperfusion.
- Group 6: ADT-OH (n=8). Animals received ADT-OH (1 µmol kg⁻¹) as an i.v. bolus contains 0.05% DMSO (v/v) 10 min before reperfusion.

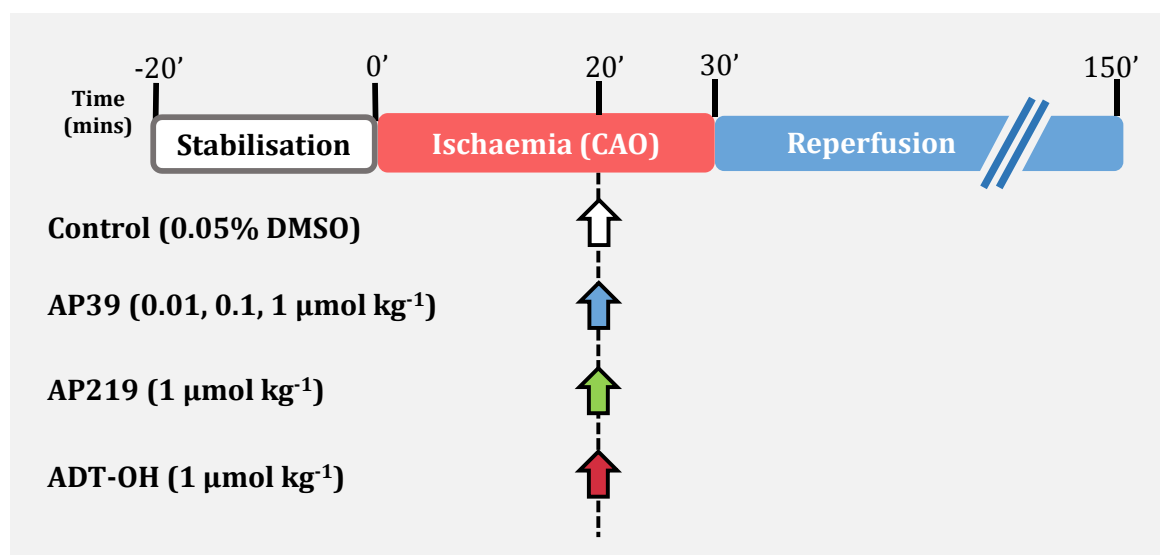


Figure 6.2 Experimental protocol of dose-response study of AP39. Following 20 minutes stabilisation period, animals underwent 30 minutes myocardial regional ischaemia followed by 120 minutes reperfusion. Arrows indicate the time of pharmacological interventions. $n= 8-10$.

6.2.3.2 Mechanistic study of AP39 postconditioning

The second series of infarct size experiments was undertaken to characterise whether AP39 relies on the RISK pathway to produce its cardioprotection. The optimum dose, within the applied dosing range, of AP39 ($1 \mu\text{mol kg}^{-1}$), selected from the first series of experiments, was concomitantly administered with specific pharmacological inhibitors for some of the RISK pathway components. Specific pharmacological inhibitors, namely the PI3K inhibitor LY294002 (Jiang et al., 2007), constitutive NOS inhibitor L-NAME (Fradorf et al., 2010) and sGC inhibitor ODQ (Routhu et al., 2010) were used at doses that have previously been reported to abrogate the activity of their targets in *in vivo* models.

Animals were randomly assigned to one of the following eight treatment groups (Figure 6.3):

- Group 1: Control (n=11). Animals received DMSO 0.05% (v/v) as an i.v. bolus 15 min before reperfusion. DMSO was used as vehicle for AP39, LY294002 and ODQ.
- Group 2: AP39 (n=8). Animals received AP39 (1 $\mu\text{mol kg}^{-1}$) as an i.v. bolus 10 min before reperfusion.
- Group 3: AP39 + L-NAME (n=8). L-NAME (20 mg kg^{-1}) was administered 15 min before reperfusion as an i.v. bolus followed by AP39 (1 $\mu\text{mol kg}^{-1}$) 10 min before reperfusion.
- Group 4: L-NAME (n=8). L-NAME (20 mg kg^{-1}) was administered 15 min before reperfusion as an i.v. bolus.
- Group 5: AP39 + LY294002 (n=8). LY294002 (0.1 mg kg^{-1}) was given 15 min before reperfusion as an i.v. bolus followed by AP39 (1 $\mu\text{mol kg}^{-1}$) 10 min before reperfusion.
- Group 6: LY294002 (n=8). LY294002 (0.1 mg kg^{-1}) was administered 15 min before reperfusion as an i.v. bolus.
- Group 7: AP39 + ODQ (n=8). ODQ (1 mg kg^{-1}) was given 15 min before reperfusion as an i.v. bolus followed by AP39 (1 $\mu\text{mol kg}^{-1}$) 10 min before reperfusion.
- Group 8: ODQ (n=8). ODQ (1 mg kg^{-1}) was administered 15 min before reperfusion as an i.v. bolus.

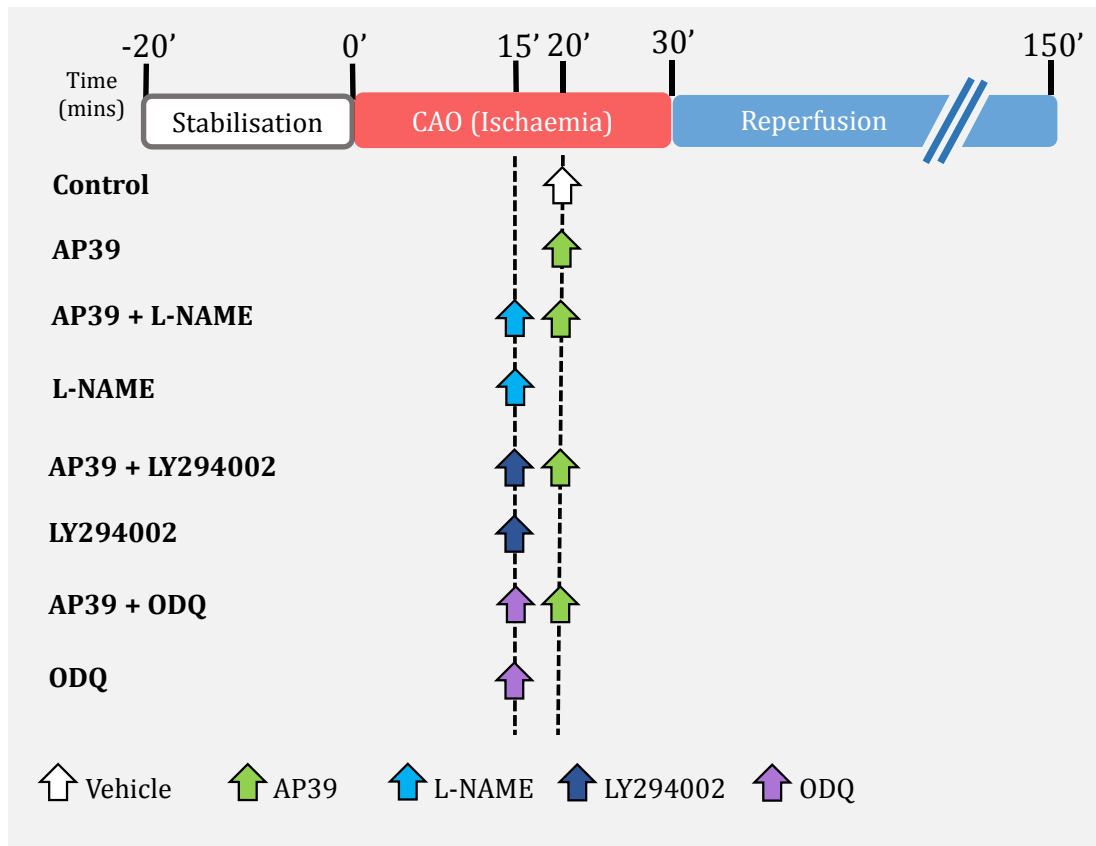


Figure 6.3 Experimental protocol of the mechanistic study of AP39. Rats were subjected to 30 left coronary occlusion and 120 minutes reperfusion. The pharmacological inhibitors were concomitantly administered with AP39 to characterise the involvement of the RISK pathway in cardioprotection established by AP39. Arrows indicate the time of pharmacological interventions. $n=8-11$.

6.2.3.3 Myocardial tissue sampling for protein analysis

The effect of AP39 on the phosphorylation of the RISK pathway components in the myocardium was further characterised in a parallel series prepared for biochemical analysis. Animals were randomised to receive either vehicle (0.05% DMSO) or AP39 ($1 \mu\text{mol kg}^{-1}$) 10 minutes before reperfusion (Figure 6.4). Animals were stabilised for 20 minutes then subjected to 30 minutes of regional myocardial ischaemia. The heart was reperfused for 5 minutes then the tissue sampling was performed as described in Chapter 2, section 2.6.1. These samples were later used to investigate the effect of AP39 on the phosphorylation of Akt, eNOS, GSK-3 β and ERK1/2 at the commencement of reperfusion using Western blotting as illustrated in Chapter 2, section 2.6.4.

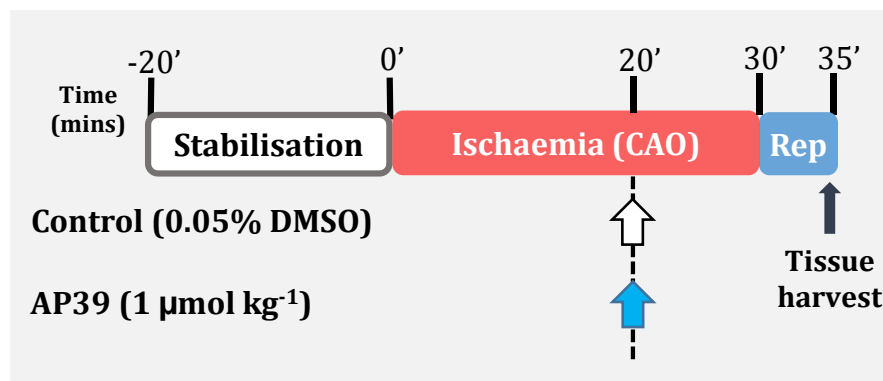


Figure 6.4 Experimental protocol of myocardial biopsies sampling following postconditioning with AP39. Animals were stabilised for 20 minutes with no further intervention following surgery then underwent 30 minutes of left coronary artery occlusion and 5 minutes reperfusion. Heart was then excised and myocardial samples from the left ventricle were snap frozen for later biochemical analysis. Rats received either vehicle or AP39 10 minutes before reperfusion. Arrows indicate the time of interventions.

6.2.4 Isolation of cardiac mitochondria

All work on isolated mitochondria was undertaken in the laboratory of Professor Rainer Schulz, Institute of Physiology, Justus-Liebig University, Giessen, Germany. The mitochondrial studies were conducted by me with the assistance of Dr Julia Bornbaum and Mrs Elvira Ungefug. The effect of specific delivery of H₂S into the mitochondria by AP39 was investigated using freshly isolated rat cardiomyocyte mitochondria *in vitro*. Two subpopulations of cardiomyocyte mitochondria, namely subsarcolemmal (SSM) and interfibrillar mitochondria (IFM), were isolated to look at the direct effect of AP39 on the mitochondria as they represent the most relevant mitochondria within the myocardium that is affected by the ischaemia and reperfusion insults.

Isolation of the two mitochondrial subpopulations was carried out by differential centrifugation (Figure 6.5) using a modified protocol of Boengler et al. (2009). Differential centrifugation is a simple, rapid and most employed technique to fractionate different cell components based on the size, density and shape (Frezza et al., 2007). It involves applying different centrifugation cycles on the tissue homogenate at an increasing relative centrifugal forces. It is worth noting that isolated mitochondria which are fractionated by this method would be contaminated with other cell components (lysosomes and peroxisomes). Nevertheless, this method preserves mitochondria integrity and relatively less stressful for the mitochondria compared with density-gradient separation.

All the procedures were undertaken at 4 °C to maintain mitochondrial integrity. Each rat was anaesthetised with 4% v/v isoflurane and the heart was quickly excised and washed with Buffer A. The ventricles were isolated and weighed, then the right ventricle was snap frozen with liquid nitrogen and used as a negative control. The left

ventricles was transferred to Buffer B, finely chopped with scissors then gently minced with 6 strokes of a teflon pestle in a glass tube. Homogenate was centrifuged at 800 g for 10 min. The supernatant was collected and centrifuged for 10 minutes at 8000 g to isolate the SSM. The sediment from the first centrifugation was re-suspended using Buffer B (10 mL 1 g⁻¹ left ventricle weight) and incubated with protease nargase (8 U g⁻¹) for 1 minute then gently minced with 5 strokes of teflon pestle and glass mortar. The homogenate was centrifuged at 800 g for 10 minutes then the supernatant was collected and centrifuged for 10 minutes at 8000 g to sediment the IFM. SSM and IFM were then washed twice with buffer A and final pellets were re-suspended in Buffer A with no ATP (i.e. incubation buffer).

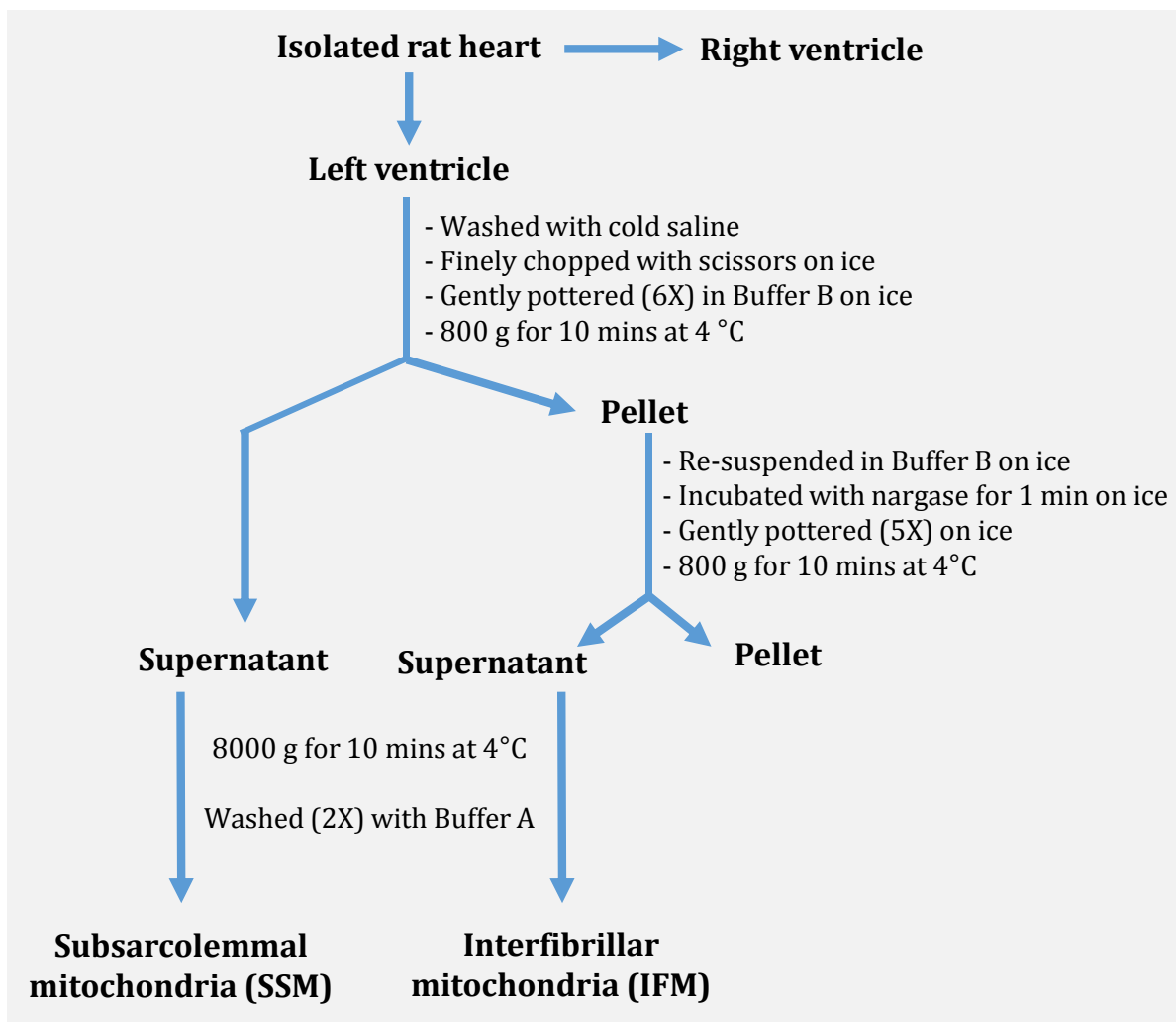


Figure 6.5 Scheme illustrating the protocol for isolation of rat-derived cardiomyocyte mitochondria using differential centrifugation.

6.2.4.1 Protein quantification of the mitochondrial samples

The total protein concentration in the mitochondrial samples was determined using Lowry assay (see Chapter Two, section 2.1.4). Lowry protein assay is based on the reaction of copper ion (Cu^+), as an indicator of the protein concentration, with Folin phenol reagent in alkaline condition (Lowry et al., 1951). A serial dilution of bovine serum albumin (BSA) was prepared (0.2, 0.4, 0.6, 0.8, 1.0, 1.2 and 1.4 mg mL^{-1}) and used as standard stocks to construct the standard curve. Samples from each subpopulation of mitochondria were taken and diluted 1:20 and 2:20 v/v with distilled water. Samples and standards were loaded onto 96-well plate in duplicate and 25 μL of a mixture of reagent A and reagent S in 1:20 v/v was added to each well. Reagent B (200 μL) was then added to each well and the absorbance was measured at 750 nm using ELISA microplate reader model (Infinite M200, Tecan, Germany).

6.2.5 Mitochondrial functions

The concentration range of AP39 used for the mitochondrial studies was equivalent to the *in vivo* doses which were used in the infarct studies. Mitochondrial toxicity studies were also conducted to investigate the effect of these concentrations of AP39 on mitochondria integrity by measuring mitochondrial membrane potential and mitochondrial autofluorescence.

6.2.5.1 Mitochondrial membrane potential

The toxicity of AP39 on cardiomyocyte mitochondria integrity was characterised using mitochondrial membrane potential as an indicator. Fluorescence probes have been often used to study the cell biology in general and the biochemical functions of its

organelles in particular including the mitochondria. In these experiments, we employed Rhodamine 123 as a cell-permeant, cationic and fluorescence dye to assess the impact of AP39, within the chosen dosing range, on mitochondrial membrane potential. Rhodamine 123 can be sequestered into the mitochondria in the presence of the membrane potential. The leakage of Rhodamine 123, which could be due to the opening of PTP or membrane rupture, from the mitochondrial into the buffered solution will indicate the disruption of the membrane potential and will appear as an increase in the fluorescence magnitude. The fluorescence of Rhodamine 123 in the Glutamate/Malate buffer was measured for 1 minute then subsarcolemmal mitochondria (0.5 mL^{-1}) were added to the solution in the cuvette. After five minutes stabilisation, mitochondria were randomly subjected to either 0.003% ethanol or AP39 (0.3, 1, 3, 5 and $10 \mu\text{M}$). The membrane potential was measured using Cary Eclipse spectrophotometer (Varian, Mulgrave, Australia) at 503/535 nm excitation/emission wavelength.

6.2.5.2 Mitochondrial autofluorescence

Autofluorescence of mitochondrial nicotinamide adenine dinucleotide (NADH) and flavin adenine dinucleotide (FADH) was used as another approach to evaluate the toxicity of AP39 on the mitochondria. NADH and FADH are electron carrier and they transfer the electrons from tricarboxylic acid cycle (TAC) to the mitochondrial electron transport chain (ECL). The level and the fluorescence of NADPH and the oxidised form of FADH (FAD) inside the mitochondria reflect the status of the ECL. Subsarcolemmal mitochondria were incubated with Glutamate/Malate buffer for 5 minutes with stirring at $25 \text{ }^\circ\text{C}$ when basal autofluorescence was measured. Mitochondria were then treated

with either vehicle (0.003% ethanol) or one of AP39's concentrations (0.3, 1, 3, 5, 10 μM). Mitochondrial autofluorescence was measured at 340/460 nm excitation/emission wavelength using Clary Eclipse spectrophotometer (Varian, Mulgrave, Australia).

6.2.5.3 Ca^{2+} retention capacity (CRC)

The opening of mitochondrial permeability transition pore (PTP) at the commencement of reperfusion represents the starting point of cell necrosis following myocardial ischaemia and reperfusion as a result of overwhelming ROS generation, pH normalisation and Ca^{2+} overload at early reperfusion. Therefore, we sought to examine if AP39 influences the mitochondrial calcium retention capacity, as an indicator of the susceptibility of PTP opening, *in vitro* using rat cardiomyocyte SSM and IFM. We used a modified protocol of Chen et al. (2012). The basis of CRC assay is that it measures mitochondrial tolerability toward Ca^{2+} which is considered as a major trigger of PTP opening. Mitochondria can retain calcium as calcium phosphate to buffer cytosolic level of calcium. However, when mitochondrial capacity to store calcium exceeded, this will lead to the opening of PTP and eventually releasing its calcium load back into the cytosol.

Freshly isolated SSM and IFM (0.1 mg mL^{-1}) were randomised to be incubated for 4 minutes in 2 mL of Glutamate/Malate buffer. The suspension was supplemented with 8 μL ADP (10 mM), 10 μL EGTA (1 mM), 6 μL CaCl_2 (5 mM) and 1 μL calcium green-5N (1 μM). Mitochondria fractions were then incubated with either vehicle (0.003% (v/v) ethanol) or AP39 (1 μM) in the presence and absence of cyclosporine A (CsA, 1 μM). CsA was used as a positive control as it is a well-known inhibitor of the PTP

opening and increases mitochondrial tolerance to Ca^{2+} overload in a CypD-dependent mechanism in the experimental settings. Pulses of Ca^{2+} (5 μmol) were added at 3 minutes intervals to the solution with stirring at 25 °C and mitochondrial calcium tolerance was expressed as μmol of Ca^{2+} mg^{-1} of protein. Fluorescence was measured with excitation and emission wavelengths 500 and 530 nm, respectively. Data were coded using random number generator (<https://www.random.org>) and the analysis was performed in a blind fashion to avoid possible bias.

6.2.5.4 Mitochondrial ROS generation

Measurement of mitochondrial ROS generation was carried out as previously described by Soetkamp et al. (2014). Freshly isolated SSM or IFM (50 μg) were separately gently suspended in Glutamate/Malate buffer and incubated randomly with either: (1) Glutamate/Malate buffer (1st Control); (2) vehicle (0.003% (v/v) ethanol) or (3) AP39 (0.3, 1, 3, 5 μM). Horseradish peroxidase (HRP, 0.1 U mL^{-1}) and 50 μmol of Amplex UltraRed were added to the suspension directly before the measurement. Amplex Ultrared is a stable and sensitive fluorogenic substrate for peroxidase detection and extensively employed in cell culture and mitochondrial studies to detect the generation of H_2O_2 . It reacts with activated HRP in 1:1 stoichiometric ratio to produce a brightly fluorescence product (Resorufin) which can be detected at excitation/emission wavelengths 565/581 nm. Amplex Ultrared offers a number of advantages over Amplex red as it is more sensitive to HRP on a per-mole basis and it is more resistant to oxidation by ROS. Moreover, it is stable over a wide pH range compared to Amplex red.

A second control group, from each subpopulation, with no intervention was employed at the end of the all measurements to ensure that any observed effects are due to AP39 and not because of the decline in the respiratory capacity (i.e. run-down of the mitochondria with the time). SSM and IFM were also incubated with rotenone (2 μM) to induce overproduction of mitochondrial ROS generation by uncoupling of complex I of the electron transport chain and used as a positive control for comparison. Mitochondrial ROS generation was measured for 4 minutes at room temperature using Cary Eclipse spectrophotometer (Agilent technologies, Santa Clara, Canada) at excitation/emission wavelengths 565/581 nm. Using random number generator (<https://www.random.org>), data were coded and slope of mito-ROS generation was calculated, as a mean fluorescence per time (a.u.), after subtracting the background fluorescence of the incubation buffer, in a blind fashion.

6.2.5.5 Mitochondrial oxygen consumption

The respiration of SSM and IFM was measured using a Mitocell Respiratory System (Strathkelvin, Glasgow, UK) at 25 °C. Mitocell is a glass chamber surrounded by circulating water jacket to maintain temperature and has a Clark-type oxygen microelectrode which consists the base of the chamber. Microelectrode consists of cathode and anode where the oxygen is reduced by the cathode when both the anode and the cathode are polarised. Reduction of each oxygen molecule consumes four electrons which create the current that flows in the circuit.

Basal mitochondrial oxygen consumption was measured in the presence and absence of either the vehicle (0.003% (v/v) ethanol) or AP39 (0.3, 1, 3, 5 μM). Mitochondria (0.1 mg ml⁻¹) were randomly incubated in two chambers simultaneously, one with

complex I substrate (5 mM glutamate and 2.5 mM malate) or with complex II substrate (5 mM succinate plus 2 μ M rotenone, to inhibit complex I activity). Respiration was stimulated by addition of 40 μ M ADP and oxygen consumption was reported as nmol of O_2 min^{-1} mg^{-1} of protein. Oxygraph charts were coded using random number generator (<https://www.random.org>) and data were analysed by a person who is blind to the treatments.

6.2.5.6 Effect of AP39 on mitochondrial GSH production

The levels of GSH and GSSG in the mitochondrial compartments following AP39 application were assessed using a glutathione assay kit. Subsarcolemmal mitochondria (SSM) were isolated as described in section 6.2.4 with some modifications to measure the mitochondrial content of GSH and GSSG after AP39 application (Figure 6.6). Left ventricle was isolated and finely chopped with scissors in Buffer A then ultrasonicated (3 X10 seconds cycle, with 5 seconds waiting interval) using an Ultra turrax homogeniser (IKA T-18, Cole Parmer, UK). Homogenate was centrifuged at 800 g for 10 minutes then the supernatant was recovered, which represents the SSM, and washed using isolation buffer 1 with centrifugation at 8000 g for 10 minutes. SSM pellet was then re-suspended in Glutamate/Malate buffer and incubation with either ultrapure water or AP39 (1 μ mol) on thermomixer (BioShake, Jena, Germany) at 650 rpm for 10 minutes at 25 °C. Stimulated mitochondria were centrifuged at 10300 g for 5 minutes, re-suspended in (200 μ L) isolation buffer 2 and added gently on the top of 4 mL of 30% Percoll in 5 mL tube then centrifuged at 32000 g for 30 minutes at 4 °C. Impurities ring was discarded and mitochondria was

recovered then washed twice with isolation buffer 2 with centrifugation at 12500 g for 5 minutes.

Purified mitochondria were re-suspended using 150 μ L of 2-(N-morpholino) ethanesulfonic acid (MES) buffer with sonication. Mitochondria sample was then deproteinated by centrifugation at 10000 g for 15 minutes and the supernatant was collected. The supernatant was mixed with metaphosphoric acid (MPA, 1.25 M) with vortexing and left to set for 5 minutes. The supernatant was then carefully collected without disturbing the precipitation.

A- To measure the total mitochondrial GSH content, the supernatant was mixed with 4 M triethanolamine (TEAM, 50 μ L of TEAM for each 1 mL supernatant) with vortexing.

B- To measure the mitochondrial GSSG content, GSSG was exclusively derived from GSH by treating the supernatant from step A with 1 M 2-vinylpyridine (10 μ L for each 1 mL of the supernatant) with vortexing and incubated for 1 hour before it was ready to assay.

A series of GSSG standard aliquots (0, 0.25, 0.5, 1.0, 2.0, 4.0, 6.0, 8.0 μ M GSSG) were prepared. Standard aliquots and the samples (50 μ L from each) were loaded in duplicate onto a 96-well plate then, 150 μ L of freshly prepared Assay Cocktail was added to each well. The plate was incubated on an orbital shaker in the dark for 25 minutes then read using an ELISA microplate reader (Infinite M200, Tecan, Germany) at 405-414 nm. Absorbance values was corrected by subtracting the absorbance value of the diluting buffer (MES) and the corrected absorbance values were plotted as a functions of either GSSG or the total GSH concentration used to construct the

standard curve. The concentration of the total GSH or GSSG was calculated by the following equation:

$$[Total\ GSH]\ or\ [GSSG] = \left[\frac{(Absorbance\ at\ 405 - 414\ nm) - (Y - intercept)}{Slope} \right] \times 2 \times Sample\ Dilution$$

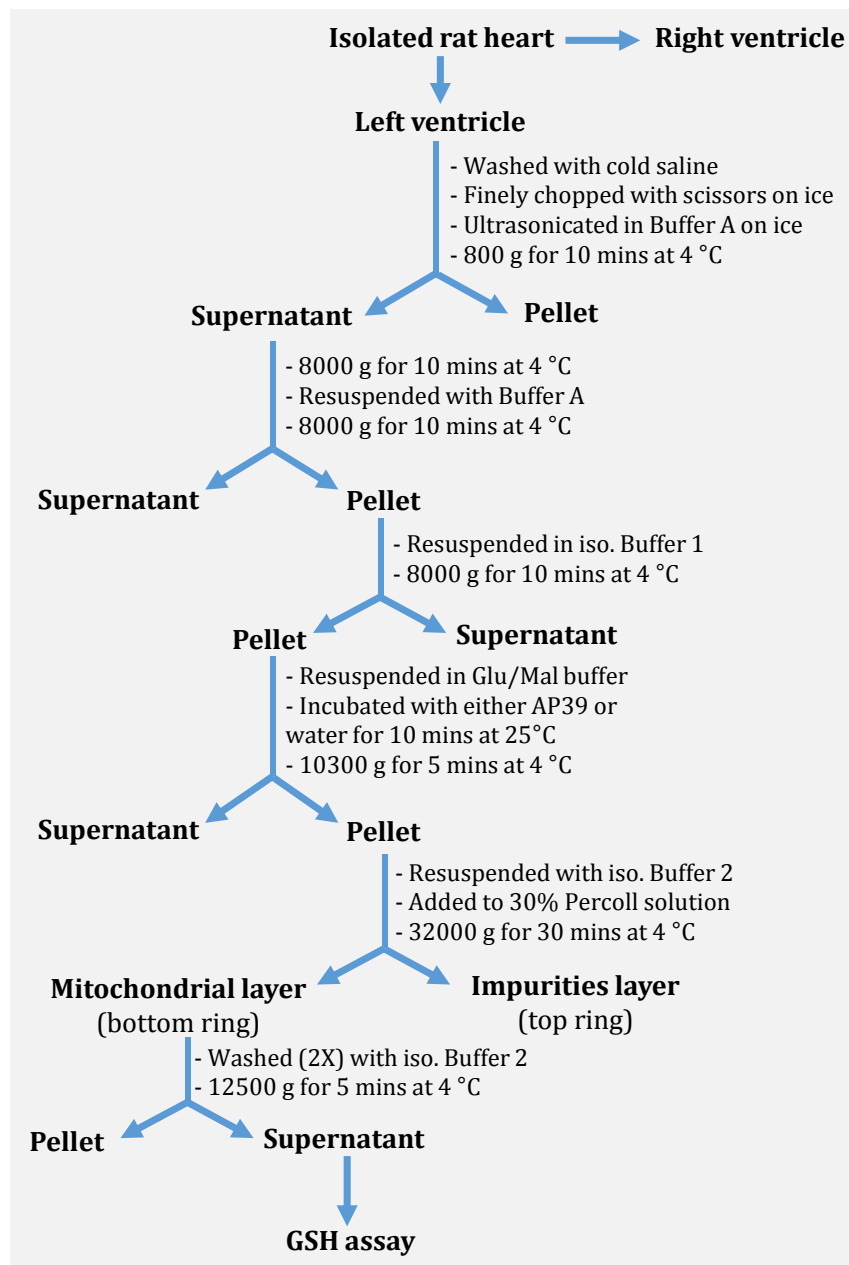


Figure 6.6 Protocol for isolation of subsarcolemmal mitochondria (SSM) and stimulation with AP39 for GSH experiments.

6.2.6 Effect of AP39 on S-nitrosylation of mitochondrial proteins

6.2.6.1 Mitochondrial preparations

Mitochondria fractions were isolated as previously described in section 6.2.6 with some modifications (Figure 6.7). Harvested rat heart was washed using ice-cold saline and the right ventricle was isolated and snap frozen with liquid nitrogen to use as a negative control then the left ventricle was weighed. Left ventricle was washed with Buffer A (3-4 times) until no blood clots were seen, then finely chopped using scissors. Cardiac tissue was further homogenised in ice-cold Buffer A (3 X 10 seconds cycle, with 5 seconds waiting after each cycle) using an Ultra turrax homogeniser (IKA T-18, Cole Parmer, UK). Mitochondria were then isolated by differential centrifugation. The homogenate was centrifuged at 800 g for 10 minutes and the supernatant, which contains the subsarcolemmal mitochondria (SSM), was transferred to 2 mL Eppendorf tubes. The pellet from the first centrifugation was then re-suspended with Buffer B and incubated with protease nargase ($8 \text{ U } 1 \text{ g}^{-1}$ left ventricle weight) for 1 minute. The tissue suspension was homogenised by potter-teflon (5 strokes) and centrifuged at 800 g for 10 minutes. Supernatant, which contained the interfibrillar mitochondria (IFM), was collected and transferred to 2 mL Eppendorf tubes. Both mitochondria pellets were centrifuged at 14300 g for 10 minutes and the produced pellets were washed twice using mitochondria isolation buffer 1 with centrifugation at 10300 g for 5 minutes. The SSM and IFM pellets were finally re-suspended in isolation buffer 1.

The total protein concentration in the final mitochondrial solutions was determined using Lowry assay as described in section 6.2.6.1. SSM and IFM (200 mg mL^{-1}) solutions were diluted with Glutamate/Malate buffer and stimulated separately in 2 mL

amber Eppendorf tubes with one of the following treatments: (1) isolation buffer 1, (2) AP39 (0.3 μmol), (3) AP39 (1 μmol) and (4) 0.5 mmol SNAP, which is a NO donor and as a positive control. The incubation was carried out on thermomixer (BioShake, Jena, Germany) at 650 rpm for 10 minutes at 25 °C, then the tubes were centrifuged at 10300 g for 5 minutes. Supernatant was discarded and the pellet was re-suspended with (200 μL) mitochondria isolation buffer 3. Mitochondria were purified using the Percoll gradient technique (Boengler et al., 2012). Re-suspended pellets were added on the top of 4 mL of 30% Percoll in 5 mL tube, then centrifuged at 32000 g for 30 minutes. After centrifugation, impurities form a ring which is attached to the interior tube surface at the top of the tube while purified mitochondria form another ring near the bottom of the tube. The impurities ring was carefully discarded and purified mitochondria were recovered and diluted with mitochondria isolation buffer 2. Mitochondria were washed twice using isolation buffer 2 with centrifugation at 12500 g for 5 minutes to remove any residue of Percoll. Purified mitochondrial proteins were then snap frozen using liquid nitrogen and kept at -80 °C.

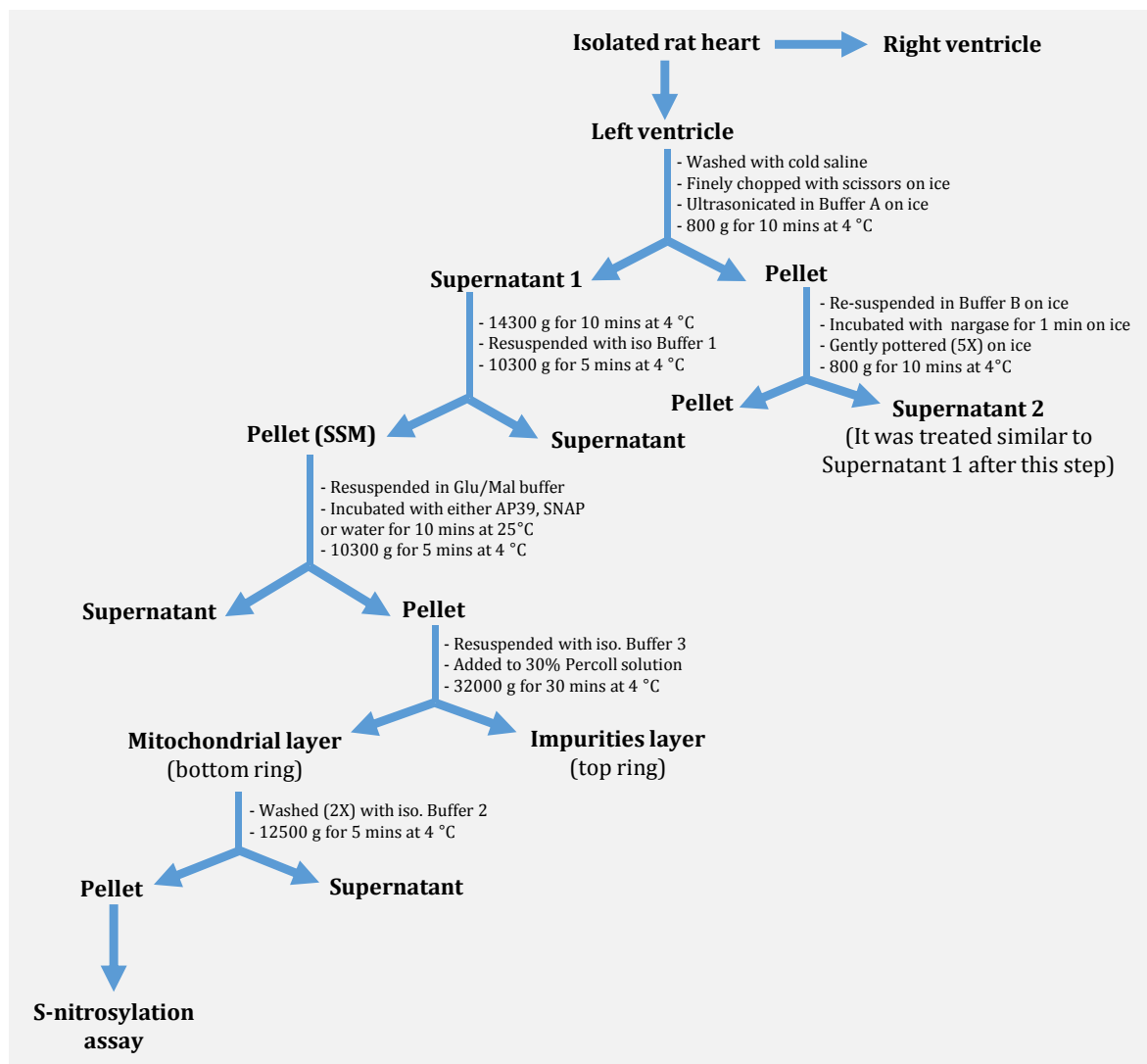


Figure 6.7 Protocol for isolation of SSM and IFM and stimulation with AP39 and SNAP for S-nitrosylation Assay.

6.2.6.2 Detecting AP39-induced S-nitrosylation using Ponceau dye

Mitochondrial proteins samples were heated at 95 °C for 5 minutes then loaded (30 µg) to 10% w/v SDS-PAGE and separated electrophoretically at (120 mV). Separated proteins were then left overnight to transfer onto nitrocellulose membrane (Amersham, Germany) at 30V. The membrane was washed with distilled water before incubated with 0.2% TCA, Ponceau[®] S solution for 15 minutes. Ponceau[®] S is a rapid and reversible dye to detect and visualise the protein bands on polyvinylidene fluoride or nitrocellulose membranes without affecting the sequence of blotted proteins. The membrane was scanned using an imaging system (Quantum ST5, Vilber, Germany).

6.2.6.3 Detecting AP39-induced S-nitrosylation using Pierce S-nitrosylation Western blot kit

Detection of mitochondrial nitrosylated protein was carried out using Pierce S-Nitrosylation Western blot kit according to the manufacturer's instructions (Figure 6.8). Purified mitochondrial proteins were re-suspended with cell lysis HENS buffer (100 mM HEPES (pH 7.8), 1 mM EDTA, 0.1 mM Neocuproine, and 1% SDS) to achieve final concentration of (100 µg 100 µL⁻¹) for each protein sample. Free sulfhydryl groups were blocked using 4 µL of methyl methanethiosulfonate (MMTS, 1 M) with vortexing for 1 minute and incubation for 30 minutes at 25 °C. The proteins were then precipitated using 600 µL pre-chilled acetone and frozen at -20 °C for 1 hour to remove MMTS. Samples were centrifuged at 10000 g for 10 minutes and left to dry for 10 minutes before re-suspending the pellet with 100 µL HENS buffer. Each sample was divided into two new Eppendorf tubes. Nitrosylated proteins were labelled using 1 µL of the 20 mM iodoTMTzero[™] Labelling reagent (iodoTMT reagent). To selectively

reduce the ntirosylated cysteine residues, 2 μ L of 1 M sodium ascorbate was added to one of the tubes from each protein samples while 2 μ L of ultrapure water was added to the other tube with brief vortexing. The reaction was proceeded for 2 hours at 25 °C. Labelled sample (10 μ L) were diluted with 5X reducing Laemmli buffer, heated at 95 C for 5 minutes then separated by pre-cast 12-well SDS-PAGE gel (Mini-Protean® TGX™ Precast gel, BioRad, Germany) at 200 mV. Separated proteins were then transferred overnight onto nitrocellulose membrane and the immunoblot was blocked with blocking solution for 1 hour. The membrane was incubated with anti-TMT antibody solution (anti-TMT antibody in 5% NFDM in TBST) for 1 hour then washed three times for 15 minutes with 1% TBST. The probed membrane was incubated with the secondary antibody (anti-mouse IgG-HRP) for 1 hour then washed three times for 15 minutes with TBST. The immunoblot was incubated with Supersignal West Pico Chemiluminescent Substrate for 5 minutes, then digitally scanned using automated imaging system (Quantum ST5, Vilber, Germany).

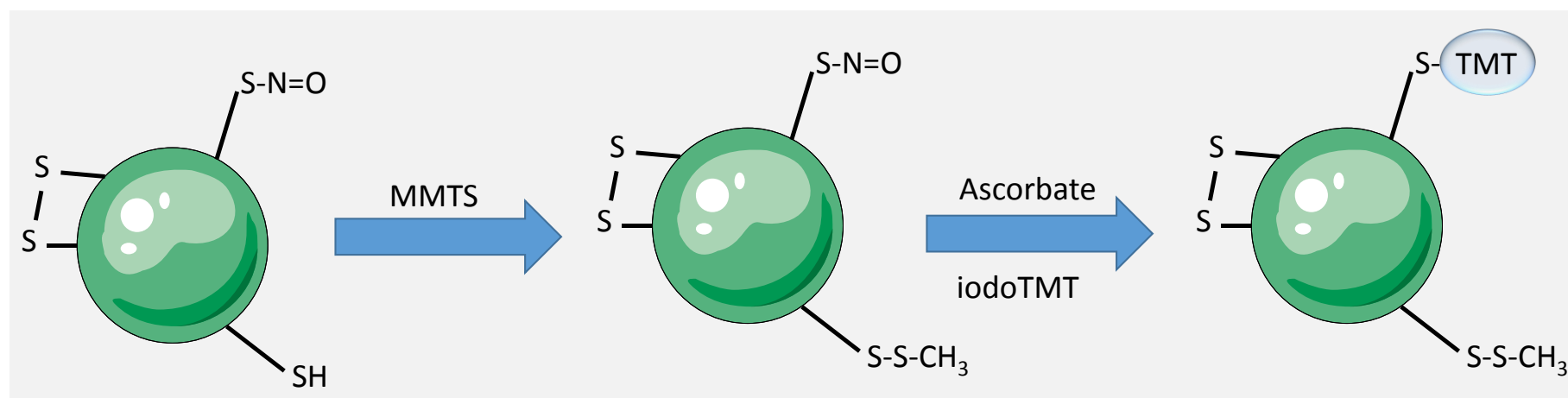


Figure 6.8 Scheme illustrating the detection of mitochondrial S-nitrosylated protein post-translational modifications using Pierce S-Nitrosylation Western blot kit. SSM and IFM were isolated and stimulated with either AP39 or SNAP. Mitochondrial extract was treated with MMTS to block the free thiol groups. S-nitrosylated residues were then specifically reduced with ascorbate and labelled with TMT to be later detected with TMT antibody using Western blotting technique.

6.3 Results

6.3.1 Inclusion/exclusion criteria

A total of 164 rats were used for these studies. For the AP39 dose-response study, 52 rats were employed, of which two were excluded: one did not have successful reperfusion and one rat did not survive ischaemia-induced ventricular fibrillation. Therefore, data from 50 successfully completed experiments are presented for series 1. In the second series, 83 rats were used, of which four were excluded: two did not complete the ischaemia/reperfusion protocol, one did not have a successful TTC staining and one did not survive reperfusion-induced arrhythmia. Thus, data from 79 rats (67 infarct size experiments which were successfully completed and 12 tissue sampling experiments) were reported for series 2. For mitochondria functional studies, data from 29 rats are reported with no exclusion.

6.3.2 Pharmacological postconditioning with AP39

6.3.2.1 Haemodynamic parameters

Baseline parameters and haemodynamic measurements for the dose-response study are shown in Table 6.2. There was no significant difference among the six experimental groups in any of the baseline parameters. Postconditioning the heart with AP39 resulted in a dose-dependent improvement in the post-ischaemia functional recovery with maximum improvement ($67.2 \pm 3.8\%$) at ($1 \mu\text{mol kg}^{-1}$) compared to the control hearts ($46.2 \pm 3.4\%$, Table 6.2). This functional recovery was represented by increased RPP at the end of reperfusion as a percentage of the pre-ischaemic RPP

(i.e. RPP recovery as a percentage of the baseline RPP). The control compounds (AP219 and ADT-OH) did not improve the functional recovery at the end of reperfusion. None of the interventions had any effect on the MAP.

6.3.2.2 Infarct limitation with AP39 postconditioning

Myocardial infarction was determined using the Evan's blue/TTC staining protocol. Area at risk (ischaemic bed) is presented as a percentage of the total ventricular volume while, infarct size was reported as a percentage of the ischaemic bed. Risk zone was similar among the experimental groups (50-60% of the total ventricular volume, Figure 6.9A). Administration of AP39 10 minutes before reperfusion resulted in a dose-dependent infarct-sparing effect compared with vehicle-treated animals (Figure 6.9B), with maximum protection seen at 1 $\mu\text{mol kg}^{-1}$ dose (infarct size $32.1 \pm 3.0\%$ vs $52.8 \pm 3.8\%$, $p < 0.001$). This represents almost 40% reduction in infarct size. The control compounds, namely AP219 and ADT-OH, did not have a significant effect on infarct size.

Table 6.2 Summary of haemodynamic parameters for AP39 dose-response study during ischaemia/reperfusion protocol

Experimental Protocol	n	BW (g)	Baseline		20 min Ischaemia		120 min Reperfusion	
			RPP (mmHg min ⁻¹)*10 ³	MAP (mmHg)	RPP (mmHg min ⁻¹)*10 ³	MAP (mmHg)	RPP (mmHg min ⁻¹)*10 ³	MAP (mmHg)
Control (0.05% DMSO)	10	342 ± 5	36.2 ± 2.1	90 ± 6	26.0 ± 1.9	70 ± 3	16.7 ± 2.2	55 ± 5
AP39 0.01 µmol kg ⁻¹	8	347 ± 7	38.4 ± 2.8	92 ± 4	27.1 ± 2.4	70 ± 5	17.7 ± 1.8	58 ± 3
AP39 0.1 µmol kg ⁻¹	8	339 ± 5	40.0 ± 2.0	89 ± 6	28.7 ± 1.2	68 ± 7	20.0 ± 1.3	54 ± 5
AP39 1 µmol kg ⁻¹	8	355 ± 5	38.5 ± 1.5	85 ± 5	29.4 ± 2.3	67 ± 3	25.8 ± 1.2*	49 ± 4
AP219 1 µmol kg ⁻¹	8	356 ± 7	37.8 ± 2.0	87 ± 7	27.6 ± 1.6	71 ± 5	16.2 ± 1.5	51 ± 6
ADT-OH 1 µmol kg ⁻¹	8	342 ± 6	39.4 ± 2.5	90 ± 4	29.1 ± 2.3	68 ± 4	17.5 ± 1.8	54 ± 5

n number of animals per group; BW body weight; RPP rate pressure product; MAP mean arterial pressure. Data are reported as mean ± SEM. (repeated measures ANOVA followed by Bonferroni post hoc test), * p < 0.05 vs control value at the same time point.

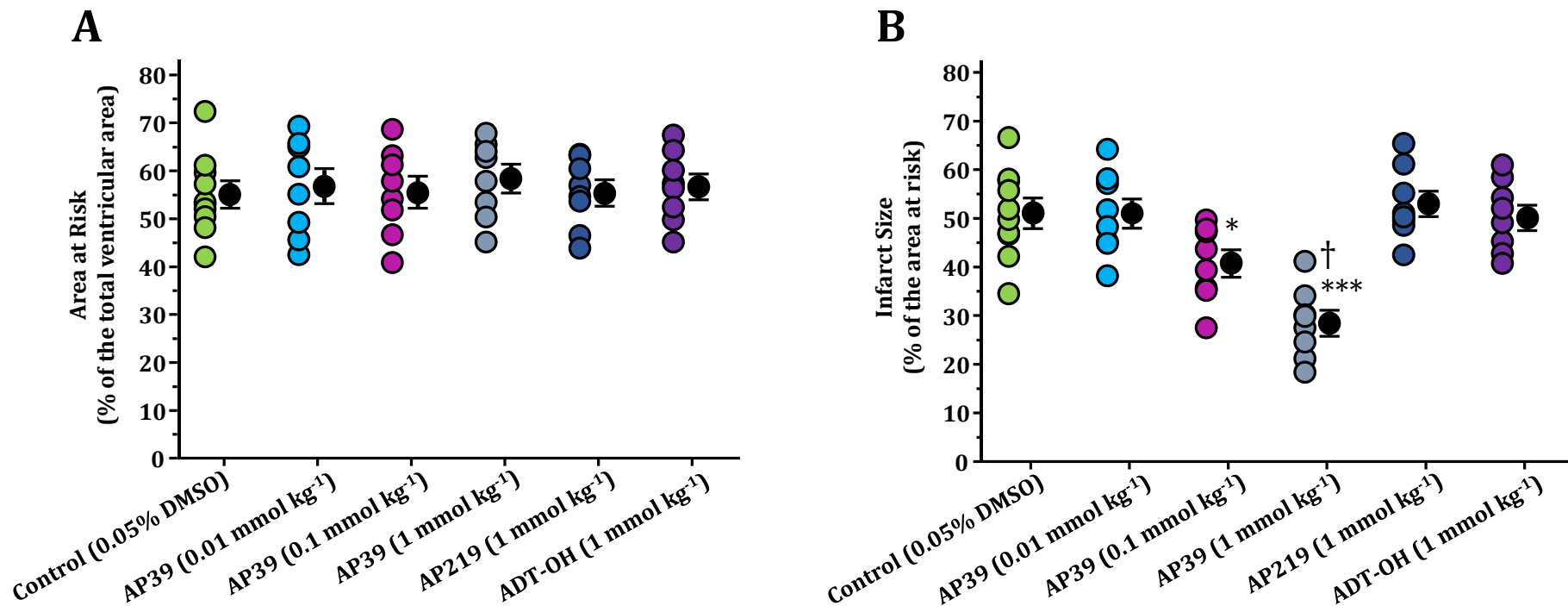


Figure 6.9 Area at risk and infarct size data for dose-response study of AP39. Infarct size was determined following 30 minutes left coronary artery occlusion and 120 minutes reperfusion using Evans' blue/TTC staining technique. **(A)** Area at risk is expressed as a percentage of the total ventricular volume and **(B)** Infarct size is reported as a percentage of area at risk. All pharmacological interventions were given 10 minutes before reperfusion. Data were analysed using one-way ANOVA followed by Newman Keuls post hoc test and expressed as mean \pm SEM, * $p < 0.05$, *** $p < 0.001$ vs control; † $p < 0.05$ vs AP39 (1 $\mu\text{mol kg}^{-1}$). The mean of infarct size is presented as a filled circle (with error bars) next to the individual value for each group (open circles).

6.3.3 Mechanistic study of AP39: involvements of PI3K/Akt and NO

6.3.3.1 Haemodynamic parameters

Baselines and cardiodynamics are shown in Table 6.3. There was no significant difference among the experimental groups in any of the baseline parameters. Similar to the first series, postconditioning with AP39 significantly increased the RPP at the end of reperfusion compared to the control (28.2 ± 1.5 vs 15.2 ± 1.8 , $p < 0.05$). This represent an improvement in the post-ischaemic functional recovery (%RPP recovery) by 29% compared to the control group. Co-administration of any of the pharmacological inhibitors, namely LY294002, L-NAME and ODQ, did not alter the %RPP recovery induced by AP39 (24.5 ± 1.6 , 27.4 ± 2.4 and 26.3 ± 1.9 , respectively) compare to vehicle-treated group. Application of AP39 did not have an effect on the MAP. Administration of any of the inhibitors alone did not affect either RPP or MAP.

Table 6.3 Summary of haemodynamic parameters throughout ischaemia/reperfusion protocol for mechanistic study of AP39 with the pharmacological inhibitors

Experimental Protocol	n	BW (g)	Baseline		20 min Ischaemia		120 min Reperfusion	
			RPP (mmHg min ⁻¹)*10 ³	MAP (mmHg)	RPP (mmHg min ⁻¹)*10 ³	MAP (mmHg)	RPP (mmHg min ⁻¹)*10 ³	MAP (mmHg)
Control	11	361 ± 5	35.5 ± 2.0	87 ± 6	26.1 ± 1.7	65 ± 4	15.2 ± 1.8	53 ± 5
AP39	8	356 ± 7	39.6 ± 3.1	92 ± 4	31.1 ± 2.0	68 ± 5	28.2 ± 1.5*	54 ± 6
AP39 + L-NAME	8	365 ± 6	36.0 ± 1.9	90 ± 7	29.5 ± 1.8	67 ± 8	27.4 ± 2.4*	53 ± 5
L-NAME	8	371 ± 9	39.3 ± 1.6	89 ± 5	28.6 ± 2.4	74 ± 5	14.4 ± 2.1	56 ± 4
AP39 + LY294002	8	359 ± 10	37.4 ± 1.5	86 ± 6	32.0 ± 2.2	70 ± 6	24.5 ± 1.6*	52 ± 5
LY294002	8	367 ± 9	42.3 ± 2.5	91 ± 4	30.2 ± 1.7	69 ± 6	16.4 ± 2.0	60 ± 7
AP39 + ODQ	8	365 ± 7	39.6 ± 1.5	93 ± 5	31.5 ± 1.6	71 ± 4	26.3 ± 1.9*	55 ± 5
ODQ	8	370 ± 8	40.3 ± 2.5	88 ± 7	28.6 ± 1.4	66 ± 5	15.6 ± 2.0	63 ± 4

n number of animals per group; BW body weight; RPP rate pressure product; MAP mean arterial pressure. Data are reported as mean ± SEM. (repeated measures ANOVA followed by Bonferroni *post hoc* test), * p < 0.05 vs control value at the same time point.

6.3.3.2 Infarct size data

We next investigated the dependency of AP39's postconditioning protection on both PI3K/Akt and NO as a relevant protective cytosolic-signalling pathway using a "signal tracing" approach (i.e. sequential interrogation of each stage in the signal transduction cascade). There was no significant difference in the risk zone (ischaemic bed) among the groups (Figure 6.10A). None of the pharmacological inhibitors alone had a significant effect on infarct size when given alone 15 minutes before reperfusion compared to the control group (Fig. 6.10B). Pharmacological postconditioning using AP39 $1 \mu\text{mol kg}^{-1}$ significantly limited the infarct size ($30.1 \pm 2.7\%$ vs $53.0 \pm 2.2\%$, $p < 0.001$) when given at 10 minutes before reperfusion as seen in series 1. This represents a 43% reduction in the final infarct size following ischaemia/reperfusion protocol. Blockade of PI3K activity with LY294002 did not abolish the infarct limitation induced by applying AP39 alone ($33.6 \pm 2.4\%$ vs $30.1 \pm 2.7\%$). Similarly, neither blockade of NO synthesis by L-NAME nor selective inhibition of its downstream effector, sGC, with ODQ attenuated the protective effect of AP39 ($38.3 \pm 2.8\%$ and $32.9 \pm 2.7\%$, respectively).

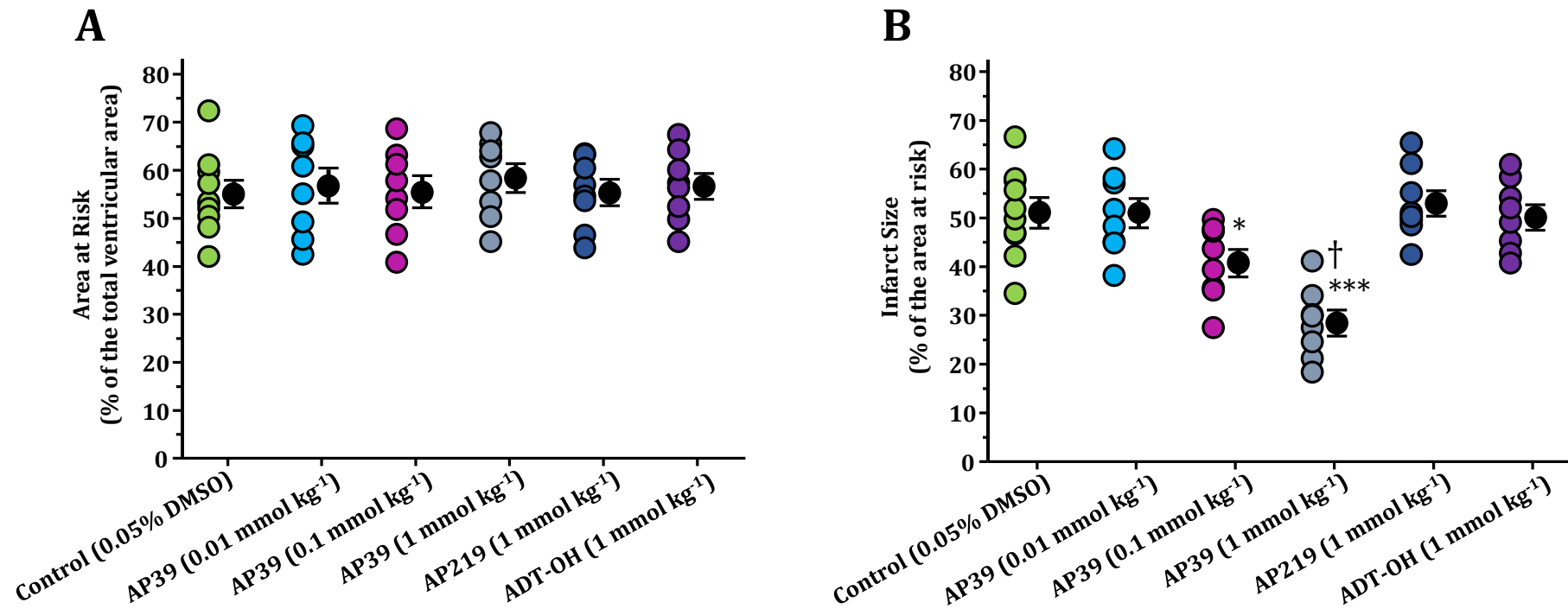


Figure 6.10 Area at risk and infarct size data for the mechanistic study of AP39 with the RISK pathway blockers. (A) Area at risk (risk zone) is expressed as a percentage of total ventricular volume and (B) myocardial infarction was reported as a percentage of the risk zone. Infarct size was determined using Evans' blue/TTC staining protocol following 30 minutes myocardial ischaemia and 2 hours reperfusion. Data were analysed using one-way ANOVA with Newman Keuls post hoc test and reported as mean \pm SEM. *** p <0.001 vs control. The mean infarction is shown as a filled circle (with error bars) next to the individual value for each group (open circles).

6.3.4 Protein phosphorylation following postconditioning with AP39

The effect of AP39, used as an adjunct to reperfusion, on the phosphorylation of key cytosolic components of the RISK pathway was also evaluated in samples harvested from the left ventricle after 5 minutes of reperfusion. Immunoblotting was carried out using phospho-specific antibodies for Akt, eNOS, GSK-3 β and ERK1/2 to outline their role in the cardioprotection. In line with the infarct size data, Western blot analysis showed that administration of AP39 at reperfusion had no significant effect on the phosphorylation of either Akt, eNOS, GSK-3 β or ERK1/2 (Figures 6.11 and 6.12). Together with the infarct data described in 6.3.3.2, these data support the hypothesis that AP39 mediated its cardioprotection in a manner independently of the activation of cytosolic RISK pathway components.

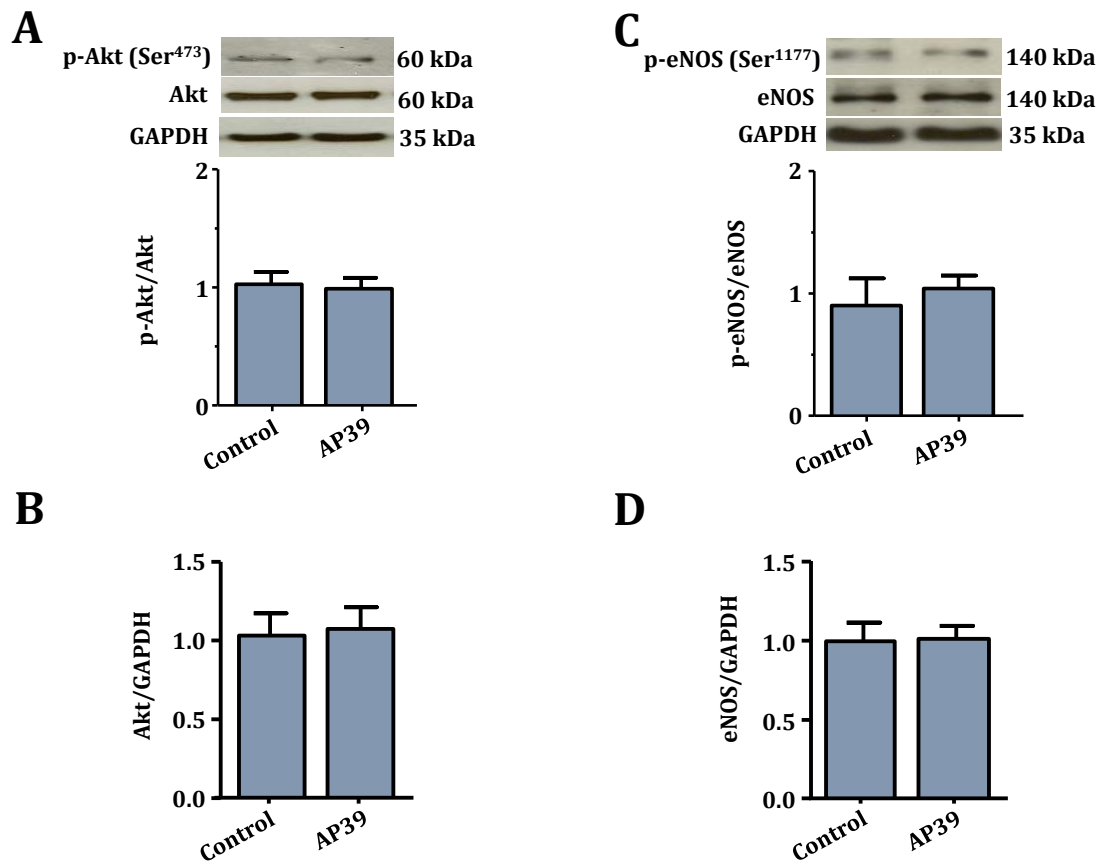


Figure 6.11 Effect of postconditioning with AP39 on the phosphorylation of Akt and eNOS at early reperfusion. Representative western blots and densitometry analysis of (A) p-Akt^{ser473}/total Akt, (B) total Akt/ GAPDH, (C) p-eNOS^{ser1177}/total eNOS and (D) total eNOS/GAPDH. Specific antibodies were used to assess the effect AP39 on the phosphorylation of Akt and eNOS in myocardial biopsies harvested from the left ventricle after 5 minutes of reperfusion. Histograms show the relative ratio of phosphorylated protein to the total level of protein. GAPDH was used as an internal standard for all quantifications. Data were analysed using unpaired student's *t*-test and presented as mean \pm SEM. There was no significant difference between AP39 and control. For all groups, *n* = 6 hearts from 6 independent experiments.

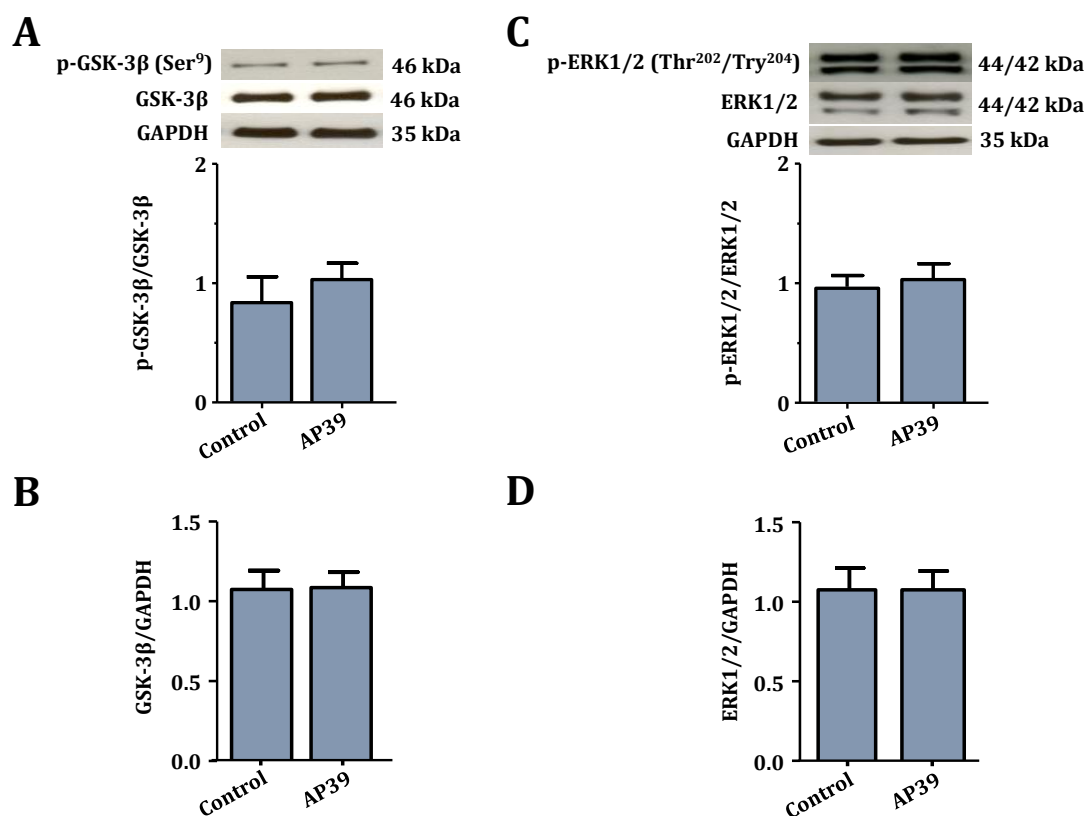


Figure 6.12 Effect of postconditioning with AP39 on the phosphorylation of GSK-3B and ERK1/2 at early reperfusion. Representative western blots and densitometry analysis of (A) p-GSK-3 β ^{ser9}/total GSK-3 β , (B) total GSK-3 β /GAPDH, (C) p-ERK1/2^{Thr202/Try204}/total ERK1/2 and (D) total ERK1/2/GAPDH. Specific antibodies were used to assess the effect AP39 on the phosphorylation of GSK-3 β and ERK1/2 in myocardial biopsies harvested from the left ventricle after 5 minutes of reperfusion. Histograms show the relative ratio of phosphorylated protein to the total level of protein. GAPDH was used as an internal standard for all quantifications. Data were analysed using unpaired student's *t*-test and presented as mean \pm SEM. No significant difference between AP39 and control. For all groups, *n*= 6 hearts from 6 independent experiments.

6.3.5 Direct mitochondrial effects of AP39

6.3.5.1 Toxicity study of AP39 on the mitochondria

The first series of mitochondria experiments involved evaluation of the toxicity of AP39 on the mitochondria using two approaches, namely mitochondrial membrane potential and autofluorescence. Mitochondria were treated with a concentration range of AP39 (0.3, 1, 3, 5, 10 μM) which was equivalent to the dosing range used *in vivo*. At the highest concentration of AP39 (10 μM), AP39 started to disturb the mitochondria integrity as an evidence of increase in Rhodamine 123 leak (Figure 6.13A) and decrease in mitochondrial autofluorescence (Figure 6.13B). None of the other concentration induced detectable effect on either mitochondrial membrane potential or autofluorescence. Accordingly, the concentration range (0.3, 1, 3 and 5 μM) of AP39 was used in the consequent mitochondrial studies.

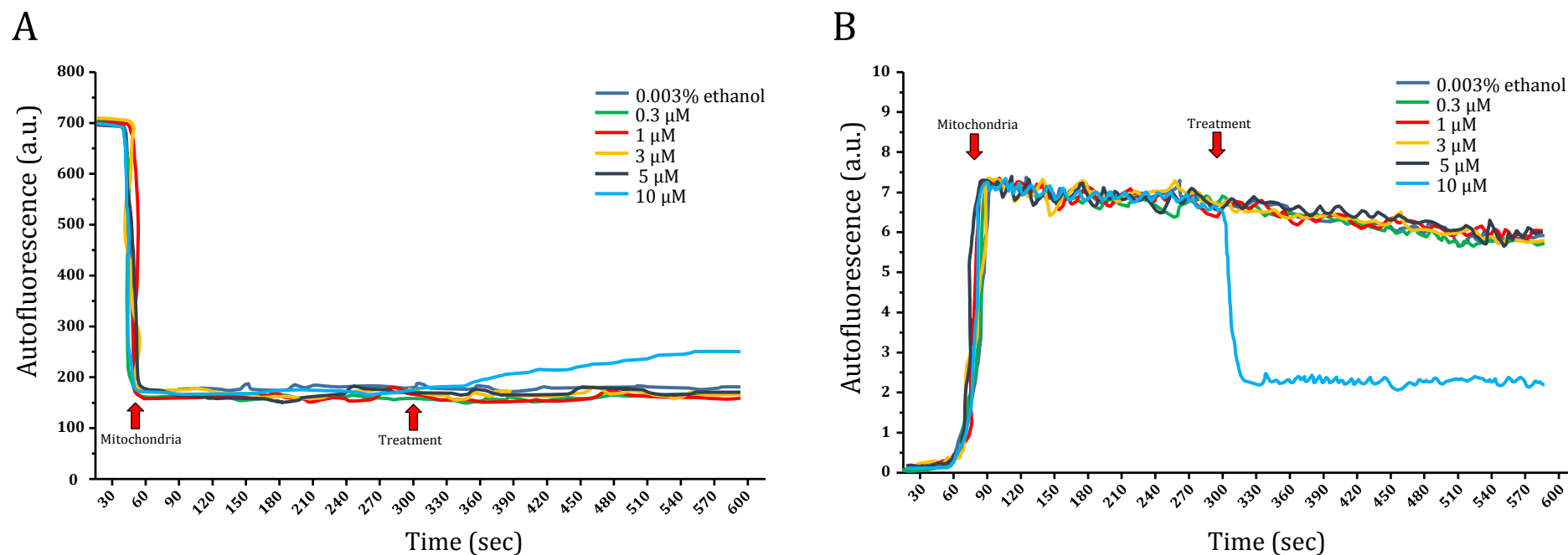


Figure 6.13 Toxicity study of AP39 on subsarcolemmal rat mitochondria *in vitro*. (A) Mitochondrial membrane potential and (B) autofluorescence were measured when mitochondria were treated with vehicle (0.003% ethanol) or with AP39 (0.3, 1, 3, 5 and 10 μM). AP39 started to disturb mitochondria integrity at 10 μM concentration. Accordingly, the concentration range (0.3-5 μM) was considered safe and used in subsequent mitochondrial studies. a.u., arbitrary unit. Arrows indicate when mitochondria were introduced and when treatments were added into the solution.

6.3.5.2 AP39's impact on Ca²⁺ overload-induced PTP opening

We examined the effect of specific-delivery of H₂S into the mitochondria on the susceptibility of PTP opening as a result of Ca²⁺ overload. We used freshly isolated rat-derived SSM and IFM and treated them with either vehicle or AP39 (1 μM). SSM and IFM were then exposed to pulses of Ca²⁺ in the presence and absence of CsA as a positive control (Figure 6.14). Untreated IFM showed a 30% higher calcium tolerance than untreated SSM (in μmol of Ca²⁺ mg⁻¹: 171 ± 9 vs 121 ± 8, p<0.001). AP39 elicited a significant inhibitory effect on PTP opening in both SSM and IFM compared to vehicle-treated mitochondria (in μmol of Ca²⁺ mg⁻¹: 163 ± 6 and 240 ± 15, respectively, p<0.001). The inhibitory effect of AP39 on PTP opening was comparable to that observed after CsA in both mitochondria fractions, which represents almost 30% increase in mitochondrial Ca²⁺ tolerance. Interestingly, AP39 showed an additive effect to CsA-induced inhibition of PTP opening. There was a further 25% increase in mitochondrial Ca²⁺ retention capacity when mitochondria were incubated with both AP39 and CSA before the exposure to Ca²⁺ pulses, compared to CsA alone (in μmol of Ca²⁺ mg⁻¹: SSM: 240 ± 9 vs 180 ± 7, p<0.001; IFM: 351 ± 19 vs 261 ± 14, p<0.001).

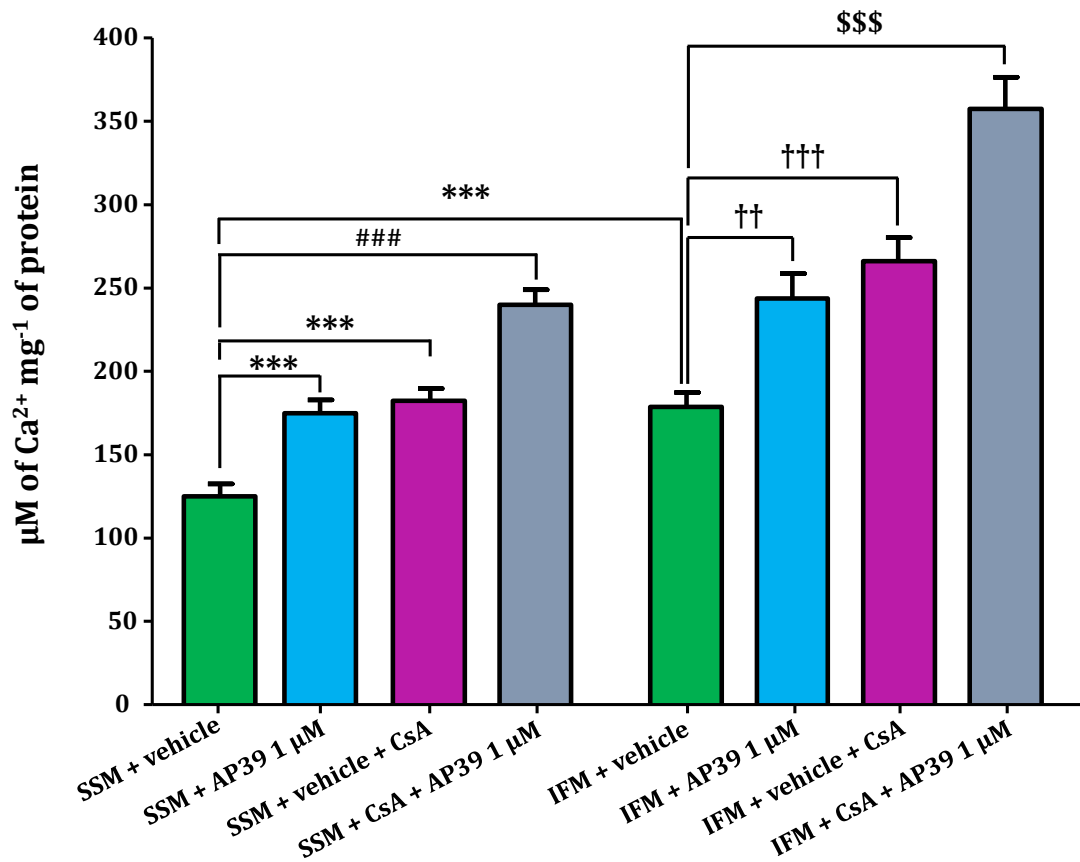


Figure 6.14 Effect of AP39 on the opening of the mitochondria permeability transition pore (PTP). Subsarcolemmal (SSM) and interfibrillar (IFM) mitochondria were individually incubated with either vehicle (0.003% ethanol) or AP39 (1 μ M). Mitochondria were then subjected to series of 5 μ M of CaCl_2 per 3 minutes at 25 $^{\circ}$ C until the opening of the PTP. CsA was used as a positive control to inhibit the opening of PTP. Data were analysed using two-way ANOVA followed by Bonferroni post hoc test and presented as mean \pm SEM, *** p <0.001 vs SSM + vehicle, ### p <0.001 vs SSM + vehicle + CsA, †† p <0.01 vs IFM + vehicle, ††† p <0.001 vs IFM + vehicle. \$\$\$ p <0.001 vs IFM + vehicle + CsA. n =10 per group.

6.3.5.3 The effect of AP39 on mito-ROS generation

Overwhelming mitochondrial ROS generation at early reperfusion is one of the main determinants of cellular injury. Therefore, we performed *in vitro* experiments to look at the direct effect of AP39 on H₂O₂ generation in the rat isolated cardiomyocyte mitochondria (Figure 6.15). SSM and IFM were incubated with: 1) no intervention, (2) vehicle (0.003% ethanol), (3) AP39 (0.3, 1, 3 and 5 μ M). In the control groups, ROS generation was significantly lower, by 20%, in IFM than SSM (0.67 ± 0.06 a.u. vs 0.84 ± 0.04 a.u., $p < 0.05$). There was no significant difference in mito-ROS generation between the first control and the second control in either mitochondria fraction. AP39 showed a dose-dependent inhibition of ROS generation in both subpopulations where AP39 (1 μ M) exerted the maximum inhibitory effect (38% in SSM and 61% in IFM) compared to control, vehicle-treated and the second control mitochondria. The maximum inhibitory effect of AP39 was significantly greater in IFM than in SSM (0.28 ± 0.03 a.u. vs 0.52 ± 0.08 a.u., $p < 0.05$). Interestingly, the inhibitory effect of AP39 on mitochondrial ROS generation was gradually reduced as the concentration was increased. Rotenone, as a positive control, resulted in overproduction of ROS to almost the same extent in both SSM and IFM (2.4 ± 0.4 a.u. and 2.7 ± 0.2 a.u., respectively). Rotenone, used as a positive control, resulted in overproduction of ROS in both SSM and IFM by 3.2 and 3.6 folds, respectively, compare to the basal ROS generation level.

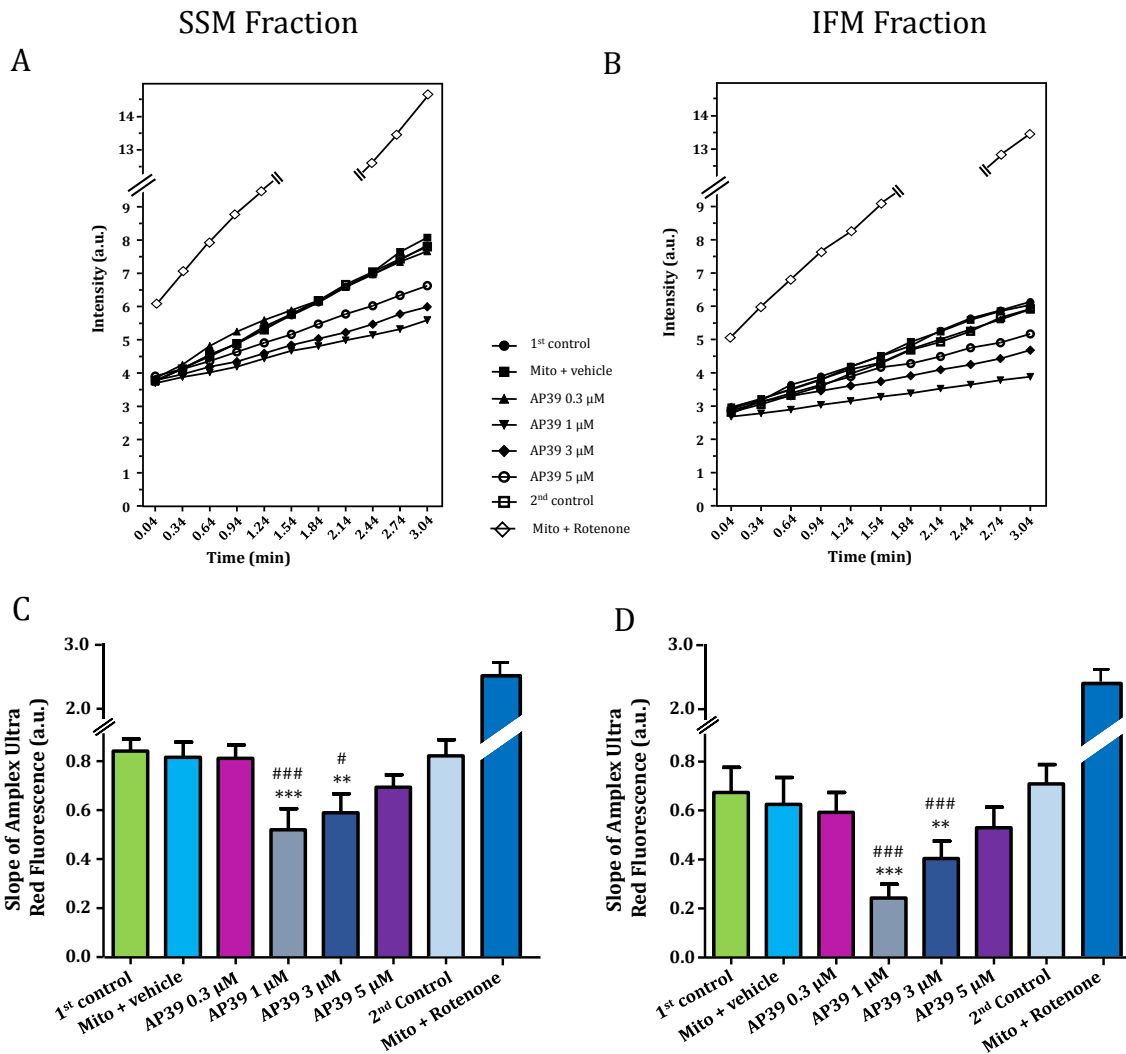
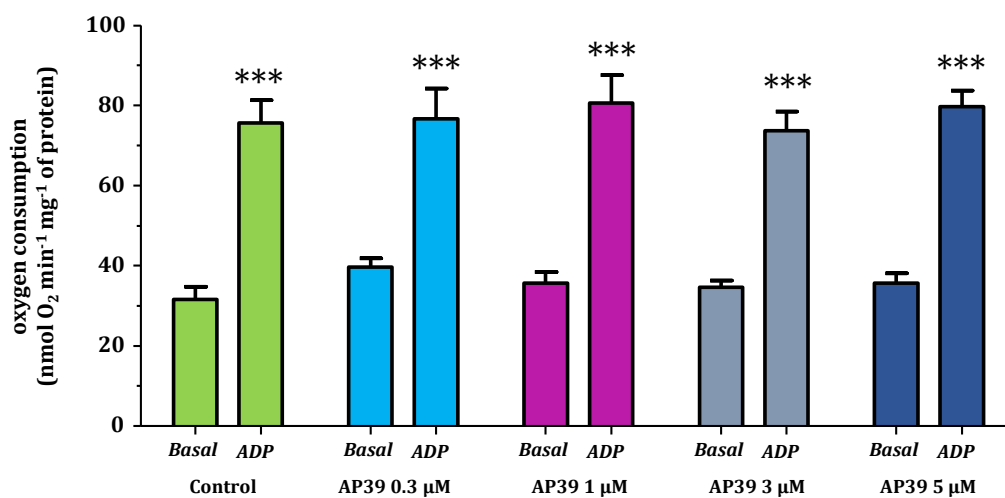


Figure 6.15 Effect of AP39 on mitochondrial-ROS generation. Mitochondria subpopulations (SSM and IFM) were incubated with either vehicle (0.05% DMSO) or different concentrations of AP39. Rotenone 123 was used as a positive control to overproduce ROS through inhibition of complex I. Second control was measured at the end of each series of experiments to avoid any false positive results due to the run-down of mitochondria fitness with the time. (A) and (B) are representative charts for the ROS generation of SSM and IFM, respectively, and error bars were removed for clarity. The slope of ROS generation was measured continuously for 4 minutes with the fluorescence indicator Amplex Ultrared both in (C) subsarcolemmal (SSM) and (D) interfibrillar (IFM) mitochondria. Data are expressed as mean \pm SEM and analysed using two-way ANOVA followed by Bonferroni post hoc test. ** $p < 0.01$, *** $p < 0.001$ vs 1st control; # $p < 0.05$, ### $p < 0.001$ vs 2nd control. $n = 10$ per group.

6.3.5.4 The effect of AP39 on mitochondrial oxygen consumption

Mitochondrial respiration was measured for both SSM and IFM using substrates for complex I (glutamate and malate) and complex II (succinate, in the presence of rotenone to inhibit complex I). There was no difference in the basal respiration of the two subpopulations of mitochondria (in $\text{nmol O}_2 \text{ min}^{-1} \text{ mg}^{-1}$: complex I - SSM: 32 ± 10 , IFM: 40 ± 16 , complex II – SSM: 56 ± 14 , IFM: 68 ± 16 , Figures 6.16 and 6.17). For the IFM, ADP-stimulated respiration was higher in IFM compared to SSM for both complexes I and II (in $\text{nmol O}_2 \text{ min}^{-1} \text{ mg}^{-1}$: complex I – SSM: 76 ± 18 , IFM 101 ± 17 , complex II – SSM: 134 ± 30 , IFM: 193 ± 23). Different concentrations of AP39 (0.3, 1, 3, 5 μM) were tested on SSM or IFM; however, none of the concentrations examined significantly influenced mitochondrial oxygen consumption.

Complex I



Complex II

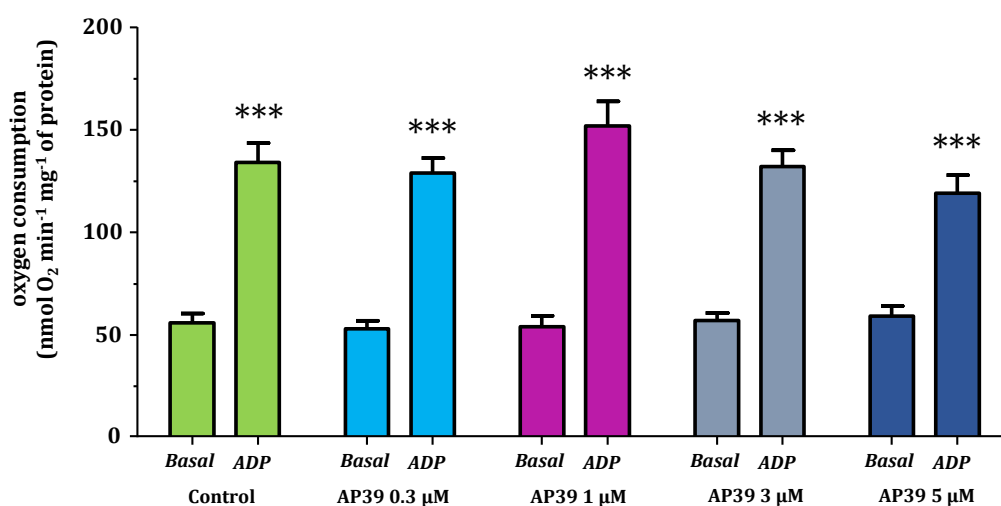
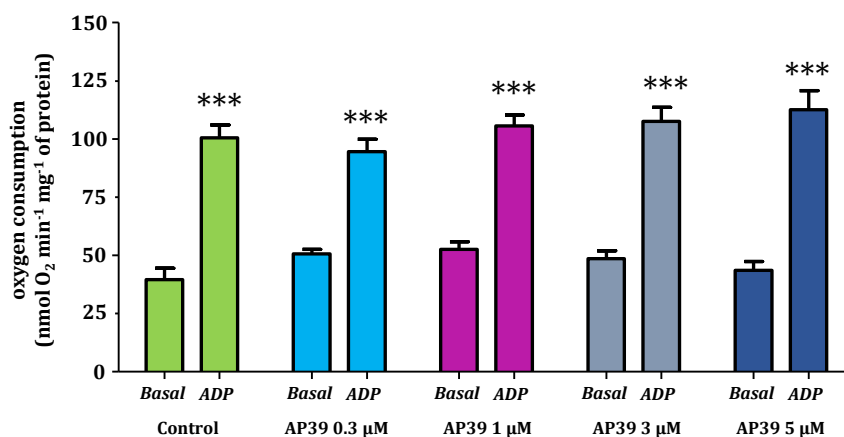


Figure 6.16 Effect of AP39 on mitochondrial oxygen consumption in subsarcolemmal (SSM) mitochondria. Mitochondrial oxygen consumption of complexes I and II of the respiratory chain was measured at the basal level and after stimulation with ADP. SSM were incubated with either vehicle (0.003% ethanol) or different concentrations of AP39 for 3 minutes before stimulating the respiration by ADP. Data were analysed via repeated measures ANOVA with Bonferroni post hoc test and reported as mean \pm SEM. *** p < 0.001 vs basal level. n = 10 per group.

Complex I



Complex II

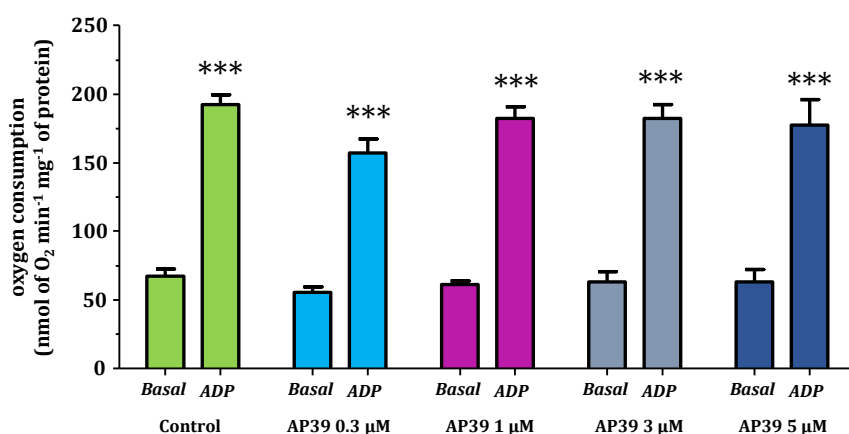


Figure 6.17 Effect of AP39 on mitochondrial oxygen consumption in interfibrillar (IFM) mitochondria. Mitochondrial oxygen consumption of complexes I and II of the respiratory chain was measured at the basal level and after stimulation with ADP. IFM were incubated with either vehicle (0.003% ethanol) or different concentrations of AP39 for 3 minutes before stimulating the respiration by ADP. Data were analysed via repeated measures ANOVA with Bonferroni post hoc test and reported as mean \pm SEM. *** $p < 0.001$ vs basal level. $n = 10$ per group.

6.3.5.5 Mitochondrial GSH and GSSG levels after AP39 application

The influence of mitochondrial application of H₂S, using AP39, on the production of mitochondrial GSH, as a possible mechanism for the limitation of mito-ROS generation observed with AP39, was evaluated *in vitro*. Incubation of SSM with AP39 did not show a significant change in the level of either GSH or GSSG compared to the control (Figure 6.18A and B). Similarly, AP39 had no effect on GSH/GSSG ratio in the SSM (Figure 6.18C).

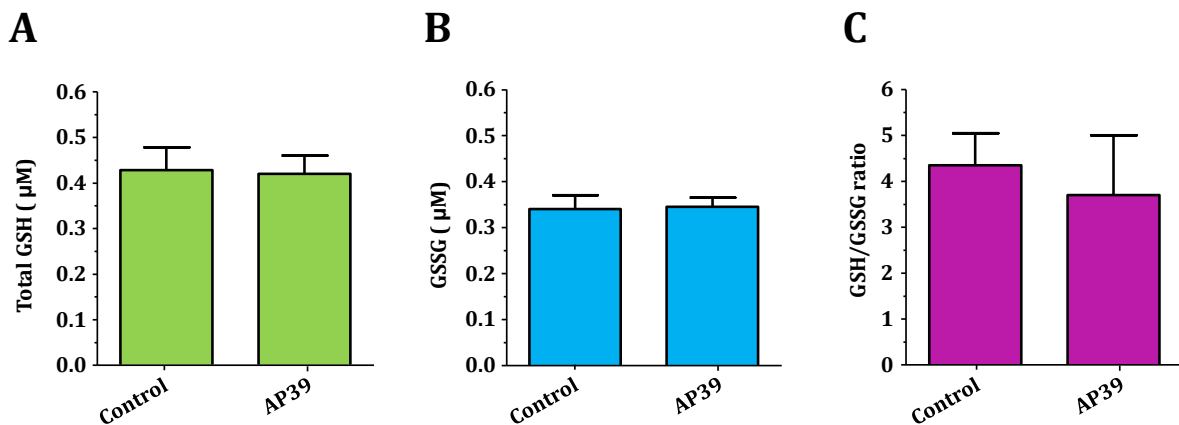


Figure 6.18 GSH and GSSG contents in the mitochondria following AP39 application. Mitochondria were incubated with either vehicle (0.003% ethanol) or AP39 (1 µM) then purified and absorbance of both total GSH and GSSG were measured. Data were analysed using unpaired student's *t*-test and reported as mean ± SEM. There was no significant difference between AP39 and control. For each groups, *n*= 3 hearts from 3 independent experiments.

6.3.5.6 The pattern of S-nitrosylation following AP39 application *in vitro*

The effect of AP39 on the S-nitrosylation of mitochondrial proteins in cardiomyocyte mitochondria both SSM and IFM, was assessed *in vitro*. The effect of AP39 (0.3 and 1 μ M) was compared with SNAP (for Ponceau S staining) and with GSNO (for Pierce S-nitrosylation western blot kit) as positive controls. Analysis of Ponceau S stained membrane did not show a significant change in the general pattern of protein expression following AP39 application in either subpopulation (Figure 6.19 and 6.20). Interestingly, incubation of either mitochondrial fraction with SNAP also did not have a significant effect on the general expression of mitochondrial proteins.

S-nitrosylation of mitochondrial proteins was also examined following AP39 application using Pierce S-nitrosylation Western blot kit. None of AP39 concentrations used in these experiments significantly altered the pattern of mitochondrial protein expression in either subpopulation of mitochondria (Figure 6.21 and 6.22). However, the positive control (GSNO) which was used in this series also did not show any significant effect on the general mitochondrial proteins expression compare to the control group in both SSM and IFM.

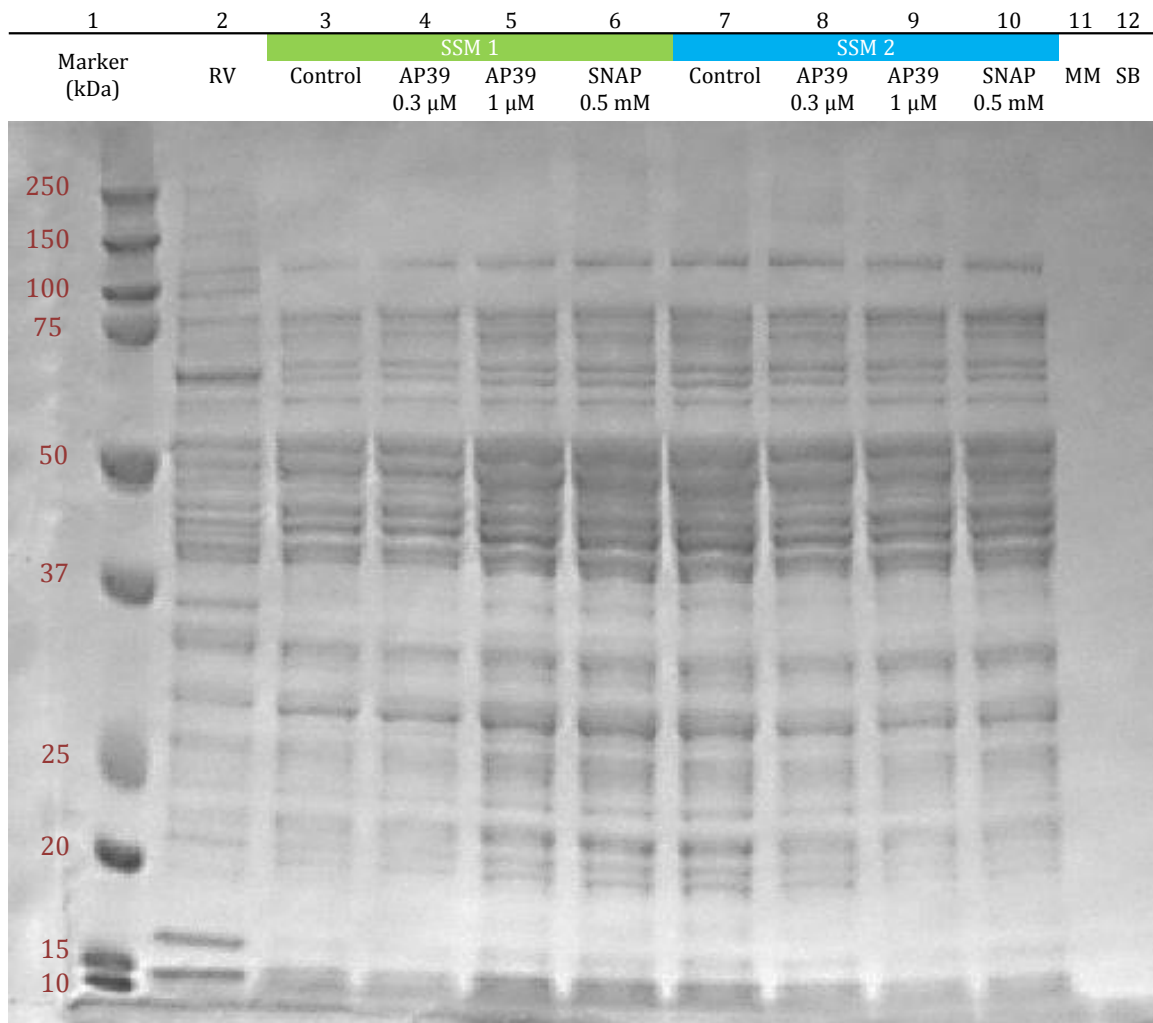


Figure 6.19 Overall SSM proteins stained with Ponceau S following treatment with AP39. SSM were stimulated with AP39 (0.3 μ M and 1 μ M) and SNAP (0.5 mM), as a positive control. The representative blot demonstrated that there was no significant difference in banding pattern between AP39-treated mitochondria and the control group. SNAP, as a positive control, also did not show a significant effect on the banding pattern compare to the control group. RV, right ventricle; MM, Master Mix; SB, sample buffer.

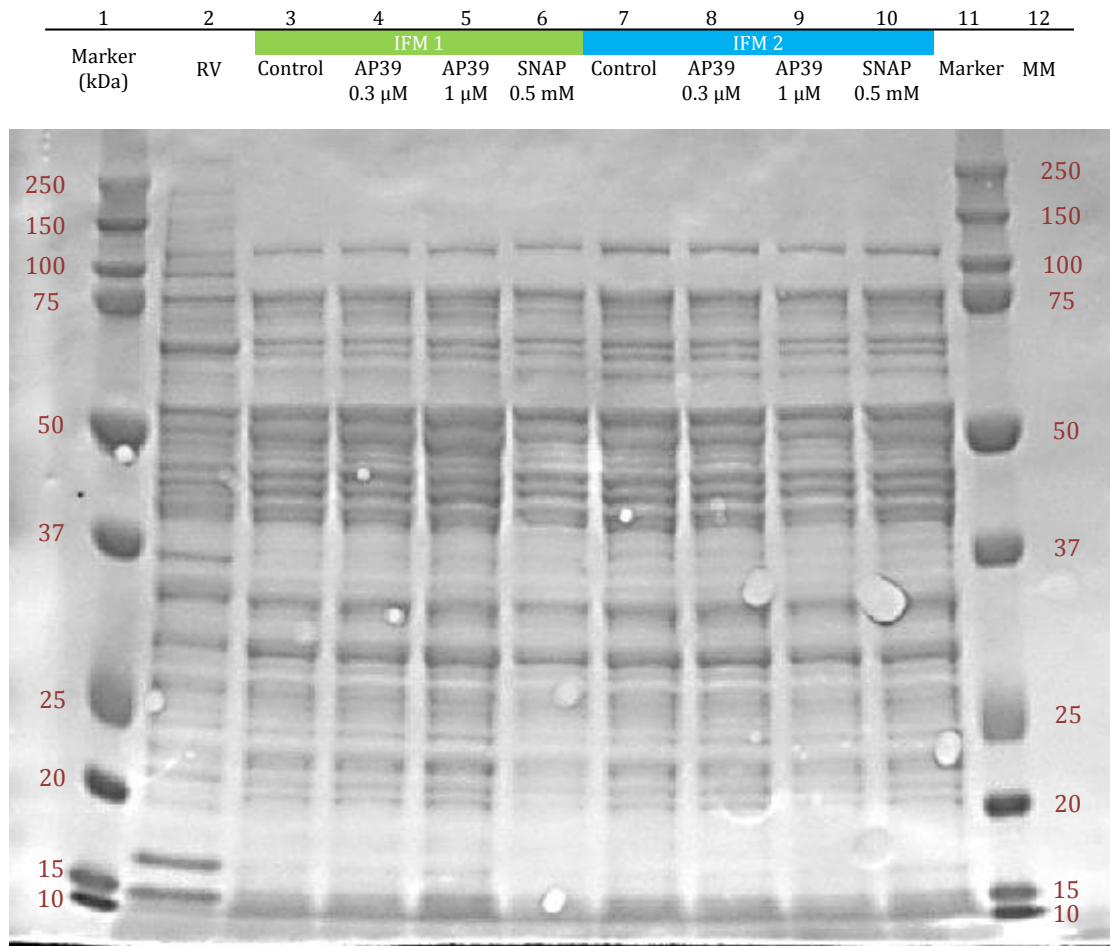


Figure 6.20 Overall IFM proteins stained with Ponceau S following treatment with AP39. IFM were stimulated with AP39 (0.3 μ M and 1 μ M) and SNAP as a positive control. The representative blot demonstrated that there was no significant difference in banding pattern between AP39-treated mitochondria and the control group. It also shows no significant difference in the positive control mitochondria which were treated with SNAP. RV, right ventricle; MM, Master Mix.

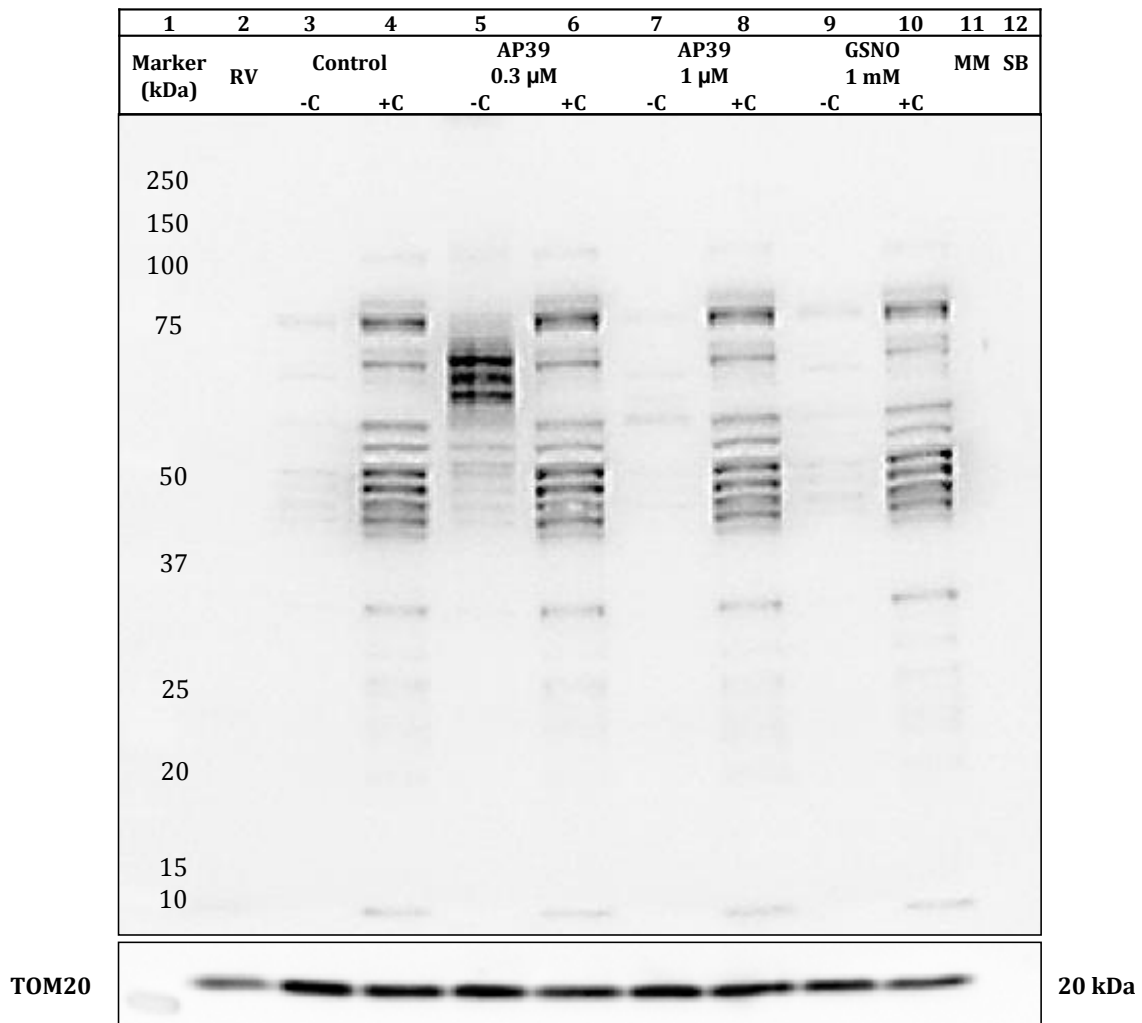


Figure 6.21 Immunoidentification of the S-nitrosylated protein in subsarcolemmal mitochondria following AP39 application. Representative blot demonstrates that none of AP39 concentrations used in this series exerted a significant effect on the S-nitrosylation pattern, neither did the positive control GSNO. The membrane was stripped and probed with a specific antibody to mitochondrial import receptor subunit (TOM20), which demonstrated that there was no significant difference in the protein loading. RV, right ventricle; +C, positive control; -C, negative control; MM, Master Mix; SB, sample buffer; TOM20, mitochondrial import receptor subunit homolog.

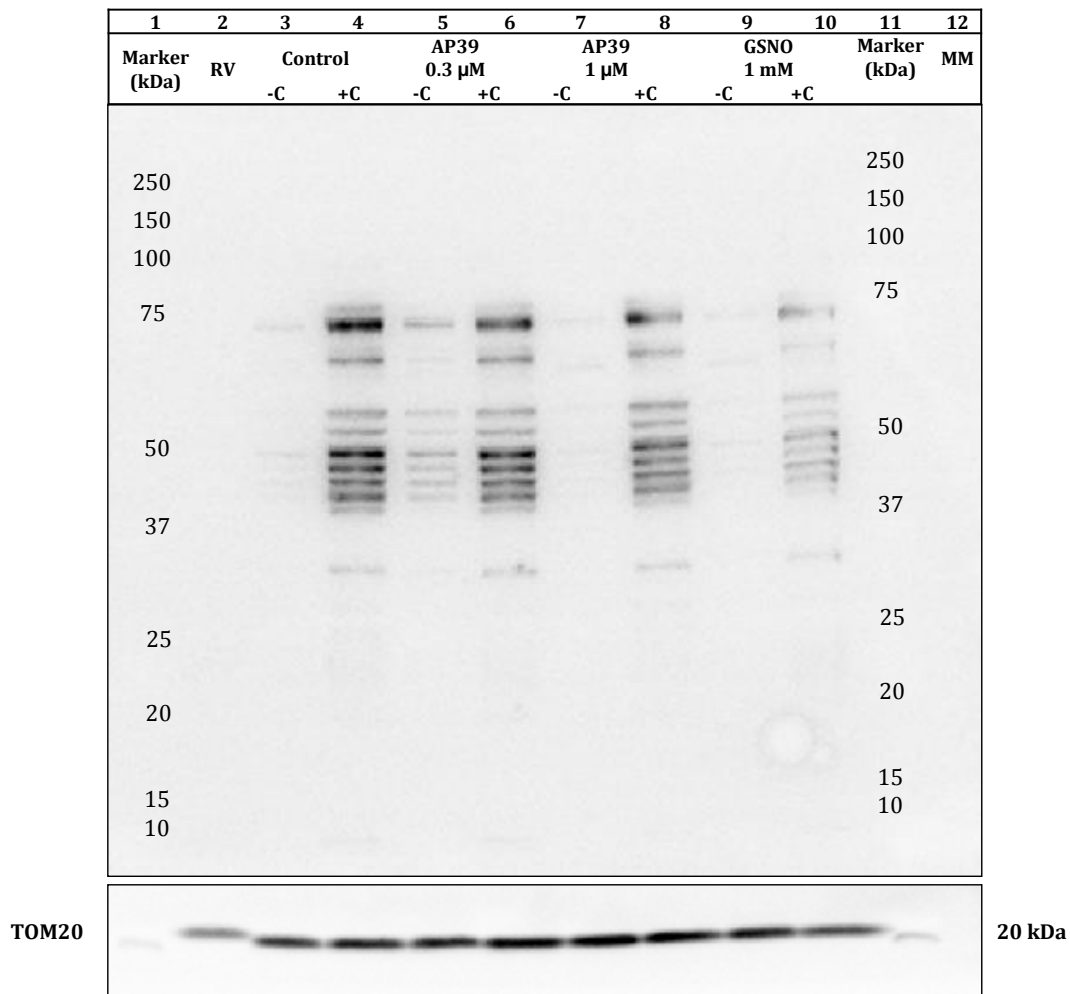


Figure 6.22 Immunoidentification of the mitochondrial S-nitrosylated protein in interfibrillar mitochondria following AP39 application. Representative blot demonstrates that none of AP39 concentrations used in this series exerted a significant effect on the S-nitrosylation pattern, neither did the positive control GSNO. The membrane was stripped and probed with a specific antibody to mitochondrial import receptor subunit (TOM20), which demonstrated that there was no significant difference in the protein loading. RV, right ventricle; +C, positive control; -C, negative control; MM, Master Mix; SB, sample buffer; TOM20, mitochondrial import receptor subunit homolog.

6.4 Discussion

The main findings of this study are:

- 1- AP39 had an infarct-limiting effect and improved post-ischaemic cardiac contractility in a postconditioning mimetic manner when given specifically at reperfusion.
- 2- Neither the mitochondria-targeting scaffold (AP219) nor the H₂S donor moiety (ADT-OH) had any detectable effect on either infarct size or RPP recovery.
- 3- Postconditioning with AP39 was attributed to directly targeting the mitochondria and in a cytosol-independent manner.
- 4- AP39 inhibited the opening of PTP in cardiomyocyte mitochondria, namely SSM and IFM, subjected to Ca²⁺ overload.
- 5- Application of AP39 limited mito-ROS generation in SSM and IFM fractions.
- 6- AP39 did not have an effect on mitochondrial oxygen consumption by complexes I and II in both SSM and IFM.
- 7- The levels of mitochondrial GSH and GSSG were not affected by AP39 application in SSM and IFM mitochondrial populations.

These results demonstrate that AP39 can protect the heart against ischaemia/reperfusion injury when given as an adjunct to reperfusion in a cytosolic-independent manner by limiting mito-ROS generation and inhibiting the opening of PTP.

6.4.1 Postconditioning the heart with AP39

Postconditioning the heart by H₂S (PostC-H₂S) has been reported to be cardioprotective by us and others who used either bolus dose of H₂S at reperfusion (King et al., 2014, Bibli et al., 2015, Karwi et al., 2016) or overexpression of CSE to increase endogenous H₂S production (Elrod et al., 2007, Calvert et al., 2010). Several mechanisms have been proposed for the cardioprotective effect of H₂S including: 1) triggering the RISK pathway (PI3K/Akt and/or ERK1/2 signalling pathway (Li et al., 2015a); 2) influencing antioxidant gene expression (Calvert et al., 2009); 3) direct effects on the mitochondria (Yao et al., 2010). However, the exact mechanism is not yet clearly identified. Part of this uncertainty is due to the nature of the commercially-available pharmacological tools which have been extensively utilised to deliver H₂S, namely NaHS and Na₂S (Whiteman et al., 2011). The purity of these salts is often questionable and their aqueous solutions cause a rapid peak in plasma H₂S level, followed by rapid clearance from the circulation (Bos et al., 2015). There have also been doubts surrounding the actual dose/concentration used in these studies that render them unreliable and uncontrollable sources of H₂S. The new slow-release series of H₂S donors, such as GYY4137 (Li et al., 2008), ATB-346 (Wallace et al., 2012) and SG-1002 (Kondo et al., 2013), have shown better pharmacokinetic profiles and more reproducible biological activities. However, the potential for translation is still hindered by the cardioprotective dose of these donors (generally >200 µM) (Le Trionnaire et al., 2014). Therefore, enhancing the activity of the existing H₂S donors or developing a new series of H₂S donors which can target particular tissues or cellular compartments has been a focus of recent research in the field of H₂S biology.

In the present study, AP39 significantly limited infarct size and improved the post-ischaemic functional recovery, both in a dose-dependent manner, when administered prior to reperfusion. Consistent with these data, Ahmed et al. (2016) recently reported that AP39 also exerted a dose-dependent attenuation in the renal damage, oxidative stress and renal inflammation when applied at reperfusion in an *in vivo* model of renal ischaemia/reperfusion injury. We observed that TPP⁺ scaffold molecule (AP219) and H₂S-generating moiety (ADT-OH), which were used as controls, had no detectable effect on either myocardial infarction or hemodynamic recovery. This is in agreement with other reports where these controls lacked biological activity when used at nanomolar or micromolar concentrations (Le Trionnaire et al., 2014, Szczesny et al., 2014). Recent work by Papapetropoulos's group (Chatzianastasiou et al., 2016) reported a "head-to-head" comparison of infarct limitation by different H₂S donors (Na₂S, GYY4137, thiovaline and AP39), and elucidation of the role of NO in mediating protection. Intriguingly, all donors had the same infarct-limiting effect in a mouse model of ischaemia/reperfusion injury. It is noteworthy that the optimum cardioprotective doses of GYY4137 and AP39 used were 26.6 μmol kg⁻¹ and 0.25 μmol kg⁻¹, respectively. Very recently, we reported that 26.6 μmole kg⁻¹ GYY4137 was not cardioprotective in an *in vivo* rat model of ischaemia/reperfusion injury with the optimum cardioprotective dose being 10-fold higher (Karwi et al., 2016). Similarly, in the present study we demonstrated that AP39 exerts an infarct-sparing effect with an optimum cardioprotective dose of 1 μmol kg⁻¹, 4-fold higher than the effective dose in mouse reported by Chatzianastasiou et al. (2016). No haemodynamic data are available to compare

AP39-induced dose-dependent improvement in post-ischaemic functional recovery in Chatzianastasiou's paper.

6.4.2 Cytosol independent cardioprotection by AP39

This study provides important mechanistic insight into AP39's cardioprotective action *in vivo*. We found that selective blockade of PI3K, which is known to mediate the cardioprotective effect of non-mitochondrial H₂S donors (Andreadou et al., 2015, Karwi et al., 2016), did not abolish the cardioprotection of AP39. Cross-talk between H₂S and NO has been suggested to be responsible for the H₂S-induced cardioprotection. King et al. (2014) and Bibli et al. (2015) have shown that H₂S-induced cardioprotection against ischaemia/reperfusion injury was not observed when eNOS was genetically silenced or pharmacologically inhibited in mice. Intriguingly, the same study by Bibli et al. (2015) reported that H₂S supplement at reperfusion was cardioprotective in rabbit through a NO-independent mechanism. Moreover, we recently reported that cardioprotection by GYY4137, a slow-releasing H₂S donor, was partially attenuated but was not abolished by L-NAME *in vivo* in a rat model of myocardial ischaemia/reperfusion injury (Karwi et al., 2016). However, the nature of this crosstalk seems to have different patterns in different organs/tissues and in various experimental conditions across species (Hancock and Whiteman, 2016). To test whether AP39 is signalling through the NO/sGC pathway, we blocked the endogenous synthesis pathway of NO and also inhibited the activity of its end effector (sGC) using L-NAME and ODQ, respectively. We found that cardioprotection by AP39 was still present when either L-NAME or ODQ were given with AP39.

These results were supported by analysis of protein phosphorylation state during early reperfusion. We observed that AP39 did not induce the phosphorylation of either Akt ser⁴⁷³ or eNOS ser¹¹⁷⁷ at 5 min reperfusion. Chatzianastasiou et al. (2016) reported that AP39 did not phosphorylate either eNOS ser¹¹⁷⁶ or VASP ser²³⁹ after 10 minutes of reperfusion and its cardioprotection was not abolished by either L-NAME or DT2, indicating a cGMP/PKG-independent mechanism in the murine model. Their data are complementary to the fuller characterisation of the potential cytosolic signalling targets of AP39 that we present here. To further characterise the cardioprotective mechanism of AP39, we also investigated the effect of AP39 on the phosphorylation of GSK-3 β , a downstream effector of the RISK pathway, and ERK1/2, a parallel arm of the RISK pathway. We observed no significant change in the phosphorylation of either GSK-3 β or ERK1/2 at early reperfusion. Viewed together, our data and those of Chatzianastasiou et al. (2016) provide persuasive evidence that, unlike other H₂S donors, AP39 mediates its cardioprotection by a mechanism that is independent of activation of the cytosolic components of the RISK signalling cascade.

6.4.3 Inhibition of PTP opening by AP39

We then investigated the potential mitochondrial mechanism involved in the cardioprotection of AP39. We first tested the hypothesis that postconditioning with AP39 protects the heart against acute myocardial infarction by inhibiting the PTP opening at early reperfusion. To do so, we have characterised for the first time the direct effect of AP39 on the most relevant subpopulations of cardiomyocyte mitochondria, namely subsarcolemmal (SSM) and interfibrillar (IFM) mitochondria. Inhibition of PTP opening in the first minutes of reperfusion

has been extensively reported to protect against reperfusion injury (Halestrap, 2010, Ong et al., 2015). It has been shown that many cardioprotective manoeuvres and interventions act to maintain PTP in a closed state at reperfusion (Hausenloy et al., 2009). With this in mind, we investigated the influence of AP39 on the opening of PTP, as a result of Ca²⁺ overload, in cardiac SSM and IFM *in vitro*, as a possible mechanism for the protective effects of AP39. We found that AP39 inhibited PTP opening in SSM and IFM with no significant difference from the inhibitory effect of CsA, which can protect the heart against ischaemia/reperfusion injury by inhibiting PTP opening at reperfusion (Hausenloy et al., 2012). We also showed that intervening with both AP39 and CsA increased mitochondrial tolerance to Ca²⁺ overload and resulted in an additive effect compared to CsA effect alone. CsA prevents the opening of PTP, multiprotein complex spanning both inner and outer mitochondrial membranes, by desensitising CypD, a proposed modulator of PTP located in the mitochondrial matrix (Bernardi and Di Lisa, 2015). Having an additive effect to the inhibitory effect of CsA suggests that AP39 may inhibit PTP opening via a CypD-independent mechanism. In line with these findings, Chatzianastasiou et al. (2016) reported that AP39 (0.3 µM *versus* 1 µM in our study), exerted an additive effect to CsA in mouse mitochondria isolated from the whole heart. However, isolating mitochondria from whole heart tissue is potentially a problematic approach as a number cell types contribute to the isolated mitochondrial fraction, for example endothelial cells, fibroblasts and other local resident cells. Even more importantly, cardiomyocyte mitochondria, namely SSM and IFM, themselves significantly differ in their main characteristics including oxygen consumption, mito-ROS generation and Ca²⁺ retention

capacity (Palmer et al., 1977, Palmer et al., 1986). Our present study characterised for the first time the effect of AP39 on the most relevant cardiomyocyte mitochondria in the context of ischaemia/reperfusion injury, namely SSM and IFM.

6.4.4 Limitation of mito-ROS generation by AP39

We investigated potential mechanisms underlying AP39-induced inhibition of PTP opening. We characterised the effect of AP39 on the mito-ROS generation *in vitro* using SSM and IFM. The detrimental effect of overwhelming mito-ROS generation, as a result of respiratory chain uncoupling and oxidation of anaerobic metabolism products, is one of the hallmarks of ischaemia/reperfusion injury (Venditti et al., 2001, Chouchani et al., 2014, Brown and Griendling, 2015). It is one of the main contributors to the opening of PTP, initiating cell apoptosis and accelerated necrosis during reperfusion (Hausenloy et al., 2009). Targeted delivery of H₂S to the mitochondria with AP39 has been shown to preserve mitochondrial function and integrity by attenuating ROS in different experimental settings (Szczesny et al., 2014, Le Trionnaire et al., 2014, Ikeda et al., 2015, Ahmad et al., 2016). Since oxidative stress and the mitochondria play central roles in ischaemia/reperfusion injury, targeting the mitochondria with selective H₂S donors is a plausible therapeutic approach to limit ischaemia/reperfusion injury. Ikeda et al. (2015) found that AP39 (10 nmol kg⁻¹) given before cardiac arrest increased H₂S level in the brain, decreased H₂O₂ level in the serum and inhibited PTP opening. In line with these studies, our data showed that AP39 limited mitochondrial ROS level in both subpopulations of cardiac mitochondria. In the present study, AP39's activity against ROS generation was attenuated as

the AP39 concentration was increased in a dose-dependent manner. This is consistent with the findings of others (Szczeny et al., 2014, Ahmad et al., 2016) who suggested that H₂S, and AP39 in particular, has a bell-shaped dose-response curve where it could be protective at low concentrations but toxic at high concentrations.

6.4.5 Selective delivery of H₂S into the mitochondria by AP39 does not affect respiratory complexes I and II

We then wanted to look at the potential protective mechanisms by which selective delivery of H₂S into the mitochondria by AP39 attenuates mito-ROS generation. There is growing evidence that H₂S is an endogenous modulator of mitochondrial function in health and disease (Guo et al., 2012). The basal mitochondrial level of H₂S is mainly generated by 3-mercaptopyruvate sulfurtransferase (3-MST) and it appears to be essential for normal function of the citric acid cycle (Modis et al., 2013b). There is a clear evidence that the intra-mitochondrial H₂S level is disturbed during oxidative stress due to the increase in H₂S degradation and reduction in its production which might contribute to cell death (Geng et al., 2004, Doeller et al., 2005, Whiteman et al., 2011, Vandiver and Snyder, 2012). This is consistent with some observations that overwhelming ROS generation during ischaemia/reperfusion injury, which also results in mitochondrial dysfunction, causes a reduction in H₂S availability (Predmore et al., 2012, Bos et al., 2015). This reduction is usually combined with translocation of the H₂S generating enzymes CBS and CSE from the cytosol to the mitochondria as a cellular adaptation to compensate for the suppression in H₂S production (Fu et al., 2012, Modis et al., 2013a, Szabo et al., 2013). Fox et al.

(2012) reported that the mitochondria of RNAi-mediated CSE knockdown in cells rendered them more vulnerable to oxidative stress and mitochondrial toxicity. H₂S replacement, either by H₂S donors (such as the non-targeting compound GYY4137) or overexpression of endogenous synthetic enzymes, has been shown to protect against ischaemia/reperfusion injury by mitigating oxidative stress and preserving mitochondrial integrity (Andreadou et al., 2015). We also investigated whether AP39 could have an effect on the mitochondrial electron transport chain which is a major source of mito-ROS generation at early reperfusion. It has been reported that H₂S at low concentration (nanomolar/low micromolar) can stimulate mitochondrial ATP production by acting as an “emergency fuel” for the electron transport chain inorganic electron donor (Szabo et al., 2014, Modis et al., 2014). It donates electrons at the level of coenzyme Q to the sulfide quinone reductase (SQR) where the electrons then transport to complex III, cytochrome c and complex IV which finally reduces molecular oxygen to water (Goubern et al., 2007). However, sulfide oxidation is an inefficient source of energy as it cost more oxygen (three mole of oxygen for each sulfide molecule) with low yield of electrons (two sulfide molecules produces two electrons) compared to other mitochondrial carbon-containing substrates, namely NADH, FADH, succinate, L-alpha-glycerophosphate (Szabo et al., 2014). Accordingly, we sought to characterise the influence of AP39 on mitochondrial respiration through complexes I and II in both SSM and IFM. We did not detect any significant effect of AP39 on the oxygen consumption of these complexes in either mitochondrial subpopulation. With these results, we can exclude the possibility that H₂S delivered by AP39 improves mitochondrial respiration over the concentration range we employed. Moreover, these data

suggest the safety margin of the applied concentration range. However, arguably it is possible that AP39 might energise Complexes III and/or IV by electron donation without altering the activity of complexes I and II. It has been demonstrated that inhibition of complex I using rotenone did not affect sulfide oxidation, while inhibiting complex III or IV by antimycin or cyanide, respectively, impeded it (Volkel and Grieshaber, 1996, Yong and Searcy, 2001, Goubern et al., 2007). Nevertheless, this needs further investigation.

6.4.6 Mitochondrial GSH/GSSG ratio is not altered by AP39 application

We then measured the levels of both GSH and GSSG following AP39 application *in vitro* as another possible antioxidant mechanism for AP39-induced abrogation of mito-ROS generation. It has been reported that H₂S can mitigate oxidative stress-induced mitochondrial damage via increasing GSH pool in the mitochondria by increased GSH production, activation of cysteine/cysteine transporters and enhanced GSH uptake (Tan et al., 2010, Kimura et al., 2010). H₂S has also been demonstrated to upregulate the endogenous antioxidant defence mechanism against oxidative stress-induced mitochondrial dysfunction, namely superoxide dismutase (SOD) isoforms (Cu/Zn-SOD and Mn-SOD), catalase, glutathione S-transferase and glutathione peroxidase (Sun et al., 2012, Wen et al., 2013). Jha et al. (2008) also found that the H₂S donor IK11001 was protective against hepatic ischaemia/reperfusion injury by increasing the expression of Trx-1, HSP-90 and Bcl-2. In the present study, there was no significant effect of AP39 on the mitochondrial level of either GSH or GSSG after 10 minutes of exposure. However, antioxidant activity established by AP39 could possibly be due to the fact that H₂S is a potent reducing agent and directly

scavenge ROS and RNS as has been shown by other investigators in different experimental models (Geng et al., 2004, Whiteman et al., 2004, Tang et al., 2010).

6.4.7 The effect of AP39 on posttranslational modifications (PTMs)

We also wanted to explore the potential PTMs following mitochondrial stimulation with AP39. The interest in H₂S-induced PTMS has tremendously increased over the last five years demonstrating an array of its biological activities could be in fact mediated through these modifications. For instance, it has been demonstrated that endogenous H₂S mediates an indispensable smooth muscle relaxation through S-sulfhydration of K_{ATP} channel facilitating the binding of (PIP₂) to open the channel (Mustafa et al., 2011). Moreover, Murphy's group (Sun et al., 2016) found that NaHS could exert an infarct-limiting effect additive to SNAP in Langendorff perfused mouse heart potentially by protein S-sulfhydration (also known as S-persulfidation) and to a greater extent by increase in S-nitrosylation. Interestingly, proteomic analysis revealed that the majority of S-nitrosylated proteins were mitochondrial proteins. Modis et al. (2016) also very recently demonstrated that endogenous H₂S plays a supportive role for mitochondrial respiration through S-sulfhydration of the α -subunit mitochondrial inner membrane protein ATP synthase (F₁F₀ ATP synthase/Complex V) at Cys²⁴⁴ and Cys²⁹⁴. Furthermore, Meng et al. (2016) demonstrated that GYY4137 mitigated myocardial hypertrophy by downregulated KLF5 expression through S-sulfhydrating of SP-1, impairing its transcriptional activity. Conversely, S-sulfhydration of Keap1 by GYY4137 enhanced its transcriptional activity and enhanced the expression of Nrf2

attenuating the diabetes-induced atherosclerosis (Xie et al., 2016). A previous study by Kai et al. (2012) found that NaHS-induced protection was abolished in mitochondria-free cells. Taken together, these studies provide persuasive evidence for H₂S-induced PTMS and that the primary target of H₂S in cardioprotection is the mitochondrion. Ponceau S solution was used as a simple and quick method to identify any significant modification in the general protein expression in mitochondrial samples. We could not detect a considerable effect of AP39 on the general protein expression in both subpopulations of mitochondria. Interestingly, the effect of SNAP, which was used as a positive control, on the general protein expression was not reproducible which made it difficult to draw any conclusion. It is highly likely that the extent of protein modification (whether by protein S-nitrosylation and/or S-sulfhydration) mediated by both AP39 and SNAP might not be clearly distinguishable using Ponceau S staining. Therefore, we then used modified biotin switch assay to selectively measure S-nitrosylated cysteine occupancy by iodoTMTzeroTM label reagent and detect this by Western blot. However, the results of these experiments also were not conclusive as no detectable change was observed in the pattern of mitochondrial proteins S-nitrosylation following stimulation with AP39 in both mitochondria fractions. Interestingly, GSNO, the positive control in this series, also did not show any detectable effect on the general S-nitrosylation pattern in both subpopulations detected with the modified biotin switch method. It is plausible that H₂S-induced PMTS are rather selective/specific modifications to certain cellular targets and are unlikely to be detected by blotting the whole spectrum of mitochondrial proteins. More importantly, the concentration of H₂S which is delivered by AP39 is remarkably low (50 to 300 fold lower) compared

to the previous reports that showed significant change in the general proteins expression following exposure to H₂S (Sun et al., 2016, Modis et al., 2016). Therefore, more selective and sensitive approach to detect H₂S-induced PTMS might be using proteomic analysis to characterise the cellular and mitochondria targets of AP39 such as iodoTMT sixplex label reagent set and proteomic analysis.

6.5 Study limitations

The exact mechanisms whereby AP39 limits ROS generation and inhibits PTP opening remains to be determined. Ikeda et al. (2015b) reported that AP39 did not influence the expression of CSE, CBS or 3-MST in the brain. That means that AP39 probably elevates mitochondrial H₂S level without interfering with the endogenous synthesis of H₂S. A convincing body of evidence supports that H₂S mediates a wide range of its physiological roles through inducing its PTMS, namely S-nitrosylation and S-sulfhydration. Intriguingly, it has been demonstrated that the activities of CypD and F₀F₁ ATP synthase, the potential triggers/modulators of the PTP opening, could be manipulated through S-nitrosylation or S-sulfhydration and that could be cardioprotective against ischaemia/reperfusion injury. Accordingly, it is tempting to suggest that AP39 possibly modulate the activity of either CypD or F₀F₁ ATP synthase to inhibit the opening of PTP. However, this still needs further investigation. The molecular mechanism of mito-ROS suppression by AP39 also still unclear. In addition, it is still unclear how AP39 attenuated mito-ROS generation in cardiomyocyte mitochondria. Whether this antioxidant effect is mediated by direct quenching of ROS by H₂S or by enhancing endogenous antioxidant system (Trx-1, SOD,

catalase, GPx, for example) still needs to be characterised. Moreover, the possibility that AP39-induced S-sulphydration could influence the antioxidant gene transcription of certain transcription factors such as Nrf2, as shown by others, should not be discounted and awaits clarification. Furthermore, understanding whether mitochondrial protection is the only mechanism of infarct limitation or if there are other possible mechanisms involved in AP39's cardioprotection, such as triggering the SAFE pathway, still needs further investigation. The metabolism of AP39 as well as the concentration of the released H₂S by AP39 inside the mitochondria needs clarification.

6.6 Conclusion

We have presented evidence that selectively targeting the mitochondria with AP39 at reperfusion can significantly limit infarct size and improve post-*ischaemic* haemodynamic recovery in an *in vivo* model of myocardial *ischaemia/reperfusion* injury. Moreover, AP39's ability to selectively deliver low concentration of H₂S to the mitochondria can minimise off-target effects and toxicity associated with the less reliable inorganic H₂S donors. The cardioprotective effect of AP39 is not mediated by the RISK pathway, which appears to be a pivotal cardioprotective mechanism activated by other H₂S donors. In isolated SSM and IFM, targeted-delivery of H₂S inhibits mito-ROS generation in both subpopulations in a dose-dependent manner without affecting mitochondrial respiration. AP39 also inhibits the opening of PTP in a CypD-independent mechanism, and provides an inhibitory effect on the PTP opening which is additive to CsA. Taken together, these findings provide proof-of-concept that direct delivery of H₂S to mitochondria by mitochondria-targeting H₂S donors,

of which AP39 is a prototype, represents a novel and effective intervention to mitigate the irreversible myocardial injury associated with reperfusion. Although the clinical use of H₂S donors still needs further investigation, future translation of this concept using AP39 or derivatives as adjunctive therapy to reperfusion would be expected to improve clinical outcome after acute myocardial infarction.

Chapter 7 General Discussion

7.1 General discussion

7.1.1 Principal findings

The most important findings of the studies included in this thesis can be summarised as follows.

Slow and stable elevation of the level of exogenous H₂S applied as an adjunct to reperfusion is a cardioprotective approach in an *in vivo* rat model of myocardial ischaemia/reperfusion injury. This was demonstrated in Chapter 4 using GYY4137 a slow-releasing H₂S donor which significantly limited myocardial infarction when administered specifically at reperfusion compare to control hearts. The cardioprotective effect of GYY4137 was also confirmed to be mediated by its payload of H₂S and not due to the parent structure of GYY4137 as depleted GYY4137 lacked any infarct-limiting effect. The lack of activity with depleted-GYY4137 is consistent with other reports (Li et al., 2009, Whiteman et al., 2010b, Fox et al., 2012, Jamroz-Wisniewska et al., 2014). Co-administration of PI3K inhibitor LY294002 completely abolished GYY4137's cardioprotection through inhibiting GYY4137-enhanced phosphorylation of Akt and GSK-3 β . This suggested the essential role of PI3K/Akt/GSK-3 β signalling pathway for GYY4137-induced infarct limitation. Blocking endogenous NO synthesis using L-NAME reduced the infarct-limiting effect of GYY4137, but did not abrogate it, by inhibiting GYY4137-induced eNOS phosphorylation. This demonstrated a partial dependency of the cardioprotective effect of GYY4137 on the bioavailability of NO at reperfusion.

In Chapter 6, it was shown that augmenting the mitochondrial H₂S level with selective mitochondrial delivery of H₂S at reperfusion protects the heart against ischaemia/reperfusion injury *in vivo*. This was interpreted as acute supplement of AP39, a mitochondria-targeting H₂S donor, specifically given at reperfusion limited the infarct size and improved post-ischaemic functional recovery in the rat model of myocardial ischaemia/reperfusion injury. We also showed in Chapter 6 that blocking the activity of PI3K with LY294002 at reperfusion does not attenuate the protective effects of AP39. The involvement of NO and its end effector sGC in the cardioprotection of AP39 were also explored. Inhibition of endogenous NO synthesis with L-NAME at reperfusion showed no significant effect on AP39-induced cardioprotection. Similarly, selective oxidation of the haem site of sGC, leading to its inhibition, did not abrogate the infarct limitation by AP39. In line with that, we also demonstrated that postconditioning the heart with AP39 does not alter the levels of p-Akt, p-eNOS, p-GSK-3 β and p-ERK1/2 in the ischaemic myocardium at early reperfusion. These data supported the hypothesis that AP39 directly targets the mitochondrion and does not trigger cytosolic salvage kinases to mediate its cardioprotection. We also explored the direct effects of AP39 on isolated cardiomyocyte mitochondria, namely SSM and IFM. We showed that AP39 inhibits the opening of PTP in both subpopulations of mitochondria. Interestingly, AP39 also elicited an additive effect to CsA-evoked desensitisation of PTP which suggests CypD independent mechanism. This is consistent with a previous study by Ikeda et al. (2015a) which reported AP39-induced inhibition of PTP opening in cortical cells 6 hours after cardiac arrest/cardiopulmonary resuscitation in mouse model. We also demonstrated that AP39 limited mito-ROS generation in both SSM and IFM in a concentration-dependent manner.

7.1.2 Context validation of the work

The studies presented in this thesis focused on exploring the potential cardioprotection of different thiol-containing compounds as potential H₂S donors, when given in clinically relevant way at reperfusion using preclinical rat model of acute myocardial infarction. These studies provided further evidence to support that exogenous supplementation of H₂S via stable and targeted H₂S donors at the time of reperfusion is a feasible and applicable cardioprotective approach against ischaemia/reperfusion injury. There is a general consensus in the field of cardioprotection that postconditioning is a reliable and relevant time point of intervention due to the unpredictable nature of myocardial ischaemia. Targeting the reperfusion phase has unveiled some of the cellular salvage kinases which can mitigate cardiac injury when specifically triggered at early reperfusion. These pathways include the RISK and the SAFE pathways. Interestingly, inhibition of the RISK pathway kinases at reperfusion does not appear to exacerbate infarct size. This emphasises the non-linearity of the RISK cascade and that these kinases are normally inactive at reperfusion. Data presented in Chapters 4 and 5 fully concur with this concept. Specific blockade of PI3K, eNOS using LY294002 and L-NAME, respectively, did not produce greater infarction compared with the control hearts.

The cardioprotective effects of exogenous thiol-containing compounds such as inorganic sulfide salts (i.e. NaHS and Na₂S) have been linked to recruitment of some components of the RISK pathway when applied before ischaemia or at reperfusion. However, the reproducibility of the generated data using these salts has been questioned due to the considerable technical difficulties associated with these salts. Sulfide salts instantly release their payload of H₂S once they

are dissolved, potentially causing a massive release of H₂S and triggering cell stress/toxicity. Neither the concentration nor the releasing pattern of H₂S by these salts relate to the physiological concentration or roles of H₂S. Therefore, there was an urgent need for developing a new generation of pharmacological tools to explore the biology of H₂S. Accordingly, this will not only improve the consistency of data but also facilitate the clinical translation of the beneficial effects of H₂S research. The development of GYY4137 is of great clinical relevance and has advanced the field of H₂S. It has been demonstrated that GYY4137 is a stable H₂S donor which releases H₂S at a slow rate which mimics the endogenous rate of H₂S production. The findings in Chapter 4 demonstrated that postconditioning the heart with GYY4137 protected against myocardial infarction via triggering PI3K/Akt/eNOS and abrogating the activity of GSK-3 β at early reperfusion. These results are of considerable clinical relevance and warrant further investigation for the possible use of GYY4137 in other disease states where impaired endogenous H₂S level contributes to the pathology of the disease. It is worth mentioning here that SG1002, a long-acting H₂S prodrug, has recently successfully passed Phase I clinical trial in patients with heart failure. This study demonstrated the ability of SG1002 to augment circulating H₂S and NO levels in both healthy subjects and heart failure patients (Polhemus et al., 2015). This trial holds a great promise considering that enhanced level of either gas has already shown cardioprotective effects in preclinical studies.

Despite the multifactorial aetiology of acute myocardial infarction, there is a large consensus that mitochondrial dysfunction at reperfusion has a central role in this pathology and is a fundamental determinant of clinical outcome. There is a compelling body of evidence demonstrating that the initial burst of mito-ROS at

the first minutes of reperfusion is the main mediator of PTP opening which initiates cell death. Application of antioxidants at early reperfusion has been reported as a promising cardioprotective intervention in experimental settings but failed to exert clinically-appreciable benefits. In part, this failure could be due to the application of a blanket approach to scavenge generated ROS with poor identification of the sources and mechanisms of mito-ROS generation during ischaemia/reperfusion injury and inability of most antioxidants to enter the mitochondria. We have demonstrated that postconditioning the heart with a mitochondria-targeted donor of H₂S (AP39) protects against injurious reperfusion. Unlike GYY4137, AP39-induced protection did not trigger any cytosolic component of the RISK pathway at early reperfusion, demonstrating that AP39 acts specifically on the mitochondrion. Cardiomyocyte mitochondria are the most relevant population of mitochondria in the myocardium which would be affected by ischaemia/reperfusion injury. Taking this into consideration, two subpopulations of cardiomyocyte mitochondria, namely subsarcolemmal (SSM) and interfibrillar (IFM) mitochondria, were specifically isolated from the left ventricle using differential centrifugation. We investigated the direct mitochondrial-effects of AP39 on mitochondrial function. We also demonstrated that AP39 increased mitochondrial Ca²⁺ tolerance thereby inhibiting Ca²⁺ overload-stimulated PTP opening. AP39 also had an additive effect to CsA-induced desensitisation of PTP. These data supported the notion that AP39 inhibits the activation of PTP via a CypD-independent mechanism. We found that AP39 limited mito-ROS generation in a concentration dependent manner. This limitation was not mediated through enhancing GSH production, a mitochondrial antioxidant system.

7.1.3 Limitations and future perspectives

All the studies in this thesis have been complimentary to each other and show a logical order of progression to investigate the cardioprotection of thiol-containing compounds. Nevertheless, there are a number of further studies which could broaden the scope of investigation and be interesting topics for further characterisation of thiol-induced cardioprotection.

The detection of H₂S level in the plasma and tissue has been a challenge despite having a crucial role in many pathologies such as ischaemia/reperfusion injury. In part this is because the majority of available H₂S probes cannot be used *in vivo* as they are fluorescent. However, Murphy's laboratory (Arndt et al., 2015) recently developed a mitochondria-targeted H₂S probe (MitoA) which preferentially accumulates in the mitochondria due to the virtue of a TTP⁺ scaffold. This probe selectively reacts with endogenous H₂S *in vitro* and *in vivo*, generating MitoN that can sensitively be detected using mass spectrometer. Although this technique is still under development and need further optimisation, its application could advance our understanding of the biological roles of endogenous H₂S. It could also guide the manipulation of H₂S level using newly developed H₂S donors in many disease states.

In Chapters 4 and 5, H₂S donors exerted a significant limitation in infarct size when they were given at reperfusion. Two hours of reperfusion was chosen in this work as it was sufficient to washout dehydrogenases from the infarcted tissue, avoiding false positive results. However, it is still unclear whether these donors will exert a comparable cardioprotection through similar mechanisms following longer period of reperfusion where there could be no-flow phenomena and late apoptosis. A suitable model to investigate that could be an *in situ* model

of myocardial ischaemia/reperfusion injury where the animal is allowed to recover for longer reperfusion following LAD ligation then sacrifice to look at potential late effects of cardioprotective H₂S donors.

There is a direct link between extent of ischaemia/reperfusion injury and arrhythmia severity (Wit and Duffy, 2008). Moreover, it has recently been shown that mitochondrial instability during regional ischaemia/reperfusion could underlie the arrhythmias (Solhjo and O'Rourke, 2015). Accordingly, it might be of interest to characterise the antioxidant effect of AP39 on the occurrence and severity of ventricular arrhythmia during simulated ischaemia/reperfusion injury using monolayers of cardiomyocyte and measuring the membrane potential and oxidative stress.

The role of the SAFE pathway in mediating the cardioprotection of H₂S still needs further investigation. This signal transduction pathway has been shown to work independently of the RISK pathway (Lecour et al., 2005), although its exact cardioprotective mechanism is still unclear. Experimentally, it has been demonstrated that JAK/STAT-3 signalling mediates, at least in part, the cardioprotection of IPC (Lecour et al., 2005) and IPost (Boengler et al., 2008a). Interestingly, Huffman et al. (2008) reported a transferable infarct-limiting effect when a virgin heart was perfused with a coronary effluent from preconditioned heart which signalled through JAK/STAT-3 pathway. Intriguingly, STAT-5 was found to be the dominant isoform triggered in patients subjected to RIPC before coronary artery bypass grafting (Heusch et al., 2012). Previous reports demonstrated that NaHS could mediate a postconditioning-mimetic effect in aging cardiomyocytes (Li et al., 2016) and isolated rat heart (Luan et al., 2012) via triggering JAK/STAT-3 signalling. These data suggest that the SAFE

pathway might be implicated in the cardioprotection of the non-targeted H₂S-donors (GYY4137) which could be an interesting topic for future investigation.

PTM produced by H₂S in the mitochondria is also an uncharted area requiring further investigation. In Chapter 5, it was concluded that AP39 limited mito-ROS in both subpopulations of cardiomyocyte mitochondria via a mechanism which is independent of enhanced GSH production. The sources of ROS generated at the first moments of reperfusion are still under debate with complexes I and III being the most likely sites of ROS generation. However, seminal work by Murphy's laboratory (Chouchani et al., 2014) recently suggested that rapid activation of complex I in the first minutes of reperfusion could be the most relevant site for detrimental mito-ROS generation. They also demonstrated that S-nitrosylation of the Cys³⁹ residue in the ND3 subunit of complex I, using mitochondria-targeted NO donor (MitoSNO), can reversibly lock complex I in the "deactivated state" at early reperfusion and prevent mito-ROS generation in murine heart. It has also been recently reported that NaHS mediated an additive effect to NO's infarct limitation through synergising NO-induced S-nitrosylation of mitochondrial proteins in mouse heart (Sun et al., 2016). Taken together, it seems tempting to suggest that AP39 could limit mito-ROS generation through S-nitrosylation of Cys³⁹ of complex I at reperfusion, although these experiments need to be performed before drawing any conclusion.

In Chapter 6, we also found that AP39-desensitised the PTP against Ca²⁺ overload possibly independently of CypD desensitisation. This conclusion was derived from the observation that AP39 had an additive effect to CsA-evoked desensitisation of PTP component in both cardiomyocyte mitochondria fractions (i.e. SSM and IFM). However, the exact mechanism of AP39-induced PTP

deactivation was not unveiled in this thesis. The ability of H₂S to trigger/induce S-nitrosylation and S-sulfhydration to shield critical mitochondrial proteins, especially when selectively delivered to mitochondria, should not be discounted. Unfortunately, the detection of mitochondrial S-nitrosylated proteins following AP39 application was not successful using Pierce™ S-nitrosylation Kit. The results were not conclusive and the assay needs further troubleshooting. Nevertheless, other assay procedures could be utilised instead such as DyLight™ Sulfhydryl-Reactive Fluors which could identify S-nitrosylated and S-sulfhydrated proteins. Despite the considerable controversy regarding the main components of the PTP, it has been reported by Murphy and colleagues (Nguyen et al., 2011a) that Cys²⁰³ residue of CypD has a crucial role in the activation of PTP. Later work by the same group later showed that mutation of Cys²⁰³ to serine residue significantly modulated the activation of PTP *in vitro* (Nguyen et al., 2011b). Furthermore, an increasing body of evidence also suggests that F₀F₁-ATP synthase (complex V), could be a major component of the PTP. Wang's laboratory have recently published data which showed the ability of H₂S to stimulate mitochondrial bioenergetics via S-sulfhydration of α -subunit of ATP synthase at Cys²⁴⁴ and Cys²⁹⁴ (Modis et al., 2016). Altogether, further studies investigating the influence of mitochondrially delivered H₂S using AP39 on the potential components of PTP would provide extremely important mechanistic insight into the cardioprotection of H₂S. The involvement of CypD in AP39's cardioprotection could be investigated using wild type and CypD null (CypD^{-/-}) mice. In addition, site-directed mutagenesis of Cys²⁴⁴ and Cys²⁹⁴ of ATP synthase could be used to explore the influence of AP39 on F₀F₁-ATP synthase *in vitro* using cell line.

7.1.4 Concluding remarks

The research carried out in this thesis represents a detailed characterisation of thiol-induced cardioprotection against ischaemia/reperfusion injury in a preclinical rodent model. The data provide new insights into the underlying cardioprotective mechanisms of thiol-containing compounds at the cellular and mitochondrial levels. The results also raise many questions regarding the exact PTMs induced by H₂S. The field of H₂S biology has been in great need of new pharmacological approaches to overcome the systemic side effects of simple sulfide salts. The H₂S donors used in this thesis are prototypes for potential therapeutic agent which offer a novel approach to mitigate irreversible myocardial infarction in the clinical setting. The work also explored the dependency of H₂S cardioprotection on eNOS activity in the myocardium and emphasises how their interactions could differ depending on the pharmacological tools employed. The concept could also possibly be extended to other pathologies, such as endothelial dysfunction and erectile dysfunction, which could help to clarify the inconclusive relationship between NO and H₂S in these pathologies.

The studies in this thesis set out to address the following questions:

1. Does Mesna at reperfusion protect the heart from ischaemia/reperfusion injury *in vivo*?
2. Does administration of GYY4137 at reperfusion limit acute myocardial infarction *in vivo*?
3. Does GYY4137 activate the RISK pathway components to mediate its infarct limitation?

4. Does GYY4137 rely on NO signalling to mediate its cardioprotection?
5. Does mitochondrial delivery of H₂S by AP39 protect against myocardial ischaemia/reperfusion *in vivo*?
6. Does AP39 trigger any of the RISK pathway components to exert its protection against reperfusion injury?
7. What effects does AP39 have on cardiomyocyte mitochondria *in vitro*?

Data in this thesis demonstrate that stable and controlled H₂S donors given at the time of reperfusion limit acute myocardial infarction in preclinical model. The cardioprotective mechanism of H₂S could significantly vary depending on its tissue concentration and the pharmacokinetic of the H₂S-releasing compound. Selectively delivering H₂S to specific organelles, such as the mitochondria, opens a wide window of opportunity of therapeutic applications of H₂S and facilitates its clinical translation. In this thesis, targeting the mitochondria with H₂S donor attenuated mito-ROS generation and inhibited the opening of PTP, the two detrimental hallmarks of what is so-called reperfusion injury. With the bewildering possibility of targeting the mitochondrion, H₂S-donating compounds represent promising therapeutic approaches to give in conjunction with PPCI to mitigate mitochondrial dysfunction and eventually improve the clinical outcome for patients who are admitted for the early reperfusion therapy.

References

- "Global status report on noncommunicable diseases 2014" [Online]. World Health Organisation (WHO). Available: <http://www.who.int/nmh/publications/ncd-status-report-2014/en/> [Accessed: 17 Nov 2016].
- Abe, K. & Kimura, H. 1996. The possible role of hydrogen sulfide as an endogenous neuromodulator. *J Neurosci*, 16, 1066-1071.
- Abramov, A. Y., Scorziello, A. & Duchen, M. R. 2007. Three distinct mechanisms generate oxygen free radicals in neurons and contribute to cell death during anoxia and reoxygenation. *J Neurosci*, 27, 1129-1138.
- Acin-Perez, R., Russwurm, M., Gunnewig, K., Gertz, M., Zoidl, G., Ramos, L., Buck, J., Levin, L. R., Rassow, J., Manfredi, G. & Steegborn, C. 2011. A phosphodiesterase 2A isoform localized to mitochondria regulates respiration. *J Biol Chem*, 286, 30423-30432.
- Acin-Perez, R., Salazar, E., Kamenetsky, M., Buck, J., Levin, L. R. & Manfredi, G. 2009. Cyclic AMP produced inside mitochondria regulates oxidative phosphorylation. *Cell Metab*, 9, 265-276.
- Ahmad, A., Olah, G., Szczesny, B., Wood, M. E., Whiteman, M. & Szabo, C. 2016. AP39, a mitochondrially targeted hydrogen sulfide donor, exerts protective effects in renal epithelial cells subjected to oxidative stress *in vitro* and in acute renal injury *in vivo*. *Shock*, 45, 88-97.
- Ahmad, A. & Szabo, C. 2016. Both the H₂S biosynthesis inhibitor aminooxyacetic acid and the mitochondrially targeted H₂S donor AP39 exert protective effects in a mouse model of burn injury. *Pharmacol Res*, 113, Part A, 348-355.
- Al-Magableh, M. R., Kemp-Harper, B. K. & Hart, J. L. 2015. Hydrogen sulfide treatment reduces blood pressure and oxidative stress in angiotensin II-induced hypertensive mice. *Hypertens Res*, 38, 13-20.
- Al-Magableh, M. R., Kemp-Harper, B. K., Ng, H. H., Miller, A. A. & Hart, J. L. 2014. Hydrogen sulfide protects endothelial nitric oxide function under conditions of acute oxidative stress *in vitro*. *Naunyn Schmiedebergs Arch Pharmacol*, 387, 67-74.
- Al-Nasser, I. & Crompton, M. 1986. The reversible Ca²⁺-induced permeabilization of rat liver mitochondria. *Biochem J*, 239, 19-29.
- Alavian, K. N., Beutner, G., Lazrove, E., Sacchetti, S., Park, H. A., Licznerski, P., Li, H., Nabili, P., Hockensmith, K., Graham, M., Porter, G. A., Jr. & Jonas, E. A. 2014. An uncoupling channel within the c-subunit ring of the F₁F₀ ATP synthase is the mitochondrial permeability transition pore. *Proc Natl Acad Sci U S A*, 111, 10580-10585.

- Alexander, B. E., Coles, S. J., Fox, B. C., Khan, T. F., Maliszewski, J., Perry, A., Pitak, M. B., Whiteman, M. & Wood, M. E. 2015. Investigating the generation of hydrogen sulfide from the phosphoramidodithioate slow-release donor GYY4137. *Med Chem Comm*, 6, 1649-1655.
- Aluise, C. D., Miriyala, S., Noel, T., Sultana, R., Jungsuwadee, P., Taylor, T. J., Cai, J., Pierce, W. M., Vore, M., Moscow, J. A., St Clair, D. K. & Butterfield, D. A. 2011. 2-Mercaptoethane sulfonate prevents doxorubicin-induced plasma protein oxidation and TNF-alpha release: implications for the reactive oxygen species-mediated mechanisms of chemobrain. *Free Radic Biol Med*, 50, 1630-1638.
- Andreadou, I., Iliodromitis, E. K., Rassaf, T., Schulz, R., Papapetropoulos, A. & Ferdinandy, P. 2015. The role of gasotransmitters NO, H₂S and CO in myocardial ischaemia/reperfusion injury and cardioprotection by preconditioning, postconditioning and remote conditioning. *Br J Pharmacol*, 172, 1587-1606.
- Arndt, S., Baeza-Garza, C. D., Logan, A., Rosa, T., Krieg, T., Hartley, R. C. & Murphy, M. P. 2015. PP8 - Determination of the endogenous hydrogen sulphide concentration in vivo using the mitochondria-targeted mass spectrometry probe MitoA. *Nitric Oxide*, 47, Supplement, S16.
- Asimakis, G. K., Inners-Mcbride, K., Medellin, G. & Conti, V. R. 1992. Ischemic preconditioning attenuates acidosis and postischemic dysfunction in isolated rat heart. *Am J Physiol*, 263, H887-H894.
- Baines, C. P., Kaiser, R. A., Purcell, N. H., Blair, N. S., Osinska, H., Hambleton, M. A., Brunskill, E. W., Sayen, M. R., Gottlieb, R. A., Dorn, G. W., Robbins, J. & Molkentin, J. D. 2005. Loss of cyclophilin D reveals a critical role for mitochondrial permeability transition in cell death. *Nature*, 434, 658-62.
- Baker, J. E., Su, J., Fu, X., Hsu, A., Gross, G. J., Tweddell, J. S. & Hogg, N. 2007. Nitrite confers protection against myocardial infarction: Role of xanthine oxidoreductase, NADPH oxidase and K_{ATP} channels. *J Mol and Cell Cardiol*, 43, 437-444.
- Barsukevich, V., Basalay, M., Sanchez, J., Mrochek, A., Whittle, J., Ackland, G. L., Gourine, A. V. & Gourine, A. 2015. Distinct cardioprotective mechanisms of immediate, early and delayed ischaemic postconditioning. *Basic Res Cardiol*, 110, 452.
- Basso, E., Fante, L., Fowlkes, J., Petronilli, V., Forte, M. A. & Bernardi, P. 2005. Properties of the permeability transition pore in mitochondria devoid of Cyclophilin D. *J Biol Chem*, 280, 18558-18561.
- Baxter, G. F., Goma, F. M. & Yellon, D. M. 1997. Characterisation of the infarct-limiting effect of delayed preconditioning: timecourse and dose-dependency studies in rabbit myocardium. *Basic Res Cardiol*, 92, 159-167.

- Bell, R. M., Mocanu, M. M. & Yellon, D. M. 2011. Retrograde heart perfusion: the Langendorff technique of isolated heart perfusion. *J Mol Cell Cardiol*, 50, 940-950.
- Beltowski, J. 2015. Hydrogen sulfide in pharmacology and medicine--An update. *Pharmacol Rep*, 67, 647-58.
- Bernardi, P. & Di Lisa, F. 2015. The mitochondrial permeability transition pore: molecular nature and role as a target in cardioprotection. *J Mol Cell Cardiol*, 78, 100-106.
- Bernardi, P. & Von Stockum, S. 2012. The permeability transition pore as a Ca²⁺ release channel: New answers to an old question. *Cell Calcium*, 52, 22-27.
- Bhatnagar, P., Wickramasinghe, K., Williams, J., Rayner, M. & Townsend, N. 2015. The epidemiology of cardiovascular disease in the UK 2014. *Heart*, 101, 1182-1189.
- Bian, J. S., Yong, Q. C., Pan, T. T., Feng, Z. N., Ali, M. Y., Zhou, S. & Moore, P. K. 2006. Role of hydrogen sulfide in the cardioprotection caused by ischemic preconditioning in the rat heart and cardiac myocytes. *J Pharmacol Exp Ther*, 316, 670-678.
- Bibli, S. I., Andreadou, I., Chatzianastasiou, A., Tzimas, C., Sanoudou, D., Kranias, E., Brouckaert, P., Coletta, C., Szabo, C., Kremastinos, D. T., Iliodromitis, E. K. & Papapetropoulos, A. 2015. Cardioprotection by H₂S engages a cGMP-dependent protein kinase G/phospholamban pathway. *Cardiovasc Res*, 106, 432-442.
- Bir, S. C., Kolluru, G. K., Mccarthy, P., Shen, X., Pardue, S., Pattillo, C. B. & Kevil, C. G. 2012. Hydrogen sulfide stimulates ischemic vascular remodeling through nitric oxide synthase and nitrite reduction activity regulating hypoxia-inducible factor-1alpha and vascular endothelial growth factor-dependent angiogenesis. *J Am Heart Assoc*, 1, e004093.
- Birnbaum, Y., Hale, S. L. & Kloner, R. A. 1997. Differences in reperfusion length following 30 minutes of ischemia in the rabbit influence infarct size, as measured by triphenyltetrazolium chloride staining. *J Mol Cell Cardiol*, 29, 657-666.
- Black, S. C. & Rodger, I. W. 1996. Methods for studying experimental myocardial ischemic and reperfusion injury. *J Pharmacol Toxicol Methods*, 35, 179-190.
- Boengler, K., Buechert, A., Heinen, Y., Roeskes, C., Hilfiker-Kleiner, D., Heusch, G. & Schulz, R. 2008a. Cardioprotection by ischemic postconditioning is lost in aged and STAT3-deficient mice. *Circ Res*, 102, 131-135.

- Boengler, K., Hilfiker-Kleiner, D., Drexler, H., Heusch, G. & Schulz, R. 2008b. The myocardial JAK/STAT pathway: from protection to failure. *Pharmacol Ther*, 120, 172-185.
- Boengler, K., Ruiz-Meana, M., Gent, S., Ungefug, E., Soetkamp, D., Miro-Casas, E., Cabestrero, A., Fernandez-Sanz, C., Semenzato, M., Di Lisa, F., Rohrbach, S., Garcia-Dorado, D., Heusch, G. & Schulz, R. 2012. Mitochondrial connexin 43 impacts on respiratory complex I activity and mitochondrial oxygen consumption. *J Cell Mol Med*, 16, 1649-1655.
- Boengler, K., Stahlhofen, S., Van De Sand, A., Gres, P., Ruiz-Meana, M., Garcia-Dorado, D., Heusch, G. & Schulz, R. 2009. Presence of connexin 43 in subsarcolemmal, but not in interfibrillar cardiomyocyte mitochondria. *Basic Res Cardiol*, 104, 141-147.
- Bogaert, J., Kalantzi, M., Rademakers, F. E., Dymarkowski, S. & Janssens, S. 2007. Determinants and impact of microvascular obstruction in successfully reperfused ST-segment elevation myocardial infarction. Assessment by magnetic resonance imaging. *Eur Radiol*, 17, 2572-2580.
- Bohl, S., Medway, D. J., Schulz-Menger, J., Schneider, J. E., Neubauer, S. & Lygate, C. A. 2009. Refined approach for quantification of *in vivo* ischemia-reperfusion injury in the mouse heart. *Am J Physiol Heart Circ Physiol*, 297, H2054-H2058.
- Bolli, R. & Marban, E. 1999. Molecular and cellular mechanisms of myocardial stunning. *Physiol Rev*, 79, 609-634.
- Bonora, M., Bononi, A., De Marchi, E., Giorgi, C., Lebedzinska, M., Marchi, S., Patergnani, S., Rimessi, A., Suski, J. M., Wojtala, A., Wieckowski, M. R., Kroemer, G., Galluzzi, L. & Pinton, P. 2013. Role of the c subunit of the Fo ATP synthase in mitochondrial permeability transition. *Cell Cycle*, 12, 674-683.
- Bos, E. M., Van Goor, H., Joles, J. A., Whiteman, M. & Leuvenink, H. G. 2015. Hydrogen sulfide: physiological properties and therapeutic potential in ischaemia. *Br J Pharmacol*, 172, 1479-1493.
- Braunersreuther, V., Montecucco, F., Asrih, M., Pelli, G., Galan, K., Frias, M., Burger, F., Quindere, A. L., Montessuit, C., Krause, K. H., Mach, F. & Jaquet, V. 2013. Role of NADPH oxidase isoforms NOX1, NOX2 and NOX4 in myocardial ischemia/reperfusion injury. *J Mol Cell Cardiol*, 64, 99-107.
- Braunwald, E. & Kloner, R. A. 1985. Myocardial reperfusion: a double-edged sword? *J Clin Invest*, 76, 1713-1719.
- Breivik, L., Helgeland, E., Aarnes, E. K., Mrdalj, J. & Jonassen, A. K. 2011. Remote postconditioning by humoral factors in effluent from ischemic

- preconditioned rat hearts is mediated via PI3K/Akt-dependent cell-survival signaling at reperfusion. *Basic Res Cardiol*, 106, 135-145.
- Brock, N. & Pohl, J. 1983. The development of mesna for regional detoxification. *Cancer Treat Rev*, 10 Suppl A, 33-43.
- Brock, N., Pohl, J. & Stekar, J. 1981a. Studies on the urotoxicity of oxazaphosphorine cytostatics and its prevention--I. Experimental studies on the urotoxicity of alkylating compounds. *Eur J Cancer*, 17, 595-607.
- Brock, N., Pohl, J. & Stekar, J. 1981b. Studies on the urotoxicity of oxazaphosphorine cytostatics and its prevention. 2. Comparative study on the uroprotective efficacy of thiols and other sulfur compounds. *Eur J Cancer Clin Oncol*, 17, 1155-1163.
- Brock, N., Pohl, J., Stekar, J. & Scheef, W. 1982. Studies on the urotoxicity of oxazaphosphorine cytostatics and its prevention--III. Profile of action of sodium 2-mercaptoethane sulfonate (mesna). *Eur J Cancer Clin Oncol*, 18, 1377-1387.
- Brown, D. I. & Griendling, K. K. 2015. Regulation of signal transduction by reactive oxygen species in the cardiovascular system. *Circ Res*, 116, 531-549.
- Bucci, M., Papapetropoulos, A., Vellecco, V., Zhou, Z., Zaid, A., Giannogonas, P., Cantalupo, A., Dhayade, S., Karalis, K. P., Wang, R., Feil, R. & Cirino, G. 2012. cGMP-dependent protein kinase contributes to hydrogen sulfide-stimulated vasorelaxation. *PLoS One*, 7, e53319.
- Bucci, M., Vellecco, V., Cantalupo, A., Brancaleone, V., Zhou, Z., Evangelista, S., Calderone, V., Papapetropoulos, A. & Cirino, G. 2014. Hydrogen sulfide accounts for the peripheral vascular effects of zofenopril independently of ACE inhibition. *Cardiovasc Res*, 102, 138-147.
- Buelke-Sam, J., Holson, J. F., Bazare, J. J. & Young, J. F. 1978. Comparative stability of physiological parameters during sustained anesthesia in rats. *Lab Anim Sci*, 28, 157-62.
- Bulluck, H. & Hausenloy, D. J. 2015. Ischaemic conditioning: are we there yet? *Heart*, 101, 1067-1077.
- Bulluck, H., Yellon, R. L. & Yellon, D. M. 2016. Promising strategies to minimize reperfusion injury in STEMI. *Minerva Cardioangiol*, 64, 284-294.
- Burguera, E. F., Vela-Anero, Á., Magalhães, J., Meijide-Faílde, R. & Blanco, F. J. 2014. Effect of hydrogen sulfide sources on inflammation and catabolic markers on interleukin 1 β -stimulated human articular chondrocytes. *Osteoarthr Cartil*, 22, 1026-1035.

- Burley, D. S., Ferdinandy, P. & Baxter, G. F. 2007. Cyclic GMP and protein kinase-G in myocardial ischaemia-reperfusion: opportunities and obstacles for survival signaling. *Br J Pharmacol*, 152, 855-869.
- Burwell, L. S., Nadtochiy, S. M. & Brookes, P. S. 2009. Cardioprotection by metabolic shut-down and gradual wake-up. *J Mol Cell Cardiol*, 46, 804-810.
- Cabrera-Fuentes, H. A., Alba-Alba, C., Aragonés, J., Bernhagen, J., Boisvert, W. A., Botker, H. E., Cesarman-Maus, G., Fleming, I., Garcia-Dorado, D., Lecour, S., Liehn, E., Marber, M. S., Marina, N., Mayr, M., Perez-Mendez, O., Miura, T., Ruiz-Meana, M., Salinas-Estefanon, E. M., Ong, S. B., Schnittler, H. J., Sanchez-Vega, J. T., Sumoza-Toledo, A., Vogel, C. W., Yarullina, D., Yellon, D. M., Preissner, K. T. & Hausenloy, D. J. 2016. Meeting report from the 2nd International Symposium on New Frontiers in Cardiovascular Research. Protecting the cardiovascular system from ischemia: between bench and bedside. *Basic Res Cardiol*, 111, 7.
- Calvert, J. W., Elston, M., Nicholson, C. K., Gundewar, S., Jha, S., Elrod, J. W., Ramachandran, A. & Lefer, D. J. 2010. Genetic and pharmacologic hydrogen sulfide therapy attenuates ischemia-induced heart failure in mice. *Circ*, 122, 9-11.
- Calvert, J. W., Jha, S., Gundewar, S., Elrod, J. W., Ramachandran, A., Pattillo, C. B., Kevil, C. G. & Lefer, D. J. 2009. Hydrogen sulfide mediates cardioprotection through Nrf2 signaling. *Circ Res*, 105, 365-374.
- Chatzianastasiou, A., Bibli, S. I., Andreadou, I., Efentakis, P., Kaludercic, N., Wood, M. E., Whiteman, M., Di Lisa, F., Daiber, A., Manolopoulos, V. G., Szabo, C. & Papapetropoulos, A. 2016. Cardioprotection by H₂S donors: nitric oxide-dependent and -independent mechanisms. *J Pharmacol Exp Ther*, 358, 431-440.
- Chen, Q., Hoppel, C. L. & Lesnefsky, E. J. 2006. Blockade of electron transport before cardiac ischemia with the reversible inhibitor amobarbital protects rat heart mitochondria. *J Pharmacol Exp Ther*, 316, 200-207.
- Chen, Q., Paillard, M., Gomez, L., Li, H., Hu, Y. & Lesnefsky, E. J. 2012. Postconditioning modulates ischemia-damaged mitochondria during reperfusion. *J Cardiovasc Pharmacol*, 59, 101-108.
- Chen, S., Bu, D., Ma, Y., Zhu, J., Sun, L., Zuo, S., Ma, J., Li, T., Chen, Z., Zheng, Y., Wang, X., Pan, Y., Wang, P. & Liu, Y. 2016a. GYY4137 ameliorates intestinal barrier injury in a mouse model of endotoxemia. *Biochem Pharmacol*, 118, 59-67.
- Chen, X., Xu, W., Wang, Y., Luo, H., Quan, S., Zhou, J., Yang, N., Zhang, T., Wu, L., Liu, J., Long, X., Zhu, N., Xie, H. & Luo, Z. 2014. Hydrogen sulfide reduces kidney injury due to urinary-derived sepsis by inhibiting NF-kappaB expression, decreasing TNF-alpha levels and increasing IL-10 levels. *Exp Ther Med*, 8, 464-470.

- Chen, Z., Zhang, Z., Zhang, D., Li, H. & Sun, Z. 2016b. Hydrogen sulfide protects against TNF- α induced neuronal cell apoptosis through miR-485-5p/TRADD signaling. *Biochem Biophys Res Commun*, 478, 1304-1309.
- Chitnis, M. K., Njie-Mbye, Y. F., Opere, C. A., Wood, M. E., Whiteman, M. & Ohia, S. E. 2013. Pharmacological actions of the slow release hydrogen sulfide donor GYY4137 on phenylephrine-induced tone in isolated bovine ciliary artery. *Exp Eye Res*, 116, 350-354.
- Chouchani, E. T., Pell, V. R., Gaude, E., Aksentijevic, D., Sundier, S. Y., Robb, E. L., Logan, A., Nadtochiy, S. M., Ord, E. N., Smith, A. C., Eyassu, F., Shirley, R., Hu, C. H., Dare, A. J., James, A. M., Rogatti, S., Hartley, R. C., Eaton, S., Costa, A. S., Brookes, P. S., Davidson, S. M., Duchon, M. R., Saeb-Parsy, K., Shattock, M. J., Robinson, A. J., Work, L. M., Frezza, C., Krieg, T. & Murphy, M. P. 2014. Ischaemic accumulation of succinate controls reperfusion injury through mitochondrial ROS. *Nature*, 515, 431-435.
- Chouchani, E. T., Pell, V. R., James, A. M., Work, L. M., Saeb-Parsy, K., Frezza, C., Krieg, T. & Murphy, M. P. 2016. A Unifying Mechanism for Mitochondrial Superoxide Production during Ischemia-Reperfusion Injury. *Cell Metab*, 23, 254-263.
- Chuah, S. C., Moore, P. K. & Zhu, Y. Z. 2007. S-allylcysteine mediates cardioprotection in an acute myocardial infarction rat model via a hydrogen sulfide-mediated pathway. *Am J Physiol Heart Circ Physiol*, 293, H2693-H2701.
- Clark, C., Foreman, M. I., Kane, K. A., McDonald, F. M. & Parratt, J. R. 1980. Coronary artery ligation in anesthetized rats as a method for the production of experimental dysrhythmias and for the determination of infarct size. *J Pharmacol Methods*, 3, 357-368.
- Clarke, S. J., Khaliulin, I., Das, M., Parker, J. E., Heesom, K. J. & Halestrap, A. P. 2008. Inhibition of mitochondrial permeability transition pore opening by ischemic preconditioning is probably mediated by reduction of oxidative stress rather than mitochondrial protein phosphorylation. *Circ Res*, 102, 1082-1090.
- Coavoy-Sanchez, S. A., Rodrigues, L., Teixeira, S. A., Soares, A. G., Torregrossa, R., Wood, M. E., Whiteman, M., Costa, S. K. & Muscara, M. N. 2016. Hydrogen sulfide donors alleviate itch secondary to the activation of type-2 protease activated receptors (PAR-2) in mice. *Pharmacol Res*, 113, 686-694.
- Cortese-Krott, M. M., Kuhnle, G. G., Dyson, A., Fernandez, B. O., Grman, M., Dumond, J. F., Barrow, M. P., Mcleod, G., Nakagawa, H., Ondrias, K., Nagy, P., King, S. B., Saavedra, J. E., Keefer, L. K., Singer, M., Kelm, M., Butler, A. R. & Feelisch, M. 2015. Key bioactive reaction products of the NO/H₂S interaction are

- S/N-hybrid species, polysulfides, and nitroxyl. *Proc Natl Acad Sci USA*, 112, E4651-E4660.
- Costigan, M. G. 2003. Hydrogen sulfide: UK occupational exposure limits. *Occup Environ Med*, 60, 308-312.
- Crestanello, J. A., Lingle, D. M., Kamelgard, J., Millili, J. & Whitman, G. J. 1996. Ischemic preconditioning decreases oxidative stress during reperfusion: a chemiluminescence study. *J Surg Res*, 65, 53-58.
- Csonka, C., Kupai, K., Kocsis, G. F., Novak, G., Fekete, V., Bencsik, P., Csont, T. & Ferdinandy, P. 2010. Measurement of myocardial infarct size in preclinical studies. *J Pharmacol Toxicol Methods*, 61, 163-170.
- Cung, T.-T., Morel, O., Cayla, G., Rioufol, G., Garcia-Dorado, D., Angoulvant, D., Bonnefoy-Cudraz, E., Guérin, P., Elbaz, M., Delarche, N., Coste, P., Vanzetto, G., Metge, M., Aupetit, J.-F., Jouve, B., Motreff, P., Tron, C., Labeque, J.-N., Steg, P. G., Cottin, Y., Range, G., Clerc, J., Claeys, M. J., Coussement, P., Prunier, F., Moulin, F., Roth, O., Belle, L., Dubois, P., Barragan, P., Gilard, M., Piot, C., Colin, P., De Poli, F., Morice, M.-C., Ider, O., Dubois-Randé, J.-L., Untersee, T., Le Breton, H., Béard, T., Blanchard, D., Grollier, G., Malquarti, V., Staat, P., Sudre, A., Elmer, E., Hansson, M. J., Bergerot, C., Boussaha, I., Jossan, C., Derumeaux, G., Mewton, N. & Ovize, M. 2015. Cyclosporine before PCI in Patients with Acute Myocardial Infarction. *NEJM*, 373, 1021-1031.
- Curtis, M. J., Macleod, B. A. & Walker, M. J. 1987. Models for the study of arrhythmias in myocardial ischaemia and infarction: the use of the rat. *J Mol Cell Cardiol*, 19, 399-419.
- Darling, C. E., Jiang, R., Maynard, M., Whittaker, P., Vinten-Johansen, J. & Przyklenk, K. 2005. Postconditioning via stuttering reperfusion limits myocardial infarct size in rabbit hearts: role of ERK1/2. *Am J Physiol Heart Circ Physiol*, 289, H1618-H626.
- Das, A., Samidurai, A., Hoke, N. N., Kukreja, R. C. & Salloum, F. N. 2015. Hydrogen sulfide mediates the cardioprotective effects of gene therapy with PKG- α . *Basic Res Cardiol*, 110, 42.
- De Paulis, D., Chiari, P., Teixeira, G., Couture-Lepetit, E., Abrial, M., Argaud, L., Gharib, A. & Ovize, M. 2013. Cyclosporine A at reperfusion fails to reduce infarct size in the *in vivo* rat heart. *Basic Res Cardiol*, 108, 1-11.
- Deuchar, G. A., Opie, L. H. & Lecour, S. 2007. TNF α is required to confer protection in an *in vivo* model of classical ischaemic preconditioning. *Life Sci*, 80, 1686-1691.
- Di Meo, I., Fagiolarini, G., Prella, A., Viscomi, C., Zeviani, M. & Tiranti, V. 2011. Chronic exposure to sulfide causes accelerated degradation of cytochrome c

- oxidase in ethylmalonic encephalopathy. *Antioxid Redox Signal*, 15, 353-362.
- Dillmann, W. H. 2008. The rat as a model for cardiovascular disease. *Drug Discov Today Dis Models*, 5, 173-178.
- Doeller, J. E., Isbell, T. S., Benavides, G., Koenitzer, J., Patel, H., Patel, R. P., Lancaster, J. R., Jr., Darley-Usmar, V. M. & Kraus, D. W. 2005. Polarographic measurement of hydrogen sulfide production and consumption by mammalian tissues. *Anal Biochem*, 341, 40-51.
- Duran, M., Aarsen, G., Fokkens, R. H., Nibbering, N. M. M., Cats, B. P., De Bree, P. K. & Wadman, S. K. 1981. 2-Mercaptoethanesulfonate-cysteinedisulfide excretion following the administration of 2-mercaptoethanesulfonate—a pitfall in the diagnosis of sulfite oxidase deficiency. *Clinica Chimica Acta*, 111, 47-53.
- Elrod, J. W., Calvert, J. W., Morrison, J., Doeller, J. E., Kraus, D. W., Tao, L., Jiao, X., Scalia, R., Kiss, L., Szabo, C., Kimura, H., Chow, C. W. & Lefer, D. J. 2007. Hydrogen sulfide attenuates myocardial ischemia-reperfusion injury by preservation of mitochondrial function. *Proc Natl Acad Sci U S A*, 104, 15560-15565.
- Elsay, D. J. 2009. Roles and mechanisms of action of the L-cysteine/cystathione-γ-lyase/hydrogen sulphide pathway in the heart. Doctor of Philosophy, Cardiff University.
- Ferdinandy, P., Hausenloy, D. J., Heusch, G., Baxter, G. F. & Schulz, R. 2014. Interaction of risk factors, comorbidities, and comedications with ischemia/reperfusion injury and cardioprotection by preconditioning, postconditioning, and remote conditioning. *Pharmacol Rev*, 66, 1142-1174.
- Filipovic, M. R., Miljkovic, J. L., Nauser, T., Royzen, M., Klos, K., Shubina, T., Koppenol, W. H., Lippard, S. J. & Ivanović-Burmazović, I. 2012. Chemical Characterization of the Smallest S-Nitrosothiol, HSNO; Cellular Cross-talk of H₂S and S-Nitrosothiols. *J Am Chem Soc*, 134, 12016-12027.
- Fiolet, J. W. & Baartscheer, A. 2000. Cellular calcium homeostasis during ischemia; a thermodynamic approach. *Cardiovasc Res*, 45, 100-106.
- Fitzgerald, R., Desantiago, B., Lee, D. Y., Yang, G., Kim, J. Y., Foster, D. B., Chan-Li, Y., Horton, M. R., Panettieri, R. A., Wang, R. & An, S. S. 2014. H₂S relaxes isolated human airway smooth muscle cells via the sarcolemmal K(ATP) channel. *Biochem Biophys Res Commun*, 446, 393-398.
- Flannigan, K. L., Agbor, T. A., Motta, J. P., Ferraz, J. G., Wang, R., Buret, A. G. & Wallace, J. L. 2015. Proresolutive effects of hydrogen sulfide during colitis are mediated through hypoxia-inducible factor-1α. *FASEB J*, 29, 1591-1602.

- Fox, B., Schantz, J. T., Haigh, R., Wood, M. E., Moore, P. K., Viner, N., Spencer, J. P., Winyard, P. G. & Whiteman, M. 2012. Inducible hydrogen sulfide synthesis in chondrocytes and mesenchymal progenitor cells: is H₂S a novel cytoprotective mediator in the inflamed joint? *J Cell Mol Med*, 16, 896-910.
- Fradorf, J., Huhn, R., Weber, N. C., Ebel, D., Wingert, N., Preckel, B., Toma, O., Schlack, W. & Hollmann, M. W. 2010. Sevoflurane-induced preconditioning: impact of protocol and aprotinin administration on infarct size and endothelial nitric-oxide synthase phosphorylation in the rat heart *in vivo*. *Anesthesiology*, 113, 1289-1298.
- Frezza, C., Cipolat, S. & Scorrano, L. 2007. Organelle isolation: functional mitochondria from mouse liver, muscle and cultured fibroblasts. *Nat Protoc*, 2, 287-95.
- Fu, M., Zhang, W., Wu, L., Yang, G., Li, H. & Wang, R. 2012. Hydrogen sulfide (H₂S) metabolism in mitochondria and its regulatory role in energy production. *Proc Natl Acad Sci U S A*, 109, 2943-2948.
- Furne, J., Saeed, A. & Levitt, M. D. 2008. Whole tissue hydrogen sulfide concentrations are orders of magnitude lower than presently accepted values. *Am J Physiol Regul Integr Comp Physiol*, 295, R1479-R1485.
- Gao, W. D., Murray, C. I., Tian, Y., Zhong, X., Dumond, J. F., Shen, X., Stanley, B. A., Foster, D. B., Wink, D. A., King, S. B., Van Eyk, J. E. & Paolucci, N. 2012. Nitroxyl-mediated disulfide bond formation between cardiac myofilament cysteines enhances contractile function. *Circ Res*, 111, 1002-1011.
- Geng, B., Chang, L., Pan, C., Qi, Y., Zhao, J., Pang, Y., Du, J. & Tang, C. 2004. Endogenous hydrogen sulfide regulation of myocardial injury induced by isoproterenol. *Biochem Biophys Res Commun*, 318, 756-763.
- Gero, D., Torregrossa, R., Perry, A., Waters, A., Le-Trionnaire, S., Whatmore, J. L., Wood, M. & Whiteman, M. 2016. The novel mitochondria-targeted hydrogen sulfide (H₂S) donors AP123 and AP39 protect against hyperglycemic injury in microvascular endothelial cells *in vitro*. *Pharmacol Res*, 113, 186-198.
- Gho, B. C., Schoemaker, R. G., Van Den Doel, M. A., Duncker, D. J. & Verdouw, P. D. 1996. Myocardial protection by brief ischemia in noncardiac tissue. *Circ*, 94, 2193-2200.
- Giorgio, M., Migliaccio, E., Orsini, F., Paolucci, D., Moroni, M., Contursi, C., Pelliccia, G., Luzi, L., Minucci, S., Marcaccio, M., Pinton, P., Rizzuto, R., Bernardi, P., Paolucci, F. & Pelicci, P. G. 2005. Electron transfer between cytochrome c and p66Shc generates reactive oxygen species that trigger mitochondrial apoptosis. *Cell*, 122, 221-233.

- Giorgio, V., Bisetto, E., Soriano, M. E., Dabbeni-Sala, F., Basso, E., Petronilli, V., Forte, M. A., Bernardi, P. & Lippe, G. 2009. Cyclophilin D modulates mitochondrial F₀F₁-ATP synthase by interacting with the lateral stalk of the complex. *J Biol Chem*, 284, 33982-33988.
- Goodwin, L. R., Francom, D., Dieken, F. P., Taylor, J. D., Warenycia, M. W., Reiffenstein, R. J. & Dowling, G. 1989. Determination of sulfide in brain tissue by gas dialysis/ion chromatography: postmortem studies and two case reports. *J Anal Toxicol*, 13, 105-109.
- Goren, M. P., Hsu, L. C. & Li, J. T. 1998. Reduction of dimesna to mesna by the isolated perfused rat liver. *Cancer Res*, 58, 4358-4362.
- Goren, M. P., Lyman, B. A. & Li, J. T. 1991. The stability of mesna in beverages and syrup for oral administration. *Cancer Chemother Pharmacol*, 28, 298-301.
- Gubern, M., Andriamihaja, M., Nubel, T., Blachier, F. & Bouillaud, F. 2007. Sulfide, the first inorganic substrate for human cells. *FASEB J*, 21, 1699-1706.
- Grambow, E., Mueller-Graf, F., Delyagina, E., Frank, M., Kuhla, A. & Vollmar, B. 2014. Effect of the hydrogen sulfide donor GYY4137 on platelet activation and microvascular thrombus formation in mice. *Platelets*, 25, 166-174.
- Grambow, E., Leppin, C., Leppin, K., Kundt, G., Klar, E., Frank, M. & Vollmar, B. 2016. The effects of hydrogen sulfide on platelet-leukocyte aggregation and microvascular thrombolysis. *Platelets*, 1-9.
- Griffiths, E. J. & Halestrap, A. P. 1993. Protection by Cyclosporin A of ischemia/reperfusion-induced damage in isolated rat hearts. *J Mol Cell Cardiol*, 25, 1461-1469.
- Griffiths, E. J. & Halestrap, A. P. 1995. Mitochondrial non-specific pores remain closed during cardiac ischaemia, but open upon reperfusion. *Biochem J*, 307 (Pt 1), 93-98.
- Guo, C., Liang, F., Shah Masood, W. & Yan, X. 2014. Hydrogen sulfide protected gastric epithelial cell from ischemia/reperfusion injury by Keap1 s-sulfhydration, MAPK dependent anti-apoptosis and NF-kappaB dependent anti-inflammation pathway. *Eur J Pharmacol*, 725, 70-78.
- Guo, W., Kan, J. T., Cheng, Z. Y., Chen, J. F., Shen, Y. Q., Xu, J., Wu, D. & Zhu, Y. Z. 2012. Hydrogen sulfide as an endogenous modulator in mitochondria and mitochondria dysfunction. *Oxid Med Cell Longev*, 2012, 878052.
- Hackfort, B. T. & Mishra, P. K. 2016. Emerging role of hydrogen sulfide-microRNA cross-talk in cardiovascular diseases. *Am J Physiol Heart Circ Physiol*, 310, H812-H812.

- Halestrap, A. P. 2010. A pore way to die: the role of mitochondria in reperfusion injury and cardioprotection. *Biochem Soc Trans*, 38, 841-860.
- Han, S. J., Kim, J. I., Park, J. W. & Park, K. M. 2015. Hydrogen sulfide accelerates the recovery of kidney tubules after renal ischemia/reperfusion injury. *Nephrol Dial Transplant*, 30, 1497-1506.
- Hancock, J. T. & Whiteman, M. 2016. Hydrogen sulfide signaling: interactions with nitric oxide and reactive oxygen species. *Ann N Y Acad Sci*, 1365, 5-14.
- Haouzi, P. 2016. Is exogenous hydrogen sulfide a relevant tool to address physiological questions on hydrogen sulfide? *Respir Physiol Neurobiol*, 229, 5-10.
- Hausenloy, D. J., Barrabes, J. A., Botker, H. E., Davidson, S. M., Di Lisa, F., Downey, J., Engstrom, T., Ferdinandy, P., Carbrera-Fuentes, H. A., Heusch, G., Ibanez, B., Iliodromitis, E. K., Inserte, J., Jennings, R., Kalia, N., Kharbanda, R., Lecour, S., Marber, M., Miura, T., Ovize, M., Perez-Pinzon, M. A., Piper, H. M., Przyklenk, K., Schmidt, M. R., Redington, A., Ruiz-Meana, M., Vilahur, G., Vinten-Johansen, J., Yellon, D. M. & Garcia-Dorado, D. 2016. Ischaemic conditioning and targeting reperfusion injury: a 30 year voyage of discovery. *Basic Res Cardiol*, 111, 70.
- Hausenloy, D. J., Boston-Griffiths, E. A. & Yellon, D. M. 2012. Cyclosporin A and cardioprotection: from investigative tool to therapeutic agent. *Br J Pharmacol*, 165, 1235-1245.
- Hausenloy, D. J., Duchen, M. R. & Yellon, D. M. 2003. Inhibiting mitochondrial permeability transition pore opening at reperfusion protects against ischaemia-reperfusion injury. *Cardiovasc Res*, 60, 617-625.
- Hausenloy, D. J., Maddock, H. L., Baxter, G. F. & Yellon, D. M. 2002. Inhibiting mitochondrial permeability transition pore opening: a new paradigm for myocardial preconditioning? *Cardiovasc Res*, 55, 534-543.
- Hausenloy, D. J., Ong, S. B. & Yellon, D. M. 2009. The mitochondrial permeability transition pore as a target for preconditioning and postconditioning. *Basic Res Cardiol*, 104, 189-202.
- Hausenloy, D. J., Tsang, A., Mocanu, M. M. & Yellon, D. M. 2005. Ischemic preconditioning protects by activating prosurvival kinases at reperfusion. *Am J Physiol Heart Circ Physiol*, 288, H971-H976.
- Hausenloy, D. J. & Yellon, D. M. 2004. New directions for protecting the heart against ischaemia-reperfusion injury: targeting the Reperfusion Injury Salvage Kinase (RISK)-pathway. *Cardiovasc Res*, 61, 448-460.

- Hausenloy, D. J. & Yellon, D. M. 2007. The evolving story of "conditioning" to protect against acute myocardial ischaemia-reperfusion injury. *Heart*, 93, 649-651.
- Hausenloy, D. J. & Yellon, D. M. 2013. Myocardial ischemia-reperfusion injury: a neglected therapeutic target. *J Clin Invest*, 123, 92-100.
- Haworth, R. A. & Hunter, D. R. 1979. The Ca²⁺-induced membrane transition in mitochondria. II. Nature of the Ca²⁺ trigger site. *Arch Biochem Biophys*, 195, 460-467.
- Hearse, D. J. & Sutherland, F. J. 2000. Experimental models for the study of cardiovascular function and disease. *Pharmacol Res*, 41, 597-603.
- Hearse, D. J. & Tosaki, A. 1987. Free radicals and reperfusion-induced arrhythmias: protection by spin trap agent PBN in the rat heart. *Circ Res*, 60, 375-383.
- Helmy, N., Prip-Buus, C., Vons, C., Lenoir, V., Abou-Hamdan, A., Guedouari-Bounihi, H., Lombes, A. & Bouillaud, F. 2014. Oxidation of hydrogen sulfide by human liver mitochondria. *Nitric Oxide*, 41, 105-112.
- Heusch, G., Kleinbongard, P., Bose, D., Levkau, B., Haude, M., Schulz, R. & Erbel, R. 2009. Coronary microembolization: from bedside to bench and back to bedside. *Circ*, 120, 1822-1836.
- Heusch, G., Musiolik, J., Kottenberg, E., Peters, J., Jakob, H. & Thielmann, M. 2012. STAT5 activation and cardioprotection by remote ischemic preconditioning in humans: short communication. *Circ Res*, 110, 111-115.
- Hoek, T. L. V., Becker, L. B., Shao, Z.-H., Li, C.-Q. & Schumacker, P. T. 2000. Preconditioning in cardiomyocytes protects by attenuating oxidant stress at reperfusion. *Circ Res*, 86, 541-548.
- Hombach, V., Grebe, O., Merkle, N., Waldenmaier, S., Hoher, M., Kochs, M., Wohrle, J. & Kestler, H. A. 2005. Sequelae of acute myocardial infarction regarding cardiac structure and function and their prognostic significance as assessed by magnetic resonance imaging. *Eur Heart J*, 26, 549-557.
- Hosoki, R., Matsuki, N. & Kimura, H. 1997. The possible role of hydrogen sulfide as an endogenous smooth muscle relaxant in synergy with nitric oxide. *Biochem Biophys Res Comm*, 237, 527-531.
- Hu, L. F., Li, Y., Neo, K. L., Yong, Q. C., Lee, S. W., Tan, B. K. & Bian, J. S. 2011. Hydrogen sulfide regulates Na⁺/H⁺ exchanger activity via stimulation of phosphoinositide 3-kinase/Akt and protein kinase G pathways. *J Pharmacol Exp Ther*, 339, 726-735.
- Huang, C., Kan, J., Liu, X., Ma, F., Tran, B. H., Zou, Y., Wang, S. & Zhu, Y. Z. 2013. Cardioprotective effects of a novel hydrogen sulfide agent-controlled

- release formulation of S-propargyl-cysteine on heart failure rats and molecular mechanisms. *PLoS One*, 8, e69205.
- Huang, Y. E., Tang, Z. H., Xie, W., Shen, X. T., Liu, M. H., Peng, X. P., Zhao, Z. Z., Nie, D. B., Liu, L. S. & Jiang, Z. S. 2012. Endogenous hydrogen sulfide mediates the cardioprotection induced by ischemic postconditioning in the early reperfusion phase. *Exp Ther Med*, 4, 1117-1123.
- Huffman, L. C., Koch, S. E. & Butler, K. L. 2008. Coronary effluent from a preconditioned heart activates the JAK-STAT pathway and induces cardioprotection in a donor heart. *Am J Physiol - Heart and Circ Physiol*, 294, H257-H262.
- Hunter, D. R. & Haworth, R. A. 1979a. The Ca²⁺-induced membrane transition in mitochondria. I. The protective mechanisms. *Arch Biochem Biophys*, 195, 453-459.
- Hunter, D. R. & Haworth, R. A. 1979b. The Ca²⁺-induced membrane transition in mitochondria. III. Transitional Ca²⁺ release. *Arch Biochem Biophys*, 195, 468-477.
- Ikeda, K., Marutani, E., Hirai, S., Wood, M. E., Whiteman, M. & Ichinose, F. 2015. Mitochondria-targeted hydrogen sulfide donor AP39 improves neurological outcomes after cardiac arrest in mice. *Nitric Oxide*, 49, 90-96.
- Imani, A., Faghihi, M., Sadr, S. S., Niaraki, S. S. & Alizadeh, A. M. 2011. Noradrenaline protects *in vivo* rat heart against infarction and ventricular arrhythmias via nitric oxide and reactive oxygen species. *J Surg Res*, 169, 9-15.
- Ishigami, M., Hiraki, K., Umemura, K., Ogasawara, Y., Ishii, K. & Kimura, H. 2009. A source of hydrogen sulfide and a mechanism of its release in the brain. *Antioxid Redox Signal*, 11, 205-214.
- Islam, K. N., Polhemus, D. J., Donnarumma, E., Brewster, L. P. & Lefer, D. J. 2015. Hydrogen Sulfide Levels and Nuclear Factor-Erythroid 2-Related Factor 2 (NRF2) Activity Are Attenuated in the Setting of Critical Limb Ischemia (CLI). *J Am Heart Assoc*, 4: e001986.
- Ito, H. 2006. No-reflow phenomenon and prognosis in patients with acute myocardial infarction. *Nat Clin Pract Cardiovasc Med*, 3, 499-506.
- Ivanciuc, T., Sbrana, E., Ansar, M., Bazhanov, N., Szabo, C., Casola, A. & Garofalo, R. P. 2016. Hydrogen sulfide: an antiviral and anti-inflammatory endogenous gasotransmitter in the airways. role in respiratory syncytial virus infection. *Am J Respir Cell Mol Biol*, 55, 684-696.
- Jain, S. K., Huning, L. & Micinski, D. 2014. Hydrogen sulfide upregulates glutamate-cysteine ligase catalytic subunit, glutamate-cysteine ligase modifier subunit, and glutathione and inhibits interleukin-1beta secretion in

- monocytes exposed to high glucose levels. *Metab Syndr Relat Disord*, 12, 299-302.
- James, A. M., Sharpley, M. S., Manas, A. R., Frerman, F. E., Hirst, J., Smith, R. A. & Murphy, M. P. 2007. Interaction of the mitochondria-targeted antioxidant MitoQ with phospholipid bilayers and ubiquinone oxidoreductases. *J Biol Chem*, 282, 14708-14718.
- Jamroz-Wisniewska, A., Gertler, A., Solomon, G., Wood, M. E., Whiteman, M. & Beltowski, J. 2014. Leptin-induced endothelium-dependent vasorelaxation of peripheral arteries in lean and obese rats: role of nitric oxide and hydrogen sulfide. *PLoS One*, 9, e86744.
- Jha, S., Calvert, J. W., Duranski, M. R., Ramachandran, A. & Lefer, D. J. 2008. Hydrogen sulfide attenuates hepatic ischemia-reperfusion injury: role of antioxidant and antiapoptotic signaling. *Am J Physiol Heart Circ Physiol*, 295, H801-H806.
- Jiang, H. L., Wu, H. C., Li, Z. L., Geng, B. & Tang, C. S. 2005. [Changes of the new gaseous transmitter H₂S in patients with coronary heart disease]. *Di Yi Jun Yi Da Xue Xue Bao*, 25, 951-954.
- Jiang, R., Zatta, A., Kin, H., Wang, N., Reeves, J. G., Mykytenko, J., Deneve, J., Zhao, Z. Q., Guyton, R. A. & Vinten-Johansen, J. 2007. PAR-2 activation at the time of reperfusion salvages myocardium via an ERK1/2 pathway in *in vivo* rat hearts. *Am J Physiol Heart Circ Physiol*, 293, H2845-H2852.
- Johansen, D., Ytrehus, K. & Baxter, G. F. 2006. Exogenous hydrogen sulfide (H₂S) protects against regional myocardial ischemia-reperfusion injury--Evidence for a role of K ATP channels. *Basic Res Cardiol*, 101, 53-60.
- Johns, T. N. & Olson, B. J. 1954. Experimental myocardial infarction. I. A method of coronary occlusion in small animals. *Ann Surg*, 140, 675-682.
- Jones, M. S., Murrell, R. D. & Shaw, I. C. 1985. Excretion of sodium 2-mercaptoethanesulphonate (MESNA) in the urine of volunteers after oral dosing. *Eur J Cancer Clin Oncol*, 21, 553-555.
- Kabasakal, L., Sehirli, A. O., Cetinel, S., Cikler, E., Gedik, N. & Sener, G. 2004. Mesna (2-mercaptoethane sulfonate) prevents ischemia/reperfusion induced renal oxidative damage in rats. *Life Sci*, 75, 2329-2340.
- Kai, S., Tanaka, T., Daijo, H., Harada, H., Kishimoto, S., Suzuki, K., Takabuchi, S., Takenaga, K., Fukuda, K. & Hirota, K. 2012. Hydrogen sulfide inhibits hypoxia- but not anoxia-induced hypoxia-inducible factor 1 activation in a von hippel-lindau- and mitochondria-dependent manner. *Antioxid Redox Signal*, 16, 203-216.

- Kaplan, P., Hendrikx, M., Mattheussen, M., Mubagwa, K. & Flameng, W. 1992. Effect of ischemia and reperfusion on sarcoplasmic reticulum calcium uptake. *Circ Res*, 71, 1123-1130.
- Karwi, Q. G., Whiteman, M., Wood, M. E., Torregrossa, R. & Baxter, G. F. 2016. Pharmacological postconditioning against myocardial infarction with a slow-releasing hydrogen sulfide donor, GYY4137. *Pharmacol Res*, 111, 442-451.
- Kempf, S. R. & Ivankovic, S. 1987. Nephrotoxicity and carcinogenic risk of cis-platin (CDDP) prevented by sodium 2-mercaptoethane-sulfonate (Mesna): experimental results. *Cancer Treat Rev*, 14, 365-372.
- Khan, A. A., Schuler, M. M., Prior, M. G., Yong, S., Coppock, R. W., Florence, L. Z. & Lillie, L. E. 1990. Effects of hydrogen sulfide exposure on lung mitochondrial respiratory chain enzymes in rats. *Toxicol Appl Pharmacol*, 103, 482-490.
- Kilkenny, C., Browne, W., Cuthill, I. C., Emerson, M., Altman, D. G. & Group, N. C. R. R. G. W. 2010. Animal research: reporting *in vivo* experiments: the ARRIVE guidelines. *Br J Pharmacol*, 160, 1577-1579.
- Kim, H. T., Kim, Y. H., Nam, J. W., Lee, H. J., Rho, H. M. & Jung, G. 1994. Study of 5'-flanking region of human Cu/Zn superoxide dismutase. *Biochem Biophys Res Commun*, 201, 1526-1533.
- Kimura, H. 2011. Hydrogen sulfide: its production and functions. *Exp Physiol*, 96, 833-835.
- Kimura, Y., Goto, Y. & Kimura, H. 2010. Hydrogen sulfide increases glutathione production and suppresses oxidative stress in mitochondria. *Antioxid Redox Signal*, 12, 1-13.
- Kimura, Y. & Kimura, H. 2004. Hydrogen sulfide protects neurons from oxidative stress. *FASEB J*, 18, 1165-1167.
- Kin, H., Zhao, Z.-Q., Sun, H.-Y., Wang, N.-P., Corvera, J. S., Halkos, M. E., Kerendi, F., Guyton, R. A. & Vinten-Johansen, J. 2004. Postconditioning attenuates myocardial ischemia-reperfusion injury by inhibiting events in the early minutes of reperfusion. *Cardiovasc Res*, 62, 74-85.
- King, A. L., Polhemus, D. J., Bhushan, S., Otsuka, H., Kondo, K., Nicholson, C. K., Bradley, J. M., Islam, K. N., Calvert, J. W., Tao, Y. X., Dugas, T. R., Kelley, E. E., Elrod, J. W., Huang, P. L., Wang, R. & Lefer, D. J. 2014. Hydrogen sulfide cytoprotective signaling is endothelial nitric oxide synthase-nitric oxide dependent. *Proc Natl Acad Sci U S A*, 111, 3182-3187.
- King, S. B. 2013. Potential biological chemistry of hydrogen sulfide (H₂S) with the nitrogen oxides. *Free Rad Biol Med*, 55, 1-7.

- Kinnally, K. W., Campo, M. L. & Tedeschi, H. 1989. Mitochondrial channel activity studied by patch-clamping mitoplasts. *J Bioenerg Biomembr*, 21, 497-506.
- Kishimoto, C., Shioji, K., Nakamura, H., Nakayama, Y., Yodoi, J. & Sasayama, S. 2001. Serum thioredoxin (TRX) levels in patients with heart failure. *Jpn Circ J*, 65, 491-494.
- Kloner, R. A. & Yellon, D. 1994. Does ischemic preconditioning occur in patients? *J Am Col Cardiol*, 24, 1133-1142.
- Koenitzer, J. R., Isbell, T. S., Patel, H. D., Benavides, G. A., Dickinson, D. A., Patel, R. P., Darley-USmar, V. M., Lancaster, J. R., Jr., Doeller, J. E. & Kraus, D. W. 2007. Hydrogen sulfide mediates vasoactivity in an O₂-dependent manner. *Am J Physiol Heart Circ Physiol*, 292, H1953-H1960.
- Kokoszka, J. E., Waymire, K. G., Levy, S. E., Sligh, J. E., Cai, J., Jones, D. P., Macgregor, G. R. & Wallace, D. C. 2004. The ADP/ATP translocator is not essential for the mitochondrial permeability transition pore. *Nature*, 427, 461-465.
- Kolluru, G. K., Shen, X., Bir, S. C. & Kevil, C. G. 2013. Hydrogen sulfide chemical biology: pathophysiological roles and detection. *Nitric Oxide*, 35, 5-20.
- Kondo, K., Bhushan, S., King, A. L., Prabhu, S. D., Hamid, T., Koenig, S., Murohara, T., Predmore, B. L., Gojon, G., Gojon, G., Wang, R., Karusula, N., Nicholson, C. K., Calvert, J. W. & Lefer, D. J. 2013. H₂S protects against pressure overload-induced heart failure via upregulation of endothelial nitric oxide synthase. *Circ*, 127, 1116-1127.
- Kottke, M., Adam, V., Riesinger, I., Bremm, G., Bosch, W., Brdiczka, D., Sandri, G. & Panfili, E. 1988. Mitochondrial boundary membrane contact sites in brain: points of hexokinase and creatine kinase location, and control of Ca²⁺ transport. *Biochim Biophys Acta*, 935, 87-102.
- Krauskopf, A., Eriksson, O., Craigen, W. J., Forte, M. A. & Bernardi, P. 2006. Properties of the permeability transition in VDAC1^{-/-} mitochondria. *Biochimica et Biophysica Acta (BBA) - Bioenergetics*, 1757, 590-595.
- Krug, A., Du Mesnil De, R. & Korb, G. 1966. Blood supply of the myocardium after temporary coronary occlusion. *Circ Res*, 19, 57-62.
- Kubickova, J., Hudecova, S., Csaderova, L., Soltysova, A., Lichvarova, L., Lencesova, L., Babula, P. & Krizanova, O. 2016. Slow sulfide donor GYY4137 differentiates NG108-15 neuronal cells through different intracellular transporters than dbcAMP. *Neuroscience*, 325, 100-110.
- Kuzuya, T., Hoshida, S., Yamashita, N., Fuji, H., Oe, H., Hori, M., Kamada, T. & Tada, M. 1993. Delayed effects of sublethal ischemia on the acquisition of tolerance to ischemia. *Circ Res*, 72, 1293-1299.

- Lacerda, L., Somers, S., Opie, L. H. & Lecour, S. 2009. Ischaemic postconditioning protects against reperfusion injury via the SAFE pathway. *Cardiovasc Res*, 84, 201-208.
- Lambert, J. P., Nicholson, C. K., Amin, H., Amin, S. & Calvert, J. W. 2014. Hydrogen sulfide provides cardioprotection against myocardial/ischemia reperfusion injury in the diabetic state through the activation of the RISK pathway. *Med Gas Res*, 4, 20.
- Lambert, T. W., Goodwin, V. M., Stefani, D. & Strosher, L. 2006. Hydrogen sulfide (H₂S) and sour gas effects on the eye. A historical perspective. *Sci Total Environ*, 367, 1-22.
- Lang, S. C., Elsasser, A., Scheler, C., Vetter, S., Tiefenbacher, C. P., Kubler, W., Katus, H. A. & Vogt, A. M. 2006. Myocardial preconditioning and remote renal preconditioning--identifying a protective factor using proteomic methods? *Basic Res Cardiol*, 101, 149-158.
- Le Trionnaire, S., Perry, A., Szczesny, B., Szabo, C., Winyard, P. G., Whatmore, J. L., Wood, M. E. & Whiteman, M. 2014. The synthesis and functional evaluation of a mitochondria-targeted hydrogen sulfide donor, (10-oxo-10-(4-(3-thioxo-3H-1,2-dithiol-5-yl)phenoxy)decyl)triphenylphosphonium bromide (AP39). *Med Chem Comm*, 5, 728-736.
- Lecour, S. 2009. Activation of the protective Survivor Activating Factor Enhancement (SAFE) pathway against reperfusion injury: Does it go beyond the RISK pathway? *J Mol Cell Cardiol*, 47, 32-40.
- Lecour, S., Suleman, N., Deuchar, G. A., Somers, S., Lacerda, L., Huisamen, B. & Opie, L. H. 2005. Pharmacological preconditioning with tumor necrosis factor- α activates signal transducer and activator of transcription-3 at reperfusion without involving classic prosurvival kinases (Akt and extracellular signal-regulated kinase). *Circ*, 112, 3911-3918.
- Lee, Z. W., Teo, X. Y., Tay, E. Y. W., Tan, C. H., Hagen, T., Moore, P. K. & Deng, L. W. 2014. Utilizing hydrogen sulfide as a novel anti-cancer agent by targeting cancer glycolysis and pH imbalance. *Br J Pharmacol*, 171, 4322-4336.
- Lee, Z. W., Zhou, J., Chen, C. S., Zhao, Y., Tan, C. H., Li, L., Moore, P. K. & Deng, L. W. 2011. The slow-releasing hydrogen sulfide donor, GYY4137, exhibits novel anti-cancer effects *in vitro* and *in vivo*. *PLoS One*, 6, e21077.
- Lencesova, L., Hudecova, S., Csaderova, L., Markova, J., Soltysova, A., Pastorek, M., Sedlak, J., Wood, M. E., Whiteman, M., Ondrias, K. & Krizanova, O. 2013. Sulfide signalling potentiates apoptosis through the up-regulation of IP3 receptor types 1 and 2. *Acta Physiol (Oxf)*, 208, 350-361.

- Lesnefsky, E. J., Chen, Q., Moghaddas, S., Hassan, M. O., Tandler, B. & Hoppel, C. L. 2004. Blockade of electron transport during ischemia protects cardiac mitochondria. *J Biol Chem*, 279, 47961-47967.
- Li, H., Wang, Y., Wei, C., Bai, S., Zhao, Y., Li, H., Wu, B., Wang, R., Wu, L. & Xu, C. 2015a. Mediation of exogenous hydrogen sulfide in recovery of ischemic post-conditioning-induced cardioprotection via down-regulating oxidative stress and up-regulating PI3K/Akt/GSK-3beta pathway in isolated aging rat hearts. *Cell Biosci*, 5, 11.
- Li, H., Zhang, C., Sun, W., Li, L., Wu, B., Bai, S., Li, H., Zhong, X., Wang, R., Wu, L. & Xu, C. 2015b. Exogenous hydrogen sulfide restores cardioprotection of ischemic post-conditioning via inhibition of mPTP opening in the aging cardiomyocytes. *Cell Biosci*, 5, 43.
- Li, J., Rohailla, S., Gelber, N., Rutka, J., Sabah, N., Gladstone, R. A., Wei, C., Hu, P., Kharbanda, R. K. & Redington, A. N. 2014. MicroRNA-144 is a circulating effector of remote ischemic preconditioning. *Basic Res Cardiol*, 109, 423.
- Li, L., Fox, B., Keeble, J., Salto-Tellez, M., Winyard, P. G., Wood, M. E., Moore, P. K. & Whiteman, M. 2013. The complex effects of the slow-releasing hydrogen sulfide donor GYY4137 in a model of acute joint inflammation and in human cartilage cells. *J Cell Mol Med*, 17, 365-376.
- Li, L., Li, M., Li, Y., Sun, W., Wang, Y., Bai, S., Li, H., Wu, B., Yang, G., Wang, R., Wu, L., Li, H. & Xu, C. 2016. Exogenous H₂S contributes to recovery of ischemic post-conditioning-induced cardioprotection by decrease of ROS level via down-regulation of NF-kappaB and JAK2-STAT3 pathways in the aging cardiomyocytes. *Cell Biosci*, 6, 26.
- Li, L., Salto-Tellez, M., Tan, C. H., Whiteman, M. & Moore, P. K. 2009. GYY4137, a novel hydrogen sulfide-releasing molecule, protects against endotoxic shock in the rat. *Free Radic Biol Med*, 47, 103-113.
- Li, L., Whiteman, M., Guan, Y. Y., Neo, K. L., Cheng, Y., Lee, S. W., Zhao, Y., Baskar, R., Tan, C. H. & Moore, P. K. 2008. Characterization of a novel, water-soluble hydrogen sulfide-releasing molecule (GYY4137): new insights into the biology of hydrogen sulfide. *Circ*, 117, 2351-2360.
- Li, Y. & Kloner, R. A. 1993. The cardioprotective effects of ischemic 'preconditioning' are not mediated by adenosine receptors in rat hearts. *Circ*, 87, 1642-1648.
- Lilyanna, S., Peh, M. T., Liew, O. W., Wang, P., Moore, P. K., Richards, A. M. & Martinez, E. C. 2015. GYY4137 attenuates remodeling, preserves cardiac function and modulates the natriuretic peptide response to ischemia. *J Mol Cell Cardiol*, 87, 27-37.

- Lim, S. Y., Yellon, D. M. & Hausenloy, D. J. 2010. The neural and humoral pathways in remote limb ischemic preconditioning. *Basic Res Cardiol*, 105, 651-655.
- Lin, S., Visram, F., Liu, W., Haig, A., Jiang, J., Mok, A., Lian, D., Wood, M. E., Torregrossa, R., Whiteman, M., Lobb, I. & Sener, A. 2016. GYY4137, a slow-releasing hydrogen sulfide donor, ameliorates renal damage associated with chronic obstructive uropathy. *J Urol*, 196, 1778-1787.
- Liu, G. S., Thornton, J., Van Winkle, D. M., Stanley, A. W., Olsson, R. A. & Downey, J. M. 1991. Protection against infarction afforded by preconditioning is mediated by A1 adenosine receptors in rabbit heart. *Circ*, 84, 350-356.
- Liu, Y. H., Lu, M., Hu, L. F., Wong, P. T., Webb, G. D. & Bian, J. S. 2012. Hydrogen sulfide in the mammalian cardiovascular system. *Antioxid Redox Signal*, 17, 141-185.
- Liu, Y. Y., Nagpure, B. V., Wong, P. T. & Bian, J. S. 2013a. Hydrogen sulfide protects SH-SY5Y neuronal cells against d-galactose induced cell injury by suppression of advanced glycation end products formation and oxidative stress. *Neurochem Int*, 62, 603-609.
- Liu, Z., Han, Y., Li, L., Lu, H., Meng, G., Li, X., Shirhan, M., Peh, M. T., Xie, L., Zhou, S., Wang, X., Chen, Q., Dai, W., Tan, C. H., Pan, S., Moore, P. K. & Ji, Y. 2013b. The hydrogen sulfide donor, GYY4137, exhibits anti-atherosclerotic activity in high fat fed apolipoprotein E(-/-) mice. *Br J Pharmacol*, 169, 1795-1809.
- Lobb, I., Jiang, J., Lian, D., Liu, W., Haig, A., Saha, M. N., Torregrossa, R., Wood, M. E., Whiteman, M. & Sener, A. 2016. Hydrogen sulfide protects renal grafts against prolonged cold ischemia-reperfusion injury via specific mitochondrial actions. *Am J Transplant*, doi: 10.1111/ajt.14080.
- Lowry, O. H., Rosebrough, N. J., Farr, A. L. & Randall, R. J. 1951. Protein measurement with the Folin phenol reagent. *J Biol Chem*, 193, 265-275.
- Lu, S., Gao, Y., Huang, X. & Wang, X. 2014. GYY4137, a hydrogen sulfide (H₂S) donor, shows potent anti-hepatocellular carcinoma activity through blocking the STAT3 pathway. *Int J Oncol*, 44, 1259-1267.
- Luan, H. F., Zhao, Z. B., Zhao, Q. H., Zhu, P., Xiu, M. Y. & Ji, Y. 2012. Hydrogen sulfide postconditioning protects isolated rat hearts against ischemia and reperfusion injury mediated by the JAK2/STAT3 survival pathway. *Braz J Med Biol Res*, 45, 898-905.
- Mani, S., Li, H., Untereiner, A., Wu, L., Yang, G., Austin, R. C., Dickhout, J. G., Lhotak, S., Meng, Q. H. & Wang, R. 2013. Decreased endogenous production of hydrogen sulfide accelerates atherosclerosis. *Circ*, 127, 2523-2534.

- Mani, S., Li, H., Yang, G., Wu, L. & Wang, R. 2015. Deficiency of cystathionine gamma-lyase and hepatic cholesterol accumulation during mouse fatty liver development. *Science Bulletin*, 60, 336-347.
- Manning, A. S. & Hearse, D. J. 1984. Reperfusion-induced arrhythmias: mechanisms and prevention. *J Mol Cell Cardiol*, 16, 497-518.
- Marber, M. S., Latchman, D. S., Walker, J. M. & Yellon, D. M. 1993. Cardiac stress protein elevation 24 hours after brief ischemia or heat stress is associated with resistance to myocardial infarction. *Circ*, 88, 1264-1272.
- Marzo, I., Brenner, C., Zamzami, N., Susin, S. A., Beutner, G., Brdiczka, D., Rémy, R., Xie, Z.-H., Reed, J. C. & Kroemer, G. 1998. The permeability transition pore complex: a target for apoptosis regulation by caspases and Bcl-2-related proteins. *J Exp Med*, 187, 1261-1271.
- Mashiach, E., Sela, S., Weinstein, T., Cohen, H. I., Shasha, S. M. & Kristal, B. 2001. Mesna: a novel renoprotective antioxidant in ischaemic acute renal failure. *Nephrol Dial Transplant*, 16, 542-551.
- Mastitskaya, S., Marina, N., Gourine, A., Gilbey, M. P., Spyer, K. M., Teschemacher, A. G., Kasparov, S., Trapp, S., Ackland, G. L. & Gourine, A. V. 2012. Cardioprotection evoked by remote ischaemic preconditioning is critically dependent on the activity of vagal pre-ganglionic neurones. *Cardiovasc Res*, 95, 487-494.
- Maxwell, M. P., Hearse, D. J. & Yellon, D. M. 1987. Species variation in the coronary collateral circulation during regional myocardial ischaemia: a critical determinant of the rate of evolution and extent of myocardial infarction. *Cardiovasc Res*, 21, 737-746.
- Mcgrath, J. C., Drummond, G. B., Mclachlan, E. M., Kilkenny, C. & Wainwright, C. L. 2010. Guidelines for reporting experiments involving animals: the ARRIVE guidelines. *Br J Pharmacol*, 160, 1573-1576.
- Mendis, S., Puska, P. & Norrving, B. 2011. *Global Atlas on Cardiovascular Disease Prevention and Control*, Geneva, World Health Organisation.
- Meng, G., Wang, J., Xiao, Y., Bai, W., Xie, L., Shan, L., Moore, P. K. & Ji, Y. 2015a. GYY4137 protects against myocardial ischemia and reperfusion injury by attenuating oxidative stress and apoptosis in rats. *J Biomed Res*, 29, 203-213.
- Meng, G., Xiao, Y., Ma, Y., Tang, X., Xie, L., Liu, J., Gu, Y., Yu, Y., Park, C. M., Xian, M., Wang, X., Ferro, A., Wang, R., Moore, P. K., Zhang, Z., Wang, H., Han, Y. & Ji, Y. 2016. Hydrogen sulfide regulates krüppel-like factor 5 transcription activity via specificity protein 1 s-sulfhydration at cys664 to prevent myocardial hypertrophy. *J Am Heart Assoc*, 5: e004160.

- Meng, G., Zhu, J., Xiao, Y., Huang, Z., Zhang, Y., Tang, X., Xie, L., Chen, Y., Shao, Y., Ferro, A., Wang, R., Moore, P. K. & Ji, Y. 2015b. Hydrogen sulfide donor GYY4137 protects against myocardial fibrosis. *Oxid Med Cell Longev*, 2015, 691070.
- Methner, C., Lukowski, R., Grube, K., Loga, F., Smith, R. A., Murphy, M. P., Hofmann, F. & Krieg, T. 2013. Protection through postconditioning or a mitochondria-targeted S-nitrosothiol is unaffected by cardiomyocyte-selective ablation of protein kinase G. *Basic Res Cardiol*, 108, 337.
- Miao, L., Shen, X., Whiteman, M., Xin, H., Shen, Y., Xin, X., Moore, P. K. & Zhu, Y. Z. 2016. Hydrogen sulfide mitigates myocardial infarction via promotion of mitochondrial biogenesis-dependent M2 polarization of macrophages. *Antioxid Redox Signal*, 25, 268-281.
- Mikami, Y., Shibuya, N., Kimura, Y., Nagahara, N., Ogasawara, Y. & Kimura, H. 2011. Thioredoxin and dihydrolipoic acid are required for 3-mercaptopyruvate sulfurtransferase to produce hydrogen sulfide. *Biochem J*, 439, 479-485.
- Minamishima, S., Bougaki, M., Sips, P. Y., Yu, J. D., Minamishima, Y. A., Elrod, J. W., Lefer, D. J., Bloch, K. D. & Ichinose, F. 2009. Hydrogen sulfide improves survival after cardiac arrest and cardiopulmonary resuscitation via a nitric oxide synthase 3-dependent mechanism in mice. *Circ*, 120, 888-896.
- Modis, K., Asimakopoulou, A., Coletta, C., Papapetropoulos, A. & Szabo, C. 2013a. Oxidative stress suppresses the cellular bioenergetic effect of the 3-mercaptopyruvate sulfurtransferase/hydrogen sulfide pathway. *Biochem Biophys Res Commun*, 433, 401-407.
- Modis, K., Bos, E. M., Calzia, E., Van Goor, H., Coletta, C., Papapetropoulos, A., Hellmich, M. R., Radermacher, P., Bouillaud, F. & Szabo, C. 2014. Regulation of mitochondrial bioenergetic function by hydrogen sulfide. Part II. Pathophysiological and therapeutic aspects. *Br J Pharmacol*, 171, 2123-2146.
- Modis, K., Coletta, C., Erdelyi, K., Papapetropoulos, A. & Szabo, C. 2013b. Intramitochondrial hydrogen sulfide production by 3-mercaptopyruvate sulfurtransferase maintains mitochondrial electron flow and supports cellular bioenergetics. *FASEB J*, 27, 601-611.
- Modis, K., Ju, Y., Ahmad, A., Untereiner, A. A., Altaany, Z., Wu, L., Szabo, C. & Wang, R. 2016. S-sulfhydration of ATP synthase by hydrogen sulfide stimulates mitochondrial bioenergetics. *Pharmacol Res*, 113, 116-124.
- Modis, K., Panopoulos, P., Coletta, C., Papapetropoulos, A. & Szabo, C. 2013c. Hydrogen sulfide-mediated stimulation of mitochondrial electron transport involves inhibition of the mitochondrial phosphodiesterase 2A, elevation of cAMP and activation of protein kinase A. *Biochem Pharmacol*, 86, 1311-1319.

- Murphy, E., Ardehali, H., Balaban, R. S., Dilisa, F., Dorn, G. W., 2nd, Kitsis, R. N., Otsu, K., Ping, P., Rizzuto, R., Sack, M. N., Wallace, D., Youle, R. J., American Heart Association Council on Basic Cardiovascular Sciences, C. O. C. C., Council on Functional, G. & Translational, B. 2016. Mitochondrial Function, Biology, and Role in Disease: A Scientific Statement From the American Heart Association. *Circ Res*, 118, 1960-1991.
- Murphy, E. & Steenbergen, C. 2013. Did a classic preconditioning study provide a clue to the identity of the mitochondrial permeability transition pore? *Circ Res*, 113, 852-855.
- Murphy, M. P. & Smith, R. A. 2007. Targeting antioxidants to mitochondria by conjugation to lipophilic cations. *Annu Rev Pharmacol Toxicol*, 47, 629-656.
- Murry, C. E., Jennings, R. B. & Reimer, K. A. 1986. Preconditioning with ischemia: a delay of lethal cell injury in ischemic myocardium. *Circ*, 74, 1124-1136.
- Murry, C. E., Richard, V. J., Reimer, K. A. & Jennings, R. B. 1990. Ischemic preconditioning slows energy metabolism and delays ultrastructural damage during a sustained ischemic episode. *Circ Res*, 66, 913-931.
- Mustafa, A. K., Sikka, G., Gazi, S. K., Stepan, J., Jung, S. M., Bhunia, A. K., Barodka, V. M., Gazi, F. K., Barrow, R. K., Wang, R., Amzel, L. M., Berkowitz, D. E. & Snyder, S. H. 2011. Hydrogen sulfide as endothelium-derived hyperpolarizing factor sulfhydrates potassium channels. *Circ Res*, 109, 1259-1268.
- Nakagawa, T., Shimizu, S., Watanabe, T., Yamaguchi, O., Otsu, K., Yamagata, H., Inohara, H., Kubo, T. & Tsujimoto, Y. 2005. Cyclophilin D-dependent mitochondrial permeability transition regulates some necrotic but not apoptotic cell death. *Nature*, 434, 652-658.
- Negoro, S., Kunisada, K., Fujio, Y., Funamoto, M., Darville, M. I., Eizirik, D. L., Osugi, T., Izumi, M., Oshima, Y., Nakaoka, Y., Hirota, H., Kishimoto, T. & Yamauchi-Takahara, K. 2001. Activation of signal transducer and activator of transcription 3 protects cardiomyocytes from hypoxia/reoxygenation-induced oxidative stress through the upregulation of manganese superoxide dismutase. *Circ*, 104, 979-981.
- Nguyen, T. T., Stevens, M. V., Kohr, M., Steenbergen, C., Sack, M. N. & Murphy, E. 2011a. Cysteine 203 of cyclophilin D is critical for cyclophilin D activation of the mitochondrial permeability transition pore. *J Biol Chem*, 286, 40184-40192.
- Nguyen, T. T. M., Stevens, M., Kohr, M., Steenbergen, C., Sack, M. & Murphy, E. 2011b. S-nitrosylation of cyclophilin D alters mitochondrial permeability transition pore. *FASEB J*, 25, 1033.1.

- Nicholls, P., Marshall, D. C., Cooper, C. E. & Wilson, M. T. 2013. Sulfide inhibition of and metabolism by cytochrome c oxidase. *Biochem Soc Trans*, 41, 1312-1316.
- Nicholson, C. K., Lambert, J. P., Molkentin, J. D., Sadoshima, J. & Calvert, J. W. 2013. Thioredoxin 1 is essential for sodium sulfide-mediated cardioprotection in the setting of heart failure. *Arterioscler Thromb Vasc Biol*, 33, 744-751.
- Nicholson, R. A., Roth, S. H., Zhang, A., Zheng, J., Brookes, J., Skrajny, B. & Bennington, R. 1998. Inhibition of respiratory and bioenergetic mechanisms by hydrogen sulfide in mammalian brain. *J Toxicol Environ Health A*, 54, 491-507.
- Nordberg, J. & Arnér, E. S. J. 2001. Reactive oxygen species, antioxidants, and the mammalian thioredoxin system1. *Free Rad Biol Med*, 31, 1287-1312.
- Okamoto, F., Allen, B. S., Buckberg, G. D., Bugyi, H. & Leaf, J. 1986. Reperfusion conditions: importance of ensuring gentle versus sudden reperfusion during relief of coronary occlusion. *J Thorac Cardiovasc Surg*, 92, 613-620.
- Olson, K. R. 2012. Mitochondrial adaptations to utilize hydrogen sulfide for energy and signaling. *J Comp Physiol B*, 182, 881-897.
- Olson, K. R., Dombkowski, R. A., Russell, M. J., Doellman, M. M., Head, S. K., Whitfield, N. L. & Madden, J. A. 2006. Hydrogen sulfide as an oxygen sensor/transducer in vertebrate hypoxic vasoconstriction and hypoxic vasodilation. *J Exp Biol*, 209, 4011-4023.
- Olson, K. R. & Straub, K. D. 2016. The role of hydrogen sulfide in evolution and the evolution of hydrogen sulfide in metabolism and signaling. *Physiol*, 31, 60-72.
- Ong, S. B., Samangouea, P., Kalkhorana, S. B. & Hausenloy, D. J. 2015. The mitochondrial permeability transition pore and its role in myocardial ischemia reperfusion injury. *J Mol Cell Cardiol*, 78, 23-34.
- Ormstad, K., Orrenius, S., Lastbom, T., Uehara, N., Pohl, J., Stekar, J. & Brock, N. 1983. Pharmacokinetics and metabolism of sodium 2-mercaptoethanesulfonate in the rat. *Cancer Res*, 43, 333-338.
- Osipov, R. M., Robich, M. P., Feng, J., Liu, Y., Clements, R. T., Glazer, H. P., Sodha, N. R., Szabo, C., Bianchi, C. & Sellke, F. W. 2009. Effect of hydrogen sulfide in a porcine model of myocardial ischemia-reperfusion: comparison of different administration regimens and characterization of the cellular mechanisms of protection. *J Cardiovasc Pharmacol*, 54, 287-297.
- Palmer, J. W., Tandler, B. & Hoppel, C. L. 1977. Biochemical properties of subsarcolemmal and interfibrillar mitochondria isolated from rat cardiac muscle. *J Biol Chem*, 252, 8731-8739.

- Palmer, J. W., Tandler, B. & Hoppel, C. L. 1986. Heterogeneous response of subsarcolemmal heart mitochondria to calcium. *Am J Physiol*, 250, H741-H748.
- Pan, T. T., Chen, Y. Q. & Bian, J. S. 2009. All in the timing: a comparison between the cardioprotection induced by H₂S preconditioning and post-infarction treatment. *Eur J Pharmacol*, 616, 160-165.
- Pan, X., Liu, J., Nguyen, T., Liu, C., Sun, J., Teng, Y., Fergusson, M. M., Rovira, I., Allen, M., Springer, D. A., Aponte, A. M., Gucek, M., Balaban, R. S., Murphy, E. & Finkel, T. 2013. The physiological role of mitochondrial calcium revealed by mice lacking the mitochondrial calcium uniporter. *Nat Cell Biol*, 15, 1464-1472.
- Papapetropoulos, A., Whiteman, M. & Cirino, G. 2015. Pharmacological tools for hydrogen sulphide research: a brief, introductory guide for beginners. *Br J Pharmacol*, 172, 1633-1637.
- Peake, B. F., Nicholson, C. K., Lambert, J. P., Hood, R. L., Amin, H., Amin, S. & Calvert, J. W. 2013. Hydrogen sulfide preconditions the db/db diabetic mouse heart against ischemia-reperfusion injury by activating Nrf2 signaling in an Erk-dependent manner. *Am J Physiol Heart Circ Physiol*, 304, H1215-H1224.
- Pell, V. R., Chouchani, E. T., Frezza, C., Murphy, M. P. & Krieg, T. 2016. Succinate metabolism: a new therapeutic target for myocardial reperfusion injury. *Cardiovasc Res*, 111, 134-141.
- Petronilli, V., Szabo, I. & Zoratti, M. 1989. The inner mitochondrial membrane contains ion-conducting channels similar to those found in bacteria. *FEBS Lett*, 259, 137-143.
- Pisarenko, O., Studneva, I., Khlopkov, V., Solomatina, E. & Ruuge, E. 1988. An assessment of anaerobic metabolism during ischemia and reperfusion in isolated guinea pig heart. *Biochim Biophys Acta*, 934, 55-63.
- Pitts, K. R., Stiko, A., Buetow, B., Lott, F., Guo, P., Virca, D. & Toombs, C. F. 2007. Washout of heme-containing proteins dramatically improves tetrazolium-based infarct staining. *J Pharmacol Toxicol Methods*, 55, 201-208.
- Polhemus, D. J., Li, Z., Pattillo, C. B., Gojon, G., Sr., Gojon, G., Jr., Giordano, T. & Krum, H. 2015. A novel hydrogen sulfide prodrug, SG1002, promotes hydrogen sulfide and nitric oxide bioavailability in heart failure patients. *Cardiovasc Ther*, 33, 216-226.
- Predmore, B. L., Julian, D. & Cardounel, A. J. 2011. Hydrogen sulfide increases nitric oxide production from endothelial cells by an akt-dependent mechanism. *Front Physiol*, 2, 104.

- Predmore, B. L., Kondo, K., Bhushan, S., Zlatopolsky, M. A., King, A. L., Aragon, J. P., Grinsfelder, D. B., Condit, M. E. & Lefer, D. J. 2012. The polysulfide diallyl trisulfide protects the ischemic myocardium by preservation of endogenous hydrogen sulfide and increasing nitric oxide bioavailability. *Am J Physiol Heart Circ Physiol*, 302, H2410-H2418.
- Prime, T. A., Blaikie, F. H., Evans, C., Nadtochiy, S. M., James, A. M., Dahm, C. C., Vitturi, D. A., Patel, R. P., Hiley, C. R., Abakumova, I., Requejo, R., Chouchani, E. T., Hurd, T. R., Garvey, J. F., Taylor, C. T., Brookes, P. S., Smith, R. A. & Murphy, M. P. 2009. A mitochondria-targeted S-nitrosothiol modulates respiration, nitrosates thiols, and protects against ischemia-reperfusion injury. *Proc Natl Acad Sci U S A*, 106, 10764-10769.
- Przyklenk, K., Bauer, B., Ovize, M., Kloner, R. A. & Whittaker, P. 1993. Regional ischemic 'preconditioning' protects remote virgin myocardium from subsequent sustained coronary occlusion. *Circ*, 87, 893-899.
- Qabazard, B., Li, L., Gruber, J., Peh, M. T., Ng, L. F., Kumar, S. D., Rose, P., Tan, C.-H., Dymock, B. W., Wei, F., Swain, S. C., Halliwell, B., Stürzenbaum, S. R. & Moore, P. K. 2014. Hydrogen sulfide is an endogenous regulator of aging in *caenorhabditis elegans*. *Antioxid Redox Signal*, 20, 2621-2630.
- Qvigstad, E., Sjaastad, I., Brattelid, T., Nunn, C., Swift, F., Birkeland, J. a. K., Krobert, K. A., Andersen, G. Ø., Sejersted, O. M., Osnes, J.-B., Levy, F. O. & Skomedal, T. 2005. Dual serotonergic regulation of ventricular contractile force through 5-HT_{2A} and 5-HT₄ receptors induced in the acute failing heart. *Circ Res*, 97, 268-276.
- Rassaf, T., Totzeck, M., Hendgen-Cotta, U. B., Shiva, S., Heusch, G. & Kelm, M. 2014. Circulating nitrite contributes to cardioprotection by remote ischemic preconditioning. *Circ Res*, 114, 1601-1610.
- Reimer, K. A., Jennings, R. B. & Hill, M. L. 1981. Total ischemia in dog hearts, *in vitro* 2. High energy phosphate depletion and associated defects in energy metabolism, cell volume regulation, and sarcolemmal integrity. *Circ Res*, 49, 901-911.
- Rey, S. & Semenza, G. L. 2010. Hypoxia-inducible factor-1-dependent mechanisms of vascularization and vascular remodelling. *Cardiovasc Res*, 86, 236-242.
- Robinson, H. & Wray, S. 2012. A new slow releasing, H₂S generating compound, GYY4137 relaxes spontaneous and oxytocin-stimulated contractions of human and rat pregnant myometrium. *PLoS One*, 7, e46278.
- Rodrigues, L., Ekundi-Valentim, E., Florenzano, J., Cerqueira, A. R. A., Schmidt, T. P., Santos, K. T., Soares, A. G., Teixeira, S. A., Ribela, M. T. C. P., De Nucci, G., Wood, M., Whiteman, M., Muscará, M. N. & Costa, S. K. P. 2016. Protective effects of exogenous and endogenous hydrogen sulfide in mast cell-

- mediated pruritus and cutaneous acute inflammation in mice. *Pharmacol Res*, <http://dx.doi.org/10.1016/j.phrs.2016.11.006>.
- Rose, P., Dymock, B. W. & Moore, P. K. 2015. GYY4137, a novel water-soluble, H₂S-releasing molecule. *Methods Enzymol*, 554, 143-167.
- Ross, R. 1993. The pathogenesis of atherosclerosis: a perspective for the 1990s. *Nature*, 362, 801-809.
- Rossoni, G., Sparatore, A., Tazzari, V., Manfredi, B., Del Soldato, P. & Berti, F. 2008. The hydrogen sulphide-releasing derivative of diclofenac protects against ischaemia-reperfusion injury in the isolated rabbit heart. *Br J Pharmacol*, 153, 100-109.
- Routhu, K. V., Tsopanoglou, N. E. & Strande, J. L. 2010. Parstatin(1-26): the putative signal peptide of protease-activated receptor 1 confers potent protection from myocardial ischemia-reperfusion injury. *J Pharmacol Exp Ther*, 332, 898-905.
- Ruiz-Meana, M., Núñez, E., Miro-Casas, E., Martínez-Acedo, P., Barba, I., Rodriguez-Sinovas, A., Inserte, J., Fernandez-Sanz, C., Hernando, V., Vázquez, J. & Garcia-Dorado, D. 2014. Ischemic preconditioning protects cardiomyocyte mitochondria through mechanisms independent of cytosol. *J Mol Cell Cardiol*, 68, 79-88.
- Saha, S., Chakraborty, P. K., Xiong, X., Dwivedi, S. K., Mustafi, S. B., Leigh, N. R., Ramchandran, R., Mukherjee, P. & Bhattacharya, R. 2016. Cystathionine beta-synthase regulates endothelial function via protein S-sulfhydration. *FASEB J*, 30, 441-456.
- Salvi, A., Bankhele, P., Jamil, J. M., Kulkarni-Chitnis, M., Njie-Mbye, Y. F., Ohia, S. E. & Opere, C. A. 2016. Pharmacological actions of hydrogen sulfide donors on sympathetic neurotransmission in the bovine anterior uvea, *in vitro*. *Neurochem Res*, 41, 1020-1028.
- Savage, J. C. & Gould, D. H. 1990. Determination of sulfide in brain tissue and rumen fluid by ion-interaction reversed-phase high-performance liquid chromatography. *J Chromatogr B Biomed Sci Appl*, 526, 540-545.
- Schott, R. J., Rohmann, S., Braun, E. R. & Schaper, W. 1990. Ischemic preconditioning reduces infarct size in swine myocardium. *Circ Res*, 66, 1133-1142.
- Schwarz, E. R., Somoano, Y., Hale, S. L. & Kloner, R. A. 2000. What is the required reperfusion period for assessment of myocardial infarct size using triphenyltetrazolium chloride staining in the rat? *J Thromb Thrombolysis*, 10, 181-187.

- Searcy, D. G., Whitehead, J. P. & Maroney, M. J. 1995. Interaction of Cu,Zn superoxide dismutase with hydrogen sulfide. *Arch Biochem Biophys*, 318, 251-263.
- Sener, G., Sehirli, O., Cetinel, S., Yegen, B. G., Gedik, N. & Ayanoglu-Dulger, G. 2005a. Protective effects of MESNA (2-mercaptoethane sulphonate) against acetaminophen-induced hepatorenal oxidative damage in mice. *J Appl Toxicol*, 25, 20-29.
- Sener, G., Sehirli, O., Ercan, F., Sirvanci, S., Gedik, N. & Kacmaz, A. 2005b. Protective effect of MESNA (2-mercaptoethane sulfonate) against hepatic ischemia/reperfusion injury in rats. *Surg Today*, 35, 575-580.
- Sener, G., Sehirli, O., Erkanli, G., Cetinel, S., Gedik, N. & Yegen, B. 2004. 2-Mercaptoethane sulfonate (MESNA) protects against burn-induced renal injury in rats. *Burns*, 30, 557-564.
- Shaw, I. C. & Graham, M. I. 1987. Mesna--a short review. *Cancer Treat Rev*, 14, 67-86.
- Shaw, I. C., Graham, M. I. & Jones, M. S. 1986. The fate of [14C]-mesna in the rat. *Arzneimittelforschung*, 36, 487-489.
- Shen, X., Peter, E. A., Bir, S., Wang, R. & Kevil, C. G. 2012. Analytical measurement of discrete hydrogen sulfide pools in biological specimens. *Free Radic Biol Med*, 52, 2276-2283.
- Shi, Y. X., Chen, Y., Zhu, Y. Z., Huang, G. Y., Moore, P. K., Huang, S. H., Yao, T. & Zhu, Y. C. 2007. Chronic sodium hydrosulfide treatment decreases medial thickening of intramyocardial coronary arterioles, interstitial fibrosis, and ROS production in spontaneously hypertensive rats. *Am J Physiol Heart Circ Physiol*, 293, H2093-H2100.
- Shibuya, N., Koike, S., Tanaka, M., Ishigami-Yuasa, M., Kimura, Y., Ogasawara, Y., Fukui, K., Nagahara, N. & Kimura, H. 2013. A novel pathway for the production of hydrogen sulfide from D-cysteine in mammalian cells. *Nat Commun*, 4, 1366.
- Shimizu, M., Tropak, M., Diaz, R. J., Suto, F., Surendra, H., Kuzmin, E., Li, J., Gross, G., Wilson, G. J., Callahan, J. & Redington, A. N. 2009. Transient limb ischaemia remotely preconditions through a humoral mechanism acting directly on the myocardium: evidence suggesting cross-species protection. *Clin Sci (Lond)*, 117, 191-200.
- Shusterman, T., Sela, S., Cohen, H., Kristal, B., Sbeit, W. & Reshef, R. 2003. Effect of the antioxidant Mesna (2-mercaptoethane sulfonate) on experimental colitis. *Dig Dis Sci*, 48, 1177-1185.

- Sidou, B. & Shaw, I. C. 1984. Determination of sodium 2-mercaptoethanesulphonate by high-performance liquid chromatography using post-column reaction colorimetry or electrochemical detection. *J Chromatogr B Biomed Sci Appl*, 311, 234-238.
- Singh, B., Randhawa, P. K., Singh, N. & Jaggi, A. S. 2016. Investigations on the role of leukotrienes in remote hind limb preconditioning-induced cardioprotection in rats. *Life Sci*, 152, 238-243.
- Singh, S., Padovani, D., Leslie, R. A., Chiku, T. & Banerjee, R. 2009. Relative contributions of cystathionine beta-synthase and gamma-cystathionase to H₂S biogenesis via alternative trans-sulfuration reactions. *J Biol Chem*, 284, 22457-22466.
- Sivakumaran, V., Stanley, B. A., Tocchetti, C. G., Ballin, J. D., Caceres, V., Zhou, L., Keceli, G., Rainer, P. P., Lee, D. I., Huke, S., Ziolo, M. T., Kranias, E. G., Toscano, J. P., Wilson, G. M., O'rourke, B., Kass, D. A., Mahaney, J. E. & Paolocci, N. 2013. HNO enhances SERCA2a activity and cardiomyocyte function by promoting redox-dependent phospholamban oligomerization. *Antioxid Redox Signal*, 19, 1185-1197.
- Sivarajah, A., Collino, M., Yasin, M., Benetti, E., Gallicchio, M., Mazzon, E., Cuzzocrea, S., Fantozzi, R. & Thiemermann, C. 2009. Anti-apoptotic and anti-inflammatory effects of hydrogen sulfide in a rat model of regional myocardial I/R. *Shock*, 31, 267-274.
- Smith, P. F., Booker, B. M., Creaven, P., Perez, R. & Pendyala, L. 2003a. Pharmacokinetics and pharmacodynamics of mesna-mediated plasma cysteine depletion. *J Clin Pharmacol*, 43, 1324-1328.
- Smith, P. K., Krohn, R. I., Hermanson, G. T., Mallia, A. K., Gartner, F. H., Provenzano, M. D., Fujimoto, E. K., Goeke, N. M., Olson, B. J. & Klenk, D. C. 1985. Measurement of protein using bicinchoninic acid. *Anal Biochem*, 150, 76-85.
- Smith, R. A., Hartley, R. C. & Murphy, M. P. 2011. Mitochondria-targeted small molecule therapeutics and probes. *Antioxid Redox Signal*, 15, 3021-3038.
- Smith, R. A., Porteous, C. M., Gane, A. M. & Murphy, M. P. 2003b. Delivery of bioactive molecules to mitochondria *in vivo*. *Proc Natl Acad Sci U S A*, 100, 5407-5412.
- Smith, R. M., Suleman, N., Lacerda, L., Opie, L. H., Akira, S., Chien, K. R. & Sack, M. N. 2004. Genetic depletion of cardiac myocyte STAT-3 abolishes classical preconditioning. *Cardiovasc Res*, 63, 611-616.
- Sodha, N. R., Clements, R. T., Feng, J., Liu, Y., Bianchi, C., Horvath, E. M., Szabo, C., Stahl, G. L. & Sellke, F. W. 2009. Hydrogen sulfide therapy attenuates the

- inflammatory response in a porcine model of myocardial ischemia/reperfusion injury. *J Thorac Cardiovasc Surg*, 138, 977-984.
- Soetkamp, D., Nguyen, T. T., Menazza, S., Hirschhauser, C., Hendgen-Cotta, U. B., Rassaf, T., Schluter, K. D., Boengler, K., Murphy, E. & Schulz, R. 2014. S-nitrosation of mitochondrial connexin 43 regulates mitochondrial function. *Basic Res Cardiol*, 109, 433.
- Sojitra, B., Bulani, Y., Putcha, U. K., Kanwal, A., Gupta, P., Kuncha, M. & Banerjee, S. K. 2012. Nitric oxide synthase inhibition abrogates hydrogen sulfide-induced cardioprotection in mice. *Mol Cell Biochem*, 360, 61-69.
- Solhjoo, S. & O'rourke, B. 2015. Mitochondrial instability during regional ischemia-reperfusion underlies arrhythmias in monolayers of cardiomyocytes. *J Mol Cell Cardiol*, 78, 90-99.
- Sary, H. C., Chandler, A. B., Dinsmore, R. E., Fuster, V., Glagov, S., Insull, W., Jr., Rosenfeld, M. E., Schwartz, C. J., Wagner, W. D. & Wissler, R. W. 1995. A definition of advanced types of atherosclerotic lesions and a histological classification of atherosclerosis. A report from the Committee on Vascular Lesions of the Council on Arteriosclerosis, American Heart Association. *Arterioscler Thromb Vasc Biol*, 15, 1512-1531.
- Su, Y. W., Liang, C., Jin, H. F., Tang, X. Y., Han, W., Chai, L. J., Zhang, C. Y., Geng, B., Tang, C. S. & Du, J. B. 2009. Hydrogen sulfide regulates cardiac function and structure in adriamycin-induced cardiomyopathy. *Circ J*, 73, 741-749.
- Suleman, N., Somers, S., Smith, R., Opie, L. H. & Lecour, S. C. 2008. Dual activation of STAT-3 and Akt is required during the trigger phase of ischaemic preconditioning. *Cardiovasc Res*, 79, 127-133.
- Sumeray, M. S. & Yellon, D. M. 1998. Characterisation and validation of a new murine model of global ischaemia-reperfusion injury. *Mol Cell Biochem*, 186, 61-68.
- Sun, H.-Y., Wang, N.-P., Kerendi, F., Halkos, M., Kin, H., Guyton, R. A., Vinten-Johansen, J. & Zhao, Z.-Q. 2005. Hypoxic postconditioning reduces cardiomyocyte loss by inhibiting ROS generation and intracellular Ca²⁺ overload. *Am J Physiol - Heart Circ Physiol*, 288, H1900-H1908.
- Sun, J., Aponte, A. M., Menazza, S., Gucek, M., Steenbergen, C. & Murphy, E. 2016. Additive cardioprotection by pharmacological postconditioning with hydrogen sulfide and nitric oxide donors in mouse heart: S-sulfhydration vs. S-nitrosylation. *Cardiovasc Res*, 110, 96-106.
- Sun, N. L., Xi, Y., Yang, S. N., Ma, Z. & Tang, C. S. 2007. [Plasma hydrogen sulfide and homocysteine levels in hypertensive patients with different blood pressure levels and complications]. *Zhonghua Xin Xue Guan Bing Za Zhi*, 35, 1145-1148.

- Sun, W. H., Liu, F., Chen, Y. & Zhu, Y. C. 2012. Hydrogen sulfide decreases the levels of ROS by inhibiting mitochondrial complex IV and increasing SOD activities in cardiomyocytes under ischemia/reperfusion. *Biochem Biophys Res Commun*, 421, 164-169.
- Sun, Y.-G., Cao, Y.-X., Wang, W.-W., Ma, S.-F., Yao, T. & Zhu, Y.-C. 2008. Hydrogen sulphide is an inhibitor of L-type calcium channels and mechanical contraction in rat cardiomyocytes. *Cardiovasc Res*, 79, 632-641.
- Sun, Y., Huang, Y., Zhang, R., Chen, Q., Chen, J., Zong, Y., Liu, J., Feng, S., Liu, A. D., Holmberg, L., Liu, D., Tang, C., Du, J. & Jin, H. 2015. Hydrogen sulfide upregulates KATP channel expression in vascular smooth muscle cells of spontaneously hypertensive rats. *J Mol Med (Berl)*, 93, 439-455.
- Susin, S. A., Zamzami, N., Castedo, M., Hirsch, T., Marchetti, P., Macho, A., Daugas, E., Geuskens, M. & Kroemer, G. 1996. Bcl-2 inhibits the mitochondrial release of an apoptogenic protease. *J Exp Med*, 184, 1331-1341.
- Suveren, E., Whiteman, M. & Baxter, G. F. 2012a. The cardioprotective effect of GYY4137, a novel H₂S donor, in ischaemia reperfusion injury. *Cardiovasc Res*, 93, S111-S111.
- Szabo, C., Coletta, C., Chao, C., Modis, K., Szczesny, B., Papapetropoulos, A. & Hellmich, M. R. 2013. Tumor-derived hydrogen sulfide, produced by cystathionine-beta-synthase, stimulates bioenergetics, cell proliferation, and angiogenesis in colon cancer. *Proc Natl Acad Sci U S A*, 110, 12474-12479.
- Szabo, C., Ransy, C., Modis, K., Andriamihaja, M., Murghes, B., Coletta, C., Olah, G., Yanagi, K. & Bouillaud, F. 2014. Regulation of mitochondrial bioenergetic function by hydrogen sulfide. Part I. Biochemical and physiological mechanisms. *Br J Pharmacol*, 171, 2099-122.
- Szabó, I., Pinto, V. D. & Zoratti, M. 1993. The mitochondrial permeability transition pore may comprise VDAC molecules. *FEBS Letters*, 330, 206-210.
- Szczesny, B., Modis, K., Yanagi, K., Coletta, C., Le Trionnaire, S., Perry, A., Wood, M. E., Whiteman, M. & Szabo, C. 2014. AP39, a novel mitochondria-targeted hydrogen sulfide donor, stimulates cellular bioenergetics, exerts cytoprotective effects and protects against the loss of mitochondrial DNA integrity in oxidatively stressed endothelial cells *in vitro*. *Nitric Oxide*, 41, 120-130.
- Tan, B. H., Wong, P. T. & Bian, J. S. 2010. Hydrogen sulfide: a novel signaling molecule in the central nervous system. *Neurochem Int*, 56, 3-10.

- Tang, X. Q., Shen, X. T., Huang, Y. E., Ren, Y. K., Chen, R. Q., Hu, B., He, J. Q., Yin, W. L., Xu, J. H. & Jiang, Z. S. 2010. Hydrogen sulfide antagonizes homocysteine-induced neurotoxicity in PC12 cells. *Neurosci Res*, 68, 241-249.
- Taylor, C. D. & Wolfe, R. S. 1974. Structure and methylation of coenzyme M(HSCH₂CH₂SO₃). *J Biol Chem*, 249, 4879-4885.
- Tomasova, L., Pavlovicova, M., Malekova, L., Misak, A., Kristek, F., Grman, M., Cacanyiova, S., Tomasek, M., Tomaskova, Z., Perry, A., Wood, M. E., Lacinova, L., Ondrias, K. & Whiteman, M. 2015. Effects of AP39, a novel triphenylphosphonium derivatised anethole dithiolethione hydrogen sulfide donor, on rat haemodynamic parameters and chloride and calcium Cav3 and RyR2 channels. *Nitric Oxide*, 46, 131-44.
- Tsang, A., Hausenloy, D. J., Mocanu, M. M. & Yellon, D. M. 2004. Postconditioning: a form of "modified reperfusion" protects the myocardium by activating the phosphatidylinositol 3-kinase-Akt pathway. *Circ Res*, 95, 230-232.
- Valls-Lacalle, L., Barba, I., Miro-Casas, E., Alburquerque-Bejar, J. J., Ruiz-Meana, M., Fuertes-Agudo, M., Rodriguez-Sinovas, A. & Garcia-Dorado, D. 2016. Succinate dehydrogenase inhibition with malonate during reperfusion reduces infarct size by preventing mitochondrial permeability transition. *Cardiovasc Res*, 109, 374-384.
- Van Den Born, J. C., Mencke, R., Conroy, S., Zeebregts, C. J., Van Goor, H. & Hillebrands, J. L. 2016. Cystathionine γ -lyase is expressed in human atherosclerotic plaque microvessels and is involved in micro-angiogenesis. *Sci Rep*, 6, 34608.
- Vandiver, M. & Snyder, S. H. 2012. Hydrogen sulfide: a gasotransmitter of clinical relevance. *J Mol Med (Berl)*, 90, 255-263.
- Venditti, P., Masullo, P. & Di Meo, S. 2001. Effects of myocardial ischemia and reperfusion on mitochondrial function and susceptibility to oxidative stress. *Cell Mol Life Sci: CMLS*, 58, 1528-1537.
- Verschraagen, M., Boven, E., Torun, E., Erkelens, C. A., Hausheer, F. H. & Van Der Vijgh, W. J. 2004. Pharmacokinetic behaviour of the chemoprotectants BNP7787 and mesna after an i.v. bolus injection in rats. *Br J Cancer*, 90, 1654-1659.
- Vishnevskii, A. A., Zakharov, G. A., Iakovlev, V. M., Gorokhova, G. I. & Kostiuhenko, L. S. 1995. [Phosphoinositide response and change in free radical oxidation in catecholamine cardionecrosis in rats]. *Biull Eksp Biol Med*, 120, 137-139.
- Volkel, S. & Grieshaber, M. K. 1996. Mitochondrial sulfide oxidation in *Arenicola marina*. Evidence for alternative electron pathways. *Eur J Biochem*, 235, 231-237.

- Wajima, T., Shimizu, S., Hiroi, T., Ishii, M. & Kiuchi, Y. 2006. Reduction of myocardial infarct size by tetrahydrobiopterin: possible involvement of mitochondrial KATP channels activation through nitric oxide production. *J Cardiovasc Pharmacol*, 47, 243-249.
- Wallace, J. L., Ferraz, J. G. & Muscara, M. N. 2012. Hydrogen sulfide: an endogenous mediator of resolution of inflammation and injury. *Antioxid Redox Signal*, 17, 58-67.
- Wang, J., Yang, H., Hu, X., Fu, W., Xie, J., Zhou, X., Xu, W. & Jiang, H. 2013. Dobutamine-mediated heme oxygenase-1 induction via PI3K and p38 MAPK inhibits high mobility group box 1 protein release and attenuates rat myocardial ischemia/reperfusion injury *in vivo*. *J Surg Res*, 183, 509-516.
- Wang, X. L., Tian, B., Huang, Y., Peng, X. Y., Chen, L. H., Li, J. C. & Liu, T. 2015. Hydrogen sulfide-induced itch requires activation of Cav3.2 T-type calcium channel in mice. *Sci Rep*, 5, 16768.
- Wang, Y., Zhao, X., Jin, H., Wei, H., Li, W., Bu, D., Tang, X., Ren, Y., Tang, C. & Du, J. 2009. Role of hydrogen sulfide in the development of atherosclerotic lesions in apolipoprotein E knockout mice. *Arterioscler Thromb Vasc Biol*, 29, 173-179.
- Warenycia, M. W., Goodwin, L. R., Benishin, C. G., Reiffenstein, R. J., Francom, D. M., Taylor, J. D. & Dieken, F. P. 1989. Acute hydrogen sulfide poisoning. Demonstration of selective uptake of sulfide by the brainstem by measurement of brain sulfide levels. *Biochem Pharmacol*, 38, 973-981.
- Wei, W. B., Hu, X., Zhuang, X. D., Liao, L. Z. & Li, W. D. 2014. GYY4137, a novel hydrogen sulfide-releasing molecule, likely protects against high glucose-induced cytotoxicity by activation of the AMPK/mTOR signal pathway in H9c2 cells. *Mol Cell Biochem*, 389, 249-256.
- Wei, X., Zhang, B., Zhang, Y., Li, H., Cheng, L., Zhao, X., Yin, J. & Wang, G. 2015. Hydrogen sulfide inhalation improves neurological outcome via NF-kappaB-mediated inflammatory pathway in a rat model of cardiac arrest and resuscitation. *Cell Physiol Biochem*, 36, 1527-1538.
- Wen, Y. D., Wang, H., Kho, S. H., Rinkiko, S., Sheng, X., Shen, H. M. & Zhu, Y. Z. 2013. Hydrogen sulfide protects HUVECs against hydrogen peroxide induced mitochondrial dysfunction and oxidative stress. *PLoS One*, 8, e53147.
- White, S. K., Hausenloy, D. J. & Moon, J. C. 2012. Imaging the myocardial microcirculation post-myocardial infarction. *Curr Heart Fail Rep*, 9, 282-292.
- Whiteman, M., Armstrong, J. S., Chu, S. H., Jia-Ling, S., Wong, B. S., Cheung, N. S., Halliwell, B. & Moore, P. K. 2004. The novel neuromodulator hydrogen

- sulfide: an endogenous peroxynitrite 'scavenger'? *J Neurochem*, 90, 765-768.
- Whiteman, M., Gooding, K. M., Whatmore, J. L., Ball, C. I., Mawson, D., Skinner, K., Tooke, J. E. & Shore, A. C. 2010a. Adiposity is a major determinant of plasma levels of the novel vasodilator hydrogen sulphide. *Diabetologia*, 53, 1722-1726.
- Whiteman, M., Le Trionnaire, S., Chopra, M., Fox, B. & Whatmore, J. 2011. Emerging role of hydrogen sulfide in health and disease: critical appraisal of biomarkers and pharmacological tools. *Clin Sci (Lond)*, 121, 459-488.
- Whiteman, M., Li, L., Kostetski, I., Chu, S. H., Siau, J. L., Bhatia, M. & Moore, P. K. 2006. Evidence for the formation of a novel nitrosothiol from the gaseous mediators nitric oxide and hydrogen sulphide. *Biochem Biophys Res Commun*, 343, 303-310.
- Whiteman, M., Li, L., Rose, P., Tan, C. H., Parkinson, D. B. & Moore, P. K. 2010b. The effect of hydrogen sulfide donors on lipopolysaccharide-induced formation of inflammatory mediators in macrophages. *Antioxid Redox Signal*, 12, 1147-1154.
- Wille, M., Nagler, T. F., Lehmann, B., Schroder, S. & Kramers, J. D. 2008. Hydrogen sulphide release to surface waters at the Precambrian/Cambrian boundary. *Nature*, 453, 767-769.
- Wit, A. L. & Duffy, H. S. 2008. Drug development for treatment of cardiac arrhythmias: targeting the gap junctions. *Am J Physiol Heart Circ Physiol*, 294, H16-H18.
- Wolfe, C. L., Sievers, R. E., Visseren, F. L. & Donnelly, T. J. 1993. Loss of myocardial protection after preconditioning correlates with the time course of glycogen recovery within the preconditioned segment. *Circ*, 87, 881-892.
- Wright, K. E., Garrod, P. & Shaw, I. C. 1985. mechanism of enhanced cysteine excretion in urine during sodium-2-mercaptoethane sulphonate (Mesna) administration. *Hum Exp Toxicol*, 4, 546.
- Wu, Z., Peng, H., Du, Q., Lin, W. & Liu, Y. 2015. GYY4137, a hydrogen sulfidereleasing molecule, inhibits the inflammatory response by suppressing the activation of nuclear factor-kappa B and mitogenactivated protein kinases in Coxsackie virus B3infected rat cardiomyocytes. *Mol Med Rep*, 11, 1837-1844.
- Xia, Y. & Zweier, J. L. 1995. Substrate control of free radical generation from xanthine oxidase in the postischemic heart. *J Biol Chem*, 270, 18797-18803.
- Xiao, X. H. & Allen, D. G. 1999. Role of Na⁺/H⁺ exchanger during ischemia and preconditioning in the isolated rat heart. *Circ Res*, 85, 723-730.

- Xie, L., Gu, Y., Wen, M., Zhao, S., Wang, W., Ma, Y., Meng, G., Han, Y., Wang, Y., Liu, G., Moore, P. K., Wang, X., Wang, H., Zhang, Z., Yu, Y., Ferro, A., Huang, Z. & Ji, Y. 2016. Hydrogen sulfide induces Keap1 S-sulfhydration and suppresses diabetes-accelerated atherosclerosis via Nrf2 activation. *Diabetes*, 65, 3171-3184.
- Xie, Z. Z., Shi, M. M., Xie, L., Wu, Z. Y., Li, G., Hua, F. & Bian, J. S. 2014. Sulfhydration of p66Shc at cysteine59 mediates the antioxidant effect of hydrogen sulfide. *Antioxid Redox Signal*, 21, 2531-2142.
- Xu, Z. S., Wang, X. Y., Xiao, D. M., Hu, L. F., Lu, M., Wu, Z. Y. & Bian, J. S. 2011. Hydrogen sulfide protects MC3T3-E1 osteoblastic cells against H₂O₂-induced oxidative damage-implications for the treatment of osteoporosis. *Free Radic Biol Med*, 50, 1314-1323.
- Yan, H., Du, J. & Tang, C. 2004. The possible role of hydrogen sulfide on the pathogenesis of spontaneous hypertension in rats. *Biochem Biophys Res Commun*, 313, 22-27.
- Yang, G., Wu, L., Jiang, B., Yang, W., Qi, J., Cao, K., Meng, Q., Mustafa, A. K., Mu, W., Zhang, S., Snyder, S. H. & Wang, R. 2008. H₂S as a physiologic vasorelaxant: hypertension in mice with deletion of cystathionine gamma-lyase. *Science*, 322, 587-590.
- Yang, G., Zhao, K., Ju, Y., Mani, S., Cao, Q., Puukila, S., Khaper, N., Wu, L. & Wang, R. 2013. Hydrogen sulfide protects against cellular senescence via S-sulfhydration of Keap1 and activation of Nrf2. *Antioxid Redox Signal*, 18, 1906-1919.
- Yao, L. L., Huang, X. W., Wang, Y. G., Cao, Y. X., Zhang, C. C. & Zhu, Y. C. 2010. Hydrogen sulfide protects cardiomyocytes from hypoxia/reoxygenation-induced apoptosis by preventing GSK-3beta-dependent opening of mPTP. *Am J Physiol Heart Circ Physiol*, 298, H1310-H1319.
- Yao, X., Tan, G., He, C., Gao, Y., Pan, S., Jiang, H., Zhang, Y. & Sun, X. 2012. Hydrogen sulfide protects cardiomyocytes from myocardial ischemia-reperfusion injury by enhancing phosphorylation of apoptosis repressor with caspase recruitment domain. *Tohoku J Exp Med*, 226, 275-285.
- Yellon, D. M., Alkhulaifi, A. M. & Pugsley, W. B. 1993. Preconditioning the human myocardium. *Lancet*, 342, 276-277.
- Yilmaz, E. R., Kertmen, H., Gurer, B., Kanat, M. A., Arikok, A. T., Erguder, B. I., Hasturk, A. E., Ergil, J. & Sekerci, Z. 2013. The protective effect of 2-mercaptoethane sulfonate (MESNA) against traumatic brain injury in rats. *Acta Neurochir (Wien)*, 155, 141-149.

- Yong, Q. C., Cheong, J. L., Hua, F., Deng, L. W., Khoo, Y. M., Lee, H. S., Perry, A., Wood, M., Whiteman, M. & Bian, J. S. 2011. Regulation of heart function by endogenous gaseous mediators-crosstalk between nitric oxide and hydrogen sulfide. *Antioxid Redox Signal*, 14, 2081-2091.
- Yong, Q. C., Lee, S. W., Foo, C. S., Neo, K. L., Chen, X. & Bian, J. S. 2008. Endogenous hydrogen sulphide mediates the cardioprotection induced by ischemic postconditioning. *Am J Physiol Heart Circ Physiol*, 295, H1330-H1340.
- Yong, R. & Searcy, D. G. 2001. Sulfide oxidation coupled to ATP synthesis in chicken liver mitochondria. *Comp Biochem Physiol B Biochem Mol Biol*, 129, 129-137.
- Ypsilantis, P., Lambropoulou, M., Tentes, I., Anagnostopoulos, K., Tsigalou, C., Papadopoulos, N., Kortsaris, A. & Simopoulos, C. 2009a. Impaired liver regeneration following partial hepatectomy using the Pringle maneuver: Protective effect of mesna. *J Gastroenterol Hepatol*, 24, 623-632.
- Ypsilantis, P., Lambropoulou, M., Tentes, I., Kortsaris, A., Papadopoulos, N. & Simopoulos, C. 2006. Mesna protects intestinal mucosa from ischemia/reperfusion injury. *J Surg Res*, 134, 278-284.
- Ypsilantis, P., Tentes, I., Anagnostopoulos, K., Kortsaris, A. & Simopoulos, C. 2009b. Mesna protects splanchnic organs from oxidative stress induced by pneumoperitoneum. *Surg Endosc*, 23, 583-589.
- Ypsilantis, P., Tentes, I., Lambropoulou, M., Anagnostopoulos, K., Papadopoulos, N., Kortsaris, A. & Simopoulos, C. 2008. Prophylaxis with mesna prevents oxidative stress induced by ischemia reperfusion in the intestine via inhibition of nuclear factor-kappaB activation. *J Gastroenterol Hepatol*, 23, 328-335.
- Ytrehus, K. 2000. The ischemic heart--experimental models. *Pharmacol Res*, 42, 193-203.
- Ytrehus, K. 2006. Models of myocardial ischemia. *Drug Discov Today: Dis Models*, 3, 263-271.
- Yuan, S. & Kevil, C. G. 2016. Nitric oxide and hydrogen sulfide regulation of ischemic vascular remodeling. *Microcirc*, 23, 134-145.
- Zhang, H., Guo, C., Wu, D., Zhang, A., Gu, T., Wang, L. & Wang, C. 2012. Hydrogen sulfide inhibits the development of atherosclerosis with suppressing CX3CR1 and CX3CL1 expression. *PLoS One*, 7, e41147.
- Zhang, W. J., Shi, Z. X., Wang, B. B., Cui, Y. J., Guo, J. Z. & Li, B. 2001. Allitridum mimics effect of ischemic preconditioning by activation of protein kinase C. *Acta Pharmacol Sin*, 22, 132-136.

- Zhao, W. & Wang, R. 2002. H₂S-induced vasorelaxation and underlying cellular and molecular mechanisms. *Am J Physiol Heart Circ Physiol*, 283, H474-H480.
- Zhao, W., Zhang, J., Lu, Y. & Wang, R. 2001. The vasorelaxant effect of H₂S as a novel endogenous gaseous K_{ATP} channel opener. *EMBO J*, 20, 6008-6016.
- Zhao, Z. Q., Corvera, J. S., Halkos, M. E., Kerendi, F., Wang, N. P., Guyton, R. A. & Vinten-Johansen, J. 2003. Inhibition of myocardial injury by ischemic postconditioning during reperfusion: comparison with ischemic preconditioning. *Am J Physiol Heart Circ Physiol*, 285, H579-H588.
- Zhong, G., Chen, F., Cheng, Y., Tang, C. & Du, J. 2003. The role of hydrogen sulfide generation in the pathogenesis of hypertension in rats induced by inhibition of nitric oxide synthase. *J Hypertens*, 21, 1879-1885.
- Zhou, L. Z., Johnson, A. P. & Rando, T. A. 2001. NF kappa B and AP-1 mediate transcriptional responses to oxidative stress in skeletal muscle cells. *Free Radic Biol Med*, 31, 1405-1416.
- Zhu, X., Tang, Z., Cong, B., Du, J., Wang, C., Wang, L., Ni, X. & Lu, J. 2013. Estrogens increase cystathionine-gamma-lyase expression and decrease inflammation and oxidative stress in the myocardium of ovariectomized rats. *Menopause*, 20, 1084-1091.
- Zhu, X. Y., Liu, S. J., Liu, Y. J., Wang, S. & Ni, X. 2010. Glucocorticoids suppress cystathionine gamma-lyase expression and H₂S production in lipopolysaccharide-treated macrophages. *Cell Mol Life Sci*, 67, 1119-1132.
- Zhu, Y. Z., Wang, Z. J., Ho, P., Loke, Y. Y., Zhu, Y. C., Huang, S. H., Tan, C. S., Whiteman, M., Lu, J. & Moore, P. K. 2007. Hydrogen sulfide and its possible roles in myocardial ischemia in experimental rats. *J Appl Physiol (1985)*, 102, 261-268.
- Zhuo, Y., Chen, P. F., Zhang, A. Z., Zhong, H., Chen, C. Q. & Zhu, Y. Z. 2009. Cardioprotective effect of hydrogen sulfide in ischemic reperfusion experimental rats and its influence on expression of survivin gene. *Biol Pharm Bull*, 32, 1406-1410.
- Zorov, D. B., Filburn, C. R., Klotz, L. O., Zweier, J. L. & Sollott, S. J. 2000. Reactive oxygen species (ROS)-induced ROS release: a new phenomenon accompanying induction of the mitochondrial permeability transition in cardiac myocytes. *J Exp Med*, 192, 1001-1014.

Publications

RESEARCH PAPER

AP39, a mitochondria-targeting hydrogen sulfide (H₂S) donor, protects against myocardial reperfusion injury independently of salvage kinase signalling

Correspondence Professor Gary F. Baxter, School of Pharmacy and Pharmaceutical Sciences, Redwood Building, King Edward VII Avenue, Cardiff CF10 3NB, UK. E-mail: baxtergf@cardiff.ac.uk

Received 29 July 2016; **Revised** 30 November 2016; **Accepted** 5 December 2016

Qutuba G Karwi^{1,2} , Julia Bornbaum³, Kerstin Boengler³, Roberta Torregrossa^{4,5}, Matthew Whiteman⁴, Mark E Wood⁵, Rainer Schulz³ and Gary F Baxter¹

¹School of Pharmacy and Pharmaceutical Sciences, Cardiff University, Cardiff, UK, ²College of Medicine, University of Diyala, Diyala, Iraq, ³Institute of Physiology, Justus-Liebig-University, Giessen, Germany, ⁴Medical School, University of Exeter, Exeter, UK, and ⁵School of Biosciences, University of Exeter, Exeter, UK

BACKGROUND AND PURPOSE

H₂S protects myocardium against ischaemia/reperfusion injury. This protection may involve the cytosolic reperfusion injury salvage kinase (RISK) pathway, but direct effects on mitochondrial function are possible. Here, we investigated the potential cardioprotective effect of a mitochondria-specific H₂S donor, AP39, at reperfusion against ischaemia/reperfusion injury.

EXPERIMENTAL APPROACH

Anaesthetized rats underwent myocardial ischaemia (30 min)/reperfusion (120 min) with randomization to receive interventions before reperfusion: vehicle, AP39 (0.01, 0.1, 1 μmol·kg⁻¹), or control compounds AP219 and ADT-OH (1 μmol·kg⁻¹). LY294002, L-NAME or ODQ were used to investigate the involvement of the RISK pathway. Myocardial samples harvested 5 min after reperfusion were analysed for RISK protein phosphorylation and isolated cardiac mitochondria were used to examine the direct mitochondrial effects of AP39.

KEY RESULTS

AP39, dose-dependently, reduced infarct size. Inhibition of either PI3K/Akt, eNOS or sGC did not affect this effect of AP39. Western blot analysis confirmed that AP39 did not induce phosphorylation of Akt, eNOS, GSK-3β or ERK1/2. In isolated subsarcolemmal and interfibrillar mitochondria, AP39 significantly attenuated mitochondrial ROS generation without affecting respiratory complexes I or II. Furthermore, AP39 inhibited mitochondrial permeability transition pore (PTP) opening and co-incubation of mitochondria with AP39 and cyclosporine A induced an additive inhibitory effect on the PTP.

CONCLUSION AND IMPLICATIONS

AP39 protects against reperfusion injury independently of the cytosolic RISK pathway. This cardioprotective effect could be mediated by inhibiting PTP via a cyclophilin D-independent mechanism. Thus, selective delivery of H₂S to mitochondria may be therapeutically applicable for employing the cardioprotective utility of H₂S.

Abbreviations

AAR, area at risk; ADT-OH, 5-(4-hydroxyphenyl)-3H-1, 2-dithiole-3-thione; AP219, mitochondria-targeting moiety; AP39, 10-oxo-10-(4-(3-thioxo-3H-1,2-dithiol-5yl)phenoxy)decyl triphenylphosphonium bromide, mitochondria-targeting H₂S donor; CsA, cyclosporine A; eNOS, endothelial NOS; GSK-3β, glycogen synthase kinase-3 β; IFM, interfibrillar mitochondria; Mito-ROS, mitochondrial ROS; PTP, permeability transition pore; RISK, reperfusion injury salvage kinase (signalling pathway); RNS, reactive nitrogen species; SSM, subsarcolemmal mitochondria; TPP⁺, triphenylphosphonium

Tables of Links

TARGETS	
PI3K	GSK-3 β
Akt (PKB)	ERK1
eNOS	ERK2
sGC	

LIGANDS
LY294002
L-NAME
ODQ
Cyclosporine A

These Tables list key protein targets and ligands in this article which are hyperlinked to corresponding entries in <http://www.guidetopharmacology.org>, the common portal for data from the IUPHAR/BPS Guide to PHARMACOLOGY (Southan *et al.*, 2016), and are permanently archived in the Concise Guide to PHARMACOLOGY 2015/16 (Alexander *et al.*, 2015).

Introduction

In myocardial ischaemia/reperfusion injury, rapid pH normalization, Ca²⁺ overload and overwhelming generation of ROS and reactive nitrogen species (RNS) at reperfusion disturb mitochondrial function and result in the opening of the mitochondrial permeability transition pore (PTP) (Hausenloy and Yellon, 2007). PTP opening leads to collapse of mitochondrial membrane potential, swelling of the mitochondria and the leakage of cytochrome c into the cytoplasm. As a result, ATP production will be impaired, initiating cell apoptosis/necrosis (Murphy *et al.*, 2016; Pell *et al.*, 2016). PTP opening at reperfusion is believed to be the no-return point of reperfusion injury (Hausenloy *et al.*, 2009). Therapeutic targeting of these processes during the first minutes of reperfusion has been investigated intensively in experimental settings as early reperfusion appears to offer a window of opportunity to prevent PTP opening and ultimately reduce lethal cell injury (Ferdinandy *et al.*, 2014).

The roles of endogenous H₂S, in a wide range of physiological systems, has been extensively explored following the discovery that it is produced by several regulated biochemical pathways in mammalian species (Kimura, 2011). In the myocardium, enhanced levels of H₂S, whether by H₂S supplement or increased endogenous production, have been shown to protect the heart against ischaemia/reperfusion injury (Johansen *et al.*, 2006; Elrod *et al.*, 2007; Karwi *et al.*, 2016). The exact cardioprotective mechanism of H₂S has yet to be clarified, but a number of molecular targets have been identified. These include activation of the reperfusion injury salvage kinase (RISK) pathway (Hausenloy, 2013), enhanced cellular and mitochondrial antioxidant defences, and preservation of mitochondrial integrity (Bos *et al.*, 2015). However, these effects have been found to vary in many experimental studies for several reasons including variations in animal species and models, different experimental conditions and inconsistencies in dosing with inorganic sulfide salts (Bos *et al.*, 2015). Inorganic sulfide salts (notably NaHS and Na₂S) have been extensively employed to explore the biological activity of H₂S. Nevertheless, these salts are impure and generate H₂S instantaneously at high (i.e. supraphysiological) concentrations, and there is increasing concern that they are unreliable sources of H₂S (Whiteman *et al.*, 2011).

We have examined cardioprotection by a novel mitochondria-targeting H₂S donor, 10-oxo-10-(4-(3-thioxo-3H-1,2-dithiol-5yl)phenoxy)decyl triphenylphosphonium bromide (AP39) (Le Trionnaire *et al.*, 2014) when given as adjunct to reperfusion and its direct effect on cardiomyocyte mitochondria, namely, subsarcolemmal (SSM) and interfibrillar mitochondria (IFM). The rationale for targeted delivery of H₂S to the mitochondria is based on the evidence that H₂S can attenuate mitochondrial ROS (mito-ROS) generation and preserves mitochondrial integrity. There are recent observations that AP39 can successfully deliver H₂S into the mitochondria when given at reperfusion and that it reproducibly protects the mitochondria in particular and the cell in general against ischaemia/reperfusion insults in the brain and kidney (Ikeda *et al.*, 2015; Ahmad *et al.*, 2016). We hypothesized that AP39 protects the heart against ischaemia/reperfusion injury when administered at reperfusion through a cytosolic-independent mechanism. We also hypothesized that AP39 attenuates mito-ROS generation and thereby inhibits PTP opening in the SSM and IFM.

Methods

Animals and ethical statement

All animal care and procedures for *in vivo* studies complied with UK Home Office Guidelines on the Animals (Scientific Procedures) Act 1986, (published by the Stationery Office, London, UK), project licence (PPL30/3032) and was approved by the Animal Welfare and Ethical Review Body at Cardiff University. Studies involving mitochondria isolation was approved by the Animal Welfare Office of the Justus-Liebig University Giessen. Male Sprague Dawley rats, 300–350 g (9–11 weeks), were obtained for *in vivo* studies from Harlan, UK. For mitochondria isolation, male Wistar rats, 300–350 g (9–11 weeks), were purchased from Harlan, France. They were housed in polypropylene cages (2–4 rats in each) on wood shavings. Animals acclimatized in the institutional animal house at constant temperature and humidity on a 12 h light/dark cycle for at least 7 days prior to experimentation, with free access to water and a small animal diet at all times. Animal studies are reported in compliance with the ARRIVE guidelines (Kilkenny *et al.*, 2010; McGrath and Lilly, 2015).

Acute myocardial infarction model

Myocardial infarction was induced as previously reported (Karwi *et al.*, 2016). Briefly, rats were anaesthetized using thiobutabarbital (Inactin® 200 mg·kg⁻¹, i.p), and anaesthesia was maintained throughout the procedure by supplemental dosing (75 mg kg⁻¹, i.v.) as required. The left jugular vein was cannulated for drug administration while the right common carotid artery was cannulated and connected to a pressure transducer (Powerlab data acquisition system, AD instruments, Abingdon, UK) to monitor the heart rate and the blood pressure throughout the experiment. The trachea was intubated and the animal ventilated with room air using a small animal ventilator (Hugo Sachs Elektronik, March, Germany) at a rate of 75 strokes min⁻¹ and tidal volume of 1.0 to 1.25 mL·100 g⁻¹. The chest was opened by midline sternotomy and the heart exposed using a retractor. The pericardium was incised and a 4/0 braided silk suture (Mersilk, Ethicon Ltd, UK) was placed around the left main coronary artery close to its origin to induce regional ischaemia. ECG was monitored using standard lead II electrodes inserted s.c. into the limbs and connected to a Powerlab data acquisition system. Rectal temperature was maintained at 37 ± 1°C using a thermal blanket (Harvard Apparatus Ltd, Cambridge, UK). The following inclusion criteria were employed during the stabilization period of 20 min: no ECG or visual signs of ischaemia, steady sinus rhythm without arrhythmia, heart rate ≥250 beats min⁻¹, and diastolic blood pressure ≥50 mmHg.

To induce regional ischaemia in the left ventricle, the left coronary artery was transiently occluded for 30 min by pulling the ligature taut through a plastic snare fixed against the epicardium. Ischaemia was confirmed by colour change of the left ventricle, a drop in the mean arterial pressure (MAP), ST-segment elevation and arrhythmia developing between 5 and 13 min of ischaemia. The ligature was then released to start reperfusion for 120 min. Successful reperfusion was confirmed by blushing of the previously ischaemic area, reperfusion-induced arrhythmia and increase in the MAP.

Infarct size determination

At the end of 120 min reperfusion, the heart was harvested and retrogradely perfused with saline through the aorta on a modified Langendorff apparatus. The ligature was re-occluded and the heart perfused with 2% Evans' blue dye to delineate the ischaemic area at risk (AAR), then quickly frozen at -20°C for 24 h. The heart was transversely sectioned into 5–6 sections of 2 mm thickness and incubated with 1% wv⁻¹TTC for 15 min. Sections were then fixed with 4% formalin in PBS for 24 h before being scanned. Sections were scanned using a digital scanner and coded using a random number generator (<https://www.random.org>), then planimetry was carried out in a blind fashion using the image analysis programme Image J (version 1.47, NIH, Bethesda, USA). The analysis determined the total ventricular area (Evans' blue positive), AAR (TTC positive) and the infarcted area (I, TTC negative), which were converted to volumes by multiplying these areas by 2 mm section thickness. Infarct size was expressed as a percentage of the AAR (% I/AAR).

Treatment protocols

The experimental protocols are summarized in Figure 1. Two series of experiments were carried out. The first series characterized the dose-dependent infarct-limiting effect of AP39 along with the control compounds (AP219 and ADT-OH) to confirm the selective effect of H₂S delivery into the mitochondria. The doses of AP39, AP219 and ADT-OH used in these experiments were derived from *in vitro* and *in vivo* studies undertaken by others (Szczeny *et al.*, 2014; Ikeda *et al.*, 2015; Ahmad *et al.*, 2016).

Animals were randomised to receive one of six interventions (Figure 1A):

- Group 1: Control ($n = 10$). Animals received a bolus dose of (0.05% DMSO, i.v.) 10 min before reperfusion. DMSO was used as a vehicle for AP39, AP219 and ADT-OH.
- Groups 2–4: Each group ($n = 8$) received AP39 at (0.01, 0.1 or 1 μmol·kg⁻¹ respectively) as an i.v. bolus 10 min before reperfusion.
- Group 5: AP219 ($n = 8$). Animals received AP219 (1 μmol·kg⁻¹) as an i.v. bolus 10 min before reperfusion.
- Group 6: ADT-OH ($n = 8$). Animals received ADT-OH (1 μmol·kg⁻¹) as an i.v. bolus 10 min before reperfusion.

The optimum dose of AP39 (1 μmol·kg⁻¹), selected from the first series of experiments, was used in a second series of experiments that investigated the involvement of the RISK pathway components using inhibitors of Akt phosphorylation (LY294002), eNOS (L-NAME) or sGC (ODQ). Animals were randomly assigned to one of the following eight treatment groups (Figure 1B).

- Group 1: Control ($n = 11$). Animals received DMSO 0.05% given as an i.v. bolus 15 min before reperfusion. DMSO was used as vehicle for AP39, LY294002 and ODQ.
- Group 2: AP39 ($n = 8$). Animals received AP39 (1 μmol·kg⁻¹) as an i.v. bolus 10 min before reperfusion.
- Group 3: AP39 + L-NAME ($n = 8$). L-NAME (20 mg·kg⁻¹) was administered 15 min before reperfusion as an i.v. bolus followed by AP39 (1 μmol·kg⁻¹) 10 min before reperfusion.
- Group 4: L-NAME ($n = 8$). L-NAME (20 mg·kg⁻¹) was administered 15 min before reperfusion as an i.v. bolus.
- Group 5: AP39 + LY294002 ($n = 8$). LY294002 (0.3 mg·kg⁻¹) was given 15 min before reperfusion as an i.v. bolus followed by AP39 (1 μmol·kg⁻¹) 10 min before reperfusion.
- Group 6: LY294002 ($n = 8$). LY294002 (0.3 mg·kg⁻¹) was administered 15 min before reperfusion as an i.v. bolus.
- Group 7: AP39 + ODQ ($n = 8$). ODQ (1 mg·kg⁻¹) was given 15 min before reperfusion as an i.v. bolus followed by AP39 (1 μmol·kg⁻¹) 10 min before reperfusion.
- Group 8: ODQ ($n = 8$). ODQ (1 mg·kg⁻¹) was administered 15 min before reperfusion as an i.v. bolus.

In a parallel series prepared for biochemical analysis of RISK pathway components, animals were randomised to receive either vehicle (0.05% DMSO) or AP39 (1 μmol·kg⁻¹) 10 min before reperfusion (Figure 1C). The heart was excised after 5 min of reperfusion and washed with saline to remove any blood residue. Tissue samples were rapidly harvested from the left ventricle, snap frozen with liquid nitrogen then kept at -80°C. These samples were used to

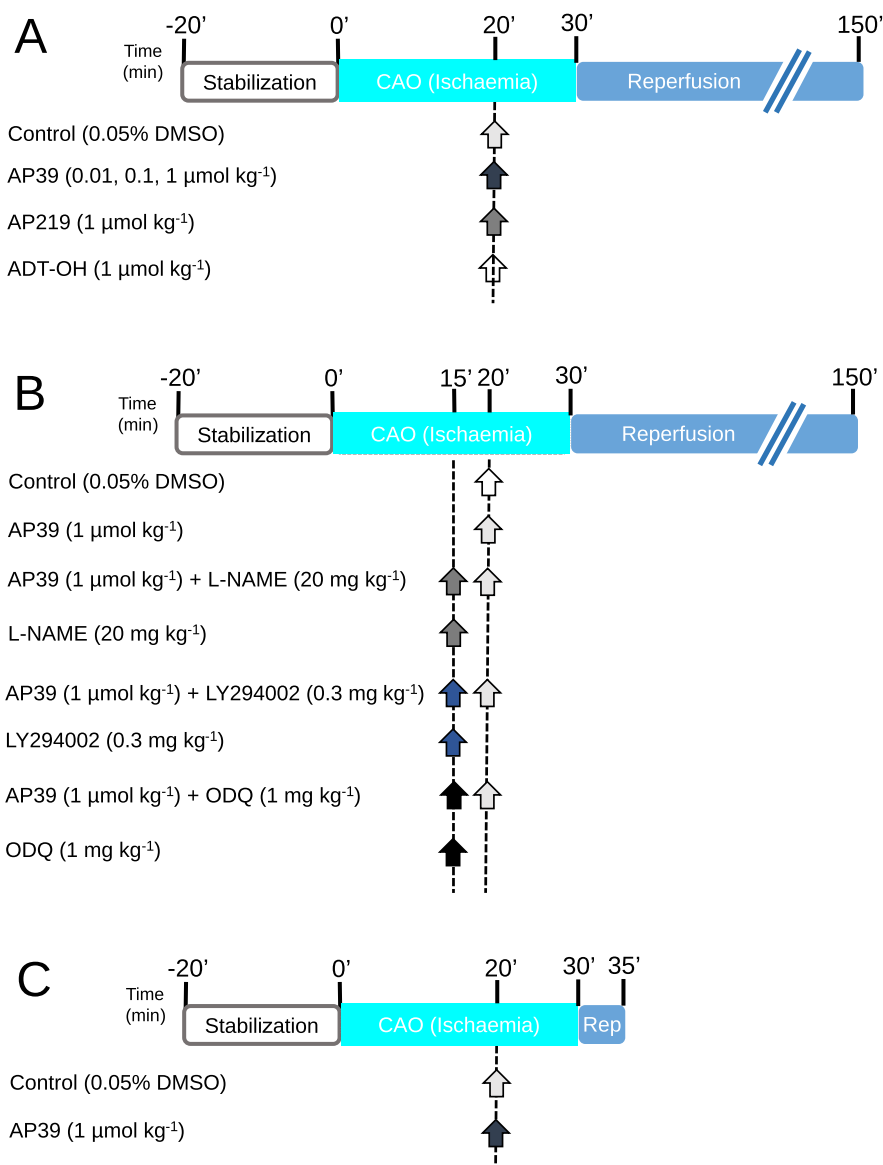


Figure 1

Experimental protocols: Animals underwent 30 min of ischaemia followed by 2 h of reperfusion. Infarct size was determined using Evans' blue/TTC staining technique. Infarction was reported as a percentage of the AAR (I/AAR %). (A) AP39 dose effect on infarct size: Animals were randomly assigned to be treated with either vehicle or AP39 or the controls (AP219 or ADT-OH) at 10 min before reperfusion. (B) Mechanistic study: Rats were randomised to receive the pharmacological inhibitors, namely LY294002, L-NAME and ODQ, at 15 min before reperfusion with or without AP39 applied at 10 min before reperfusion. Control group only received the vehicle (0.05% DMSO) 10 min before reperfusion. (C) Myocardium sampling protocol: Rats were randomised to receive either vehicle (0.05% DMSO) or AP39 10 minutes before reperfusion. Myocardial biopsies were harvested at 5 minutes of reperfusion from the left ventricle. Arrows indicate the time of the pharmacological interventions.

investigate the effect of AP39 on the phosphorylation of Akt, eNOS, GSK-3 β and ERK1/2 at the commencement of reperfusion using western blotting.

Isolation of cardiac mitochondria

Isolation of two mitochondrial subpopulations, subsarcolemmal mitochondria (SSM) and interfibrillar mitochondria (IFM), was carried out using a modified protocol of that described by Boengler *et al.* (2009). All the procedures were undertaken at 4°C to maintain mitochondrial integrity. Each rat was anaesthetized with 4% v.v⁻¹ isoflurane, and

the heart was quickly excised and washed with buffer A (100 mM KCl, 50 mM 3-[N-morpholino]-propanesulfonic acid (MOPS), 5 mM MgSO₄, 1 mM ATP and 1 mM EGTA, pH 7.4). The ventricles were isolated and weighed. Ventricles were transferred to buffer B (buffer A + 0.04% BSA), finely chopped with scissors then gently minced with six strokes of a teflon pestle in a glass tube. Homogenate was centrifuged at 800 *g* for 10 min. The supernatant from the first centrifugation was collected and centrifuged for 10 min at 8000 *g* to isolate the SSM. The sediment of the first centrifugation was resuspended for 1 min in buffer B

with protease nargase ($8 \text{ U}\cdot\text{g}^{-1}$) then gently minced with five strokes of the teflon pestle and glass mortar. The homogenate was centrifuged at 800 g for 10 min, then the supernatant was collected and centrifuged for 10 min at 8000 g to sediment the IFM. The SSM and IFM were washed with buffer A and final pellets were resuspended in buffer A with no ATP. Protein concentration was determined using Lowry assay (BioRad, Hercules, Canada).

Calcium retention capacity

Mitochondrial tolerance to calcium overload, a trigger to PTP opening, was investigated in the presence and absence of AP39 using a modified protocol of Chen *et al.* (2012). Freshly isolated SSM and IFM ($0.1 \text{ mg}\cdot\text{mL}^{-1}$) were randomised to be incubated for 4 min in 2 mL (in mM: KCl 125, Tris-MOPS 10, KH_2PO_4 1.2, MgCl_2 1.2, glutamate 5, malate 2.5). The suspension was supplemented with $8 \mu\text{L}$ ADP (10 mM), $10 \mu\text{L}$ EGTA (1 mM), $6 \mu\text{L}$ CaCl_2 (5 mM) and calcium green-5 N ($1 \mu\text{M}$, Invitrogen, Carlsbad, Canada). Mitochondria were treated with vehicle (0.003% ethanol) or AP39 ($1 \mu\text{M}$) during the incubation period. Cyclosporine A (CsA) ($1 \mu\text{M}$) was used as a positive control as it is a well-known inhibitor of the PTP opening and increases mitochondrial tolerance to Ca^{2+} overload by a cyclophilin D-dependent mechanism. Pulses of Ca^{2+} ($5 \mu\text{M}$) were added at 3 min intervals to the solution with stirring at 25°C and mitochondrial calcium tolerance was expressed as μM of $\text{Ca}^{2+} \text{ mg}^{-1}$ of protein. Fluorescence was measured with excitation and emission wavelengths 530/530 nm, respectively. Data were coded using a random number generator (<https://www.random.org>) and blindly analysed.

Mitochondrial oxygen consumption

The respiration of SSM and IFM was measured using a Clark-type oxygen electrode (Strathkelvin, Glasgow, UK) at 25°C . The concentrations range of AP39 used for the mitochondrial studies were equivalent to the *in vivo* doses and after assessing the direct effect of AP39 on the mitochondria autofluorescence and membrane potential (data not shown). Basal mitochondrial oxygen consumption was measured in the presence and absence of either the vehicle (0.003% ethanol) or AP39 (0.3, 1, 3, 5 μM). Mitochondria ($0.1 \text{ mg}\cdot\text{mL}^{-1}$) were randomised to receive one of the treatments and were incubated in two chambers simultaneously, one with complex I substrate (5 mM glutamate and 2.5 mM malate) and the other with complex II substrate (5 mM succinate plus $2 \mu\text{M}$ of rotenone, to inhibit complex I activity). Respiration was stimulated by addition of $40 \mu\text{M}$ of ADP, and oxygen consumption was reported as $\text{nmol of O}_2\cdot\text{min}^{-1}\cdot\text{mg}^{-1}$ of protein. Oxygraph charts were randomly coded (<https://www.random.org>) and blindly analysed.

Mito-ROS generation

Measurement of mito-ROS generation was carried out as previously described by Soetkamp *et al.* (2014). Freshly isolated SSM or IFM ($50 \mu\text{g}$) were suspended in incubation buffer (in mM: Tris-MOPS 10, EGTA 0.02, KCl 125, glutamate 5, malate 2.5, Pi-Tris 1.2, MgCl_2 1.2, pH 7.4). Then $0.1 \text{ U}\cdot\text{mL}^{-1}$ HRP (Roche Diagnostic, Grenzach, Germany) and $50 \mu\text{mol}$ Amplex UltraRed (Invitrogen, Eugene, OR) were added to the suspension directly before the measurements were

performed. Cardiomyocyte mitochondria were randomly incubated with: (i) no intervention; (ii) vehicle (0.003% ethanol); and (iii) AP39 (0.3, 1, 3 and 5 μM). A second control group with no intervention was employed at the end of the all measurements to ensure that any observed effects are due to AP39 and not because of the decline in the respiratory capacity. SSM and IFM were also incubated with rotenone ($2 \mu\text{M}$) to induce overproduction of mito-ROS generation and used as a positive control. Mito-ROS generation was measured for 4 min at room temperature using Cary Eclipse spectrophotometer (Agilent technologies, Santa Clara, Canada) at excitation/emission wavelengths 565/581 nm. Using a code generator (<https://www.random.org>), data were coded and the slope of mito-ROS generation was calculated, as a mean fluorescence per time (a.u.), by an operator blind to the treatments after subtracting the background fluorescence of the incubation buffer.

Western blot analysis

Myocardial samples were homogenized and lysed using a hard tissue lysing kit (Stretton Scientific Ltd, Stretton, UK). Then $30 \mu\text{g}$ of protein was loaded into each well of a 10% w. v⁻¹ SDS-PAGE and separated electrophoretically at 120 mV . Separated proteins were transferred onto nitrocellulose membrane (Amersham, Germany), and the membrane was blocked for non-specific binding with 5% skimmed milk for 2 h. The membrane was then probed with the primary antibody overnight at 4°C . The membrane was then incubated with secondary antibody (goat anti-rabbit HRP, 1:15 000, Cell Signalling, UK) for 1 h at room temperature. Super Signal West Dura Extended Duration Substrate (Thermo Scientific, UK) was added on the surface of the membrane to laminate the bands and the bands were visualized on X-ray film. Films were scanned and coded, and densitometry was carried out in blind fashion using Image J software (1.48v, National Institutes of Health USA). All protein bands were expressed as the relative density of myocardium sample, harvested after 20 min of stabilization (baseline), and then normalised for corresponding GAPDH bands, which served as an internal standard.

Antibodies

The following antibodies were used for Western blotting: Akt (1:1000), phospho- ser⁴⁷³Akt (1:1000), endothelial NOS (eNOS 1:500), phospho- ser¹¹⁷⁷eNOS (1:500), GSK-3 β (1:1000), phospho- ser⁹GSK-3 β (1:1000), ERK 1/2 (1:1000), phospho- Thr²⁰²/Tyr²⁰⁴ ERK 1/2 (1:1000) and GAPDH (1:50 000).

Statistical analysis

The data and statistical analysis comply with the recommendations on experimental design and analysis in pharmacology (Curtis *et al.*, 2015). All data passed the Kolmogorov–Smirnov normality test of distribution. Statistical analysis was performed using GraphPad Prism® software (2007, Version 5.01, USA), and data are presented as mean \pm SEM. Infarct size data were analysed using one-way ANOVA with Newman–Keuls *post hoc* test, and Western blot analysis was performed using Student's unpaired *t*-test. Haemodynamic and mitochondrial data were statistically analysed using repeated measures ANOVA supported by

Bonferroni's *post hoc* test. $P < 0.05$ was considered statistically significant. Post tests were only carried out if $P < 0.05$ was achieved in the ANOVA.

Materials

AP39 and the control compounds, the mitochondria-targeting moiety, AP219, and the H₂S-releasing moiety, ADT-OH (5-(4-hydroxyphenyl)-3H-1, 2-dithiole-3-thione), were synthesized by us as previously reported (Le Trionnaire *et al.*, 2014; Szczesny *et al.*, 2014; Tomasova *et al.*, 2014). The purity of the compounds was determined by NMR spectroscopy (¹H, ³¹P and ¹³C). The irreversible haem-site soluble GC (sGC) inhibitor 1H-[1,2,4]oxadiazolo[4,3-a]quinoxalin-1-one (ODQ), the constitutive NOS inhibitor L-nitroarginine methyl ester (L-NAME), the PI3K inhibitor LY294002, thiobutabarbital sodium salt hydrate (Inactin® hydrate), Evans blue dye, triphenyltetrazolium chloride (TTC) and DMSO were all purchased from Sigma-Aldrich, Gillingham, UK. Western blotting antibodies were all sourced from Cell Signalling, UK.

Results

For the AP39 dose–response study, 52 rats were used, of which two were excluded: one did not have successful reperfusion, and one rat did not survive ischaemia-induced ventricular fibrillation. Therefore, data from 50 successfully completed experiments are presented. In the second series, 83 rats were used, of which, four were excluded: two did not complete the ischaemia–reperfusion protocol, one did not have successful TTC staining and one did not survive reperfusion-induced arrhythmia. Thus, data from 79 rats, 67 infarct size experiments that were successfully completed and 12 tissue sampling experiments were reported. For mitochondria functional studies, data from 20 rats are reported.

Pharmacological postconditioning with AP39

Baseline parameters for infarct size studies are shown in (Table 1). There was no difference among the 14 experimental groups in any of the baseline parameters. Risk zone was similar among the experimental groups (50–60% of the total ventricular volume, Figure 2A). Administration of AP39 10 min before reperfusion resulted in a dose-dependent infarct-sparing effect compared with vehicle-treated animals (Figure 2B). The maximum cardioprotection was seen at 1- $\mu\text{mol}\cdot\text{kg}^{-1}$ dose with almost 40% reduction in infarct size compared with vehicle-treated animals. Postconditioning with AP39 (1 $\mu\text{mol}\cdot\text{kg}^{-1}$) also dose-dependently increased in the post-ischaemic functional recovery [% rate pressure product (RPP) recovery as a percentage of pre-ischaemia RPP] measured at the end of reperfusion ($67.2 \pm 3.8\%$) compared with the control hearts ($46.2 \pm 3.8\%$, Table 1). The control compounds, namely AP219 and ADT-OH, did not have a significant effect on either RPP recovery or infarct size, confirming that selective delivery of H₂S to the mitochondria mediates AP39's cardioprotection.

Cytosol-independent mechanism of postconditioning with AP39

We next investigated the effect of AP39 on the RISK pathway as a relevant protective cytosolic-signalling pathway using a 'signal tracing' technique. Specific pharmacological inhibitors, namely the PI3K inhibitor LY294002 (Jiang *et al.*, 2007), constitutive NOS inhibitor L-NAME (Fradorf *et al.*, 2010) and sGC inhibitor ODQ (Routhu *et al.*, 2010) were used at doses that have previously been reported to abrogate the activity of their targets in *in vivo* models.

There was no significant difference in either the baseline characteristics or the risk zone (ischaemic bed) among the groups (Figure 3A). None of the pharmacological inhibitors had a significant effect on infarct size when given alone 15 min before reperfusion compared with the control group (Figure 3B). Blockade of PI3K activity with LY294002 did not abolish the infarct limitation by AP39. Similarly, neither blockade of NO synthesis by L-NAME nor selective inhibition of its downstream effector, sGC, with ODQ attenuated the protective effect of AP39.

The effect of AP39, used as an adjunct to reperfusion, on the key cytosolic components of the RISK pathway was also evaluated in samples harvested from the left ventricle after 5 min of reperfusion (Figure 4). Immunoblotting was carried out using phospho-specific antibodies for Akt, eNOS, GSK-3 β and ERK1/2 to outline their role in the cardioprotection. In line with the infarct size data, Western blot analysis showed that administration of AP39 at reperfusion had no significant effect on the phosphorylation of either Akt, eNOS, GSK-3 β or ERK1/2. This confirms that AP39 mediated its cardioprotection independently of these cytosolic components on the RISK pathway.

Mitochondrial effects of AP39

We examined the effect of specific-delivery of H₂S into the mitochondria on the susceptibility to PTP opening. We used freshly isolated SSM and IFM and treated them with vehicle or AP39 (1 μM). SSM and IFM were exposed to pulses of Ca²⁺ in the presence and absence of CsA as a positive control (Figure 5). Untreated IFM showed 30% higher calcium tolerance than untreated SSM. AP39 elicited a significant inhibitory effect on the PTP opening in both SSM and IFM, which represents 30% increase in Ca²⁺ overload tolerance, compared with vehicle-treated mitochondria. The inhibitory effect of AP39 on PTP opening was comparable with that observed after CsA in SSM and IFM. Interestingly, AP39 showed 25% additive effect to CsA-induced inhibition of PTP opening when either SSM or IFM were incubated with both AP39 and CsA before the exposure to Ca²⁺ pulses, compared with CsA alone.

Mitochondrial respiration was measured for both SSM and IFM using substrates for complex I (glutamate and malate) and complex II (succinate, in the presence of rotenone to inhibit complex I). There was no difference in the basal respiration of the two subpopulations of mitochondria. ADP-stimulated respiration was higher in IFM (by 25% and 31% for complex I and II respectively) compared with SSM. Different concentrations of AP39 (0.3, 1, 3, 5 μM) were tested on SSM or IFM; however, none of

Table 1

Summary of the baseline parameters and haemodynamic data throughout the ischaemia–reperfusion protocol

Experimental protocol	n	BW (g)	Baseline			20 min ischaemia			120 min reperfusion		
			HR (beats·min ⁻¹)	RPP (mmHg·min ⁻¹ ·10 ³)	MAP (mmHg)	HR (beats·min ⁻¹)	RPP (mmHg·min ⁻¹ ·10 ³)	MAP (mmHg)	HR (beats·min ⁻¹)	RPP (mmHg·min ⁻¹ ·10 ³)	MAP (mmHg)
Series 1											
Control (0.05% DMSO)	10	342 ± 5	342 ± 10	36.2 ± 2.1	90 ± 6	311 ± 14	26.0 ± 1.9	70 ± 3	257 ± 9	16.7 ± 2.2	55 ± 5
AP39 0.01 μmol·kg ⁻¹	8	347 ± 7	351 ± 8	38.4 ± 2.8	92 ± 4	302 ± 10	27.1 ± 2.4	70 ± 5	245 ± 12	17.7 ± 1.8	58 ± 3
AP39 0.1 μmol·kg ⁻¹	8	339 ± 5	349 ± 12	40.0 ± 2.0	89 ± 6	299 ± 14	28.7 ± 1.2	68 ± 7	278 ± 8	20.0 ± 1.3	54 ± 5
AP39 1 μmol·kg ⁻¹	8	355 ± 5	356 ± 9	38.5 ± 1.5	85 ± 5	303 ± 10	29.4 ± 2.3	67 ± 3	332 ± 10	25.8 ± 1.2*	49 ± 4
AP219 1 μmol·kg ⁻¹	8	356 ± 7	341 ± 10	37.8 ± 2.0	87 ± 7	315 ± 9	27.6 ± 1.6	71 ± 5	250 ± 9	16.2 ± 1.5	51 ± 6
ADT-OH 1 μmol·kg ⁻¹	8	342 ± 6	355 ± 12	39.4 ± 2.5	90 ± 4	309 ± 11	29.1 ± 2.3	68 ± 4	243 ± 11	17.5 ± 1.8	54 ± 5
Series 2											
Control (0.05% DMSO)	11	361 ± 5	352 ± 12	35.5 ± 2.0	87 ± 6	302 ± 12	26.1 ± 1.7	65 ± 4	255 ± 12	15.2 ± 1.8	53 ± 5
AP39 1 μmol·kg ⁻¹	8	356 ± 7	346 ± 9	39.6 ± 3.1	92 ± 4	289 ± 10	31.1 ± 2.0	68 ± 5	320 ± 9	28.2 ± 1.5*	54 ± 6
AP39 1 μmol·kg ⁻¹ + L-NAME 20 mg·kg ⁻¹	8	365 ± 6	345 ± 11	36.0 ± 1.9	90 ± 7	285 ± 15	29.5 ± 1.8	67 ± 8	314 ± 13	22.4 ± 2.4*	53 ± 5
L-NAME 20 mg·kg ⁻¹	8	371 ± 9	343 ± 10	39.3 ± 1.6	89 ± 5	281 ± 12	28.6 ± 2.4	74 ± 5	230 ± 8	14.4 ± 2.1	56 ± 4
AP39 1 μmol·kg ⁻¹ + LY294002 0.3 mg·kg ⁻¹	8	359 ± 10	350 ± 7	37.4 ± 1.5	86 ± 6	291 ± 10	32.0 ± 2.2	70 ± 6	306 ± 10	24.5 ± 1.6*	52 ± 5
LY294002 0.3 mg·kg ⁻¹	8	367 ± 9	351 ± 11	42.3 ± 2.5	91 ± 4	305 ± 14	30.2 ± 1.7	69 ± 6	235 ± 12	16.4 ± 2.0	60 ± 7
AP39 1 μmol·kg ⁻¹ + ODQ 1 mg·kg ⁻¹	8	365 ± 7	350 ± 11	39.6 ± 1.5	93 ± 5	291 ± 11	31.5 ± 1.6	71 ± 4	329 ± 9	26.3 ± 1.9*	55 ± 5
ODQ 1 mg·kg ⁻¹	8	370 ± 8	342 ± 9	40.3 ± 2.5	88 ± 7	300 ± 10	28.6 ± 1.4	66 ± 5	228 ± 15	15.6 ± 2.0	63 ± 4

Animals body weight and haemodynamic parameters for infarct size studies at the end of stabilization period (baseline), after 20 min of ischaemia and at the end of reperfusion. BW, body weight; n, number of animals per group. There was no significant difference among experimental groups in the baselines or the application of the pharmacological inhibitors on the haemodynamics. Values expressed as mean ± SEM. (Two-way ANOVA followed by Bonferroni *post hoc* test).

**P* < 0.05 versus control value at the same time point

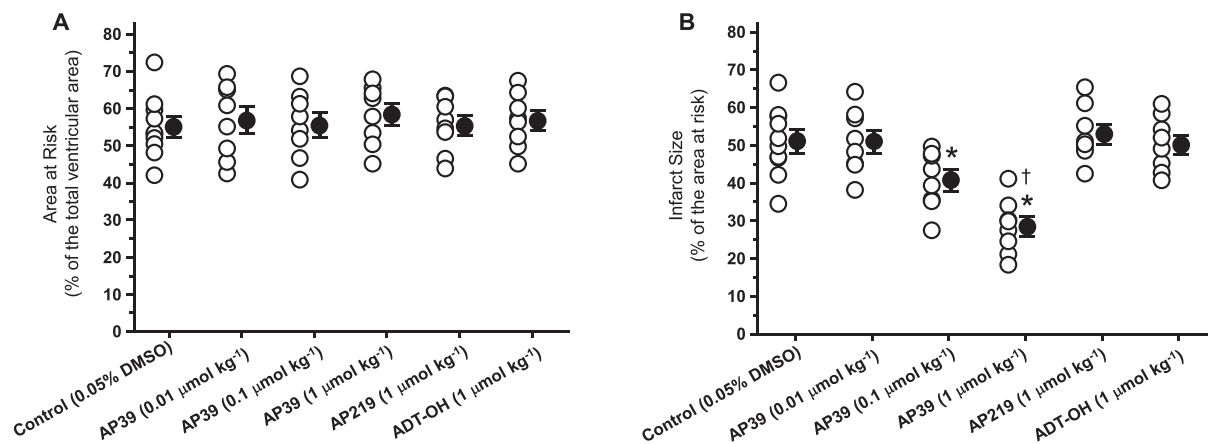


Figure 2

Infarct-limiting effect of AP39 at reperfusion: (A) area at risk (AAR) reported as a percentage of the total ventricular volume. (B) Infarct size presented as a percentage of the AAR. Data were analysed using one-way ANOVA with Neuman Keuls *post hoc* test and presented as mean \pm SEM, $n = 8$ for all groups except the control group (0.05% DMSO) where $n = 10$. The mean of the infarct size for each group is represented by a filled circle (with error bars) next to the individual values (open circles). * $P < 0.05$ versus control, † $P < 0.05$ versus AP39 0.1 $\mu\text{mol kg}^{-1}$.

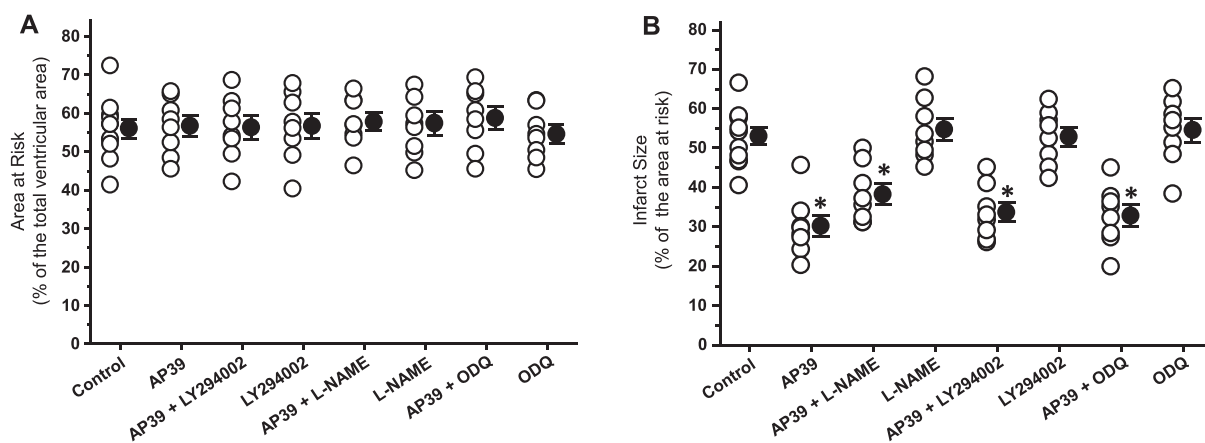


Figure 3

Effect of pharmacological inhibitors of the RISK pathway on infarct-limitation by AP39: (A) risk zone measurements of experimental groups expressed as a percentage of the total ventricular area. (B) Myocardial infarction data are expressed as a percentage of the risk zone. Individual animal data in each group are represented by empty circles while the mean of infarct size is presented by a full circle. Data were analysed via one-way ANOVA followed by Newman Keuls *post hoc* test and reported as mean \pm SEM, $n = 8$ for all groups except the control group where $n = 11$. * $P < 0.05$ versus control.

the concentrations examined significantly influenced mitochondrial oxygen consumption.

Overwhelming mito-ROS generation at early reperfusion is one of the main determinants of cellular injury. Therefore, we performed *in vitro* experiments to look at the direct effect of AP39 on H_2O_2 generation in the isolated rat left ventricle mitochondria (Figure 7A–D). In the control groups, ROS generation was significantly lower by 20% in IFM than SSM. AP39 showed a dose-dependent inhibition of ROS generation in both SSM and IFM. AP39 (1 μM) exerted the maximum inhibitory effect (38% in SSM and 61% in IFM) compared with control, vehicle-treated and the second control

mitochondria. Interestingly, the inhibitory effect of AP39 on mito-ROS generation was gradually reduced as the concentration was increased. Rotenone, as a positive control, resulted in overproduction of ROS in both SSM and IFM by 65% and 75%, respectively, compare the basal ROS generation level.

Discussion

The lipophilic triphenylphosphonium (TPP^+) scaffold is an attractive moiety for investigating mitochondrial function as it selectively accumulates (100- to 500-fold vs. cytosol) in

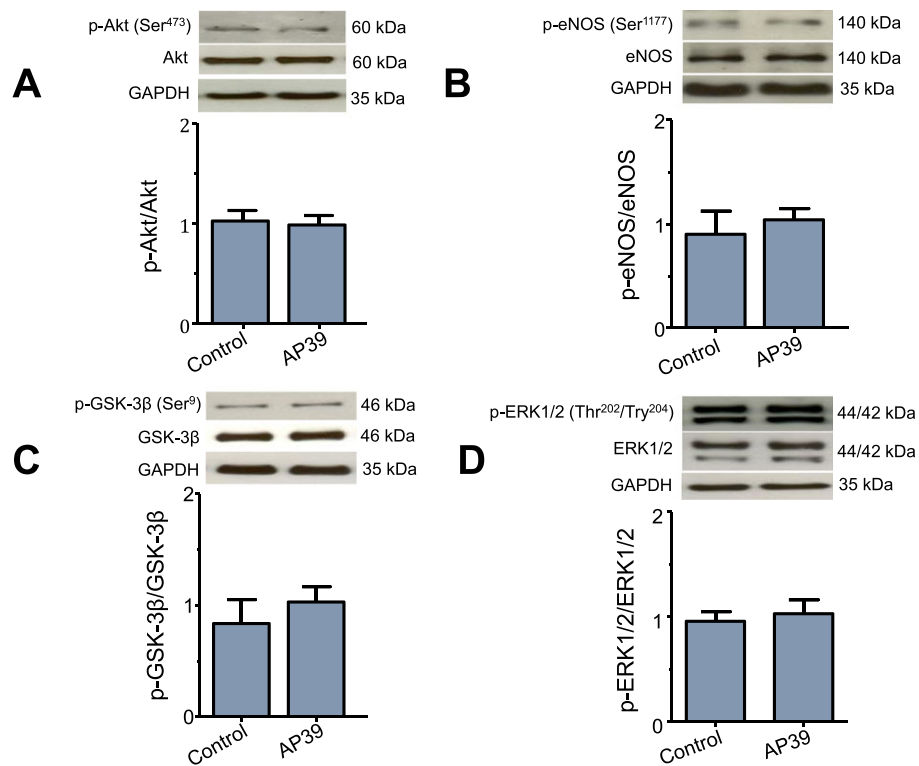


Figure 4

Effect of AP39 on RISK pathway proteins at early reperfusion: representative western blots and densitometry analysis of (A) pAkt^{S473}, total Akt and GAPDH; (B) p-eNOS^{S1177}, total eNOS and GAPDH; (C) p-GSK-3β^{S9}, GSK-3β and GAPDH; (D) p-ERK1/2^{Thr202/Tyr204}, ERK1/2 and GAPDH. Specific antibodies were used to assess the effect of AP39 on the phosphorylation of the RISK components in myocardial biopsies harvested from the left ventricle at early reperfusion. Histograms show the relative ratio of phosphorylated protein to the total level of protein. GAPDH was used as an internal standard for all quantifications. Data were analysed using Student's *t*-test and presented as mean ± SEM, *n* = 6 per group.

the mitochondrial matrix (Murphy and Smith, 2007; Smith *et al.*, 2011). Previous work (Prime *et al.*, 2009) demonstrated infarct limitation using a mitochondria-targeted NO donor (MitoSNO) with an NO-releasing moiety linked to TPP⁺. Work by Krieg's group (Methner *et al.*, 2013) showed that MitoSNO works independently of cytosolic protein kinase G that mediates the cardioprotective effect of non-mitochondrial-targeted NO donors. AP39 represents the first successful attempt to deliver H₂S selectively and at low concentration to the mitochondria (Le Trionnaire *et al.*, 2014; Szczesny *et al.*, 2014; Tomasova *et al.*, 2014; Ikeda *et al.*, 2015; Ahmad *et al.*, 2016).

In the present study, AP39 significantly limited infarct size (Figure 2B) and improved the post-ischaemic functional recovery (Table 1), both in a dose-dependent manner, when administered prior to reperfusion. Consistent with these data, Ahmad *et al.* (2016) reported that AP39 also exerted attenuation in renal damage, oxidative stress and renal inflammation when applied at reperfusion in an *in vivo* renal ischaemia/reperfusion injury model. We observed that the TPP⁺ scaffold molecule (AP219) and the H₂S-generating moiety (ADT-OH), which were used as controls, had no effect on myocardial injury. This is in agreement with other reports where these controls lacked biologically activity when used at nanomolar or micromolar concentrations (Le Trionnaire *et al.*, 2014; Szczesny *et al.*, 2014; Ahmad *et al.*, 2016).

At the time of finalizing this manuscript, recent work with AP39 by Papapetropoulos's group (Chatzianastasiou *et al.*, 2016) has appeared. The main focus of Chatzianastasiou's work is 'head-to-head' comparison of infarct limitation by different H₂S donors (Na₂S, GYY4137, thiovaline and AP39) and elucidation of the role of NO in mediating protection. Intriguingly, all donors had the same infarct-limiting effect in a mouse model of ischaemia/reperfusion injury. It is noteworthy that the optimum cardioprotective doses of GYY4137 and AP39 used were 26.6 and 0.25 μmol·kg⁻¹ respectively. Very recently, we reported that 26.6 μmol·kg⁻¹ GYY4137 was not cardioprotective in an *in vivo* rat model of ischaemia/reperfusion injury with the optimum cardioprotective dose being 10-fold higher (Karwi *et al.*, 2016). Similarly, in the present study, we demonstrated that AP39 exerts an infarct-sparing effect with an optimum cardioprotective dose of 1 μmol·kg⁻¹, fourfold higher than the effective dose in mouse reported by Chatzianastasiou *et al.* (2016). No haemodynamic data are available to compare AP39-induced dose-dependent improvement in post-ischaemic functional recovery with Chatzianastasiou's paper.

Our present study provides important mechanistic insight into AP39's cardioprotective action *in vivo*. We found that selective blockade of PI3K, which is known to mediate the cardioprotective effect of non-mitochondrial H₂S donors (Andreadou *et al.*, 2015; Karwi *et al.*, 2016), did not abolish

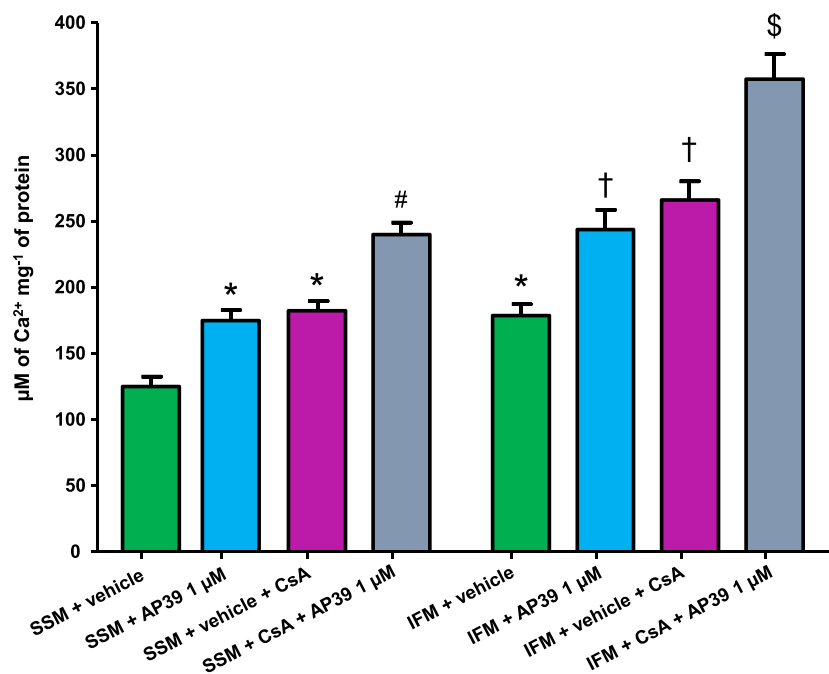


Figure 5

Effect of AP39 on mitochondrial PTP opening: SSM and IFM were incubated individually with vehicle (0.003% ethanol) or different concentrations of AP39 and subjected to pulses of 5 μM of CaCl₂ per 3 min at 25°C until the opening of PTP in the presence and absence of CsA. Data expressed as mean ± SEM, $n = 10$, * $P < 0.05$ versus SSM + vehicle, # $P < 0.05$ versus SSM + vehicle + CsA, † $P < 0.05$ versus IFM + vehicle, \$ $P < 0.05$ versus IFM + vehicle + CsA (two-way ANOVA followed by Bonferroni *post hoc* test, $n = 10$).

cardioprotection (Figure 3B). Crosstalk/interaction between H₂S and NO has different patterns depending on organs/tissues, experimental conditions and species (King *et al.*, 2014; Bibli *et al.*, 2015; Karwi *et al.*, 2016). To test if NO/sGC pathway mediates the effect of AP39, we blocked the endogenous NO synthesis pathway and also inhibited the activity of its end effector (sGC) using L-NAME and ODQ respectively. We found that cardioprotection by AP39 was still observed in the presence of L-NAME or ODQ, supported by analysis of protein phosphorylation during early reperfusion. We observed that AP39 did not induce phosphorylation of Akt, eNOS, GSK-3β, a downstream effector of the RISK pathway, or ERK1/2, a parallel arm of the RISK pathway at 5 min reperfusion (Figure 4A–D). Chatzianastasiou *et al.* (2016) reported that AP39 did not phosphorylate either eNOS ser¹¹⁷⁶ or VASP ser²³⁹ after 10 min of reperfusion and its cardioprotection was not abolished by either L-NAME or DT2, indicating a cGMP/PKG-independent mechanism in the murine model. Their data are complementary to the fuller characterization of the potential cytosolic signalling targets of AP39 that we present here. Viewed together, our data and those of Chatzianastasiou *et al.* (2016) provide persuasive evidence that, unlike other H₂S donors, AP39 mediates its cardioprotection by a mechanism that is independent of activation of the cytosolic components of the RISK signalling cascade.

Intra-mitochondrial H₂S is essential for normal function of the citric acid cycle. Levels are disturbed during oxidative stress due to increased H₂S degradation and reduced production (Geng *et al.*, 2004; Doeller *et al.*, 2005; Whiteman *et al.*, 2011; Vandiver and Snyder, 2012). H₂S supplements or

overexpression of endogenous synthetic enzymes have been shown to protect against ischaemia/reperfusion injury by mitigating oxidative stress and preserving mitochondrial integrity (Andreadou *et al.*, 2015). Interestingly, Kai *et al.* (2012) found that NaHS-induced protection was abolished in mitochondria-free cells. Nevertheless, whether H₂S directly interacts with mitochondria or triggers cytosolic signalling pathways that converge on the mitochondria may depend on the intracellular level of H₂S. Therefore, we have characterized for the first time the direct effect of AP39 on the most relevant subpopulations of cardiomyocyte mitochondria, namely SSM and IFM. Inhibition of the PTP opening in the first minutes of reperfusion has been extensively reported to protect against reperfusion injury (Halestrap, 2010; Ong *et al.*, 2014). It has been shown that many cardioprotective interventions act to maintain PTP in a closed state (Hausenloy *et al.*, 2009). With this in mind, we investigated the influence of AP39 on the opening of PTP, as a result of Ca²⁺ overload, in cardiac SSM and IFM. We found that AP39 inhibited PTP opening in SSM and IFM (Figure 5) with no significant difference from the inhibitory effect of the positive control, CsA, which can protect myocardium against ischaemia/reperfusion injury (Hausenloy *et al.*, 2012). We observed that AP39 and CsA in combination increased mitochondrial tolerance to Ca²⁺ overload and resulted in an additive effect compared with either compound alone. CsA prevents the opening of PTP by desensitizing cyclophilin-D, a component of the multiprotein complex spanning the inner and outer mitochondrial membranes, which is a modulator of PTP located in the mitochondrial matrix (Bernardi and Di Lisa,

2015). Having an additive effect to CsA suggests that AP39 may inhibit PTP opening via a cyclophilin-D independent mechanism. Chatzianastasiou *et al.* (2016) reported that AP39 (0.3 vs. 1 μM in our study), exerted an additive effect to CsA in mouse mitochondria isolated from the whole heart. However, isolating mitochondria from whole heart tissue is potentially problematic as a number of cell types contribute to the isolated mitochondrial fraction, for example endothelial cells, fibroblasts and other local resident cells. Even more important, cardiomyocyte mitochondria, namely SSM and IFM, themselves significantly differ in their main characteristics including oxygen consumption, mito-ROS generation and calcium retention capacity (Palmer *et al.*, 1977; Palmer *et al.*, 1986). Our present study confirms for the first time the effect of AP39 in both IFM and SSM subpopulations.

It has been reported that H_2S can stimulate mitochondrial ATP production by acting as an electron donor for the electron transport chain (Modis *et al.*, 2014; Szabo *et al.*, 2014). Accordingly, we explored the influence of AP39 on mitochondrial respiration through complexes I and II in both SSM and IFM. The respiration control ratio (RCR), an index for the coupling between mitochondrial respiration and oxidative phosphorylation, for isolated mitochondria fractions in this study was around 2.5. Although this result is comparable with our previously data (Boengler *et al.* 2009), others have reported higher RCR ratios (Chen *et al.*, 2008; Asemu *et al.*, 2013; Gao *et al.*, 2013). This could be due to either measuring oxygen consumption at 30°C instead of 25°C, using trypsin instead

of nargase to release the IFM or stimulating the mitochondria with higher concentration of ADP than what was used in this study. We did not detect any significant effect of AP39 on the oxygen consumption of these complexes in either mitochondrial subpopulation (Figure 6). These data suggest the safety margin of the applied concentration range. More importantly and in line with others, these results show that electron supply by H_2S (at low concentration) to the electron transport chain occurs at the level of coenzyme Q where sulfide quinone reductase activity is involved. Following that, electrons will flow forward toward Complex III and Complex IV without affecting either Complexes I or II (Gouvern *et al.*, 2007; Szabo *et al.*, 2014). It has been demonstrated that inhibition of Complex I using rotenone did not affect sulfide oxidation while inhibition of Complex III or VI by antimycin or cyanide, respectively, impeded it (Volkel & Grieshaber, 1996; Yong & Searcy, 2001; Gouvern *et al.*, 2007). Investigating the effect of AP39 on mitochondrial respiration at 37°C also needs further investigation in future work.

The detrimental effect of overwhelming mito-ROS generation, as a result of respiratory chain uncoupling, is one of the hallmarks of ischaemia/reperfusion injury (Venditti *et al.*, 2001; Brown and Griendling, 2015). It is a major contributor to the opening of PTP, initiating cell apoptosis and accelerated necrosis during reperfusion (Hausenloy *et al.*, 2009). Since oxidative stress and the mitochondria play central roles in ischaemia/reperfusion injury, targeting the mitochondria with selective H_2S donors is a plausible therapeutic approach to limit ischaemia/reperfusion injury. Here, we

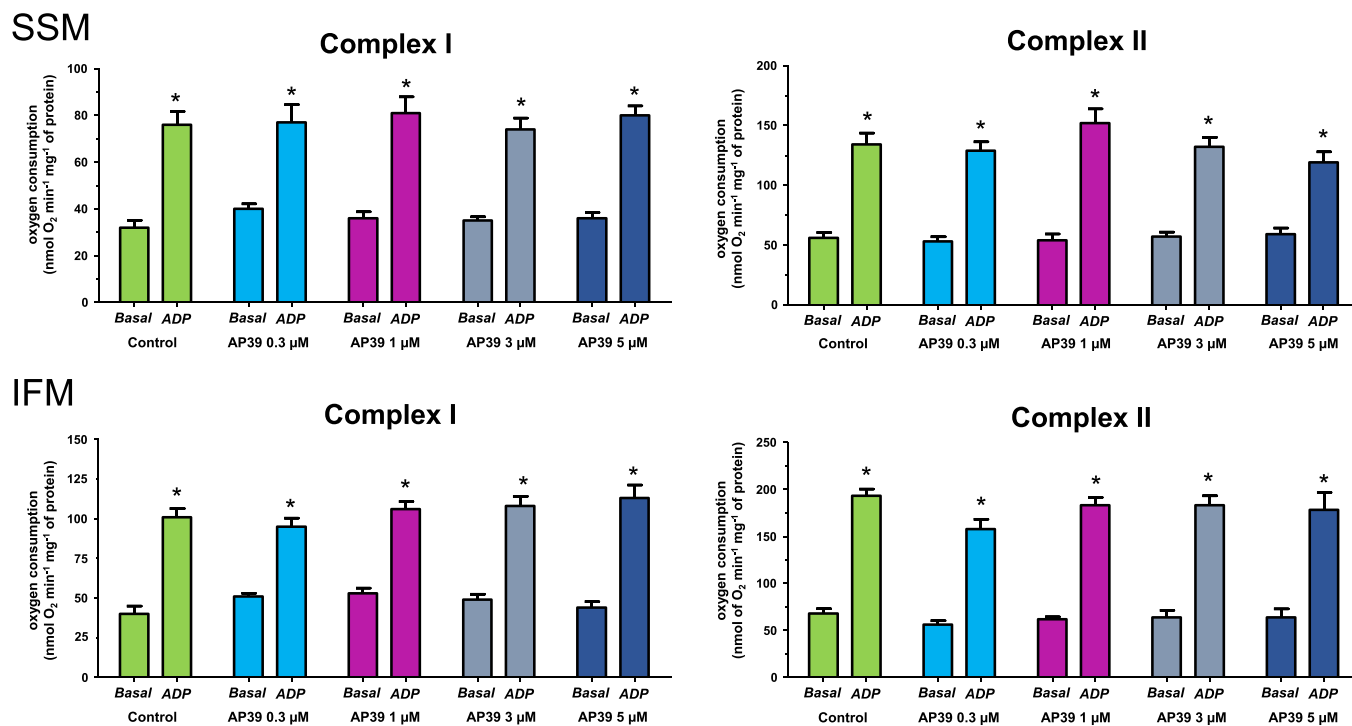


Figure 6

Effect of AP39 on mitochondrial respiration: Respiration of complexes I and II were measured at basal level and after ADP-stimulation in the presence and absence of the vehicle or different concentrations of AP39 in SSM and IFM mitochondria. Data were analysed by two-way ANOVA with Bonferroni *post hoc* test and reported as mean \pm SEM, $n = 10$, * $P < 0.05$ versus basal respiration.

have investigated for the first time the influence of AP39 on mito-ROS generation in both SSM and IFM. We found that AP39 limited mito-ROS level in both subpopulations (Figure 7), which is in line with other studies of mito-ROS reduction with AP39 (Le Trionnaire *et al.*, 2014; Szczesny *et al.*, 2014; Ikeda *et al.*, 2015; Ahmad *et al.*, 2016). We also observed an attenuation in AP39's activity as its concentration was increased, consistent with the findings of others (Szczesny *et al.*, 2014; Ahmad *et al.*, 2016).

Although we have provided novel mechanistic insights into how AP39 could mediate cardioprotection, there are several caveats and current limitations. Assessing the extent of mitochondrial H₂S level increase following AP39

application remains a challenge due to the lack of sensitive probes. Ikeda *et al.* (2015) reported that AP39 did not influence the expression of cystathionine γ lyase (CSE), cystathionine β synthase (CBS) or 3-mercaptopyruvate sulphurtransferase (3-MST) in the brain. This suggests that AP39 probably elevates mitochondrial H₂S level without interfering with the endogenous synthesis of H₂S. The focus of ongoing work is to investigate whether AP39 suppresses oxidative stress by increasing GSH production or by up-regulating mito-ROS scavenging pathways or by directly scavenging ROS. The exact mechanism/target whereby AP39 inhibits PTP opening also remains to be determined. It may be interesting to identify what happens to these

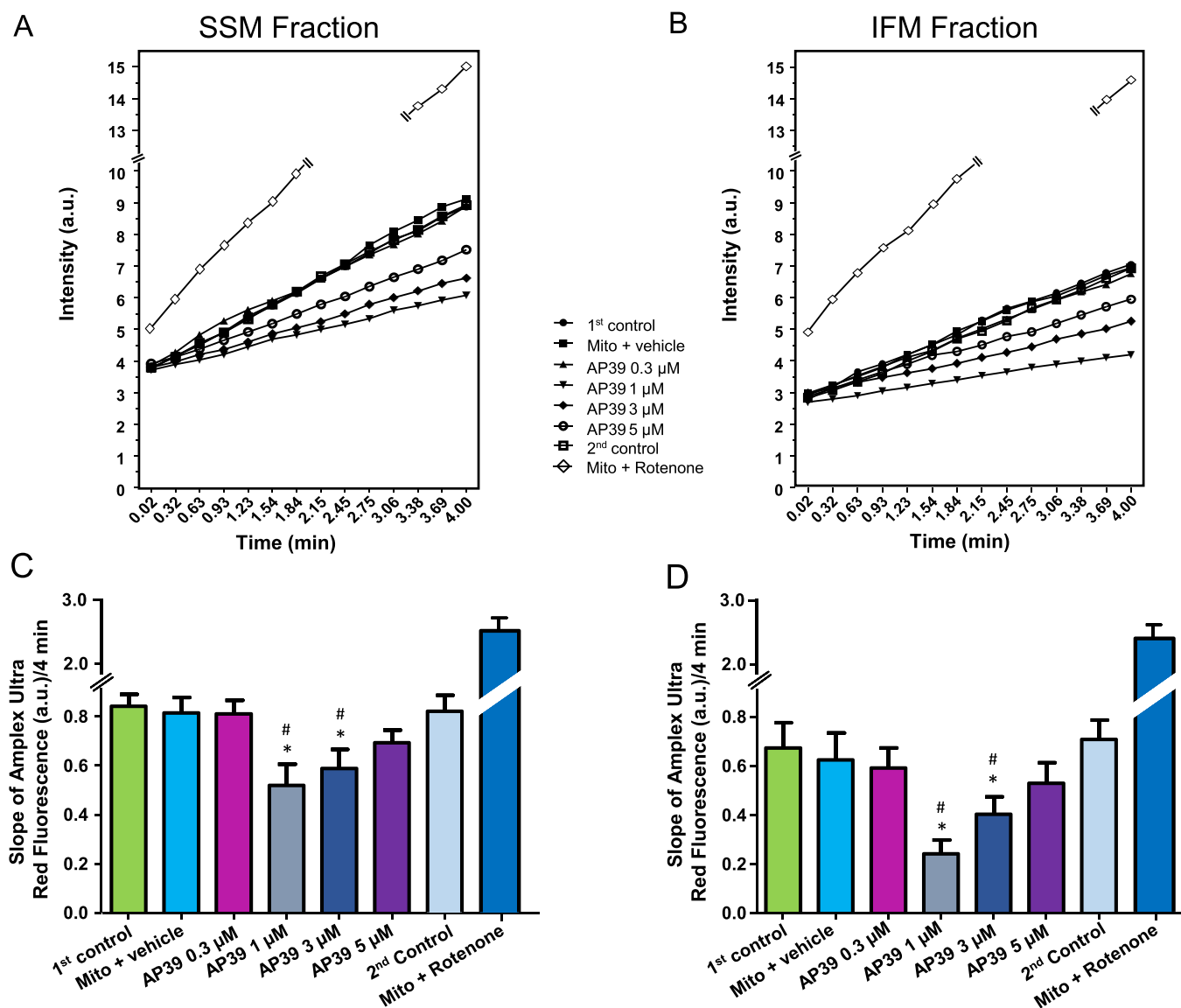


Figure 7

Effect of AP39 on mitochondrial-ROS generation: Mitochondria were incubated with either vehicle (0.05% DMSO) or different concentrations of AP39. (A) and (B) are representative charts for the ROS generation of SSM and IFM, respectively, and error bars were removed for clarity. The slope of ROS generation was measured continuously for 4 min with the fluorescence indicator Amplex UltraRed both in (C) SSM and (D) IFM mitochondria. Data are expressed as mean \pm SEM, $n = 10$, * $P < 0.05$ versus first control, [#] $P < 0.05$ versus second control (two-way ANOVA with Bonferroni post hoc test, $n = 10$).

subpopulations in the animal treated with AP39. Both subpopulations play significant roles in mediating cardioprotection, although it is possible this includes persulfidation (also called S-sulfhydration) of mitochondrial proteins such as ATP synthase (Modis *et al.*, 2016; Wedmann *et al.*, 2016). Very recent work by Murphy's group (Sun *et al.*, 2016) also proposed that postconditioning with NaHS protected against myocardial infarction via an increase in S-nitrosylation and most of the S-nitrosylated proteins were mitochondrial proteins. This further emphasizes the physiological importance of post-translation modifications of H₂S and its interaction with NO in the mitochondria, a phenomenon that we are now seeking to characterize.

In conclusion, our results confirm that AP39 can protect the heart against myocardial infarction when given at reperfusion in a manner that is independent of classical cytosolic signalling mechanisms. We also report for the first time that AP39 inhibits mito-ROS generation and PTP opening in both SSM and IFM, probably in a cyclophilin D-independent manner without affecting mitochondrial respiration. These findings provide proof-of-concept that direct delivery of H₂S to mitochondria by mitochondria-targeting H₂S donors, of which AP39 is a prototype of several compounds in this class under development, represents a novel and effective adjunctive intervention to mitigate the irreversible myocardial injury associated with reperfusion.

Acknowledgements

Q.K. acknowledges the generous support of the Iraqi Ministry of Higher Education and Scientific Research. R.T. is the recipient of The Brian Ridge Scholarship. M.W. and M.E.W. would like to thank the Medical Research Council (UK) MR/M022706/1 for their generous support. Authors also thank Elvira Ungefug, Anna Reis, Sabrina Bohme and Christine Hirschhauser for their support.

Author contributions

Q.G.K. and G.F.B. conceived and designed the studies and wrote the first draft of the manuscript. Q.K. performed all the *in vivo* studies, biochemical studies and mitochondrial studies. J.B., K.B. and R.S. designed the mitochondrial studies and assisted Q.K. with performing mitochondrial experiments and analysis of mitochondrial function data. M.E.W., R.T. and M.W. designed, synthesized and characterized AP39 and related compounds. All authors contributed to revision of the manuscript prior to finalization for submission by Q.K. and G.F.B.

Conflict of interest

M.W., M.E.W. and the University of Exeter have intellectual property (patent filings) on AP39, related compounds and their use.

Declaration of transparency and scientific rigour

This Declaration acknowledges that this paper adheres to the principles for transparent reporting and scientific rigour of preclinical research recommendation by funding agencies, publishers and other organizations engaged with supporting research.

References

- Ahmad A, Olah G, Szczesny B, Wood ME, Whiteman M, Szabo C (2016). AP39, a mitochondrially targeted hydrogen sulfide donor, exerts protective effects in renal epithelial cells subjected to oxidative stress *in vitro* and in acute renal injury *in vivo*. *Shock* 45: 88–97.
- Alexander SP, Fabbro D, Kelly E, Marrion N, Peters JA, Benson HE *et al.* (2015). The concise guide to PHARMACOLOGY 2015/16: Enzymes. *Br J Pharmacol* 172: 6024–6109.
- Andreadou I, Iliodromitis EK, Rassaf T, Schulz R, Papapetropoulos A, Ferdinandy P (2015). The role of gasotransmitters NO, H₂S and CO in myocardial ischaemia/reperfusion injury and cardioprotection by preconditioning, postconditioning and remote conditioning. *Br J Pharmacol* 172: 1587–1606.
- Asemu G, O'Connell KA, Cox JW, Dabkowski ER, Xu W, Ribeiro RF Jr *et al.* (2013). Enhanced resistance to permeability transition in interfibrillar cardiac mitochondria in dogs: effects of aging and long-term aldosterone infusion. *Am J Physiol Heart Circ Physiol* 304: H514–H528.
- Bernardi P, Di Lisa F (2015). The mitochondrial permeability transition pore: molecular nature and role as a target in cardioprotection. *J Mol Cell Cardiol* 78: 100–106.
- Bibli SI, Andreadou I, Chatzianastasiou A, Tzimas C, Sanoudou D, Kranias E *et al.* (2015). Cardioprotection by H₂S engages a cGMP-dependent protein kinase G/phospholamban pathway. *Cardiovasc Res* 106: 432–442.
- Boengler K, Stahlhofen S, van de Sand A, Gres P, Ruiz-Meana M, Garcia-Dorado D *et al.* (2009). Presence of connexin 43 in subsarcolemmal, but not in interfibrillar cardiomyocyte mitochondria. *Basic Res Cardiol* 104: 141–147.
- Bos EM, van Goor H, Joles JA, Whiteman M, Leuvenink HG (2015). Hydrogen sulfide: physiological properties and therapeutic potential in ischaemia. *Br J Pharmacol* 172: 1479–1493.
- Brown DI, Griendling KK (2015). Regulation of signal transduction by reactive oxygen species in the cardiovascular system. *Circ Res* 116: 531–549.
- Chatzianastasiou A, Bibli SI, Andreadou I, Efentakis P, Kaludercic N, Wood ME *et al.* (2016). Cardioprotection by H₂S donors: nitric oxide-dependent and -independent mechanisms. *J Pharmacol Exp Ther*. doi:10.1124/jpet.116.235119.
- Chen Q, Moghaddas S, Hoppel CL, Lesnfsky EJ (2008). Ischemic defects in the electron transport chain increase the production of reactive oxygen species from isolated rat heart mitochondria. *Am J Physiol Cell Physiol* 294: C460–C466.
- Chen Q, Paillard M, Gomez L, Li H, Hu Y, Lesnfsky EJ (2012). Postconditioning modulates ischemia-damaged mitochondria during reperfusion. *J Cardiovasc Pharmacol* 59: 101–108.

- Curtis MJ, Bond RA, Spina D, Ahluwalia A, Alexander SP, Giembycz MA *et al.* (2015). Experimental design and analysis and their reporting: new guidance for publication in BJP. *Br J Pharmacol* 172: 3461–3471.
- Doeller JE, Isbell TS, Benavides G, Koenitzer J, Patel H, Patel RP *et al.* (2005). Polarographic measurement of hydrogen sulfide production and consumption by mammalian tissues. *Anal Biochem* 341: 40–51.
- Elrod JW, Calvert JW, Morrison J, Doeller JE, Kraus DW, Tao L *et al.* (2007). Hydrogen sulfide attenuates myocardial ischemia–reperfusion injury by preservation of mitochondrial function. *Proc Natl Acad Sci U S A* 104: 15560–15565.
- Ferdinandy P, Hausenloy DJ, Heusch G, Baxter GF, Schulz R (2014). Interaction of risk factors, comorbidities, and comedications with ischemia/reperfusion injury and cardioprotection by preconditioning, postconditioning, and remote conditioning. *Pharmacol Rev* 66: 1142–1174.
- Fradorf J, Huhn R, Weber NC, Ebel D, Wingert N, Preckel B *et al.* (2010). Sevoflurane-induced preconditioning: impact of protocol and aprotinin administration on infarct size and endothelial nitric-oxide synthase phosphorylation in the rat heart in vivo. *Anesthesiology* 113: 1289–1298.
- Gao XH, Qanungo S, Pai HV, Starke DW, Steller KM, Fujioka H *et al.* (2013). Aging-dependent changes in rat heart mitochondrial glutaredoxins--Implications for redox regulation. *Redox Biol* 1: 586–598.
- Geng B, Chang L, Pan C, Qi Y, Zhao J, Pang Y *et al.* (2004). Endogenous hydrogen sulfide regulation of myocardial injury induced by isoproterenol. *Biochem Biophys Res Commun* 318: 756–763.
- Gubern M, Andriamihaja M, Nubel T, Blachier F, Bouillaud F (2007). Sulfide, the first inorganic substrate for human cells. *FASEB J* 21: 1699–1706.
- Halestrap AP (2010). A pore way to die: the role of mitochondria in reperfusion injury and cardioprotection. *Biochem Soc Trans* 38: 841–860.
- Hausenloy DJ (2013). Cardioprotection techniques: preconditioning, postconditioning and remote conditioning (basic science). *Curr Pharm Des* 19: 4544–4563.
- Hausenloy DJ, Boston-Griffiths EA, Yellon DM (2012). Cyclosporin A and cardioprotection: from investigative tool to therapeutic agent. *Br J Pharmacol* 165: 1235–1245.
- Hausenloy DJ, Ong SB, Yellon DM (2009). The mitochondrial permeability transition pore as a target for preconditioning and postconditioning. *Basic Res Cardiol* 104: 189–202.
- Hausenloy DJ, Yellon DM (2007). The evolving story of “conditioning” to protect against acute myocardial ischaemia-reperfusion injury. *Heart* 93: 649–651.
- Ikeda K, Marutani E, Hirai S, Wood ME, Whiteman M, Ichinose F (2015). Mitochondria-targeted hydrogen sulfide donor AP39 improves neurological outcomes after cardiac arrest in mice. *Nitric Oxide* 49: 90–96.
- Jiang R, Zatta A, Kin H, Wang N, Reeves JG, Mykytenko J *et al.* (2007). PAR-2 activation at the time of reperfusion salvages myocardium via an ERK1/2 pathway in in vivo rat hearts. *Am J Physiol Heart Circ Physiol* 293: H2845–H2852.
- Johansen D, Ytrehus K, Baxter GF (2006). Exogenous hydrogen sulfide (H₂S) protects against regional myocardial ischemia–reperfusion injury--Evidence for a role of K ATP channels. *Basic Res Cardiol* 101: 53–60.
- Kai S, Tanaka T, Daijo H, Harada H, Kishimoto S, Suzuki K *et al.* (2012). Hydrogen sulfide inhibits hypoxia- but not anoxia-induced hypoxia-inducible factor 1 activation in a von hippel–lindau- and mitochondria-dependent manner. *Antioxid Redox Signal* 16: 203–216.
- Karwi QG, Whiteman M, Wood ME, Torregrossa R, Baxter GF (2016). Pharmacological postconditioning against myocardial infarction with a slow-releasing hydrogen sulfide donor, GYY4137. *Pharmacol Res* 111: 442–451.
- Kilkenny C, Browne W, Cuthill IC, Emerson M, Altman DG, Group NCRRGW (2010). Animal research: reporting in vivo experiments: the ARRIVE guidelines. *Br J Pharmacol* 160: 1577–1579.
- Kimura H (2011). Hydrogen sulfide: its production and functions. *Exp Physiol* 96: 833–835.
- King AL, Polhemus DJ, Bhushan S, Otsuka H, Kondo K, Nicholson CK *et al.* (2014). Hydrogen sulfide cytoprotective signaling is endothelial nitric oxide synthase-nitric oxide dependent. *Proc Natl Acad Sci U S A* 111: 3182–3187.
- Le Trionnaire S, Perry A, Szczesny B, Szabo C, Winyard PG, Whatmore JL *et al.* (2014). The synthesis and functional evaluation of a mitochondria-targeted hydrogen sulfide donor, (10-oxo-10-(4-(3-thioxo-3H-1,2-dithiol-5-yl)phenoxy)decyl)triphenylphosphonium bromide (AP39). *Med Chem Comm* 5: 728–736.
- McGrath JC, Lilley E (2015). Implementing guidelines on reporting research using animals (ARRIVE etc.): new requirements for publication in BJP. *Br J Pharmacol* 172: 3189–3193.
- Methner C, Lukowski R, Grube K, Loga F, Smith RA, Murphy MP *et al.* (2013). Protection through postconditioning or a mitochondria-targeted S-nitrosothiol is unaffected by cardiomyocyte-selective ablation of protein kinase G. *Basic Res Cardiol* 108: 337–343.
- Modis K, Bos EM, Calzia E, van Goor H, Coletta C, Papapetropoulos A *et al.* (2014). Regulation of mitochondrial bioenergetic function by hydrogen sulfide. Part II. Pathophysiological and therapeutic aspects. *Br J Pharmacol* 171: 2123–2146.
- Modis K, Ju Y, Ahmad A, Untereiner AA, Altaany Z, Wu L *et al.* (2016). S-sulfhydration of ATP synthase by hydrogen sulfide stimulates mitochondrial bioenergetics. *Pharmacol Res* 113: 116–124.
- Murphy E, Ardehali H, Balaban RS, DiLisa F, Dorn GW 2nd, Kitsis RN *et al.* (2016). Mitochondrial function, biology, and role in disease: a scientific statement from the american heart association. *Circ Res* 118: 1960–1991.
- Murphy MP, Smith RA (2007). Targeting antioxidants to mitochondria by conjugation to lipophilic cations. *Annu Rev Pharmacol Toxicol* 47: 629–656.
- Ong SB, Samangouei P, Kalkhoran SB, Hausenloy DJ (2014). The mitochondrial permeability transition pore and its role in myocardial ischemia reperfusion injury. *J Mol Cell Cardiol* 78: 23–34.
- Palmer JW, Tandler B, Hoppel CL (1977). Biochemical properties of subsarcolemmal and interfibrillar mitochondria isolated from rat cardiac muscle. *J Biol Chem* 252: 8731–8739.
- Palmer JW, Tandler B, Hoppel CL (1986). Heterogeneous response of subsarcolemmal heart mitochondria to calcium. *Am J Physiol* 250: H741–H748.
- Pell VR, Chouchani ET, Frezza C, Murphy MP, Krieg T (2016). Succinate metabolism: a new therapeutic target for myocardial reperfusion injury. *Cardiovasc Res* 111: 134–141.
- Prime TA, Blaikie FH, Evans C, Nadtochiy SM, James AM, Dahm CC *et al.* (2009). A mitochondria-targeted S-nitrosothiol modulates respiration, nitrosates thiols, and protects against

- ischemia–reperfusion injury. *Proc Natl Acad Sci U S A* 106: 10764–10769.
- Routhu KV, Tsopanoglou NE, Strande JL (2010). Parstatin (1-26): the putative signal peptide of protease-activated receptor 1 confers potent protection from myocardial ischemia–reperfusion injury. *J Pharmacol Exp Ther* 332: 898–905.
- Smith RA, Hartley RC, Murphy MP (2011). Mitochondria-targeted small molecule therapeutics and probes. *Antioxid Redox Signal* 15: 3021–3038.
- Soetkamp D, Nguyen TT, Menazza S, Hirschhauser C, Hendgen-Cotta UB, Rassaf *et al.* (2014). S-nitrosation of mitochondrial connexin 43 regulates mitochondrial function. *Basic Res Cardiol* 109: 433–451.
- Southan C, Sharman JL, Benson HE, Faccenda E, Pawson AJ, Alexander SP *et al.* (2016). The IUPHAR/BPS Guide to PHARMACOLOGY in 2016: towards curated quantitative interactions between 1300 protein targets and 6000 ligands. *Nucleic Acids Res* 44: D1054–D1068.
- Sun J, Aponte AM, Menazza S, Gucek M, Steenbergen C, Murphy E (2016). Additive cardioprotection by pharmacological postconditioning with hydrogen sulfide and nitric oxide donors in mouse heart: S-sulphydration vs. S-nitrosylation. *Cardiovasc Res* 110: 96–106.
- Szabo C, Ransy C, Modis K, Andriamihaja M, Murghes B, Coletta C *et al.* (2014). Regulation of mitochondrial bioenergetic function by hydrogen sulfide. Part I. Biochemical and physiological mechanisms. *Br J Pharmacol* 171: 2099–2122.
- Szczesny B, Modis K, Yanagi K, Coletta C, Le Trionnaire S, Perry A *et al.* (2014). AP39, a novel mitochondria-targeted hydrogen sulfide donor, stimulates cellular bioenergetics, exerts cytoprotective effects and protects against the loss of mitochondrial DNA integrity in oxidatively stressed endothelial cells in vitro. *Nitric Oxide* 41: 120–130.
- Tomasova L, Pavlovicova M, Malekova L, Misak A, Kristek F, Grman M *et al.* (2014). Effects of AP39, a novel triphenylphosphonium derivatised anethole dithiolethione hydrogen sulfide donor, on rat haemodynamic parameters and chloride and calcium Ca3 and RyR2 channels. *Nitric Oxide* 46: 131–144.
- Vandiver M, Snyder SH (2012). Hydrogen sulfide: a gasotransmitter of clinical relevance. *J Mol Med* 90: 255–263.
- Venditti P, Masullo P, Di Meo S (2001). Effects of myocardial ischemia and reperfusion on mitochondrial function and susceptibility to oxidative stress. *Cell Mol Life Sci* 58: 1528–1537.
- Volkel S, Grieshaber MK (1996). Mitochondrial sulfide oxidation in *Arenicola marina*. Evidence for alternative electron pathways. *Eur J Biochem* 235: 231–237.
- Wedmann R, Onderka C, Wei S, Szijártó IA, Miljkovic JL, Mitrovic A *et al.* (2016). Improved tag-switch method reveals that thioredoxin acts as depersulfidase and controls the intracellular levels of protein persulfidation. *Chem Sci* 7: 3414–3426.
- Whiteman M, Le Trionnaire S, Chopra M, Fox B, Whatmore J (2011). Emerging role of hydrogen sulfide in health and disease: critical appraisal of biomarkers and pharmacological tools. *Clin Sci* 121: 459–488.
- Yong R, Searcy DG (2001). Sulfide oxidation coupled to ATP synthesis in chicken liver mitochondria. *Comp Biochem Physiol B Biochem Mol Biol* 129: 129–137.



Pharmacological postconditioning against myocardial infarction with a slow-releasing hydrogen sulfide donor, GYY4137



Qutuba G. Karwi^a, Matthew Whiteman^b, Mark E. Wood^c, Roberta Torregrossa^{b,c}, Gary F. Baxter^{a,*}

^a School of Pharmacy and Pharmaceutical Sciences, Cardiff University, UK

^b University of Exeter, Medical School, Exeter, UK EX1 2LU

^c School of Biosciences, University of Exeter, UK

ARTICLE INFO

Article history:

Received 30 March 2016

Received in revised form 27 June 2016

Accepted 30 June 2016

Available online 1 July 2016

Chemical compounds studied in this article:

GY4137-Morphilino salt (PubChem CID: 469337261)

LY294002 (PubChem CID: 3973)

N-Nitro-L-arginine methyl ester hydrochloride (PubChem: 39836)

Keywords:

Postconditioning

Hydrogen sulfide

Ischemia-reperfusion

Myocardial infarction

Reperfusion

ABSTRACT

Exogenous hydrogen sulfide (H₂S) protects against myocardial ischemia/reperfusion injury but the mechanism of action is unclear. The present study investigated the effect of GYY4137, a slow-releasing H₂S donor, on myocardial infarction given specifically at reperfusion and the signalling pathway involved. Thiobutabarbital-anesthetised rats were subjected to 30 min of left coronary artery occlusion and 2 h reperfusion. Infarct size was assessed by tetrazolium staining. In the first study, animals randomly received either no treatment or GYY4137 (26.6, 133 or 266 μmol kg⁻¹) by intravenous injection 10 min before reperfusion. In a second series, involvement of PI3K and NO signalling were interrogated by concomitant administration of LY294002 or L-NAME respectively and the effects on the phosphorylation of Akt, eNOS, GSK-3β and ERK1/2 during early reperfusion were assessed by immunoblotting. GYY4137 266 μmol kg⁻¹ significantly limited infarct size by 47% compared to control hearts (P < 0.01). In GYY4137-treated hearts, phosphorylation of Akt, eNOS and GSK-3β was increased 2.8, 2.2 and 2.2 fold respectively at early reperfusion. Co-administration of L-NAME and GYY4137 attenuated the cardio-protection afforded by GYY4137, associated with attenuated phosphorylation of eNOS. LY294002 totally abrogated the infarct-limiting effect of GYY4137 and inhibited Akt, eNOS and GSK-3β phosphorylation. These data are the first to demonstrate that GYY4137 protects the heart against lethal reperfusion injury through activation of PI3K/Akt signalling, with partial dependency on NO signalling and inhibition of GSK-3β during early reperfusion. H₂S-based therapeutic approaches may have value as adjuncts to reperfusion in the treatment of acute myocardial infarction.

© 2016 Elsevier Ltd. All rights reserved.

1. Introduction

In acute myocardial infarction, prompt restoration of coronary blood flow with appropriate reperfusion interventions is essential to salvage ischemic myocardium. Paradoxically, sudden reperfusion induces further irreversible cell injury and death beyond

Abbreviations: AAR, area at risk; Akt, protein kinase B; DATS, diallyltrisulfide; eNOS, endothelial nitric oxide synthase; ERK1/2, extracellular signal-regulated kinases 1/2 (p42/p44 mitogen activated protein kinase); GSK-3β, glycogen synthase kinase-3 Beta; GYY4137, morpholin-4-ium 4-methoxyphenyl-morpholinophosphinodithioate; H₂S, hydrogen sulfide; IPost-C, ischemic postconditioning; mPTP, mitochondrial permeability transition pore; NO, nitric oxide; PBS, phosphate buffered saline; PI3K, phosphatidylinositol-3-kinase; RISK, reperfusion injury salvage kinase (signalling pathway).

* Corresponding author at: School of Pharmacy and Pharmaceutical Sciences, Redwood Building, King Edward VII Avenue, Cardiff CF10 3NB, UK.

E-mail address: baxtergf@cardiff.ac.uk (G.F. Baxter).

<http://dx.doi.org/10.1016/j.phrs.2016.06.028>

1043-6618/© 2016 Elsevier Ltd. All rights reserved.

that caused by ischemia. Therefore, reperfusion injury contributes to overall clinical outcome since ultimate infarct size will be determined by both ischemic and reperfusion injuries [12]. Reperfusion injury is a challenging but important therapeutic target. The molecular pathology of reperfusion injury is complex and is likely to involve overwhelming oxidative/nitrosative stress, sudden intracellular pH normalisation and cytosolic Ca²⁺ oscillation, precipitating opening of the mitochondrial permeability transition pore (mPTP) during the early moments of reperfusion which initiates necrosis [47,7].

Ischemic postconditioning (IPost-C) is an experimental manoeuvre in which very brief intermittent periods of ischemia are introduced immediately after reperfusion [58]. This intervention has been shown to limit infarct size significantly, most likely through the activation of survival signalling mechanisms that reduce opening of the mPTP [19]. The so-called “reperfusion injury salvage kinase” (RISK) pathway includes as key components

Table 1

Baseline and cardiodynamics for series 1 and 2 at the end of stabilisation period, after 20 min of ischaemia and at the end of reperfusion.

Experimental Protocol	n	BW (g)	Baseline		20 min Ischaemia		120 min Reperfusion	
			RPP (mmHg min ⁻¹ *10 ³)	MAP (mmHg)	RPP (mmHg min ⁻¹ *10 ³)	MAP (mmHg)	RPP (mmHg min ⁻¹ *10 ³)	MAP (mmHg)
Series 1								
Control	10	355 ± 6	37.5 ± 2.0	88 ± 4	27.9 ± 1.8	68 ± 4	24.0 ± 1.4	53 ± 3
GY4137 26.6 μmol kg ⁻¹	8	360 ± 9	40.3 ± 3.0	90 ± 6	29.1 ± 2.1	71 ± 5	26.3 ± 2.0	59 ± 4
GY4137 133 μmol kg ⁻¹	8	346 ± 7	41.4 ± 1.8	94 ± 6	29.5 ± 2.2	70 ± 6	24.3 ± 1.5	53 ± 4
GY4137 266 μmol kg ⁻¹	8	368 ± 6	39.1 ± 1.7	83 ± 4	28.6 ± 2.0	65 ± 5	20.9 ± 1.6	45 ± 3
D-GY4137	6	368 ± 6	38.4 ± 2.3	85 ± 5	26.3 ± 2.1	69 ± 4	22.7 ± 1.3	48 ± 4
Series 2								
Control	7	384 ± 7	36.3 ± 2.2	85 ± 5	24.8 ± 2.2	61 ± 6	21.2 ± 2.0	48 ± 4
GY4137	7	379 ± 8	41.3 ± 3.0	96 ± 6	26.8 ± 1.6	66 ± 6	21.6 ± 1.1	47 ± 2
GY4137 + L-NAME	7	387 ± 7	39.3 ± 2.5	88 ± 5	29.5 ± 2.4	69 ± 5	19.4 ± 2.4	50 ± 6
L-NAME	6	381 ± 9	39.3 ± 1.6	97 ± 3	30.4 ± 2.1	76 ± 7	22.4 ± 5.1	57 ± 9
GY4137 + LY294002	6	362 ± 8	39.3 ± 1.8	88 ± 4	30.2 ± 1.8	71 ± 5	24.2 ± 0.6	53 ± 1
LY294002	6	367 ± 11	44.5 ± 2.8	98 ± 4	29.6 ± 1.2	72 ± 4	25.0 ± 0.7	54 ± 2

RPP = Rate pressure product, MAP = mean arterial pressure. Data are reported as Mean ± SEM. There was no significant difference among the experimental groups (One way ANOVA + Newman Keuls post-hoc), $p > 0.05$.

phosphatidylinositol-3-kinase (PI3K)/Akt, and endothelial nitric oxide synthase (eNOS). Other kinases have been described as part of the RISK pathway including extracellular regulated kinase (ERK1/2; p42/p44 mitogen activated protein kinase) and glycogen synthase-3β (GSK-3β). Although IPost-C is of limited clinical applicability, a number of pharmacological approaches that mimic IPost-C have been described, including the administration of autacoids and other mediators thought to activate the kinases of the RISK cascade [5].

Hydrogen sulfide (H₂S) has attracted considerable interest as a cardiovascular autacoid. Although produced endogenously within the myocardium and coronary vasculature [35,16], in coronary artery disease, there may be reduced H₂S production [56,17,22]. The administration of exogenous H₂S donor compounds or increasing endogenous production of H₂S has been well documented to reduce ischemia-reperfusion injury in experimental models [11,8,26]. There is also evidence that H₂S is a mediator of IPost-C [3,56,20,10]. However, potential therapeutic extrapolation of this knowledge has been hindered by the limitations of H₂S donor compounds. Much of the experimental literature has reported studies with inorganic sulfide salts (Na₂S and NaSH) which are impure in commercial form and unstable. Despite them being water soluble and inexpensive, a particular issue is that the H₂S release is largely uncontrollable as they dissociate in aqueous medium instantly to generate H₂S at high concentration in a short-lasting burst [41]. In contrast to Na₂S and NaSH, GY4137 (morpholin-4-ium 4-methoxyphenyl-morpholino-phosphinodithioate) is a donor compound which releases H₂S at a slow steady rate at physiological pH and temperature [33]. Several studies have suggested that GY4137 effectively delivers H₂S in various physiological systems [32,34,29,44,36,15,39]. Recent work by Meng et al. [38] showed that GY4137 given prior to myocardial ischemia protected against injury development and improved post-ischemic recovery of function. However, the therapeutically relevant time window for acute myocardial infarction implies administration as a postconditioning mimetic *i.e.* immediately prior to reperfusion since this is the time at which clinical therapeutic intervention can feasibly be made.

The aim of the present study was to investigate for the first time the injury limiting effects of GY4137 at early reperfusion *when given specifically as an adjunct to reperfusion* in a rat model of acute myocardial infarction. We hypothesised that GY4137 was able to limit reperfusion injury when given just prior to reperfusion, thereby limiting ultimate infarct size. We further hypothesised that the protective action was due to H₂S release and the activation of key components of the RISK signalling cascade at the first minutes

of reperfusion associated with postconditioning, namely PI3K/Akt and eNOS.

2. Materials and methods

2.1. Animals

Male Sprague Dawley rats, 300–350 g, were purchased from Harlan, UK. They were acclimatised in the institutional animal house at constant temperature and humidity on a 12 h light/dark cycle for at least seven days prior to experimentation, with free access to water and a small animal diet (Teklad global 14% protein rodent maintenance diet) at all times. All handling and procedures were carried out in accordance with UK Home Office Guidelines on the Animals (Scientific Procedures) Act 1986, (published by the Stationery Office, London, UK). The reporting of animal studies was in accordance with ARRIVE guidelines [25,37].

2.2. Materials

GY4137 and 'depleted' GY4137 were synthesised in-house as described [1,33] and purity determined by NMR spectroscopy (1H, 31P and 13C). The purity of GY4137 was identical to a commercial sample from SigmaAldrich. The constitutive nitric oxide synthase (NOS) inhibitor L-nitroarginine methyl ester (L-NAME), the phosphatidylinositol-3-kinase (PI3K) inhibitor LY294002, thiobutabarbital sodium salt hydrate (Inactin® hydrate), Evans blue dye, triphenyltetrazolium chloride (TTC) and dimethylsulfoxide (DMSO) were all purchased from Sigma-Aldrich, Gillingham, UK. Western blotting antibodies were all sourced from Cell Signalling, UK.

2.3. Acute myocardial infarction model

Rats were anaesthetised by intraperitoneal injection of thiobutabarbital sodium (200 mg kg⁻¹) and maintained by intravenous supplemental dosing (75 mg kg⁻¹) as required to maintain surgical anesthesia throughout the procedure. Body temperature was maintained at 37 ± 1 °C *via* rectal thermometer attached to a thermo-regulated blanket unit (Harvard Apparatus Ltd, Cambridge, UK). The right common carotid artery was cannulated and connected to a pressure transducer to measure heart rate and blood pressure throughout the procedure (Powerlab data acquisition system, AD instruments, Abingdon, UK). The left jugular vein was cannulated for drug administration. The trachea was cannulated *via* tracheotomy and the animal ventilated with room air by a

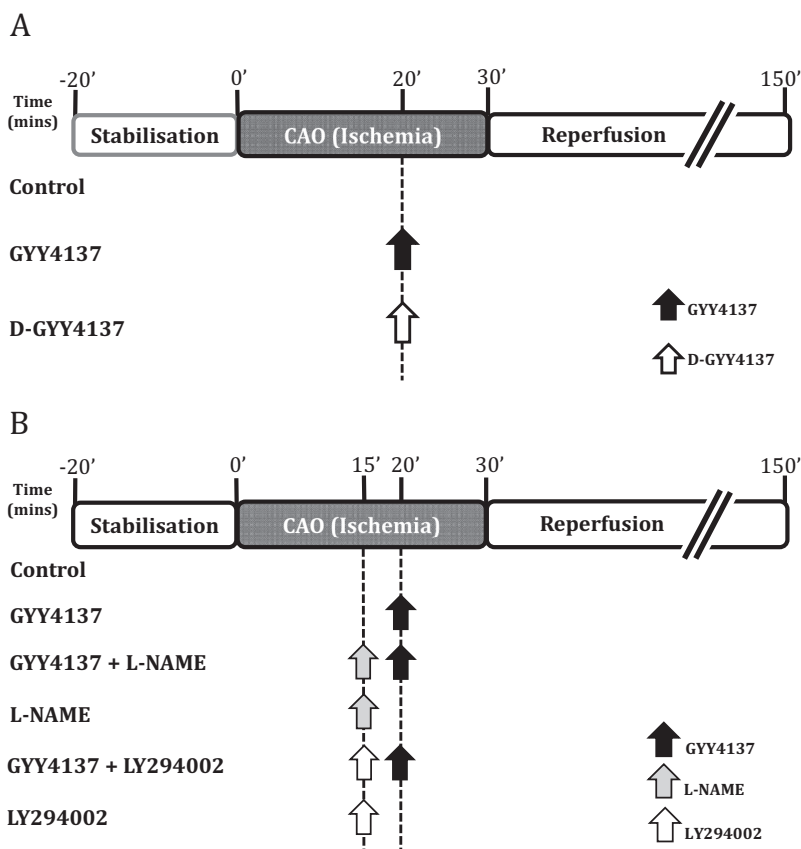


Fig. 1. Treatment protocols. (A) **Series 1 infarct studies.** After surgical preparation, rats were stabilised for 20 min then subjected to 30 min of left coronary artery occlusion (CAO) followed by 120 min of reperfusion. Control rats did not receive any further intervention, while treatment groups received one of three GYY4137 doses or depleted GYY4137 (D-GYY4137) 10 min before reperfusion. Hearts were excised at the end of reperfusion for infarct size determination, $n=6-10$. Arrows indicate the time of pharmacological interventions. (B) **Series 2 infarct studies.** Following stabilisation, rats were subjected to 30 min of left coronary artery occlusion and 120 min of reperfusion. Animals were randomised into six groups. Control heart did not receive any further intervention. GYY4137 was administered 10 min before reperfusion. LY294002 and L-NAME were administered 15 min before reperfusion. Hearts were excised at the end of reperfusion for infarct size determination, $n=6-7$. Parallel groups, $n=4$, were prepared identically but hearts were excised 5 min after reperfusion for analysis by immunoblotting. Arrows indicate the time of pharmacological interventions.

small animal volume controlled ventilator (Hugo Sachs Elektronik, March, Germany) at a rate of 75 strokes min^{-1} and tidal volume of 1.0–1.25 mL 100 g^{-1} . The electrocardiogram was recorded using standard lead II electrodes inserted subcutaneously into the limbs and connected to a Powerlab data acquisition system. A midline sternotomy was performed and the chest opened using a metal retractor to expose the heart. After pericardiotomy, a 4/0 braided silk suture (Mersilk, Ethicon Ltd, UK) was placed around the left main coronary artery close to its origin from the left border of the pulmonary conus. The animal was left to stabilise for 20 min during which the two ends of the silk ligature remained loose. For each animal to be included it had to achieve the following hemodynamic parameters during the stabilisation period: heart rate ≥ 250 beats per minute, diastolic blood pressure ≥ 50 mmHg, steady sinus rhythm, no signs of ischemia or arrhythmia during the stabilisation period.

After stabilisation, the ligature was pulled taut through a plastic snare and fastened against the epicardium to induce regional ischemia for 30 min. Ischemia was confirmed by a drop in the mean arterial pressure (MAP), a colour change of the left ventricle (from red to pale), and ECG changes (ST-segment elevation). After 30 min, the snare was released to allow reperfusion for 120 min. Successful reperfusion was confirmed by hyperemic colour change of the ischemic tissue bed, occurrence of reperfusion-induced arrhythmia during the first minute after reperfusion, and an increase in the MAP.

2.4. Infarct size determination

After 120 min reperfusion, the heart was excised and perfused via the aorta with saline on a modified Langendorff apparatus. After re-occluding the coronary ligature, the heart was perfused with 2% Evans' blue dye to identify the ischemic zone (area at risk, AAR). The heart was then frozen at -20°C for 5–24 h. The frozen heart was transversely sliced at 2 mm thickness into 5–6 sections from apex to base and the sections incubated with triphenyltetrazolium chloride (TTC) 1% w/v in phosphate buffered saline (PBS; pH 7.4) at 37°C for 15 min. TTC is reduced to a red formazan pigment in viable tissue while necrotic tissue is unstained. Stained sections were fixed in 4% formalin in PBS for 24 h before being scanned. Planimetry was conducted using the image analysis program Image J (version 1.47, NIH, Bethesda, USA). Sections were coded so that image analysis was undertaken in a blinded fashion to obviate bias. Planimetric analysis determined the total ventricular area, the AAR (Evans blue negative), and the infarcted area (TTC negative). These areas were then converted into volumes by multiplying each total area by 2 mm section thickness and the infarct size was reported as a percentage of the area at risk volume (% I/AAR).

2.5. Treatment protocols

Treatment protocols are illustrated in Fig. 1. Two separate series of experiments were undertaken. The first series examined the dose-dependent effects of GYY4137 on infarct size and the involve-

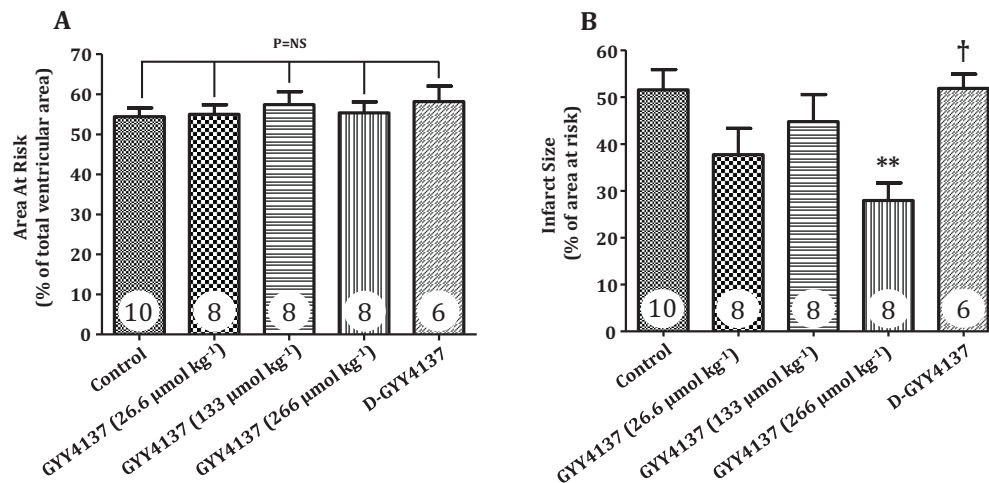


Fig. 2. Infarct size data: GYY4137 dose-response study (Series 1). Area at risk was determined Evans' blue exclusion and infarction was assessed by TTC staining. GYY4137 was administered at 26.6, 133, or 266 $\mu\text{mol kg}^{-1}$ 10 min before reperfusion. (A) Area at risk as a percentage of the total ventricular volume. (B) Myocardial infarction expressed as a percentage of the area at risk. Numbers in histograms indicate sample size. ** $P < 0.01$ versus Control; † $p < 0.05$ versus GYY4137 266 $\mu\text{mol kg}^{-1}$ (one way ANOVA with Newman Keuls *post hoc* test).

ment of H_2S in mediating any responses. The dose range employed in these studies was derived from previous studies in the rat heart *ex vivo* by our group [50] and *in vivo* studies conducted by others [33,38]. Animals were randomly assigned to one of five groups (Fig. 1A):

- Group 1: Control (n=9). Animals were subjected to coronary occlusion and reperfusion with saline given as a slow i.v. bolus 10 min before reperfusion.
- Group 2–4: Each group (n=8) received GYY4137 at 26.6, 133 or 266 $\mu\text{mol kg}^{-1}$, respectively as a slow i.v. bolus (500 $\mu\text{L min}^{-1}$) 10 min before reperfusion.
- Group 5: Depleted GYY4137 (n=6). GYY4137 solution (100 mg mL^{-1}) was prepared in saline and left uncovered for 72 h at room temperature to dissipate all H_2S , then administered at a dose of 266 $\mu\text{mol kg}^{-1}$ i.v. 10 min before reperfusion.

The second series of experiments explored the involvement of RISK pathway components in the cardioprotective effect of GYY4137. The optimum dose of GYY4137 (266 $\mu\text{mol kg}^{-1}$) was selected from the first series and animals were randomised into six treatment groups (Fig. 1B).

Group 6: Control (n=7). Animals were subjected to coronary occlusion and reperfusion with saline or DMSO 5% given as a slow i.v. bolus 15 min before reperfusion. DMSO was used as vehicle for LY294002. Since DMSO exerted no effect on cardiodynamics or infarct size, saline and DMSO treated animals are reported collectively.

- Group 7: GYY4137 (n=7). A slow bolus dose of GYY4137 (266 $\mu\text{mol kg}^{-1}$, 500 $\mu\text{L min}^{-1}$) was administered at 10 min before reperfusion.
- Group 8: GYY4137 + L-NAME (n=7). An intravenous bolus dose of L-NAME (20 mg kg^{-1}) was administered 15 min before reperfusion followed by GYY4137 (266 $\mu\text{mol kg}^{-1}$, 500 $\mu\text{L min}^{-1}$) 10 min before reperfusion.
- Group 9: L-NAME (n=6). An intravenous bolus dose of L-NAME (20 mg kg^{-1}) was administered 15 min before reperfusion.
- Group 10: GYY4137 + LY294002 (n=6). An intravenous bolus dose of LY294002 (0.1 mg kg^{-1} in 5% DMSO) was given 15 min before reperfusion followed by GYY4137 (266 $\mu\text{mol kg}^{-1}$, 500 $\mu\text{L min}^{-1}$) 10 min before reperfusion.

- Group 11: LY294002 (n=6). A bolus dose of LY294002 (0.1 mg kg^{-1} in 5% DMSO) was administered intravenously 15 min before reperfusion.

In a parallel series of experiments, rats were subjected to the same interventions as in groups 6–11 to prepare samples for biochemical analysis. After 5 min of reperfusion, the experiment was terminated and myocardial biopsies were harvested from the left ventricle, rapidly frozen in liquid nitrogen then kept at -80°C for Western blotting of Akt, eNOS, GSK-3 β and ERK1/2.

2.6. Western blotting analysis

To investigate the involvement of Akt, eNOS, GSK-3 β and ERK1/2, protein immunoblotting was carried out to analyse protein phosphorylation at 5 min of reperfusion. Myocardial biopsies were homogenised and lysed using a hard tissue lysing kit (Stretton Scientific Ltd, Stretton, UK). Equal amounts of protein were loaded onto 10% w/v sodium dodecyl sulfate-polyacrylamide gel, separated electrophoretically (120 mV) and transferred onto nitrocellulose membrane (Amersham, Germany). The membrane was then blocked with 5% skimmed milk for 2 h and probed with the primary antibody overnight at 4°C . The following antibodies were used: Akt (1:1000), phospho- ser⁴⁷³ Akt (1:1000), endothelial nitric oxide synthase (eNOS 1:500), phospho- ser¹¹⁷⁷ eNOS (1:500), glycogen-synthase kinase-3 beta (GSK-3 β 1:1000), phospho- ser⁹ GSK-3 β (1:1000), extracellular signal-regulated kinases ERK 1/2 (1:1000), phospho- Thr²⁰²/Tyr²⁰⁴ ERK 1/2 (1:1000) and GAPDH (1:50000). The immunoblots were probed with secondary antibody (goat anti-rabbit HRP, 1:15000, Cell Signalling UK) for 1 h then probed with Super Signal West Dura Extended Duration Substrate (Thermo Scientific) to visualise the bands on X-ray film. The film was scanned and densitometry was conducted in a blinded fashion using Image J software (1.48 v, National Institutes of Health USA). Phosphorylated and total protein bands were normalised to corresponding GAPDH bands and to baseline samples, harvested after 20 min of stabilisation, loaded at either side of each gel.

2.7. Statistical analysis

All data are reported as arithmetic mean \pm SEM. Data were analysed using GraphPad Prism[®] software (2007, Version 5.01, USA). Cardiodynamics including rate-pressure product (RPP, heart rate

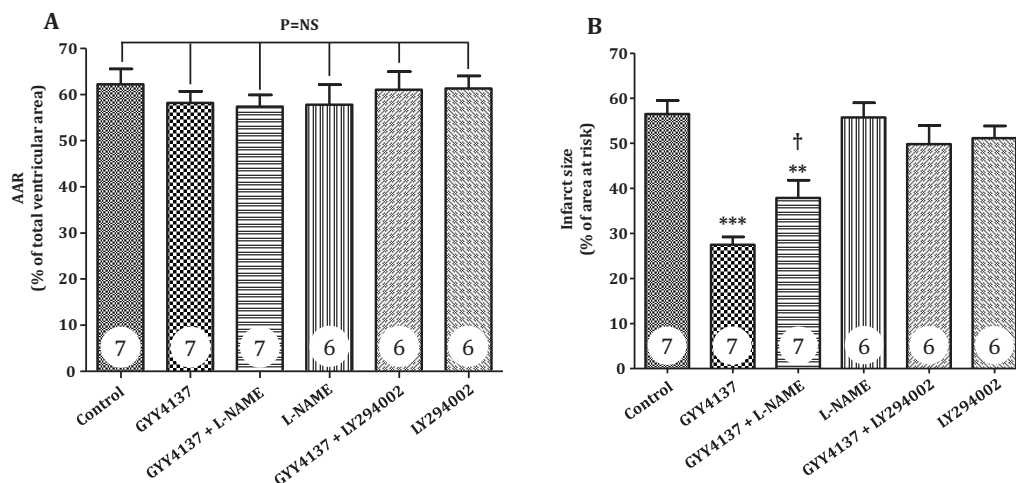


Fig. 3. Infarct size data: GYY4137 with pharmacological inhibitors (Series 2). Area at risk was determined Evans' blue exclusion and infarction was assessed by TTC staining. GYY4137 was administered at $266 \mu\text{mol kg}^{-1}$ 10 min before reperfusion. LY294002 or L-NAME were given 15 min before reperfusion. (A) Area at risk expressed as a percentage of the total ventricular volume. (B) Infarct size expressed as a percentage of the area at risk. Numbers in histograms indicate sample size. ** $p < 0.01$ versus Control; *** $p < 0.001$ versus control; † $p < 0.01$ versus GYY4137 (one way ANOVA with Newman Keuls *post hoc* test).

* systolic blood pressure) and mean arterial pressure (MAP, diastolic pressure + $1/3$ [systolic pressure – diastolic pressure]) were statistically analysed using repeated measures ANOVA supported by Bonferroni's *post hoc* test. Baseline data including body weight, RPP, and MAP passed the Kolmogorov-Smirnov normality test of distribution. Infarct size data were analysed using one way ANOVA supported by Newman-Keuls *post hoc* test. Differences between groups were considered significant if $p < 0.05$.

3. Results

In series 1, 42 rats were used, of which two were excluded from final analysis, one due to failure of TTC staining and one rat which did not survive the ischemia-reperfusion protocol. Thus data for 40 successfully completed experiments are reported. In series 2, 66 rats were employed, of which three did not complete the ischemia-reperfusion protocol. Thus, data from a total of 63 completed experiments are reported in series 2: these comprised 39 completed infarct size experiments and 24 preparations for Western blot analysis.

3.1. Hemodynamic parameters

Baseline hemodynamics for series 1 and 2 are summarised in Table 1. There was no significant difference in any of the parameters among the experimental groups. Cardiodynamics (MAP and RPP) measurements before ischemia, during ischemia and at the end of reperfusion are also presented in Table 1. GYY4137 had no detectable effect on cardiodynamics during the ischemia-reperfusion protocol.

3.2. Infarct size following GYY4137 postconditioning

Series 1 examined the response to three doses of GYY4137 on infarct size (Fig. 2). AAR constituted approximately 40–60% of the total ventricular volume with no significant differences among the treatment groups (Fig. 2A). Control infarct size (%I/AAR) was $52.5 \pm 4.7\%$ (Fig. 2B). GYY4137 ($266 \mu\text{mol kg}^{-1}$) produced significant infarct limitation when given 10 min before reperfusion compared to control hearts ($27.9 \pm 3.8\%$ vs $52.5 \pm 4.7\%$, $p < 0.01$). This represents a 47% relative reduction in infarct size. In contrast, depleted-GYY4137 (produced as described in [1] which lacked H_2S donating potential but was otherwise structurally identical had no

effect on infarct size at the same dose ($51.9 \pm 3.1\%$), confirming the dependency of GYY4137's infarct-limiting action on H_2S release.

3.3. Involvement of PI3K/Akt and eNOS in GYY4137 postconditioning

The second series of experiments was undertaken to examine components of the RISK signalling pathway in the protective effect of GYY4137 (Fig. 3). There was no significant difference in the AAR among the experimental groups (Fig. 3A). GYY4137 ($266 \mu\text{mol kg}^{-1}$) elicited a significant reduction in I/AAR compared to control ($27.6 \pm 2.0\%$ vs $56.8 \pm 3.5\%$, respectively, $p < 0.001$, Fig. 3B). Pharmacological inhibition of eNOS with L-NAME prior to GYY4137 almost halved the cardioprotective effect of GYY4137 ($41.1 \pm 6.3\%$ vs $27.6 \pm 2.0\%$, respectively, $p < 0.05$), but did not abolish it ($41.1 \pm 6.3\%$ vs $56.8 \pm 3.5\%$, respectively, $p < 0.01$, Fig. 3B). Concomitant administration of LY294002 to inhibit PI3K activity completely abrogated the cardioprotective effect of GYY4137 ($49.8 \pm 4.2\%$ vs $56.8 \pm 3.5\%$, respectively, $p > 0.05$). Neither L-NAME nor LY294002 had any effect on infarct size when given alone ($55.7 \pm 3.3\%$ and $51.2 \pm 2.7\%$ respectively, both $p > 0.05$ vs control).

The extent of phosphorylation of Akt, eNOS, GSK-3 β and ERK1/2 in early reperfusion was investigated with phospho-specific antibodies to determine the possible roles in cardioprotection by GYY4137. Immunoreactivity measurements were performed using myocardial tissue samples harvested from the left ventricle 5 min after reperfusion and are presented in Fig. 4A–D. There was no significant difference in protein expression to GAPDH of Akt, eNOS, GSK-3 β or ERK1/2 among any of the experimental groups. There was a significant 2.8-fold increase ($p < 0.001$ vs. control) in phospho-ser⁴⁷³ Akt at reperfusion following GYY4137 treatment (Fig. 4A). Prior administration of L-NAME did not limit this increase in Akt phosphorylation. However, administration of LY294002 alone or prior to GYY4137 abolished Akt phosphorylation (Fig. 5A). Postconditioning with GYY4137 also increased eNOS phosphorylation at the activating ser¹¹⁷⁷ site by 2.2-fold in early reperfusion ($p < 0.01$ vs. control; Fig. 4B). This activation was abrogated by prior administration of either L-NAME or LY294002. Ser⁹ phosphorylation of GSK-3 β was also increased 2.2-fold by GYY4137 (Fig. 4C). This phosphorylation, leading to inactivation of GSK-3 β , was not affected by L-NAME. However, pre-treatment with LY294002 prior to GYY4137 abrogated GSK-3 β phosphorylation. GYY4137 had no

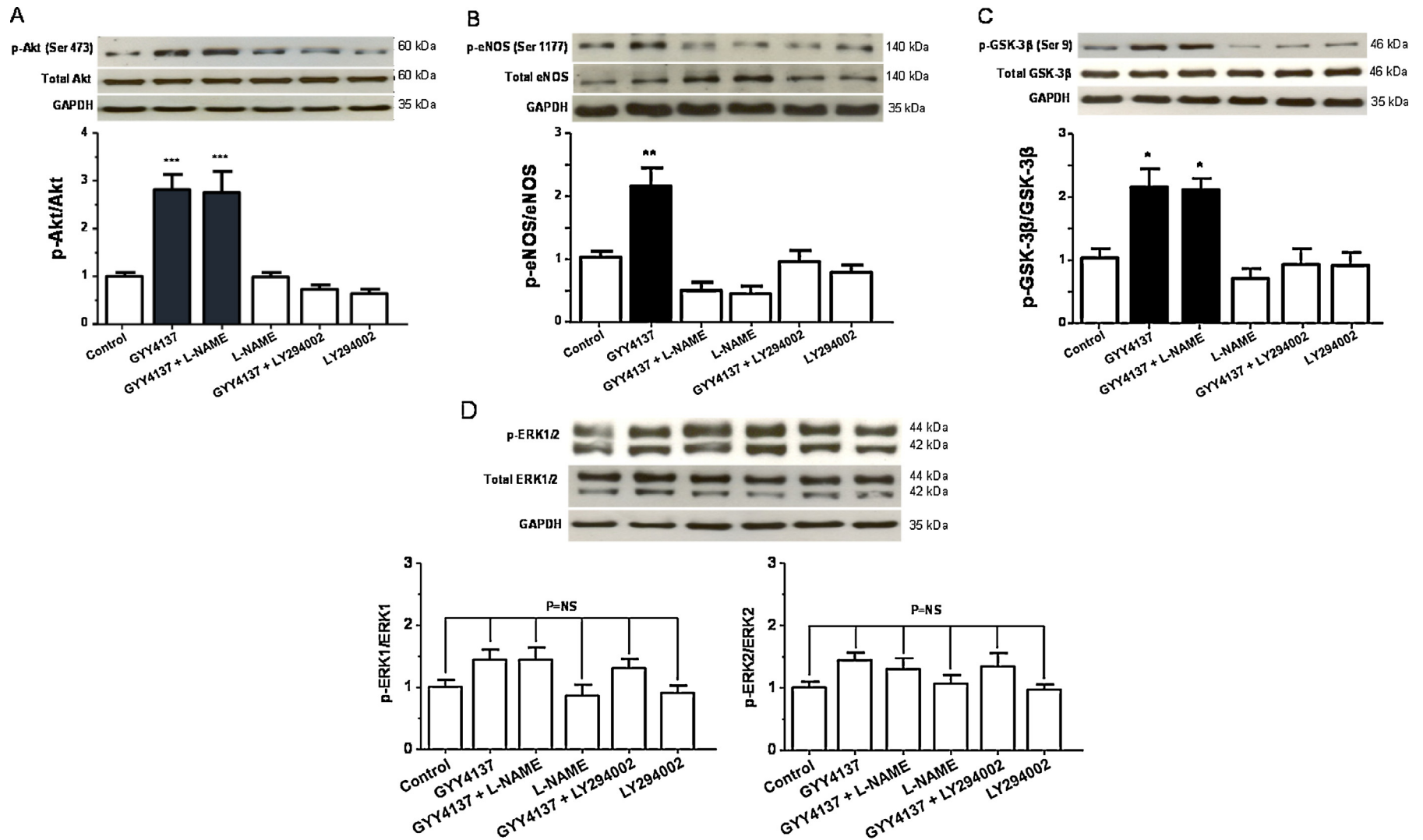


Fig. 4. Western blot analysis of left ventricular myocardium harvested from the area at risk 5 min after reperfusion. Histograms show densitometric ratios of phosphorylated to total protein. GAPDH was used as loading control for all determinations. (A) p-Akt, total Akt and GAPDH. (B) p-eNOS, total eNOS and GAPDH. (C) p-GSK-3 β , total GSK-3 β and GAPDH. (D) p-ERK1/2, total ERK1/2 and GAPDH. * $p < 0.05$, ** $p < 0.01$, *** $p < 0.001$ versus control. In all groups, $n = 4$.

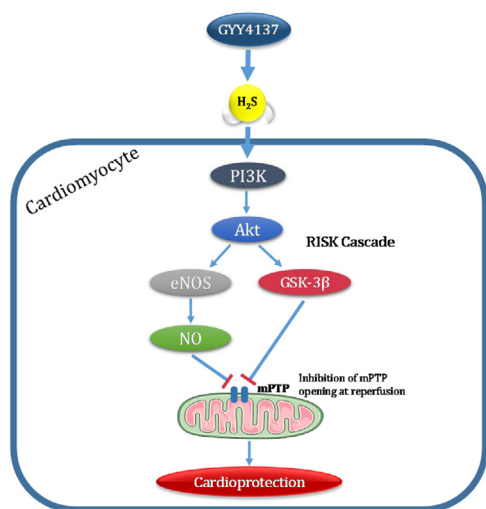


Fig. 5. GYY4137, a donor of H₂S, induces marked limitation of myocardial infarct size when given shortly before reperfusion. Based on the present experimental data, we present a mechanistic scheme by which GYY4137 mediates its cardioprotection against reperfusion injury. GYY4137 releases H₂S which triggers a key component of the reperfusion injury salvage kinase cascade, namely PI3K/Akt activation at reperfusion. Downstream of activated Akt, phosphorylation of eNOS and GSK-3β are induced by GYY4137 treatment. Although not yet determined, it seems plausible that GYY4137 eventually inhibits the opening of mPTP at early reperfusion as a result of the increase in NO level and inhibition GSK-3β activity, resulting in reduced cardiomyocyte susceptibility to lethal reperfusion injury.

significant effect on the phosphorylation of ERK1/2 at early reperfusion (Fig. 4D).

4. Discussion

The principal observations of this study can be summarised as follows:

- 1 GYY4137 limited myocardial infarction *in vivo* when given specifically prior to reperfusion indicating potent attenuation of lethal reperfusion injury in a postconditioning-like manner.
- 2 The infarct-limiting effect of GYY4137 at early reperfusion was mediated through activation of the PI3K/Akt survival cascade.
- 3 There was a partial dependency of GYY4137's protective effect on increased eNOS activation.
- 4 GYY4137 inhibited GSK-3β activity at early reperfusion by increasing the phosphorylation of its ser⁹ site downstream of PI3K/Akt signalling.

These findings support the hypothesis that administration of GYY4137 at reperfusion can protect the heart against reperfusion injury by activating the key components of the RISK cascade (PI3K/Akt/NO) and inhibition of GSK-3β activity.

4.1. Infarct limitation by GYY4137

The results show for the first time the effect of GYY4137, as a slow-releasing H₂S donor, on myocardial infarction in an *in vivo* model. Intracellular levels of H₂S are reported to be decreased during ischaemia-reperfusion as a result of overwhelming ROS generation which limits H₂S synthesis and increases its degradation [51]. GYY4137 elicited significant infarct limitation when administered prior to reperfusion. Depleted GYY4137 [1] was employed as a control to ensure that any detectable effect was due to H₂S released and not by the parent molecule or by-products formed from GYY4137 decomposition. Depleted GYY4137 had no effect on infarct size and this is consistent with previous studies where

loss of H₂S from GYY4137 was shown to be associated with loss of biological activity [32,53,13,23,1].

This is the first study of pharmacological postconditioning against reperfusion injury *in vivo* using GYY4137 as a stable H₂S donor. Although inorganic H₂S generators (NaSH and Na₂S) have been used in different experimental species, the specific targeting of reperfusion injury by GYY4137 in this study is novel. Several studies have investigated the effect of H₂S against myocardial ischemia-reperfusion when commercially available sulfide salts were perfused or given pre-ischemia. For example, Johansen et al. [24] were the first to show that NaSH limited infarct size in a rat isolated heart preparation, while Pan et al. [40], Sivarajah et al. [46], Zhuo et al. [59] and Yao et al. [55] all showed that NaSH limited infarct size in an *in vivo* rat model through diverse mechanisms. Part of this variation is arguably due to the unstable nature of these H₂S sources, in addition to the different experimental conditions and end-points of interest. Using garlic derivative as an organic source of H₂S, Zhang et al. [57] and Chuah et al. [9] reported that allitridum and S-allylcysteine respectively also elicited cardioprotection against myocardial infarction when given before ischemia. Preconditioning the heart with the thiol derivative S-diclofenac was also protective partially through the opening of mitochondrial K_{ATP} channels [45]. Investigators also have examined the possibility of postconditioning the myocardium using NaSH and Na₂S. For example, Elrod et al. [11], Sodha et al. [48] and Lambert et al. [28] all reported that Na₂S protected mouse heart against myocardial infarction *in vivo* when given at reperfusion. Bibli et al. [4] showed that a bolus dose of NaSH 10 min before reperfusion then continuous infusion of NaSH till the end of reperfusion was required to significantly exert cardioprotection in rabbit. In comparison with these results, in this study we showed that a single bolus dose of GYY4137 at reperfusion had a significant cardioprotective effect against myocardial infarction in the rat. To our knowledge, the only other long-lasting H₂S donors that have been reported are the polysulfide diallyl trisulfide (DATS) and SG-1002, a thiol-activated H₂S donor. Despite generating 10 times less H₂S than Na₂S, DATS was shown to improve mitochondrial respiration and stimulate eNOS at reperfusion in an *in vivo* mouse model of ischemia-reperfusion injury. However, DATS is a polysulfide compound, and thus cannot be considered a pure H₂S donor with the possibility of off-target effects. Moreover, H₂S release from GYY4137 is reported to last longer compare to DATS [33,43]. In the setting of pressure-overload-induced heart failure, SG-1002-treated hearts were protected during transverse aortic constriction *via* triggering VEGF/Akt/eNOS/NO/cGMP pathway. Recently, SG-1002 has successfully passed Phase I clinical study in patient with heart failure (ClinicalTrials.gov #NCT01989208 and #NCT02278276), by increasing blood H₂S level and circulating NO bioavailability [42]. However, none of these studies have shown that the observed effects are due to H₂S release due to the lack of negative control (like depleted GYY4137, for example). Therefore, there is persuasive experimental evidence that a stable level of H₂S release confers effective cardioprotection against ischemia-reperfusion injury. The present study confirms for the first time that administration of GYY4137 prior to reperfusion (postconditioning), rather than prior to coronary artery occlusion (preconditioning), exerts a marked cardioprotective effect due to H₂S-releasing capacity.

4.2. GYY4137 postconditioning activates PI3K/Akt signalling

The second series of experiments aimed to explore the signalling mechanisms underpinning the protective effect of GYY4137. The involvement during early reperfusion of specific kinase mechanisms, notably activation of PI3K/Akt and/or ERK1/2, activation of eNOS and inhibition of GSK-3β, has attracted considerable attention in relation to cardiac conditioning phenomena, especially

postconditioning. Elucidation of the RISK pathway has confirmed that it is a key modulator of protection against reperfusion injury in many species, although not all. Here, we explored the effects of pharmacological inhibition of two key components, PI3K/Akt and eNOS, confirmed by assessment of the phosphorylation status of these proteins. We found that the PI3K inhibitor LY294002 abrogated the infarct-limiting effect of GYY4137 which indicated the involvement of PI3K/Akt survival pathway in cardioprotection established by GYY4137. This was supported by the observation that GYY4137 increased Akt phosphorylation in left ventricular myocardium during early reperfusion, an effect abolished by LY294002. Li et al. [30] showed that NaSH at reperfusion limited cell death by activating PI3K/Akt pathway in aging rat heart and cardiomyocytes. However, Lambert et al. [28] demonstrated that in diabetic rats NaSH-induced postconditioning might signal through the other arm of the RISK pathway, namely ERK1/2. LY294002 alone had no significant effect on either the infarct size or Akt phosphorylation compared to control which is consistent with the findings of other investigators [52,2]. This suggests that the PI3K/Akt pathway is almost inactive at basal physiological levels of H₂S.

We also investigated the involvement of ERK1/2 in cardioprotection established by GYY4137. In contrast to Akt phosphorylation, we observed no significant increase in ERK1/2 phosphorylation at early reperfusion following postconditioning with GYY4137. It has been reported by others that a bolus dose of Na₂S at reperfusion could activate ERK1/2 and also inhibit GSK-3β [28,31,4]. However, since in our hands GSK-3β phosphorylation (leading to enzyme inhibition) by GYY4137 was abrogated by LY294002, this suggests it is downstream of PI3K/Akt, rather than ERK1/2. It again emphasises the physiological differences between bolus sulfide (with NaSH or Na₂S) and H₂S generated in a more physiological manner (with GYY4137).

4.3. Dependency of GYY4137-postconditioning on NO

Inhibition of NO synthesis using L-NAME had no effect on the infarct size *per se* which is consistent with other investigators [14,21]. This observation implies that NO does not afford any cardioprotection against myocardial infarction at basal physiological levels. GYY4137 treatment induced an increase in the phosphorylation of eNOS at its activating site, ser¹¹⁷⁷ suggesting that NO bioavailability is increased following GYY4137 treatment. L-NAME prior to GYY4137 administration limited the phosphorylation of eNOS and partially attenuated infarct limitation but did not completely abolish the protective effect. These data suggest that enhancing NO bioavailability synergises the cardioprotection of GYY4137 against reperfusion injury but blocking eNOS phosphorylation only partially limits the cardioprotection of GYY4137, suggesting the involvement of parallel NO-independent pathway(s). There has been considerable interest in cross-regulation of NO and H₂S but the nature of their interactions is uncertain, at least in part because of the large variation in experimental conditions.

SG-1002, H₂S donor, was protective and increased NO bioavailability in an *in vivo* model of heart failure [27]. An increase in NO metabolites following DATS treatment was also observed by Lefler and co-workers [43], in mouse heart. King et al. [26] found that H₂S did not limit infarction in eNOS phospho-mutant (S1179A) or eNOS knockout mice. Considered together, these studies suggest that an increase in one of the gaseous mediators can eventually lead to an increase in the other but the picture is obscured by variations across species, pathological models and tissue types. The NO-dependency of H₂S has recently been studied by Bibli et al. [4] in an *in vivo* model of myocardial infarction using two species, rabbit and mouse. Pharmacologically limiting NO availability with L-NAME did not limit the protection of NaSH in rabbits, while genetic mutation or pharmacological blockade of eNOS totally abolished

H₂S-induced protection in mice. Dependency of NaSH-induced cardioprotection on NO in mice was previously reported by Sojitra et al. [49]. Together and in line with our data, it seems plausible that NO involvement in the infarct-limiting effect of H₂S could be tissue and/or species-dependent. Further detailed work needs to be carried out for better understanding of the molecular pharmacology of these molecules and to enhance the clinical implementation of H₂S-delivering systems.

4.4. GYY4137 postconditioning attenuates GSK-3β phosphorylation

GSK-3β has been proposed as one of the key end effectors of some cardioprotective manoeuvres, particularly ischemic conditioning phenomena. It has been demonstrated that GSK-3β promotes the opening of mPTP during reperfusion, an event thought to be a major determinant of cell death [7]. In isolated cardiomyocytes, Yao et al. [54] and Li et al. [31] found that NaSH protected against hypoxia/reoxygenation induced cell death by inhibiting GSK-3β-dependent opening of mPTP. In line with these results, the present study demonstrated that GYY4137 increased the phosphorylation of GSK-3β at Ser⁹ site at reperfusion. This was abolished by LY294002, but not by L-NAME, suggesting that GYY4137 induced inhibition of GSK-3β is downstream of PI3K/Akt. There is evidence that the increase in Akt phosphorylation [18] and NO bioavailability [6] at early reperfusion may also inhibit the opening of mPTP. Considering these data together, it seems plausible that postconditioning with GYY4137 is associated with a reduced susceptibility of mPTP opening, although this remains to be determined by specific measurements of mPTP opening.

4.5. Study limitations

There are still questions which this study did not address and they could be interesting topics for further investigations. This study found that GYY4137 activates the RISK pathway at early minutes of reperfusion to limit the infarct size where infarction was quantified after 2 h of reperfusion. Nevertheless, whether GYY4137 could exert a comparable cardioprotection *via* similar or different mechanism(s) with longer reperfusion protocol, where there could be no-flow phenomena or late apoptosis, needs to be investigated. Although spent-GYY4137 did not exert any cardioprotection, the direct effect of GYY4137 administration on the level of H₂S in the heart and circulation needs to be measured. Similarly, measuring the proposed elevation in NO bioavailability as a result of activating eNOS at reperfusion by GYY4137 administration could also underpin the conclusion.

5. Conclusion

In summary, we have demonstrated that the slow-releasing H₂S donor GYY4137, but not its H₂S-depleted control, protected the heart against lethal reperfusion injury when administered as an adjunct treatment prior to reperfusion. This cardioprotective action is dependent on activation of PI3K/Akt signalling pathway at early reperfusion, which in turn, increases NO bioavailability by increasing eNOS phosphorylation, and increases the phosphorylation of GSK-3β (see Fig. 5, Graphical Abstract). Thus, stable slow-releasing H₂S donor compounds may be promising candidates for the development of adjunct therapies to reperfusion for the treatment of acute myocardial infarction.

Conflicts of interest

None.

Acknowledgements

QK acknowledges the generous support of the Iraqi Ministry of Higher Education and Scientific Research. RT is the recipient of The Brian Ridge Scholarship.

Appendix A. Supplementary data

Supplementary data associated with this article can be found, in the online version, at <http://dx.doi.org/10.1016/j.phrs.2016.06.028>.

References

- [1] B.E. Alexander, S.J. Coles, B.C. Fox, T.F. Khan, J. Maliszewski, A. Perry, M.B. Pitak, M. Whiteman, M.E. Wood, Investigating the generation of hydrogen sulfide from the phosphoramidodithioate slow-release donor GYY4137, *Med. Chem. Commun.* 6 (2015) 1649–1655.
- [2] V. Barsukevich, M. Basalay, J. Sanchez, A. Mrochek, J. Whittle, G.L. Ackland, A.V. Gourine, A. Gourine, Distinct cardioprotective mechanisms of immediate, early and delayed ischaemic preconditioning, *Basic Res. Cardiol.* 110 (2015) 452.
- [3] J.S. Bian, Q.C. Yong, T.T. Pan, Z.N. Feng, M.Y. Ali, S. Zhou, P.K. Moore, Role of hydrogen sulfide in the cardioprotection caused by ischemic preconditioning in the rat heart and cardiac myocytes, *J. Pharmacol. Exp. Ther.* 316 (2006) 670–678.
- [4] S.I. Bibli, I. Andreadou, A. Chatzianastasiou, C. Tzimas, D. Sanoudou, E. Kranias, P. Brouckaert, C. Coletta, C. Szabo, D.T. Kremastinos, E.K. Iliodromitis, A. Papapetropoulos, Cardioprotection by H₂S engages a cGMP-dependent protein kinase G/phospholamban pathway, *Cardiovasc. Res.* 106 (2015) 432–442.
- [5] D.S. Burley, G.F. Baxter, Pharmacological targets revealed by myocardial preconditioning, *Curr. Opin. Pharmacol.* 9 (2009) 177–188.
- [6] D.S. Burley, P. Ferdinandy, G.F. Baxter, Cyclic GMP and protein kinase-G in myocardial ischaemia-reperfusion: opportunities and obstacles for survival signaling, *Br. J. Pharmacol.* 152 (2007) 855–869.
- [7] H.A. Cabrera-Fuentes, C. Alba-Alba, J. Aragonés, J. Bernhagen, W.A. Boisvert, H.E. Botker, G. Cesarman-Maus, I. Fleming, D. Garcia-Dorado, S. Lecour, E. Liehn, M.S. Marber, N. Marina, M. Mayr, O. Perez-Mendez, T. Miura, M. Ruiz-Meana, E.M. Salinas-Estefanon, S.B. Ong, H.J. Schnittler, J.T. Sanchez-Vega, A. Sumoza-Toledo, C.W. Vogel, D. Yarullina, D.M. Yellon, K.T. Preissner, D.J. Hausenloy, Meeting report from the 2nd International Symposium on New Frontiers in Cardiovascular Research. Protecting the cardiovascular system from ischemia: between bench and bedside, *Basic Res. Cardiol.* 111 (2016) 7.
- [8] J.W. Calvert, S. Jha, S. Gundewar, J.W. Elrod, A. Ramachandran, C.B. Pattillo, C.G. Kevil, D.J. Lefer, Hydrogen sulfide mediates cardioprotection through Nrf2 signaling, *Circ. Res.* 105 (2009) 365–374.
- [9] S.C. Chuah, P.K. Moore, Y.Z. Zhu, S-allylcysteine mediates cardioprotection in an acute myocardial infarction rat model via a hydrogen sulfide-mediated pathway, *Am. J. Physiol. Heart Circ. Physiol.* 293 (2007) H2693–H2701.
- [10] A. Das, A. Samidurai, N.N. Hoke, R.C. Kukreja, F.N. Salloum, Hydrogen sulfide mediates the cardioprotective effects of gene therapy with PKG-1 α , *Basic Res. Cardiol.* 110 (2015) 42.
- [11] J.W. Elrod, J.W. Calvert, J. Morrison, J.E. Doeller, D.W. Kraus, L. Tao, X. Jiao, R. Scalia, L. Kiss, C. Szabo, H. Kimura, C.W. Chow, D.J. Lefer, Hydrogen sulfide attenuates myocardial ischemia-reperfusion injury by preservation of mitochondrial function, *Proc. Natl. Acad. Sci. U. S. A.* 104 (2007) 15560–15565.
- [12] P. Ferdinandy, D.J. Hausenloy, G. Heusch, G.F. Baxter, R. Schulz, Interaction of risk factors, comorbidities, and comedications with ischemia/reperfusion injury and cardioprotection by preconditioning, postconditioning, and remote conditioning, *Pharmacol. Rev.* 66 (2014) 1142–1174.
- [13] B. Fox, J.T. Schantz, R. Haigh, M.E. Wood, P.K. Moore, N. Viner, J.P. Spencer, P.G. Winyard, M. Whiteman, Inducible hydrogen sulfide synthesis in chondrocytes and mesenchymal progenitor cells: is H₂S a novel cytoprotective mediator in the inflamed joint? *J. Cell. Mol. Med.* 16 (2012) 896–910.
- [14] J. Fradorf, R. Huhn, N.C. Weber, D. Ebel, N. Wingert, B. Preckel, O. Toma, W. Schlack, M.W. Hollmann, Sevoflurane-induced preconditioning: impact of protocol and aprotinin administration on infarct size and endothelial nitric-oxide synthase phosphorylation in the rat heart in vivo, *Anesthesiology* 113 (2010) 1289–1298.
- [15] E. Grambow, F. Mueller-Graf, E. Delyagina, M. Frank, A. Kuhla, B. Vollmar, Effect of the hydrogen sulfide donor GYY4137 on platelet activation and microvascular thrombus formation in mice, *Platelets* 25 (2014) 166–174.
- [16] B.T. Hackfort, P.K. Mishra, Emerging role of hydrogen sulfide-microRNA cross-talk in cardiovascular diseases, *Am. J. Physiol. Heart Circ. Physiol.* ajpheart 00660 (2016) 2015.
- [17] S.J. Han, J.I. Kim, J.W. Park, K.M. Park, Hydrogen sulfide accelerates the recovery of kidney tubules after renal ischemia/reperfusion injury, *Nephrol. Dial. Transplant.* 30 (2015) 1497–1506.
- [18] D.J. Hausenloy, S.B. Ong, D.M. Yellon, The mitochondrial permeability transition pore as a target for preconditioning and postconditioning, *Basic Res. Cardiol.* 104 (2009) 189–202.
- [19] D.J. Hausenloy, D.M. Yellon, Reperfusion injury salvage kinase signalling: taking a RISK for cardioprotection, *Heart Fail. Rev.* 12 (2007) 217–234.
- [20] Y.E. Huang, Z.H. Tang, W. Xie, X.T. Shen, M.H. Liu, X.P. Peng, Z.Z. Zhao, D.B. Nie, L.S. Liu, Z.S. Jiang, Endogenous hydrogen sulfide mediates the cardioprotection induced by ischemic preconditioning in the early reperfusion phase, *Exp. Ther. Med.* 4 (2012) 1117–1123.
- [21] A. Imani, M. Faghihi, S.S. Sadr, S.S. Niaraki, A.M. Alizadeh, Noradrenaline protects in vivo rat heart against infarction and ventricular arrhythmias via nitric oxide and reactive oxygen species, *J. Surg. Res.* 169 (2011) 9–15.
- [22] K.N. Islam, D.J. Polhemus, E. Donnarumma, L.P. Brewster, D.J. Lefer, Hydrogen sulfide levels and nuclear factor-erythroid 2-related factor 2 (NRF2) activity are attenuated in the setting of critical limb ischemia (CLI), *J. Am. Heart Assoc.* 4 (2015).
- [23] A. Jamroz-Wisniewska, A. Gertler, G. Solomon, M.E. Wood, M. Whiteman, J. Beltowski, Leptin-induced endothelium-dependent vasorelaxation of peripheral arteries in lean and obese rats: role of nitric oxide and hydrogen sulfide, *PLoS One* 9 (2014) e86744.
- [24] D. Johansen, K. Ytrehus, G.F. Baxter, Exogenous hydrogen sulfide (H₂S) protects against regional myocardial ischemia-reperfusion injury-Evidence for a role of K⁺ATP channels, *Basic Res. Cardiol.* 101 (2006) 53–60.
- [25] C. Kilkenny, W. Browne, I.C. Cuthill, M. Emerson, D.G. Altman, N. C. R. G. W. Group, Animal research: reporting in vivo experiments: the ARRIVE guidelines, *Br. J. Pharmacol.* 160 (2010) 1577–1579.
- [26] A.L. King, D.J. Polhemus, S. Bhushan, H. Otsuka, K. Kondo, C.K. Nicholson, J.M. Bradley, K.N. Islam, J.W. Calvert, Y.X. Tao, T.R. Dugas, E.E. Kelley, J.W. Elrod, P.L. Huang, R. Wang, D.J. Lefer, Hydrogen sulfide cytoprotective signaling is endothelial nitric oxide synthase-nitric oxide dependent, *Proc. Natl. Acad. Sci. U. S. A.* 111 (2014) 3182–3187.
- [27] K. Kondo, S. Bhushan, A.L. King, S.D. Prabhu, T. Hamid, S. Koenig, T. Murohara, B.L. Predmore, G. Gojon SR, G. Gojon JR, R. Wang, N. Karusula, C.K. Nicholson, J.W. Calvert, D.J. Lefer, H₂S protects against pressure overload-induced heart failure via upregulation of endothelial nitric oxide synthase, *Circulation* 127 (2013) 1116–1127.
- [28] J.P. Lambert, C.K. Nicholson, H. Amin, S. Amin, J.W. Calvert, Hydrogen sulfide provides cardioprotection against myocardial/ischemia reperfusion injury in the diabetic state through the activation of the RISK pathway, *Med. Gas Res.* 4 (2014) 20.
- [29] Z.W. Lee, J. Zhou, C.S. Chen, Y. Zhao, L. Li, L.W. Deng, The slow-releasing hydrogen sulfide donor, GYY4137, exhibits novel anti-cancer effects in vitro and in vivo, *PLoS One* 6 (2011) e21077.
- [30] H. Li, Y. Wang, C. Wei, S. Bai, Y. Zhao, H. Li, B. Wu, R. Wang, L. Wu, C. Xu, Mediation of exogenous hydrogen sulfide in recovery of ischemic post-conditioning-induced cardioprotection via down-regulating oxidative stress and up-regulating PI3K/Akt/GSK-3 β pathway in isolated aging rat hearts, *Cell Biosci.* 5 (2015) 11.
- [31] H. Li, C. Zhang, W. Sun, L. Li, B. Wu, S. Bai, H. Li, X. Zhong, R. Wang, L. Wu, C. Xu, Exogenous hydrogen sulfide restores cardioprotection of ischemic post-conditioning via inhibition of mPTP opening in the aging cardiomyocytes, *Cell Biosci.* 5 (2015) 43.
- [32] L. Li, M. Salto-Tellez, C.H. Tan, M. Whiteman, P.K. Moore, GYY4137, a novel hydrogen sulfide-releasing molecule, protects against endotoxic shock in the rat, *Free Radic. Biol. Med.* 47 (2009) 103–113.
- [33] L. Li, M. Whiteman, Y.Y. Guan, K.L. Neo, Y. Cheng, S.W. Lee, Y. Zhao, R. Baskar, C.H. Tan, P.K. Moore, Characterization of a novel, water-soluble hydrogen sulfide-releasing molecule (GYY4137): new insights into the biology of hydrogen sulfide, *Circulation* 117 (2008) 2351–2360.
- [34] M. Lisjak, N. Srivastava, T. Teklic, L. Civalo, K. Lewandowski, I. Wilson, M.E. Wood, M. Whiteman, J.T. Hancock, A novel hydrogen sulfide donor causes stomatal opening and reduces nitric oxide accumulation, *Plant Physiol.* Biochem. 48 (2010) 931–935.
- [35] Y.H. Liu, M. Lu, L.F. Hu, P.T. Wong, G.D. Webb, J.S. Bian, Hydrogen sulfide in the mammalian cardiovascular system, *Antioxid. Redox Signal.* 17 (2012) 141–185.
- [36] Z. Liu, Y. Han, L. Li, H. Lu, G. Meng, X. Li, M. Shirhan, M.T. Peh, L. Xie, S. Zhou, X. Wang, Q. Chen, W. Dai, C.H. Tan, S. Pan, P.K. Moore, Y. Ji, The hydrogen sulfide donor, GYY4137, exhibits anti-atherosclerotic activity in high fat fed apolipoprotein E(-/-) mice, *Br. J. Pharmacol.* 169 (2013) 1795–1809.
- [37] J.C. Mcgrath, G.B. Drummond, E.M. McLachlan, C. Kilkenny, C.L. Wainwright, Guidelines for reporting experiments involving animals: the ARRIVE guidelines, *Br. J. Pharmacol.* 160 (2010) 1573–1576.
- [38] G. Meng, J. Wang, Y. Xiao, W. Bai, L. Xie, L. Shan, P.K. Moore, Y. Ji, GYY4137 protects against myocardial ischemia and reperfusion injury by attenuating oxidative stress and apoptosis in rats, *J. Biomed. Res.* 29 (2015) 203–213.
- [39] G. Meng, J. Zhu, Y. Xiao, Z. Huang, Y. Zhang, X. Tang, L. Xie, Y. Chen, Y. Shao, A. Ferro, R. Wang, P.K. Moore, Y. Ji, Hydrogen sulfide donor GYY4137 protects against myocardial fibrosis, *Oxid. Med. Cell Longevity* 2015 (2015) 691070.
- [40] T.T. Pan, Y.Q. Chen, J.S. Bian, All in the timing: a comparison between the cardioprotection induced by H₂S preconditioning and post-infarction treatment, *Eur. J. Pharmacol.* 616 (2009) 160–165.
- [41] A. Papapetropoulos, M. Whiteman, G. Cirino, Pharmacological tools for hydrogen sulphide research: a brief, introductory guide for beginners, *Br. J. Pharmacol.* 172 (2015) 1633–1637.

- [42] D.J. Polhemus, Z. Li, C.B. Pattillo, G. Gojon SR., G. Gojon JR., T. Giordano, H. Krum, A novel hydrogen sulfide prodrug, SG1002, promotes hydrogen sulfide and nitric oxide bioavailability in heart failure patients, *Cardiovasc. Ther.* 33 (2015) 216–226.
- [43] B.L. Predmore, K. Kondo, S. Bhushan, M.A. Zlatopolsky, A.L. King, J.P. Aragon, D.B. Grinsfelder, M.E. Condit, D.J. Lefer, The polysulfide diallyl trisulfide protects the ischemic myocardium by preservation of endogenous hydrogen sulfide and increasing nitric oxide bioavailability, *Am. J. Physiol. Heart Circ. Physiol.* 302 (2012) H2410–8.
- [44] H. Robinson, S. Wray, A new slow releasing, H(2)S generating compound, GYY4137 relaxes spontaneous and oxytocin-stimulated contractions of human and rat pregnant myometrium, *PLoS One* 7 (2012) e46278.
- [45] G. Rossoni, A. Sparatore, V. Tazzari, B. Manfredi, P. Del Soldato, F. Berti, The hydrogen sulphide-releasing derivative of diclofenac protects against ischaemia-reperfusion injury in the isolated rabbit heart, *Br. J. Pharmacol.* 153 (2008) 100–109.
- [46] A. Sivarajah, M. Collino, M. Yasin, E. Benetti, M. Gallicchio, E. Mazzon, S. Cuzzocrea, R. Fantozzi, C. Thiernemann, Anti-apoptotic and anti-inflammatory effects of hydrogen sulfide in a rat model of regional myocardial I/R, *Shock* 31 (2009) 267–274.
- [47] J.P. Sluijter, G. Condorelli, S.M. Davidson, F.B. Engel, P. Ferdinandy, D.J. Hausenloy, S. Lecour, R. Madonna, M. Ovize, M. Ruiz-Meana, R. Schulz, L.W. Van Laake, Nucleus of the European Society of Cardiology Working Group Cellular Biology of the Heart, Novel therapeutic strategies for cardioprotection, *Pharmacol. Ther.* 144 (2014) 60–70.
- [48] N.R. Sodha, R.T. Clements, J. Feng, Y. Liu, C. Bianchi, E.M. Horvath, C. Szabo, G.L. Stahl, F.W. Sellke, Hydrogen sulfide therapy attenuates the inflammatory response in a porcine model of myocardial ischemia/reperfusion injury, *J. Thorac. Cardiovasc. Surg.* 138 (2009) 977–984.
- [49] B. Sojitra, Y. Bulani, U.K. Putcha, A. Kanwal, P. Gupta, M. Kuncha, S.K. Banerjee, Nitric oxide synthase inhibition abrogates hydrogen sulfide-induced cardioprotection in mice, *Mol. Cell. Biochem.* 360 (2012) 61–69.
- [50] E. Suveren, M. Whiteman, G.F. Baxter, The cardioprotective effect of GYY4137, a novel H₂S donor, in ischaemia reperfusion injury, *Cardiovasc. Res.* 93 (2012), S111–S111.
- [51] M. Vandiver, S.H. Snyder, Hydrogen sulfide: a gasotransmitter of clinical relevance, *J. Mol. Med. (Berl.)* 90 (2012) 255–263.
- [52] J. Wang, H. Yang, X. Hu, W. Fu, J. Xie, X. Zhou, W. Xu, H. Jiang, Dobutamine-mediated heme oxygenase-1 induction via PI3K and p38 MAPK inhibits high mobility group box 1 protein release and attenuates rat myocardial ischemia/reperfusion injury in vivo, *J. Surg. Res.* 183 (2013) 509–516.
- [53] M. Whiteman, L. Li, P. Rose, C.H. Tan, D.B. Parkinson, P.K. Moore, The effect of hydrogen sulfide donors on lipopolysaccharide-induced formation of inflammatory mediators in macrophages, *Antioxid. Redox Signal.* 12 (2010) 1147–1154.
- [54] L.L. Yao, X.W. Huang, Y.G. Wang, Y.X. Cao, C.C. Zhang, Y.C. Zhu, Hydrogen sulfide protects cardiomyocytes from hypoxia/reoxygenation-induced apoptosis by preventing GSK-3 β -dependent opening of mPTP, *Am. J. Physiol. Heart Circ. Physiol.* 298 (2010) H1310–9.
- [55] X. Yao, G. Tan, C. He, Y. Gao, S. Pan, H. Jiang, Y. Zhang, X. Sun, Hydrogen sulfide protects cardiomyocytes from myocardial ischemia-reperfusion injury by enhancing phosphorylation of apoptosis repressor with caspase recruitment domain, *Tohoku J. Exp. Med.* 226 (2012) 275–285.
- [56] Q.C. Yong, S.W. Lee, C.S. Foo, K.L. Neo, X. Chen, J.S. Bian, Endogenous hydrogen sulphide mediates the cardioprotection induced by ischemic postconditioning, *Am. J. Physiol. Heart Circ. Physiol.* 295 (2008) H1330–H1340.
- [57] W.J. Zhang, Z.X. Shi, B.B. Wang, Y.J. Cui, J.Z. Guo, B. Li, Allitridum mimics effect of ischemic preconditioning by activation of protein kinase C, *Acta Pharmacol. Sin.* 22 (2001) 132–136.
- [58] Z.Q. Zhao, J.S. Corvera, M.E. Halkos, F. Kerendi, N.P. Wang, R.A. Guyton, J. Vinten-Johansen, Inhibition of myocardial injury by ischemic postconditioning during reperfusion: comparison with ischemic preconditioning, *Am. J. Physiol. Heart Circ. Physiol.* 285 (2003) H579–88.
- [59] Y. Zhuo, P.F. Chen, A.Z. Zhang, H. Zhong, C.Q. Chen, Y.Z. Zhu, Cardioprotective effect of hydrogen sulfide in ischemic reperfusion experimental rats and its influence on expression of survivin gene, *Biol. Pharm. Bull.* 32 (2009) 1406–1410.



Background: Hypoxic postconditioning (HpostC) is the cardioprotective strategy consisting in gradual recovery of oxygen supply after severe ischemia or hypoxia for to prevent oxidative heart injury in first minutes of reperfusion. Aim of this study was to verify possibilities to improve beneficial HpostC-induced effect by co-administration of molecular hydrogen (H₂). H₂ is considered as a selective antioxidant which reduces strong oxidants and simultaneously spares a physiological prosurvival cell signalling mediated by several oxygen free radicals (•O₂⁻, NO).

Methods: Experiments were performed on isolated rat hearts perfused with Krebs-Henseleit buffer (KHB) and exposed to 30-min zero-flow ischemia and 120-min reperfusion – ischemia-reperfusion (I/R) injury. HpostC was induced by 4 cycles of 1-min perfusion with oxygen-free KHB intercepted by 1 min perfusion with normal KHB. Treatment by H₂ was administrated in a setting of HpostC where the oxygen-free KHB was saturated with H₂ (H₂+HpostC). Severity of I/R injury was determined according to evaluation of infarct size (TTC staining) and contractile recovery (LVDP) at the end of reperfusion.

Results: HpostC reduced infarct size by 36% and even more H₂+HpostC by 57% (p<0.05, both groups vs. non-HpostC controls-C). LVDP in H₂+HpostC was improved to the levels of statistical significance (p<0.05 vs. C).

Conclusions: Molecular hydrogen improved the prosurvival effect of hypoxic postconditioning. Molecular mechanisms behind remains to be elucidated.

Grants: VEGA SR 2/0201/15, 2/0021/15, APVV-0102-11, APVV-0241-11

19 Postconditioning with H₂S: Molecular Pharmacology

Q. Karwi^a, M. Whiteman^b, M. Wood^c, G. Baxter^a

^aSchool of Pharmacy and Pharmaceutical Sciences, Cardiff University, Cardiff, United Kingdom

^bMedical School, University of Exeter, Exeter, United Kingdom

^cBiosciences, College of Life and Environmental Science, University of Exeter, Exeter, United Kingdom

Background: Hydrogen sulfide (H₂S) has a crucial role in maintaining normal function of the cardiovascular system. It has been shown that administration of exogenous H₂S is protective against myocardial ischaemia-reperfusion (MI/R) injury. However, the mechanism involved is yet to be identified in clinically relevant models and regimens. In the present study, we investigated the molecular targets of two H₂S donors (GYY4137, a slow-releasing H₂S donor, and AP39, a mitochondria-targeting H₂S donor) in an in vivo model of MI/R injury.

Methods: Rats were subjected to 30 minutes myocardial ischaemia/120 minutes reperfusion and both H₂S donors were given 10 minutes before reperfusion (GYY4137 226 μmol/kg; AP39 1 μmol/kg).

Results: H₂S donors significantly limited infarct size with no detectable effect on haemodynamics. Decomposed GYY4137, AP219 the TPP⁺ moiety of AP39, or ADT-OH, the H₂S releasing moiety of AP39 had no effect on haemodynamics or infarct size. Co-administration of L-NAME attenuated but did not abolished GYY4137-induced infarct limitation while LY294002 totally abrogated the cardioprotection. AP39-induced cardioprotection was not affected by either L-NAME, LY294002 or ODQ. Western blot analysis showed that GYY4137 increased Ser⁴⁷³Akt and Ser¹¹⁷⁷eNOS phosphorylation at early reperfusion with no effect on ERK1/2 phosphorylation. It also increased Ser⁹GSK-3β phosphorylation and plausibly decrease

susceptibility of mPTP opening. AP39 had no effect on Akt, eNOS, GSK-3β or ERK1/2 phosphorylation

Conclusions: Data suggest that AP39 has a cytosolic-independent cardioprotective mechanism, supporting the notion of mitochondrial-targeted H₂S delivery. Further characterization of the cardioprotective mechanism of GYY4137 and AP39 is the aim of work in progress now using different subpopulations of myocardial mitochondria, namely, subsarcolemmal and interfibrillar mitochondria.

20 Impact of diabetes on the efficacy of pre-conditioning in a series of patients with ST-elevation myocardial infarction

André Luz^a, Inês Silveira^a, Bruno Brochado^a, Raquel Guimarães^a, Maria João Sousa^a, Patrícia Rodrigues^a, Rui Magalhães^b, Severo Torres^{a,b}, Adelino F. Leite-Moreira^c, Henriques Carvalho^{a,b}

^aServiço de Cardiologia, Centro Hospitalar do Porto, Portugal

^bInstituto de Ciências Biomédicas “Abel Salazar” – Universidade do Porto, Portugal

^cDepartamento de Fisiologia e Cirurgia Cardio-Torácica, Faculdade de Medicina – Universidade do Porto, Portugal

Background: Diabetes blunts ischemic conditioning in basic experiments. However, data in humans is lacking. Pre-Conditioning, manifested as pre-infarct angina (PIA), is a strong stimulus to reduce ischemia-reperfusion injury and thereby infarct size (IS) in patients suffering ST-elevation myocardial infarction (STEMI). We aimed to study the impact of PIA in diabetic (DM) and in non-DM STEMI-patients undergoing primary angioplasty.

Methods: PIA was considered as at least one episode of chest, arm or jaw pain in the preceding 48h before STEMI diagnosis. IS was estimated by peak Troponin-T (logarithmic-transformed TnT-ng/ml), area at risk (AAR-%) was angiographically estimated by the APPROACH score. Regression models were constructed separately to DM and non-DM patients, the interaction of PIA with AAR was tested versus IS as dependent variable.

Results: In a retrospective analysis of 832 consecutive STEMI-patients, 199 (24%) had DM. Proportion of PIA was well balanced for both DM (66/199 = 33%) and non-DM (205/633=32%) groups. In DM-patients, PIA reduced IS (1.3±1.1 vs. 1.6 ± 1.0, p=0.021), whereas for no-DM, PIA had a marginal effect (1.3±1.1 vs. 1.5 ± 1.0, p=0.054). No interaction was found between AAR and PIA for both DM and non-DM groups (p=0.967 and p=0.293, respectively). By multivariable analysis, PIA and creatinine clearance were independent predictors of reduced IS, whereas AAR and total ischemic time were related to increased IS.

Conclusions: In this large series, the effect of PIA was more pronounced in diabetics, independently from the AAR. This may suggest that the diabetic human heart is somehow more susceptible to Pre-Conditioning.

21 Role of altered Ca²⁺ homeostasis during adverse cardiac remodeling after ischemia/reperfusion

A. Domínguez-Rodríguez^a, I. Díaz^a, E. Sánchez de Rojas-de Pedro^a, A. Hmadcha^b, E. Calderón-Sánchez^a, J.P. Benitah^c, A.M. Gómez^c, T. Smani^a, A. Ordóñez^a

Infarct Limitation by GYY4137 at Reperfusion, a Slow-Releasing Hydrogen Sulfide Donor, in the Rat *In Vivo*

Administration of exogenous hydrogen sulfide (H₂S) donors has been shown to protect the heart against ischaemia/reperfusion injury when given at reperfusion by a mechanism that is not fully defined. We sought to characterise the effect of GYY4137, a slow-releasing H₂S donor (morpholin-4-ium 4-methoxyphenyl (morpholino) phosphinodithioate), when given specifically at reperfusion and the involvement of PI3K/Akt signalling in mediating its effects. . All the handling and procedures were carried out in accordance with Home Office Guideline of the Animal (Scientific Procedure) ACT, 1986. Adult male Sprague Dawley rats were anaesthetised with thiobutabarbital (800 µmol/kg, i.p.) and regional myocardial ischaemia was induced by occluding the left descending coronary artery for 30 minutes followed by 2 hours of reperfusion. Animals were randomly assigned (n=6 per group) to receive: 1) no further intervention, 2) GYY4137 (266 µmol/kg, i.v.) 10 minutes before reperfusion, 3) Endothelial nitric oxide synthase (eNOS) inhibitor (L-NAME, 74.2 µmol/kg, i.v.) 5 minutes prior to GYY4137 dose, 4) PI3K inhibitor LY294002 (872.6 nmol/kg, i.v.) 5 minutes prior to GYY4137 dose. In two additional groups, L-NAME and LY294002 were given alone as previously. In a parallel series of experiments (n=4 in per group), tissue samples were harvested from the left ventricle at 5 minutes of reperfusion and snap frozen for biochemical analysis. Infarct size is reported as a percentage of the area at risk. Data, reported as mean±SEM, were analysed using one-way ANOVA supported by Newman Keuls post hoc test, when appropriate. In GYY4137-treated hearts, the phosphorylation of Akt, eNOS and GSK-3β increased at 5 minutes of reperfusion. GYY4137 significantly limited infarct size by 51% compared to untreated-hearts (27.6 ± 2.0% vs 56.8 ± 3.5%, p<0.001). Co-administration of L-NAME with GYY4137 attenuated but did not abolish the cardio protection established by GYY4137 (41.1 ± 6.3% vs 27.6 ± 2.0%, p<0.05) by limiting the phosphorylation of eNOS. LY294002 totally abrogated the infarct-limiting effect of GYY4137 (55.7 ± 3.3%) and inhibited the phosphorylation of Akt, eNOS and GSK-3β. These data indicate that GYY4137 can protect the heart against ischaemia/reperfusion injury through activating the PI3K/Akt/NO signalling pathway and increasing the phosphorylation of GSK-3β at early reperfusion.



Methods and Results: DEX (60 mg/kg) was found to provide almost complete protection against chronic ANT cardiotoxicity induced by daunorubicin (DAU, 3 mg/kg/week for 10 weeks) in rabbits. Using HPLC/MS analysis ADR-925 was determined in plasma and myocardium after DEX administration to rabbits. We have confirmed that administration of ADR-925 (60 mg/kg, *i.v.* alone or with additional *s.c.* dose after 150 min) is able to reach same or even higher concentrations than those after parent drug (DEX) for 5–6 and 9–12 hours, respectively. This allowed direct assessment of cardioprotective effects of ADR-925 on the same rabbit model. The results clearly showed that ADR-925 is unable to provide a significant cardioprotection regardless of schedule of administration as judged by functional, morphological or molecular parameters (e.g. LV dp/dt_{max} decreased as compared to controls by 46%, 39% and 41% in DAU and both ADR-925 combination groups, respectively, $p < 0.05$).

Conclusion: Our data strongly suggest that metal chelating metabolite ADR-925 is not responsible for effective protection induced by DEX against chronic ANT cardiotoxicity. Instead, other mechanisms presumably associated with parent DEX molecule may deserve further study. Supported by GACR 13-15008S and PRVOUK 37/05.

Abstract n° P-19-06

Infarct limitation by GYY4137 at reperfusion, a slow-releasing hydrogen sulfide donor, is PI3K/Akt-dependant with partial dependency on endothelial NO in the rat *in vivo*

Qutuba G KARWI¹; Matthew Whiteman²; Mark E. Wood³; William R Ford¹; Gary F Baxter¹

¹School of Pharmacy and Pharmaceutical Sciences, Cardiff University, UK

²Medical School, University of Exeter, UK

³Biosciences, College of Life and Environmental Science, University of Exeter, UK

Background: Exogenous hydrogen sulfide has been reported as a potential therapy to protect the heart against ischaemia/reperfusion injury in preclinical models when given at reperfusion. GYY4137, a slow hydrogen sulfide-releasing compound, has been shown to be long-lasting H₂S generator with cytoprotective and anti-inflammatory properties by diverse signalling actions. The aim of this study was to investigate for the first time the effect of GYY4137 administration at reperfusion. We hypothesised that GYY4137 given as an adjunct to reperfusion, limits reperfusion injury leading to reduction of infarct size.

Method: Myocardial infarction was induced in 33 male Sprague Dawley rats by occluding the left descending coronary artery for 30 minutes followed by 2 hours of reperfusion. Rats were randomised to receive either no treatment or one of three GYY4137 doses (10, 50 or 100 mg/kg), given intravenously 10 minutes before reperfusion. A second experimental series used PI3K inhibitor (LY294002 0.3 mg/kg) and eNOS inhibitor (L-NAME 20 mg/kg) prior to GYY4137. Risk zone size was determined by Evans' blue exclusion and infarct size was assessed using triphenyltetrazolium staining. Infarct size was expressed as a percentage of the area at risk (AAR).

Results: The highest dose of GYY4137 depressed blood pressure but this was not statistically significant in comparison with the control. While the AAR was similar among all groups, GYY4137 (100 mg/kg) significantly limited infarct size by 47% compared to control group (27.9 ± 3.8 vs $52.5 \pm 4.7\%$, $p < 0.01$, Figure 1, A). In a further study, PI3K inhibition with LY294002 abrogated the protective effect of GYY4137 (100 mg/kg) while eNOS inhibitor attenuated but did not abolish the effect of GYY4137 (Figure 1, B).

Conclusion: These results indicate that GYY4137 can markedly limit lethal reperfusion injury, signalling through PI3K/Akt survival pathway. Nevertheless, the data suggest a partial dependency on NO to mediate its protection. Further studies are ongoing to explore the molecular mechanisms of this powerful cardioprotective effect, including the roles of H₂S, NO and the PI3K/Akt reperfusion injury salvage kinase pathway.

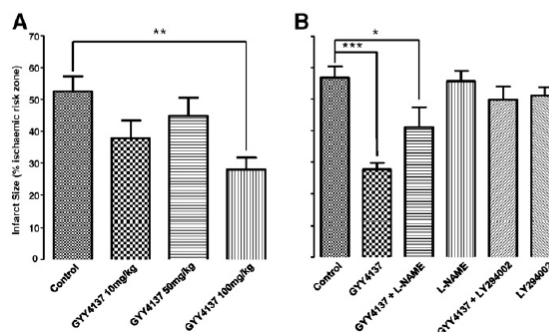


Figure 1. Summary of infarct size measurement expressed as a percentage of the area at risk for (A) GYY4137 dose response study (B) Co-administration of GYY4137 (100 mg/kg) plus L-NAME or LY294002. Data are mean \pm SEM. * = $P < 0.05$ ** = $P < 0.01$, *** = $P < 0.001$ (ANOVA with Dunnett's post hoc test); n = 6–9 in each group.

Abstract n° P-20-01

Imaging Myocardial Glucose Metabolism in an Experimental Model of Uraemic Cardiomyopathy using ¹⁸F-FDG PET

Robert ATKINSON^a; Christopher Cawthorne^a; Torsten Ruest^a; Sunil Bhandari^b; Anne-Marie L Seymour^a

^aSchool of Biological, Biomedical and Environmental Sciences, University of Hull

^bDepartment of Renal Medicine, Hull and East Riding NHS Hospital Trust.

Introduction: *In vivo* positron emission tomography (PET) provides a unique opportunity with which to investigate the metabolic remodeling underpinning the progression of heart disease to failure. Previous studies on uraemic cardiomyopathy (UCM) have identified an enhanced reliance on glucose as a substrate *ex vivo* in the isolated perfused rat heart using ¹³C NMR spectroscopy [1]. The aim of this study was to investigate longitudinally cardiac glucose uptake and metabolism *in vivo* using ¹⁸F-fluorodeoxyglucose (¹⁸F-FDG) PET in a model of UCM.

Methods: Experimental uraemia was induced in male Sprague-Dawley rats via a subtotal nephrectomy. Dynamic PET/CT scans were acquired in list mode at 5 and 13 weeks (wk) post-surgery using a bolus intravenous injection of 40 MBq ¹⁸F-FDG. Data were reconstructed using the 3D ordered subset maximisation algorithm and visualised using Amide software (Figure 1). Time activity curves were generated by manually drawing a region of interest around the left ventricle and the standardized uptake value (SUV) calculated using the final frame of the data set. Cardiac hypertrophy (CH) was determined *ex vivo* after 13 weeks using the heart weight-to-tibia length ratio. The extent of uraemia and anaemia was assessed using serum biochemistry.

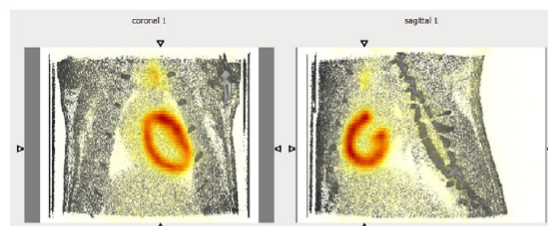


Figure 1 Coronal and sagittal images highlighting ¹⁸F-FDG uptake in the uraemic rat heart visualised using Amide software.